SMI CCSG
Centre for Coal Seam Gas

Recharge Estimation in the Surat Basin

FINAL REPORT

The University Of Queensland
AUSTRALIA

Research Team

Lucy Reading[1], Neil McIntyre[1], Josh Larsen[2], Nevenka Bulovic[1], Abdollah Jarihani[2], Long Dinh[1], Warren Finch[1]

[1] Centre for Water in the Minerals Industry, Sustainable Minerals Institute, The University of Queensland
[2] School of Geography, Planning and Environmental Management, The University of Queensland

Acknowledgements

This research was performed by the Centre for Water in the Minerals Industry (part of Sustainable Minerals Institute) in collaboration with the School of Geography, Planning and Environmental Management, on behalf of the Centre for Coal Seam Gas, The University of Queensland.

The research team would like to acknowledge the kind assistance of the Project Industry Partner Contacts: St.John Herbert (Arrow Energy Pty Ltd), Andrew Moser and Peter Evans (APLNG), Lindsey Campbell and Patrick McKelvey (QGC), Dave Gornall (Santos), Linda Foster and Mark Silburn (DNRM), and Sanjeev Pandey (formerly DNRM).

The research team would also like to acknowledge the following for their kind assistance and helpful input in no particular order: Allison Hortle (CSIRO), Elad Dafny (USQ), Adrian Butler (Imperial College London), Andrew Ireson (University of Saskatchewan), Ofer Dahan (Ben-Gurion University of the Negev) and Jim Underschultz (CCSG).

SMI CWiMI
Centre for Water in the Minerals Industry
Centre for Water in the Minerals Industry
Sustainable Minerals Institute
The University of Queensland, Australia
cwimi@smi.uq.edu.au
www.cwimi.uq.edu.au

SMI CCSG
Centre for Coal Seam Gas
Centre for Coal Seam Gas
Sustainable Minerals Institute
The University of Queensland, Australia
ccsg@smi.uq.edu.au

www.ccsg.uq.edu.au

Centre for Coal Seam Gas

Disclosure

1. The UQ, Centre of Coal Seam Gas is currently funded by the University of Queensland 25% ($5 million) and the Industry members 75% ($15 million) over 5 years.

2. For more information about the Centre's activities and governance see: http://www.ccsg.uq.edu.au/AboutCCSG/FAQs

Disclaimer

The information, opinions and views expressed in this report do not necessarily represent those of the University of Queensland, the UQ, Centre for Coal Seam Gas or its constituent members or associated companies.

Researchers within or working with the Centre for Coal Seam Gas are bound by the same policies and procedures as other researchers within The University of Queensland, which are designed to ensure the integrity of research. You can view these policies at:

http://ppl.app.uq.edu.au/content/4.-research-and-research-training

The Australian Code for the Responsible Conduct of Research outlines expectations and responsibilities of researchers to further ensure independent and rigorous investigations.

This report has not yet been independently peer reviewed.

ISBN: 978 1 74272 139 2

Document Control Sheet

Project number: CLX 148323

Version #	Reviewed by	Revision Date	Brief description of changes
1.0	Lucy Reading Neil McIntyre Jim Underschultz		
2.0	Lucy Reading Neil McIntyre	28.11.14	Incorporate feedback on version 1.0 from the project technical group

Executive Summary

The Recharge Estimation project aims to improve our understanding of spatial and temporal distributions of groundwater recharge in the Surat Basin. Phase 1 of this project has brought together existing relevant data sets and knowledge, developed new recharge estimates particularly for the Surat Basin, provided a short-list of possible experimental sites and conceptual models, and produced an outline of designs for potential field experiments at those sites. These outcomes have been guided by industry partners and external experts at a series of six project workshops and numerous separate meetings.

The outcomes of the project are presented in two separate reports. This report covers the review and recharge estimation. The second report covers the field experiment design.

The objectives of this report are to provide:

1. A review of recharge estimation methods used globally
2. A review of previous recharge studies in the Surat
3. New recharge estimates based on analysis of existing data
4. Recommendations for further research based on identified knowledge gaps

A literature review of current techniques used globally was conducted to determine which recharge estimation methods might be suitable for recharge estimation in the Surat Basin. Key findings from the literature review were: 1. multiple methods should ideally be applied because of the considerable uncertainty in any one approach, and 2. individual approaches are tailored to a particular range of time and space scales. The review also concludes that extensive field measurements are an essential part of developing models and achieving useful levels of reliability in recharge estimates.

Recharge Estimation:

A number of recharge estimation methods have been applied in the Surat Basin prior to this study, e.g. groundwater hydrograph analyses, groundwater chloride mass balance, unsaturated zone chloride mass balance and soil water balance modelling. These previous recharge estimates included a range of spatial scales but were typically limited to long term averages with limited information about temporal variation.

Analysis and interpretation of available data provided here examines this gap and has resulted in new estimates of the spatial and temporal distribution of groundwater recharge in the Surat Basin.

The regional groundwater flow directions in different aquifers were plotted by fitting potentiometric surfaces to available borehole data. However due to various data limitations, the potentiometric surfaces are only broadly indicative of regional groundwater flow paths and require improvement. Higher quality and quantity of water level data is necessary with better characterisation of source aquifers and borehole location.

The water table fluctuation method was applied to selected groundwater hydrographs producing new estimates of groundwater recharge. Calculated annual average recharge rates varied between 4 and 37 mm/year depending on location, but were restricted to a limited number of bores with sufficient data and where aquifers are unconfined, water tables are shallow, and pumping impacts are limited. If suitable locations are targeted for additional groundwater monitoring, this method could easily be used to extend recharge rate estimation further throughout the unconfined Main Range Volcanics and Walloon Coal Measures.

Analysis of surface water data was also used to quantify groundwater recharge. This is a powerful method because it only requires streamflow records; however it has important assumptions, including the need to assume that recharge appears as stream baseflow at the outlet of the surface catchment. Annual average recharge rates using this method varied between 0 and 3.2 mm/year.

There are a number of potential ways forward for the surface water analyses including extending it to other parts of the Surat Basin, examining recharge on larger time scales such as annual or seasonal, and applying alternative baseflow separation and recession analysis methods.

Deep Drainage Estimation:

The combined remote sensing and modelling product from CSIRO, the Australian Water Availability Project (http://www.csiro.au/awap/) gives regional deep drainage estimates at a 5 km grid resolution at monthly and annual timescales. The CSIRO data, supplemented with additional remote sensed soil moisture data, were used to investigate the spatial and temporal variability of recharge throughout the whole Surat and for separate geological units. For

example, over the Walloon-Injune units, the annual average deep drainage rate ranged between 2 and 34 mm/year; while across the Main Range Volcanics the rate varied between 1 and 105 mm/year. Averaging deep drainage over the whole of the Surat, the range changed from 3 to 64 mm/year when moving from a particularly dry to a particularly wet year. Although they provide the sought spatial and temporal resolutions, the CSIRO deep drainage estimates are based on national scale water balance generalisations, only partially use the available remote sensed data, and provide deep drainage rather than actual recharge rates. Hence these data should not yet be assumed to be suitable for groundwater impacts assessment in the Surat Basin, and further analysis and development is recommended.

Deep drainage within the Surat Basin as a whole was found to exhibit a high degree of spatial variability, and areas of higher deep drainage are driven by a combination of higher precipitation and /or soil and landscape properties.

The temporal distribution of deep drainage shows large variability around the long term mean values. These results show the potential importance of including recharge as a time varying input (at least annually varying) to groundwater models.

Summary:
Phase 1 of the Recharge Estimation project demonstrated some of the approaches that can be used to generate improved estimates of recharge and deep drainage; and has developed local and regional scale estimates using the most easily accessible existing data. However, to date the local scale data analysed represent only small parts of the recharge areas, and do not provide the process understanding needed to extrapolate these estimates across the key Surat Basin recharge areas. Furthermore, Phase 1 has not included merging of local scale and regional scale data. We therefore recommend that the project moves into Phases 2 and 3, which will develop new process understanding through field experiments that can be used to calibrate local scale recharge estimates and finally extrapolate to regional scale products.

Table of Contents

List of Figures

List of Tables

Introduction

Groundwater modelling studies and aquifer water balances rely on an accurate determination of recharge rates so that sustainable yields, potential impacts of extraction, and susceptibility to change can be properly quantified. However, accurate determination of recharge is often elusive because of complex flow paths and a lack of data available to inform processes or constrain uncertainty.

Where there are potential aquifer impacts from activities such as CSG development, an accurate knowledge of recharge rates in both space and time is critical for a reliable assessment of this impact likelihood and an understanding of risk. Within the context of the Surat Basin specifically, there is a need to develop improved knowledge about groundwater recharge mechanisms and improved estimates of groundwater recharge rates because: 1) The quantity and distribution of recharge across the basin are expected to influence groundwater levels during CSG production as well as during the post-production recovery period; 2) The quantity and distribution of recharge may influence the attribution of groundwater pressure changes; 3) The current gaps in scientific knowledge limit the robustness of current recharge models and estimates; and 4) Representation of recharge varies widely between groundwater impacts assessment models.

The Recharge Estimation project aims to improve our understanding of spatial and temporal distributions of groundwater recharge in the Surat Basin. Phase 1 of this project has brought together existing relevant data sets and knowledge, developed new recharge estimates, compiled a short-list of experimental sites and conceptual models, and designed field experiments. Two reports have been produced from Phase 1. While this report focuses on the literature review and development of new recharge estimates, the “Field Experimental Design” report focuses on the short-listed experimental sites and proposed field measurements.

The objectives of this report are to provide:

1. A review of recharge estimation methods
2. A review of previous recharge studies in the Surat
3. A summary of testing of different recharge estimation methods based on analysis of existing data
4. Recommendations for further research based on identified knowledge gaps

Recharge Estimation Methods

Groundwater recharge is the flux of water that reaches the groundwater table (Bond, 1998). This differs from “deep drainage” which is the downwards movement of water across the bottom of the root zone.

Recharge can reach groundwater tables through a number of pathways. These pathways can generally be categorised into “diffuse” recharge and “focussed” recharge. Whilst “diffuse” recharge can potentially occur across the landscape, “focussed” recharge only occurs through streams, cracks and other preferential flow pathways. Preferential flow encompasses a range of hydrological processes such as macropore flow, funnelling and unstable flow fingering and means that recharge can reach to deeper depths at greater speeds than would occur via diffuse recharge alone (Cuthbert and Tindimugaya, 2010). Diffuse recharge is strongly influenced by local vegetation and climate characteristics, which are largely dependent on climate types (Barron et al., 2012).

In general, the most suitable approach to estimating groundwater recharge is to derive a conceptual model for recharge processes first, then determine groundwater recharge using one or more of several suitable methods (Scanlon et al., 2002). A suitable conceptual model may include aspects of location, timing and likely unsaturated flow pathways. As part of the development of a conceptual model, available hydrologic data including precipitation records, stream-flow records and groundwater level records should be evaluated (Scanlon et al., 2002).

There are limitations to the well-established recharge estimation methods, most of which yield results that are method and scale dependent (de Vries and Simmers, 2002). In cases where recharge estimation is required for large, complex groundwater basins, it is therefore appropriate to apply multiple estimation techniques including techniques that are applicable at different scales (Delin et al., 2007). Complex processes such as preferential flow, which exert a strong control on recharge are often not simulated in regional scale studies (Ordens et al., 2014). Comparison of estimates from multiple methods can also provide information to test hypotheses.

The different scales at which recharge may be estimated range from point scale to regional scale. Figure 1 lists approaches to recharge estimation methods and illustrates the scales over which they are commonly applied.

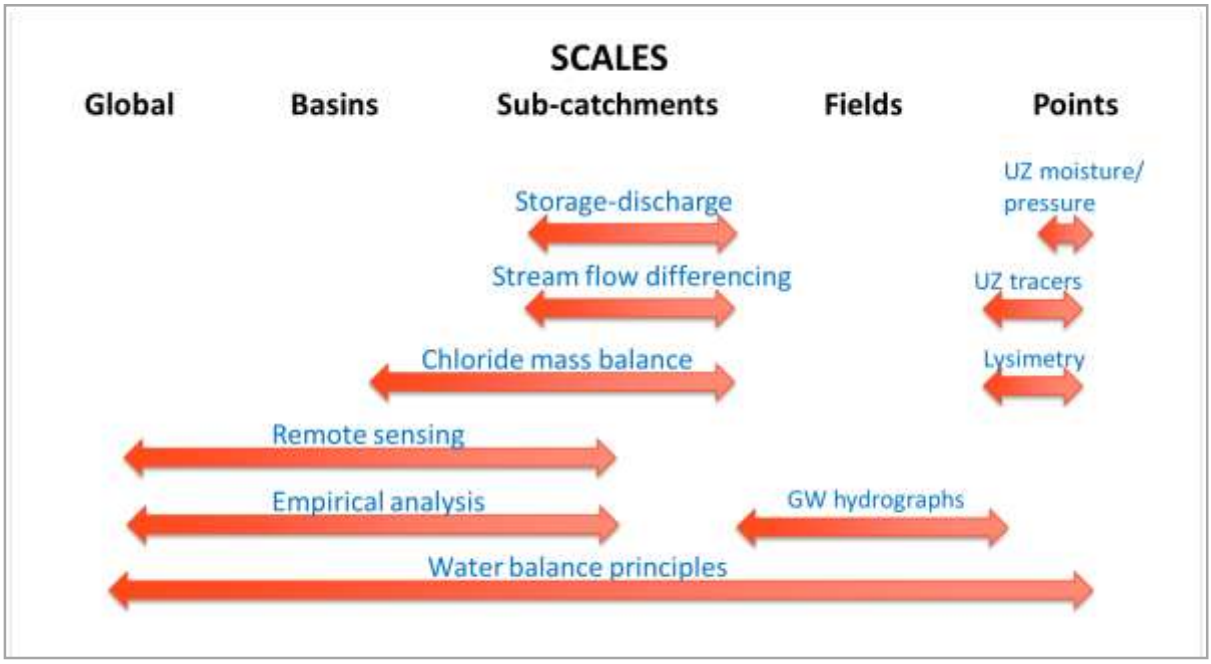

Figure 1 – Indicative scales for commonly applied recharge estimation methods (where UZ = unsaturated zone).

A brief description of the available recharge estimation methods is provided in Sections 0 to 0. Detailed descriptions of the applied recharge estimation methods are provided at the start of Sections 6, 7 and 8.

Empirical Approaches and Remote Sensing

Commonly applied regional scale estimation approaches include empirical approaches and remote-sensing based approaches. Empirical approaches involve taking local estimates of recharge (using one of the other methods) and relating these estimates to easily observable properties such as soil type and vegetation indices. These approaches have previously been applied at the national scale (Crosbie et al., 2010), who developed empirical relationships for use across Australia based on a dataset of field scale recharge estimates. . For global scale estimation of recharge, a simple equation has been used to relate physical factors such as hydrogeology, soil texture, precipitation intensity and relief to diffuse recharge rates (Doll and Fiedler, 2008).

Remote sensing has been a widely applied measurement tool within hydrology. Remote sensing cannot directly measure groundwater recharge; instead the data must be able to account for the other major elements in the water balance (evapotranspiration, surface runoff, soil water storage, surface storage and precipitation) and recharge inferred from this (Becker 2006).

Groundwater Tracers

The chloride mass balance (CMB) approach is the most widely used technique for estimating recharge (Scanlon et al., 2006). This approach has previously been applied for recharge estimation at the regional scale using groundwater chloride and rainfall chloride data (Wood and Sanford, 1995) but care needs to be taken with regards to interpolating between sparse groundwater chloride measurements and combining groundwater chloride data from multiple different aquifers. Some key assumptions of the chloride mass balance method are that: the chloride in the groundwater originates only from precipitation and that there is no recycling or concentration of chloride within the aquifer (Wood, 1999). As the groundwater chloride concentrations represent chloride that may have accumulated over many years, the method is typically used to give long-term average recharge rates rather than time distributions.

Remotely sensed data can be used to estimate the space and time distributions of recharge (Brunner, 2004). These estimates can then be adjusted by calibration to more accurate but lower resolution values of recharge, e.g. derived from the chloride method (Brunner, 2004).

In addition to the CMB method, there are a number of other groundwater chemical tracer techniques (including isotopic techniques) that can be applied to estimate recharge rates. Groundwater chemical methods for quantifying recharge can be divided into two broad categories: methods which rely on mass balance of solutes to deduce information about the magnitudes of recharge to the aquifer; and methods which seek to estimate the age or residence time of the groundwater (Cook and Herczeg, 1998). All of these methods produce long-term average estimates of recharge rates.

Surface Water Analysis Based Methods

There are also a number of recharge estimation methods that rely on surface water data and are applied at either the river reach scale or the sub-catchment scale (Shanafield and Cook,

2014). Streamflow differencing can be used to estimate transmission losses in perennial streams (by measuring the difference between upstream and downstream flow while taking into account other flow sources and sinks, including evaporation) (Shanafield and Cook, 2014).

Quantification of “mountain block recharge” has recently been achieved using recession flow analysis (Ajami et al., 2011). The method relies on the application of catchment storage-discharge relationships proposed by Kirchner (2009) and is based on certain assumptions, such as low evapotranspiration (ET) rates during dry periods and perennial flow conditions at the gauge, and that interflow and other catchment losses are negligible (Ajami et al., 2011).

Field and Point Scale Methods

Finally, there are a plethora of recharge estimation methods that can be applied at the field scale to the point scale. These include lysimeters, unsaturated zone soil moisture measurements, unsaturated zone tracers, groundwater hydrograph analyses and water balance measurements and modelling.

Lysimetry can be used to make direct measurements of drainage and evapotranspiration (Allison et al., 1994). Some of the problems associated with using lysimeters to determine recharge are the expense of construction and maintenance, soil and vegetation disturbance, modification of the bottom boundary condition relative to that prevailing in the open field and the localized nature of the data obtained (Gee and Hillel, 1988). Recent studies have found that passive wick lysimeters (where a wetted fibreglass wick acts as a hanging water column that develops suction in the soil water depending on the flux) are capable of achieving minimal disturbance to the native flow regime (Louie et al., 2000).

Unsaturated zone moisture monitoring traditionally involves the use of water content sensors, such as time-domain reflectometry (TDR) probes and tensiometers for water-pressure measurements (Dahan et al., 2009). Measurement of percolation of both water and contaminants through deep unsaturated zones can be achieved by installing FTDR (flexible time-domain reflectometry) probes and VSP (vadose zone sampling ports) into the upper sidewall of an uncased small-diameter slanted borehole (Dahan et al., 2009). Downward flux rates of water can then be determined by combining the calculated wetting-front propagation velocity with the measured change in water content (Dahan et al., 2009).

The natural tracers most commonly for unsaturated zone based recharge estimates are ^{3}H, ^{14}C, ^{36}Cl, ^{15}N, ^{18}O, ^{2}H, ^{13}C and Cl (Allison et al., 1994). The mechanisms of infiltration will affect the interpretation of results (so multiple tracers are required) (Allison et al., 1994).

The most common assumption applied in unsaturated zone tracer methods is that piston flow is occurring, but there is mounting evidence that water movement along preferred pathways is the rule rather than the exception (Allison et al., 1994). In cases where bypass flow occurs, deep drainage rates are underestimated when using unsaturated zone tracer methods (Ringrose-Voase and Nadelko, 2011).

In arid and semi-arid environments, desiccation cracks can make up a substantial proportion of the soil's volume, especially near the surface (Baram et al., 2012b). While it was previously though that plowing and irrigation would prevent the development of crack networks and promote matrix percolation through clay soils (Kurtzman and Scanlon, 2011), recent research has found that naturally formed desiccation cracks can remain open year-round, even at high sediment water contents (Baram et al., 2012b).

Evidence of preferred pathway flow has been presented recently through a vadose zone monitoring study where major differences were detected in the solute concentrations between the mobile flowing phase and the sediment profile (Rimon et al., 2011). Comparison of recharge estimates from different methods can be used to help determine whether preferential flow is occurring. For example, discrepancies between vadose zone based methods and groundwater based methods can indicate the occurrence of preferential flow (Kurtzman and Scanlon, 2011).

Analysis of groundwater hydrographs can be used to calculate recharge rates at the groundwater table. A commonly applied method is the water-table fluctuation (WTF) method. This method requires knowledge of specific yield and changes in water levels over time (Healy and Cook, 2002). Advantages of this approach include its simplicity and an insensitivity to the mechanism by which water moves through the unsaturated zone (Healy and Cook, 2002).

Recharge estimates derived using the WTF method can be assumed to represent an area of at least several square meters around an observation bore (Healy and Cook, 2002). Uncertainty in estimates generated by this method relate to the limited accuracy with which

specific yield can be determined and to the extent to which assumptions inherent in the method are valid (Healy and Cook, 2002).

There can be considerable variation in rates of recharge over the scale of a few meters (Allison et al., 1994). For this reason, when point scale recharge estimation methods are applied, multiple sampling locations are often required to capture the variability in groundwater recharge.

Water Balance Measurements

Water balance measurements are implicit to some of the methods previously described, which use various forms of measurement (remote sensing, groundwater levels, etc) to help close the water balance and to determine the space and time distribution of the water balance. At smaller scales, field experiments are often used to estimate recharge by directly measuring all other components of the water balance. This direct approach reduces the chance of over- or under-estimation (Lerner et al., 1990).

Mdaghri-Alaoui and Eugster (2001) measured the components of the water balance at an experimental site to quantify recharge through a highly heterogeneous unsaturated zone. Numerous other examples exist of field scale water balance measurements (Freeze and Banner, 1970; Ireson et al., 2006; Lerner et al., 1990; Marshall et al., 2009; Rutter et al., 2014).

Any errors associated with estimating or measuring the individual components of the water balance may reduce the accuracy of recharge estimates based on water balance measurements (Herczeg and Love, 2007). The water balance approaches are therefore ideally coupled with deep vadose zone percolation measurements and/or groundwater hydrograph monitoring.

Field based water balance measurements can also be readily combined with recharge process modelling. Rockhold et al. (2009) used field monitoring of the water balance at a waste disposal field site to refine and improve recharge estimates from numerical simulations. The approach used in this study encompassed lysimetry, water flux measurements (Gee et al., 2002) and measurements of unsaturated zone water content and matric potential.

The combination of field based measurements and process based modelling has recently been applied for regional scale recharge estimation in China (Lu, Jin et al. 2011) and Denmark (Andreasen et al., 2013). Lu et al. (2011) calibrated a 1D unsaturated flow model (HYDRUS-1D) at five representative sites using field data of climate, soil moisture and groundwater levels. While Andreasen et al. (2013) calibrated the 1D soil-vegetation-atmosphere transfer model Daisy against soil moisture measurements from 30 stations and three depths.

Modelling Approaches

Unsaturated zone process models simulate the stores and fluxes of water at different levels in the soil (and in some cases surface and interception stores and fluxes), driven by rainfall inputs and evapotranspiration demands. The deep drainage estimates are the downward fluxes from the bottom store.

Model types range from relatively simple soil moisture accounting models such as PERFECT (Littleboy et al., 1989) and APSIM-SoilWat (McCown et al., 1996), where drainage is based on simplistic storage-drainage approximations; to more complex physics-based models such as HYDRUS (Simunek and van Genuchten, 2008), where pore water pressure is simulated using soil water-pressure characteristic curves, and drainage rates are based on pressure gradients.

The use of these models to estimate recharge requires an assumption about the pressure gradient or the storage-discharge equation at the interface of the unsaturated and saturated zone. Typically, it is assumed that there is no interaction and a ‘free drainage’ boundary condition applies. An alternative method is the use of models which fully couple unsaturated zone and saturated zone processes. This approach has been illustrated using several models including HYDRUS-2D (Reading et al., 2010) and MIKESHE (Christiaens and Feyen, 2001).

Regional groundwater recharge can also be estimated using inverse numerical groundwater modelling. However, during inverse modelling, recharge and hydraulic conductivity are typically estimated (calibrated) simultaneously (Sanford, 2002). Independent measurements of recharge rates are therefore required in order to constrain model calibration (Sanford, 2002).

Comparing Recharge Estimates

There is value in directly comparing recharge estimates derived using different recharge estimation methods. However, the assumptions and the relevant temporal and spatial scale need to be kept in mind when comparing estimates derived from different recharge estimation techniques. A brief summary of some of the limitations of different techniques (included those related to scale) is provided in Table 1.

Inconsistencies in estimates derived from different recharge estimation methods may provide insight into measurement errors or the validity of assumptions underlying a method and thus may provide direction for revising the conceptual model (Healy and Scanlon, 2010). However, many methods are applicable for estimating recharge that occurs via multiple recharge mechanisms e.g. both diffuse and focussed recharge. One reason for inconsistencies in estimates is that the quantity measured is different i.e. methods that estimate potential recharge (or deep drainage) may give different recharge estimates from those methods that estimate actual recharge (Crosbie et al., 2010).

Table 1 - Recharge estimation methods

Method Description	**Parameters required**	**Main advantages**	**Main limitations**
Groundwater hydrograph analyses ("water table fluctuation" method)	Groundwater levels, specific yield, rainfall and groundwater pumping.	Can make use of available groundwater level data. Additional monitoring is cheap. Recharge estimation at the water table.	Requires knowledge of specific yield and good water level records. Works at small scales but is difficult to extend to larger areas without extensive monitoring systems. Restricted by assumptions regarding other influences on groundwater levels.
Discharge-storage relationships	Stream-flow time-series.	Can make use of available streamflow data. Provides a "lower bound" recharge estimate / estimates "net recharge".	Assumes that baseflow volumes equal recharge volumes. Limited to water sheds where lateral fluxes, pumping, leakage and water storage changes are minimal.

Lysimetry	Deep drainage is directly measured but data on rainfall, irrigation and soil hydraulic properties may be useful in interpreting lysimetry results.	Can provide accurate data on deep drainage and crop water use.	Lysimeters are expensive to construct and are not transportable. Only provide point estimates of deep drainage. Soil hydraulic properties will be disturbed during installation of the lysimeter.
Unsaturated zone moisture measurements	Soil moisture content and soil hydraulic properties.	Relatively simple measurement techniques can be used (unless deep profiles are monitored).	Requires data on both water content and water pressure. Only provides point estimates of deep drainage (unless monitoring extends to the water table in which case, provides point estimates of recharge).
Unsaturated zone process models	Rainfall, irrigation, runoff, climate variables for calculating evapotranspiration. Ideally soil moisture and pressure. For simple models, soil "bucket" parameters need to be calibrated or estimated using regionalisation. For Richards' equation models, hydraulic properties need to be calibrated, estimated using regionalisation or laboratory or in-situ experiments.	Can be applied regionally when simple (bucket-type) models are used. Where more complex (e.g. Richards' equation) models are used, the modelling may be too computationally demanding to use regionally; but can be used for local recharge and to improve our understanding of recharge processes. Can provide high resolution recharge estimates.	Requires knowledge of other components of water balance (some of these components can have high uncertainty). Limited by how well the chosen model represents the physical system. Model parameter uncertainty can be high. Typically used to provide estimates of deep drainage (but can be used to provide estimates of groundwater recharge if the entire unsaturated zone is simulated).
Water Balance calculation using remotely sensed data	Remote sensing data can be used to estimate: Precipitation; near-surface soil moisture; evapotranspiration; land cover; in some cases large river flows and groundwater levels.	Reasonable spatial and temporal resolution; near-global coverage.	Unknown uncertainty in conversion of raw remote sensing signals to hydrological data. Generally does not account for deep unsaturated zone changes in storage.

	Independent estimates of surface flow are usually needed.		
Groundwater modelling - Calibration of recharge	Geological model, aquifer and aquitard hydraulic properties, groundwater levels, groundwater pumping etc.	Can make use of existing groundwater models.	Recharge is controlled by hydraulic properties and boundary conditions (therefore non-unique).
Darcy's Law (i.e. relating the groundwater flow rate through a cross-sectional area of the aquifer to the surface area that contributes to recharge)	Hydraulic conductivity, hydraulic gradient and surface area for geological formations of interest.	Potential to integrate over large spatial scales.	This method suffers significantly from reliable estimates of hydraulic conductivity. Considering the natural variation in hydraulic conductivity and the difficulty in scaling up regional values of hydraulic conductivity, the method at best would provide order of magnitude estimates of recharge.
Groundwater chloride mass balance	Chloride concentrations in groundwater and rainfall.	Can make use of readily available data (therefore there is potential for regional recharge estimation using this method).	Based on long term average precipitation and chloride concentrations in rain and groundwater or soil water. Assumes steady state conditions (provides long term average estimates of recharge).
Groundwater age dating	Tracer concentrations in groundwater.		Not a direct measure of flux (bounding fluxes must be determined indirectly). Assumptions relating to GW flow paths and solute sources/sinks.
Unsaturated zone solute tracers	Solutes in rainfall, solutes in the unsaturated zone.	Relatively cheap (therefore it is possible to make measurements at multiple locations).	Only provide point estimates of deep drainage. Piston flow reduces the value of this method.

Water balance measurements	As many components of the water balance are measured as possible (e.g. rainfall, potential evaporation, soil moisture, groundwater levels, surface water levels, plant/tree water uptake).	Reduced reliance on models and indirect measurements.	The recharge rates are site specific i.e. controlled by the physical characteristics of the site.

Recharge in the Surat Basin

The Great Artesian Basin is the largest confined groundwater basin within Australia, covering the majority of Queensland and extending into New South Wales, South Australia and the Northern Territory. The basin is made up of multiple layers of aquifers, predominantly comprised of sandstone, which are interbedded by layers of mudstone and siltstone that commonly act as aquitards (Habermehl, 1980). The basin is of a synclinal shape, with a general tilt towards the southwest (Habermehl, 1980).

The Surat Basin is a structural sub-basin within the GAB. Due to the vast area of the Surat Basin, covering an area of approximately 270,000 km^2, many of the hydrological characteristics are highly variable across the basin.

The Surat Basin sits within the “subtropical” climate zone. Average annual rainfall ranges from 500 mm/year in the west to 800 mm/year in the east. Potential evaporation rates greatly exceed average annual rainfall (average annual open pan evaporation is greater than 1200mm/year). Rainfall is highly variable and seasonal within the basin with occasional periods of high intensity rain and runoff alternating with extended periods of severe drought and low stream flow (Preston et al., 2007).

The basin is roughly bounded to the north and east by the Great Dividing Range; however the surface water catchments within the Surat Basin do not line up with the groundwater basin boundaries. In fact, multiple surface water basins coincide with the Surat geological basin (including the Fitzroy River Basin, the Condamine-Balonne River Basin, the Moonie River Basin and the Border Rivers Basin). As a result, there are several surface water divides within the Surat Basin.

Due to the vast scale of the Surat Basin, multiple recharge mechanisms pathways may be present. However, the majority of the recharge flux probably occurs within a small area along the basin boundaries (Kellett et al., 2003). Within this broad context, groundwater recharge processes in the Basin can be separated into 1) recharge to the shallow, unconfined alluvial aquifers associated with the surface hydrology, and 2) the direct recharge to the aquifers of the Great Artesian Basin (GAB).

Recharge pathways for 1) will occur as a direct hydraulic connection (permanent or temporary) with river channels (Winter et al., 1998) and via the unsaturated zone of the wide expanse of floodplain soils (diffuse recharge). Recharge pathways for 2) include preferential flow, diffuse recharge and recharge via surface channels. The latter recharge pathways have traditionally been considered to occur primarily within the extent of "GAB intake beds" (Figure 2), or locations where the GAB aquifers outcrop and thus become exposed to the surface and atmosphere. These intake beds are located at the margins of the GAB (Radke et al., 2000) comprise a layered sequence of sandstone aquifers and interbedded mudstone confining beds (Kellett et al., 2003) and have been mapped previously using a combination of geological, geophysical and remote sensing methods (Bierwirth and Welsh, 2000).

The majority of the recharge in the GAB intake beds occurs following high intensity, short duration rainfall events and is therefore likely to be associated with localised preferential flow pathways (Habermehl, 2002; Kellett et al., 2003). However, a robust conceptual model incorporating these pathways and surface interactions is yet to be developed.

Recent assessments by CSIRO (Herczeg and Love, 2007; Smerdon et al., 2012a) suggest that there is also potential for recharge to occur to GAB aquifers outside of the GAB intake beds. The Office for Groundwater Impact Assessment (OGIA) model also assumes that recharge occurs outside of the GAB intake beds (to the "Primary Recharge Areas as shown in Figure 2). There is therefore a clear research need to more conclusively demonstrate the recharge processes and pathways to GAB aquifers, which will in turn allow a better assessment of the relative contributions of recharge via the "GAB intake beds" versus recharge outside of these beds.

There are very little data available to confirm whether "indirect" recharge to the GAB formations is occurring via other geologic units. In addition to the uncertainty surrounding

recharge locations and pathways, there is only limited information about the recharge rates and the spatial variability of these rates.

RECHARGE ESTIMATION IN THE SURAT BASIN

SMI CWiMI
Centre for Water in the Minerals Industry

Surat basin, GAB intake beds and primary recharge areas

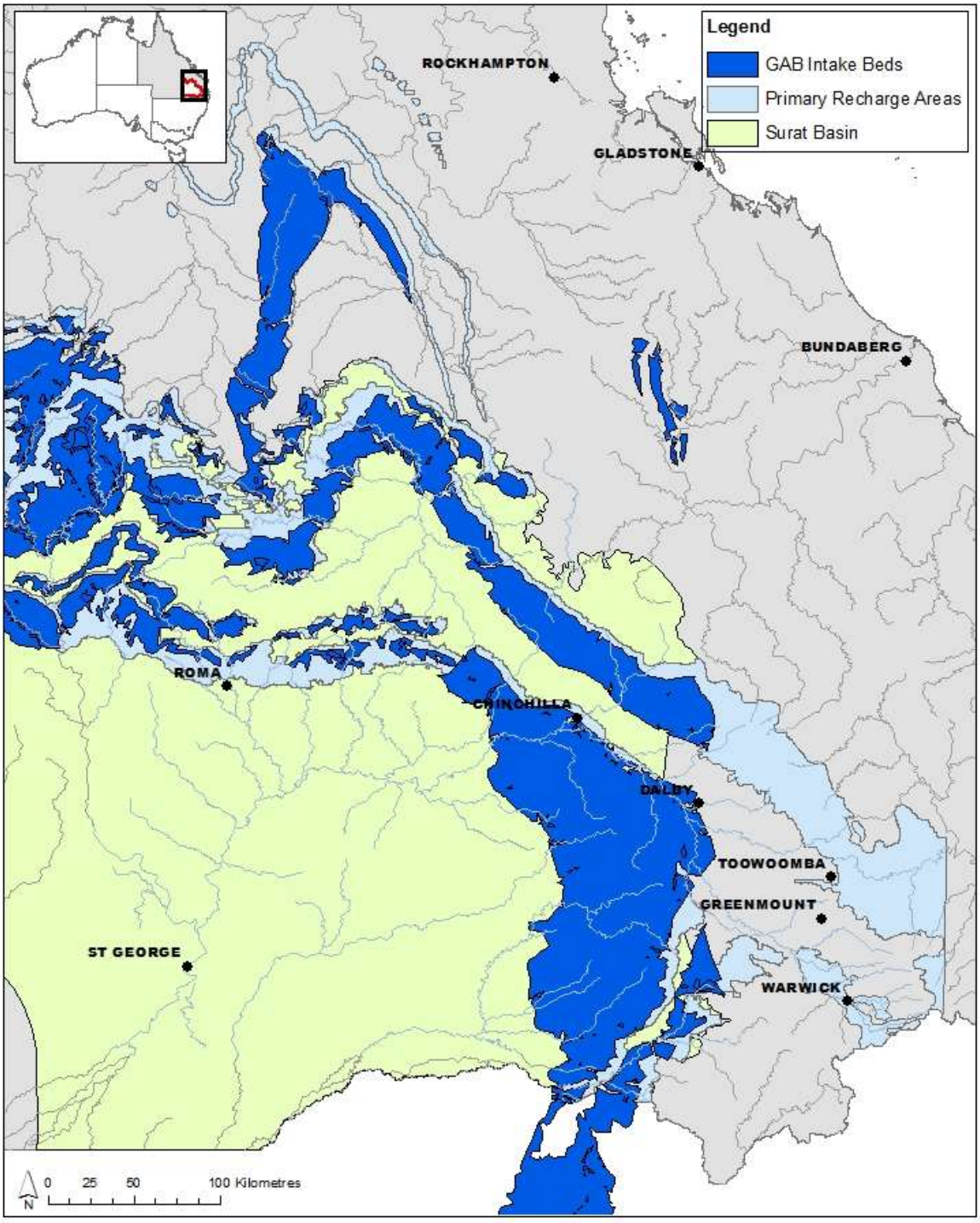

Figure 2 - Location of the Surat Basin, the "GAB intake beds" and the "primary recharge areas"

Recharge Pathways and Mechanisms

Three separate pathways have been suggested for recharge to the GAB formations. These are: recharge exclusively through the “GAB intake beds”, recharge through the Main Range Volcanics and recharge through the unconfined alluvial aquifers.

Recharge through the “GAB intake beds”

The “GAB intake beds” coincide with the locations where the GAB formations outcrop. There is some disagreement on which formations contribute significant recharge to the GAB. While some definitions for the “intake beds” encompass both aquifers and aquitards e.g. Kellett et al. (2003), others define the “intake beds” as consisting exclusively of GAB aquifers (Smerdon and Ransley, 2012).

The “intake beds” were originally defined based on available geological mapping (Kellett et al., 2003). It was hoped that delineation of the recharge beds could be improved using remotely sensed data sets. In particular, it was hoped that differentiation could be made between the low permeability materials and the higher permeability materials. However, data from gamma-radiometrics surveys of the GAB “intake beds” did not appear to discriminate between low permeability units and higher permeability units such as sandstones. It was hypothesized that this may be due to weathering effects causing the potassium values to be low for all units; alternatively, there may be errors within the geological mapping.

According to the Kellett et al. (2003) recharge estimation study, the formations included in the intake beds within Queensland are: Bungil, Mooga, Gubberamunda, Hooray, Kumbarilla, Ronlow, Gilbert, Southlands, Springbok, Adori, Hutton, Marburg, Boxvale, Precipice, Clematis and Warang. The majority of these formations consist of fine to coarse quartzose sandstones with limited information available about the presence or absence of fractures. Many of these formations contain either interbedded mudstone and siltstone or kaolinitic clays infilling pore spaces. The permeabilities of sandstone formations in the outcrop zones are expected to be controlled in part by the presence of clays and carbonate minerals existing in certain horizons (Arditto, 1983).

The hydraulic properties of the soils that overlie the outcrops may limit groundwater recharge volumes or contribute to significant time lags between rainfall events and the occurrence of recharge. The dominant soil types mapped within the intake beds are: Chromosol (loam),

Sodosol (sandy loam), Tenosol and Rudosol (sand) with lessor amounts of Vertosol (clay), Kandasol and Ferrosol. The range of clay percentages in the A horizon is approximately 5 to 60. Based on this information, the soils that overlie geological outcrops within the intake beds would be expected to display wide ranging hydraulic properties.

Land use may also play a role in controlling groundwater recharge potential by altering infiltration capacity and runoff occurrence and/or by consuming water that may otherwise have been available for deep percolation and eventually groundwater recharge. Land uses that are present within the GAB recharge beds include livestock grazing, semi-intensive agriculture, production forestry and national parks (Kellett et al., 2003).

There is evidence that both diffuse recharge and preferential flow occur throughout the GAB intake beds (Kellett et al., 2003). Preferential flow is likely to be the dominant recharge process in the GAB intake beds (Kellett et al., 2003). Preferential flow pathways within the GAB intake beds include creeks, cracks in clay soils and fractures in geological formations. There is evidence from international studies that preferential flow can be responsible for up to 75% of total recharge in fractured rock environments (Sukhija et al., 2003), however, the information about the location and density of fractures within the GAB intake beds is very limited.

Rainfall of greater than 200 mm during a one month period was found to be necessary to generate preferential flow as it was hypothesized that the unsaturated zone typically needs to be saturated before preferential flow can occur (Kellett et al., 2003). Yet, recent studies have shown that the unsaturated zone typically does not need to be saturated in order for preferential flow to occur through cracking clay soils (Greve et al., 2010).

Desiccation cracks can serve as water conduits and preferentially transport water and solutes into deep sections of the vadose zone during high rainfall events (Baram et al., 2012a). However, preferential flow may also occur in between these high rainfall events as soil cracks can remain pathways for preferential flow even when they are closed at the soil surface (Greve et al., 2010).

Habermehl (2002) introduced the idea of “induced recharge” through GAB intake beds. He claimed that: “abstraction by waterbores has caused a large scale lowering of the potentiometric surface and a steepening of the hydraulic gradient, which allowed more recharge water to enter the system.” There is currently some speculation regarding the

possibility of this occurring in response to coal seam dewatering but the theory has not yet undergone further investigation. The conditions that would be required in order for depressurisation of the coal measures to induce increased recharge rates include: shallow, highly permeable unsaturated zones or direct connection of groundwater with surface water. These conditions are important because they could lead to a situation where recharge processes are driven by the hydraulic gradient in the groundwater as well as unsaturated zone properties and processes.

Recharge to GAB formations through the Main Range Volcanics

When developing a regional groundwater flow model for the Surat "Cumulative Management Area", the Office for Groundwater Impact Assessment (OGIA) identified the potential for recharge to occur to the east of the previously mapped intake beds, through the Main Range Volcanics. This is contrary to an assumption in Kellett (2003) that the basalt areas are unlikely to contribute significantly to recharge due to associations between the basalts and "relatively impermeable soils". Yet, within the area underlain by the Main Range Volcanics, there are actually a range of soil types present and even the least permeable of these soils have previously been found to drain readily (Silburn et al., 2006).

The entire sequence of basalts within the Main Range Volcanics is intensely jointed with very well developed vertical joints (Armstrong, 1974). The joints and weathered zones are of great significance in the groundwater cycle since the basalt itself is extremely compact and impervious (Armstrong, 1974). Beneath the hills there is a thick cover of soil and weathered mantle below which vertical joints in the basalt form a network of narrow channels through which recharge reaches the water table and makes a limited contribution to the storage capacity (Armstrong, 1974). There is evidence that groundwater flow to the west within the Main Range Volcanics is considerable (Armstrong, 1974).

There remains some debate, however, about the potential for recharge to the Main Range Volcanics to flow into the GAB formations such as the Walloon Coal Measures. The Walloon Coal Measures directly underlie the Main Range Volcanics and are exposed as fine grained sandstone and shale, sometimes masked by shallow soils (Free, 1989). The Walloon Coal Measures consist of grey mudstone, siltstone, fine-grained labile sandstone, coal seams and minor limestone (Free, 1989).

If the basalts hold groundwater directly above the Walloon Coal Measures and some hydraulic connectivity exists, it is expected that groundwater would flow to the Walloon Coal Measures if they are depressurised. Available groundwater level data suggest that there is potential for groundwater flow from the basalts to the Walloon Coal Measures (see section 5 of this report). In addition, there is geochemical evidence that groundwater recharge is occurring through the basalts into the Walloon Coal Measures. While there is some variability in groundwater composition within the Walloon Coal Measures, there is an area within the Walloon Coal Measures that is geographically close to the Main Range Volcanics where the groundwater composition is geochemically similar to groundwater in the Main Range Volcanics.

Recharge to GAB formations via unconfined alluvial aquifers

A recent study by Herczeg and Love (2007) into conceptual models of recharge in the GAB concluded that recharge can occur where the GAB intake beds are exposed or are close to the land surface, or anywhere in the unconfined parts of the GAB. Recharge to GAB formations in central part of the Surat could only occur via vertical leakage in locations where the predominant vertical hydraulic gradient is downwards rather than upwards. There is still some debate about whether diffuse recharge through unconfined formations such as the Condamine alluvium has the potential to be transmitted downwards to the GAB formations (Hillier, 2010).

In order to assess the potential for focussed recharge to occur through stream beds (both within the Condamine alluvium and throughout the Surat Basin), it is important to consider previous studies into possible surface water – groundwater interactions in the Surat Basin.

Ransley et al. (2007) developed a new method to map potential hydraulic connection between groundwater and river systems and evaluated this mapping method in the Border Rivers catchment. This mapping method uses depth to water table as the basis for distinguishing connected and disconnected streams and combines this information with information about the hydraulic conductance of the geological material beneath the base of a river.

Parsons et al. (2008) conducted an assessment of surface-groundwater connectivity throughout the Murray Darling Basin. The connectivity mapping involved determining the direction and magnitude of groundwater flux to or from major rivers for a given point in time.

An example of the results of this study (for the Condamine and Balonne Rivers) is provided in Figure 3.

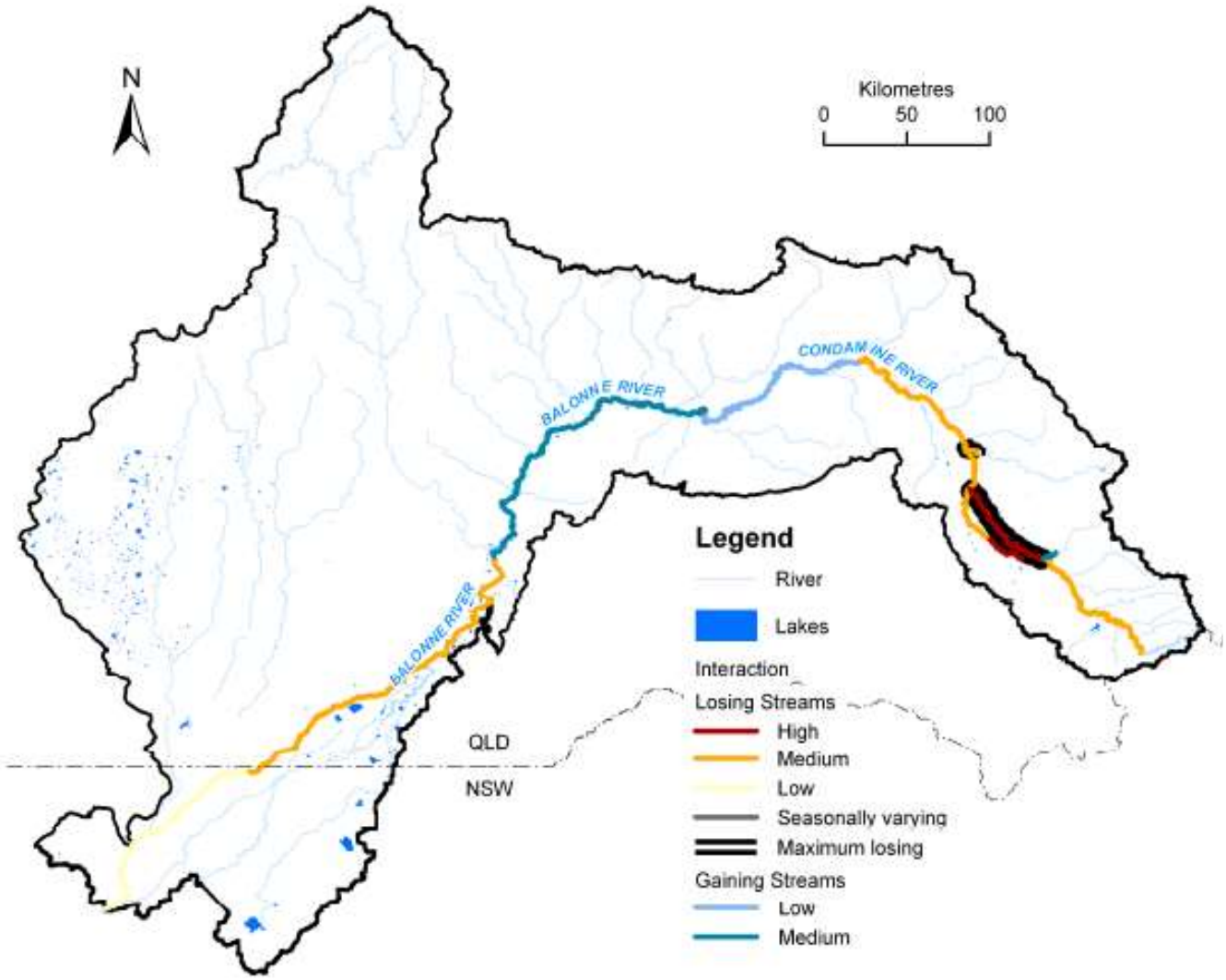

Figure 3 - Surface water / groundwater interactions: Condamine and Balonne Rivers (Parsons, Evans et al. 2008)

The Australasian Groundwater & Environmental Consultants Pty Ltd (2005) conducted a desktop assessment to determine if any of the surface water systems in the Great Artesian Basin might be receiving baseflow. The following spatial data were used in this assessment: the locations and extent of major surface water systems, GAB Intake Beds and GAB springs; the surface topography and groundwater bore data (including locations, aquifer assignments and water levels). The assessment highlighted a number of creeks (including within the

Kumbarilla Beds, Hutton Sandstone and Hooray Sandstone outcrops) that may potentially be receiving baseflow.

Groundwater Recharge in the Surat – previous estimates

Some of the recharge estimation methods identified in Section 2.1 have already been applied in the Surat Basin. These methods have included groundwater hydrograph analyses, groundwater chloride mass balance, unsaturated zone chloride mass balance and soil water balance modelling. A summary of the relevant studies is provided below and a summary of the recharge estimates produced is provided in Table 3 at the end of Section 2.

Groundwater Recharge in the GAB Intake Beds (Kellett, Ransley et al. 2003)

Kellett et al. (2003) calculated recharge rates within GAB intake beds along the eastern margin of the GAB, with the exception of the intake beds in far north Queensland. Measurements were focussed on the shallowest GAB aquifers that are intercepted by water bores, namely the Hooray and Hutton Sandstones (Kellett et al., 2003). Groundwater recharge was assessed using several methods including hydrograph analyses, chloride mass balance calculations, radiocarbon dating of groundwater and stable isotope analyses.

Based on the hydrograph for a shallow observation bore in one of the sandstone formations, the Mooga Sandstone, a recharge rate of 4-7 mm/year was calculated. The dynamic nature of hydrographs for some of the bores within the GAB intake beds indicated that streambed leakage to the underlying aquifers is an important recharge process (Kellett et al., 2003).

The chloride mass balance technique was used to determine the spatial distribution of long term average recharge rates within the GAB intake beds. The recharge rates ranged from <0.5 mm/year to >10 mm/year. The results of radiocarbon age dating of groundwater generally supported the chloride mass balance results as older waters were detected in locations with lower estimated recharge rates. From the results of stable isotope analyses for groundwater, it was determined that significant recharge only occurs following high rainfall events, i.e. >200 mm within a one month period. Kellett et al. (2003) also identified a number of locations where streams flow across GAB intake beds

Soil water balance modelling, soil chloride mass balance and lysimeter studies

Outside of the GAB intake beds, deep drainage estimates have been made using the PERFECT soil water balance model for the Queensland Murray Darling Basin (Yee Yet and Silburn, 2003) and the Fitzroy Basin (Owens et al., 2007). These two surface water basins cover more than 90% of the Surat and Bowen basins. In the Murray Darling Basin study, deep drainage estimates were summarised using look-up tables of drainage for a range of soil, land use and climate combinations. Estimates of average annual deep drainage for the Murray Darling Basin study ranged from 1 mm/year to 455 mm/year (Yee Yet and Silburn, 2003). The modelled deep drainage results for the Fitzroy Basin are shown in Figure 4. The estimates that fall within the recharge estimation project "study area" ranged from close to 0 mm/year to 139 mm/year.

Chloride mass balance estimates of deep drainage were also conducted in the Murray Darling Basin (Owens et al., 2004) and the Fitzroy Basin (Radford et al., 2009) to complement the modelling studies.

Researchers working in the Murray Darling Basin have found compelling evidence (based on transient chloride mass balance calculations) that deep drainage occurred despite heavy clay soils and a semi-arid climate (Silburn et al., 2011). Deep drainage since clearing was determined to be greater under cropping (mean 10 mm/year) than under pasture (mean 3 mm/year) or native vegetation (0.1-0.3 mm/year) (Silburn et al., 2011).

Starting in 2002, 27 non-weighing drainage barrel lysimeters were installed across nine irrigated cropping sites in the Northing Darling Basin of QLD and NSW to monitor deep drainage (Silburn and Montgomery, 2004). Deep drainage was measured under a range of cotton and grain crops. Sites in Queensland included St. George, Macalister and Dalby.

The deep drainage estimates from a range of studies conducted between 2004 and 2011 (including soil Cl mass balance, lysimetry and soil water balance studies) have been compiled in Figure 5. Details of the previous studies with their corresponding legends are in Table 2.

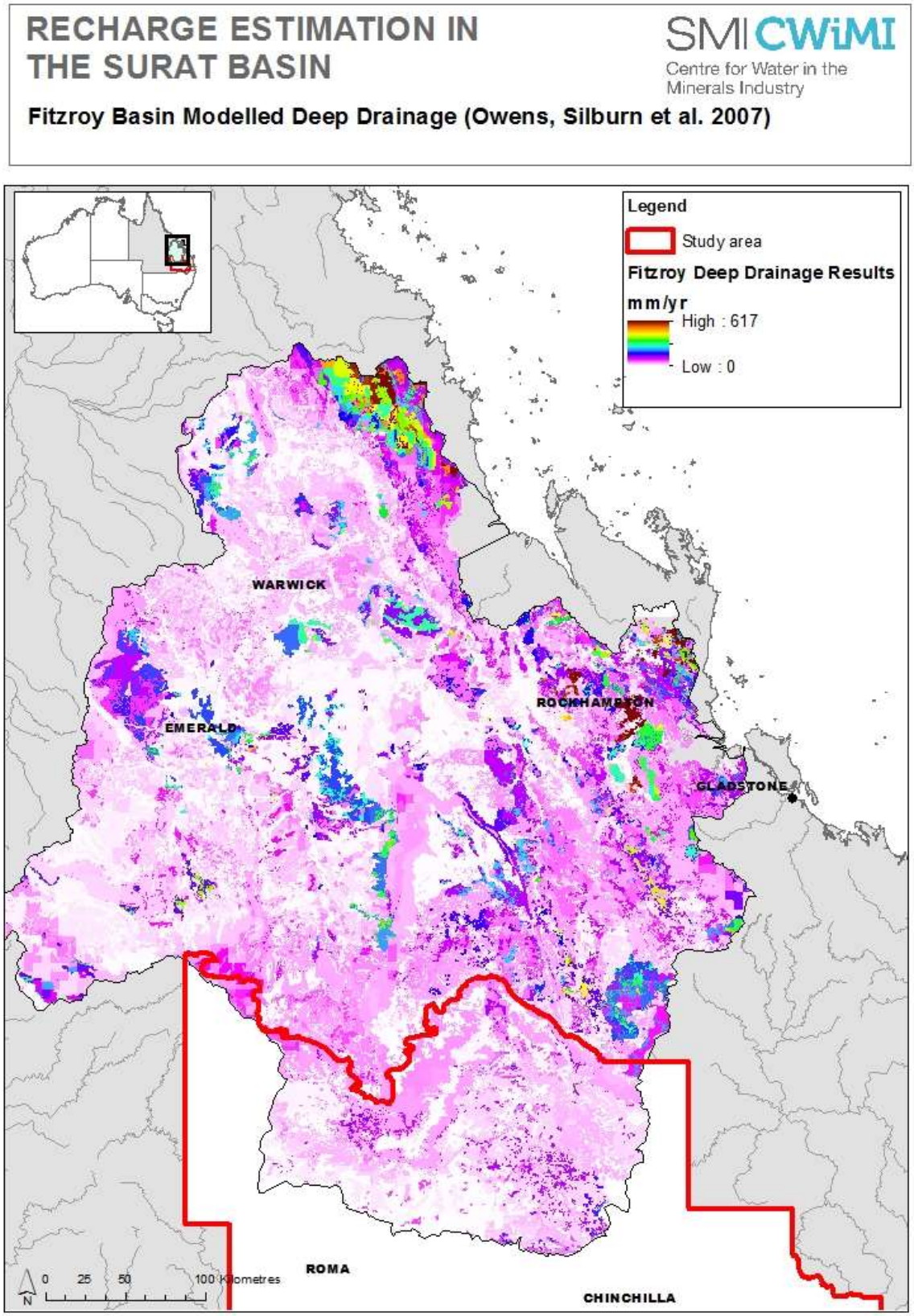

Figure 4 - Fitzroy Basin Modelled Deep Drainage

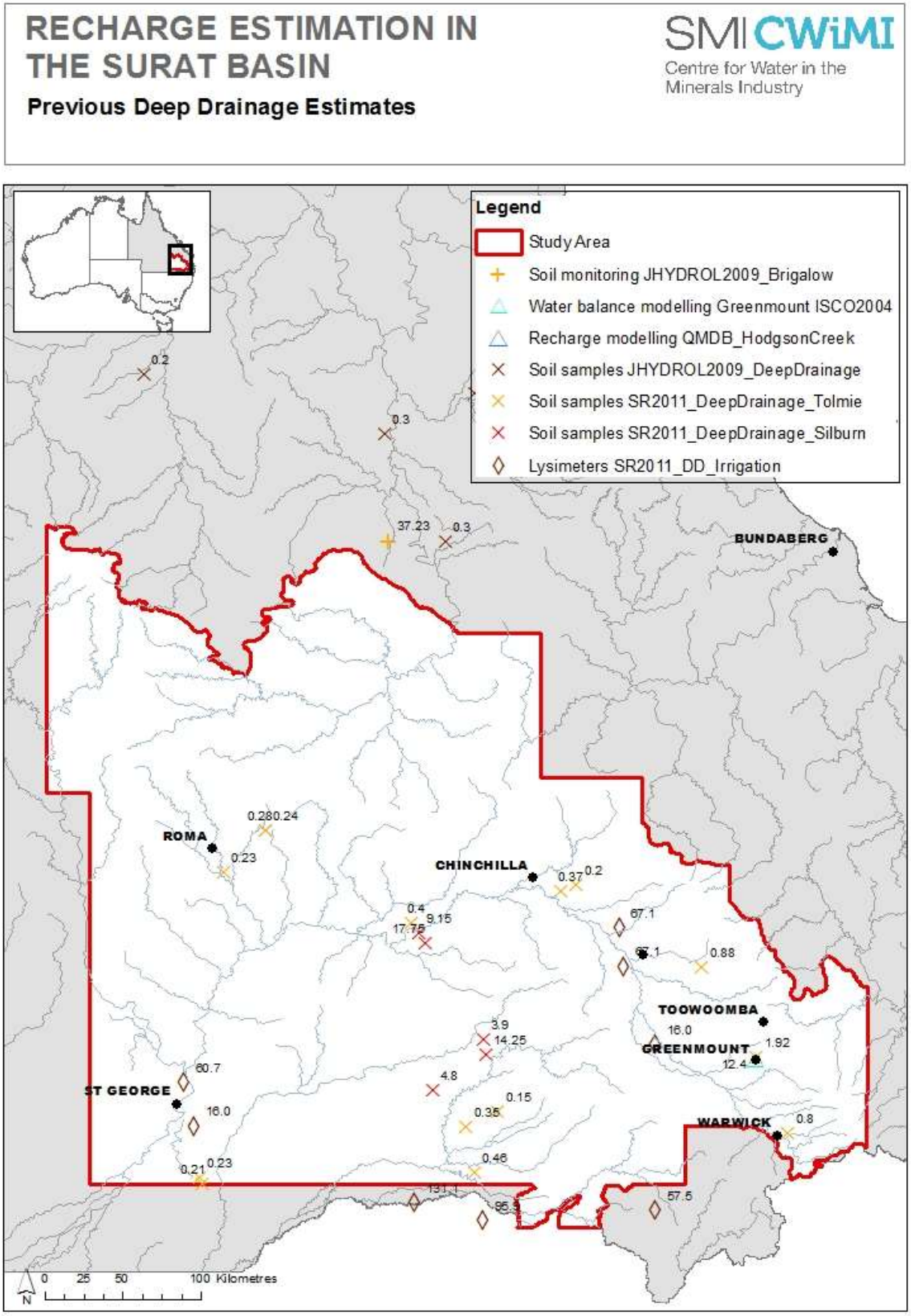

Figure 5 - Previous Deep Drainage Estimates (mm/yr)

Table 2 - Previous Deep Drainage Studies

Literature Reference	Method used	Corresponding legend
The Brigalow Catchment Study revisited: Effects of land development on deep drainage determined from non-steady chloride profiles (2009) D.M. Silburn, B.A. Cowie, C.M. Thornton	Research station. Three permanent monitoring sites (soil profile used for deep drainage and chloride mass analysis)	Soil monitoring JHYDROL 2009_Brigalow
Validating modelled deep drainage estimates for the Queensland Murray-darling basin (2004) J.S. Owens, P.E. Tolmie and D.M. Silburn	Water balance modelling at Greenmount. Runoff and soil erosion from previous model + use of PERFECT	Water balance modelling Greenmount ISCO2004
Soil chloride and deep drainage responses to land clearing for cropping at seven sites in central Queensland, northern Australia (2009) B.J. Radford, D.M. Silburn, B.A. Forster	Soil sampling. Sites previously used in the project ‘‘Sustainable Farming Systems for Central Queensland” in which data on soil characteristics was collected.	Soil Samples JHDROL2009_DeepDrainage
Deep drainage and soil salt loads in the Queensland Murray–Darling Basin using soil chloride: comparison of land uses (2011) P. E. Tolmie, D. M. Silburn, and A. J. W. Biggs	Composited or averaged Cl profiles were collected Previous Cl, pH and EC data. Use of past runoff studies and cropping-tillage studies.	Soil Samples SR2011_DeepDrainage_Tolmie
Deep drainage rates of Grey Vertosols depend on land use in semi-arid subtropical regions of Queensland, Australia (2011) D. M. Silburn,F, P. E. Tolmie, A. J. W. Biggs, J. P. M. Whish, and V. French	Hydraulic soil coring rig was used. Soil samples for chemical analysis and soil water content	Soil Samples SR2011_DeepDrainage_Silburn
Deep drainage through Vertosols in irrigated fields measured with drainage lysimeters (2011) T. A. Gunawardena, D. McGarry, J. B. Robinson, and D. M. Silburn	Three drainage lysimeters per site. One near each of the head and tail ditches, and one at the mid-point. All irrigated sites. Lysimeters still there but no longer monitored.	Lysimeter SR2011_DD_irrigation

Hodgson Creek, QMDB—salinity and recharge studies and 2CSalt modelling (2006) D.M. Silburn, J.S. Owens, S. Dutta, R.G. Cresswell, V. McNeil	Recharge modelling. NRMW bores and salinity study bores. Measure of stream flow, salinity and ionic chemistry.	Recharge modelling QMDB_HodgsonCreek

CSIRO – groundwater chloride mass balance

The chloride mass balance method has been used recently to estimate recharge across the intake beds as shown in Figure 6 (Ransley and Smerdon, 2012). This method was selected as it allows recharge to be estimated over larger spatial scales and provides a smoothing effect that dampens the annual variations in rainfall and chloride. Chloride concentrations in rainfall were obtained from a recently constructed map of chloride deposition for Australia (Davies and Crosbie, 2011) and chloride concentrations in groundwater were obtained from the recharge studies by Kellett et al. (2003) and Habermehl et al. (2009). There may be potential to apply this method to other geological formations, such as the Walloon Coal Measures. However, our ability to apply this method to specific areas is limited by the availability of groundwater chloride data and rainfall chloride data.

OGIA groundwater model

In the OGIA groundwater model, recharge was allowed to vary on a zonal basis during model calibration i.e. different recharge rates were applied to different formation outcrops throughout the Surat Basin (GHD, 2012). In most zones, recharge was allowed to vary between 1 and 30 mm/yr, based on maximum and minimum long-term average estimates reported by Kellett et al. (2003) and an initial value of 15 mm/year was assumed. The assumed recharge rates for aquifers were typically the same as for the aquitards.

However, it was expected that a significant proportion of the “recharge” assigned to aquitard units would be rejected due to the limited capacity of these units to transmit water, hence the “net recharge” is close to zero. The “net recharge” for each geological formation is equal to water table recharge plus inflow from adjacent formations minus discharge to local shallow groundwater systems (GHD, 2012). The total “net recharge” was estimated to be 125,267 ML/year (GHD, 2012). To provide some context to this figure, groundwater extractions for agriculture, industry, urban, stock and domestic uses were estimated to be 215,000 ML/year and over the life of the CSG industry, water extraction was predicted to average approximately 95,000 ML/year (QWC, 2012b).

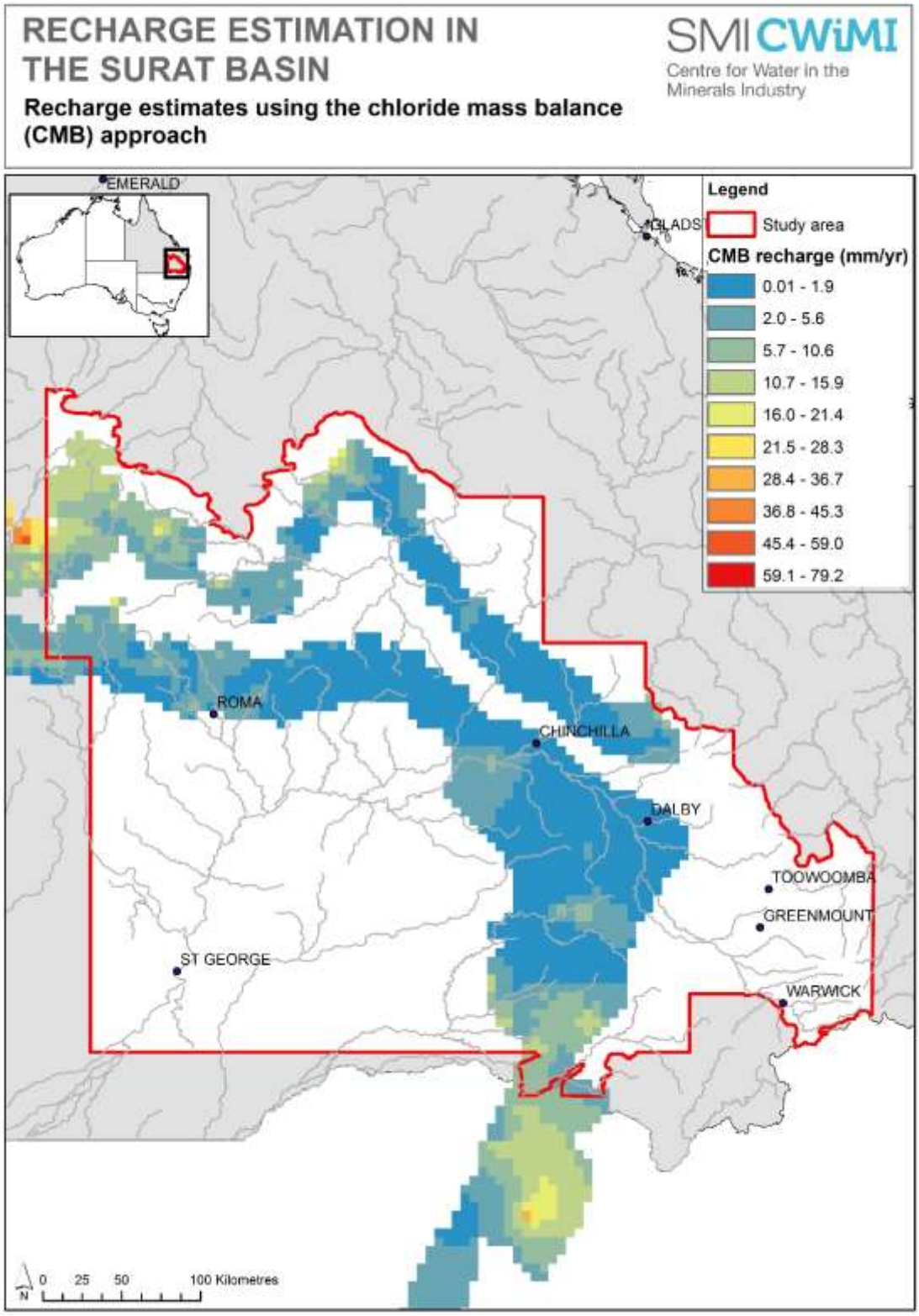

Figure 6 - Recharge estimates using the chloride mass balance method (Ransley and Smerdon, 2012)

RECHARGE ESTIMATION IN THE SURAT BASIN
Recharge estimates using the chloride mass balance (CMB) approach
SMI CWiMI
Centre for Water in the Minerals Industry

Table 3 - Previous recharge estimates

Method Used	Spatial Scale	Time Period	Estimated Recharge Rate (mm/year)	Reference
Groundwater Hydrograph Analysis	Single bore in the Mooga Sandstone	1993-2001	4-7	(Kellett et al., 2003)
Groundwater Chloride Mass Balance	GAB intake beds	N/A	<0.5 - >10	(Kellett et al., 2003)
PERFECT Model	Queensland Murray Darling Basin	1900-2001	1-455	(Yee Yet and Silburn, 2003)
PERFECT Model	Fitzroy Basin	1900-2005	0-139*	(Owens et al., 2007)
PERFECT Model	Greenmount Site	1977-1996	12	(Owens et al., 2004)
Soil Chloride Mass Balance	Greenmount Site	1977-1996	14	(Tolmie et al., 2004)
Soil Chloride Mass Balance	13 cropped sites in the Queensland Murray Darling Basin	1985-2001	2-16	(Tolmie et al., 2004)
Soil Chloride Mass Balance	5 paired sites (pasture/annual cropping) in southern Queensland	N/A	0.1-25	(Silburn et al., 2011)
Lysimeters	7 irrigated sites in the Queensland Murray Darling Basin	2002-2009	0-235	(Gunawardena et al., 2011)
Groundwater Chloride Mass Balance	GAB intake beds	N/A	0-79	(Ransley and Smerdon, 2012)

OGIA groundwater model – calibrated "net recharge"	Surat CMA	N/A	0-5.2	(GHD, 2012)

*only recharge estimates for the portion of the Fitzroy Basin that coincides with the "Recharge Estimation Project Study Area" are reported here

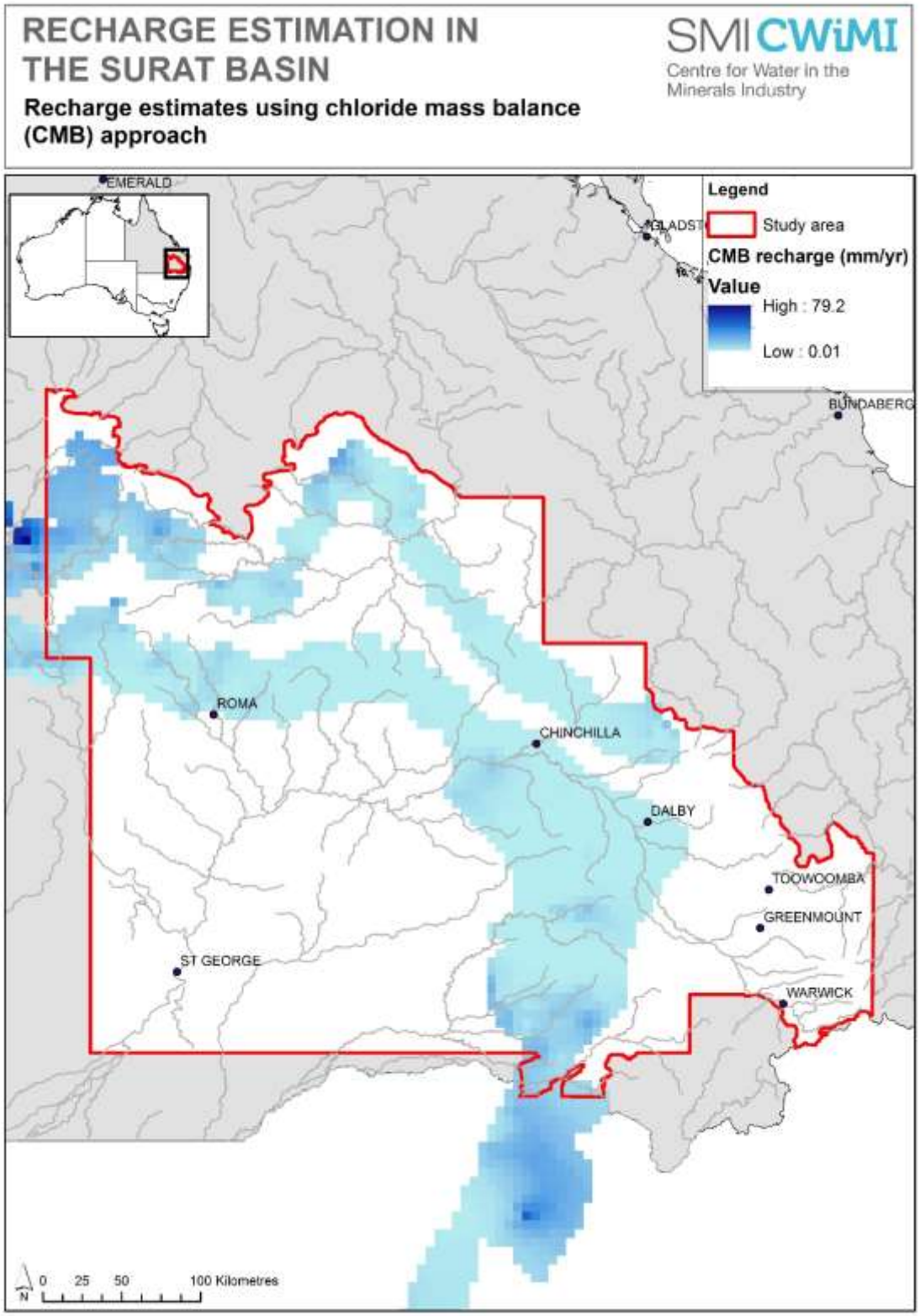
RECHARGE ESTIMATION IN THE SURAT BASIN
Recharge estimates using chloride mass balance (CMB) approach
SMI CWiMI
Centre for Water in the Minerals Industry
EMERALD
Legend
Study area
CMB recharge (mm/yr)
Value
High : 79.2
Low : 0.01
BUNDABERG
ROMA
CHINCHILLA
DALBY
TOOWOOMBA
GREENMOUNT
ST GEORGE
WARWICK
0 25 50 100 Kilometres
N

Recharge Estimation Using Analysis of Available Data - Introduction

The boundary for the recharge estimation project was derived by extending the Surat "Cumulative Management Area" boundary to include the "primary recharge areas" identified by OGIA in their underground water impact report (QWC, 2012b) . The extended boundary is shown in Figure 7. The data analyses that are described within the remainder of this report include only data from within this "study area" boundary. Analysis of existing data was used to improve our understanding of recharge processes and develop refined recharge estimates.

The methods used were:

1. Re-analysis of previous deep drainage results
2. Analysis of groundwater potentiometric surfaces
3. Analysis of groundwater hydrographs
4. Analysis of remote sensing data, principally the outputs of CSIRO's Australian Water Availability Project
5. Analysis of surface water hydrographs

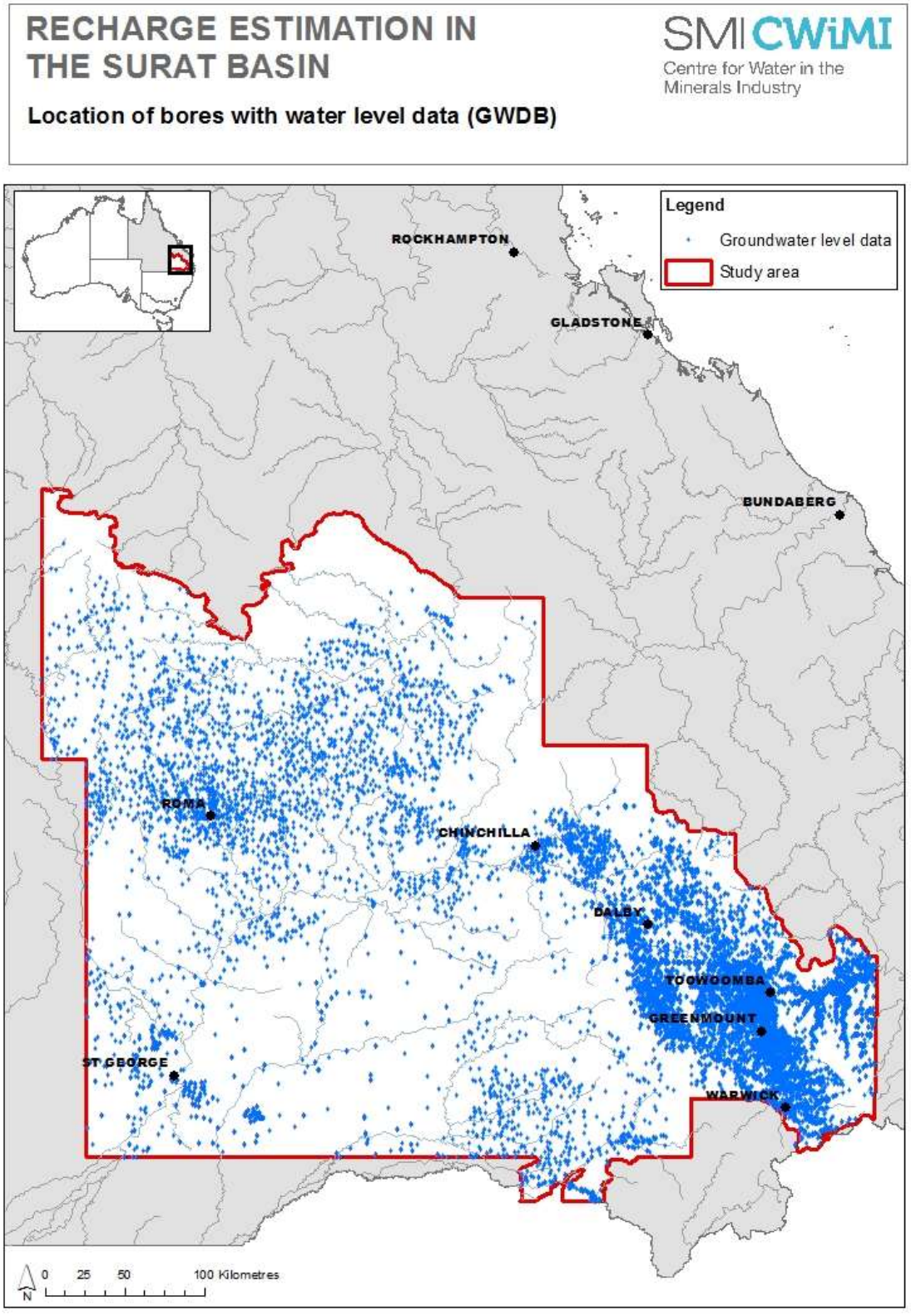

Figure 7 - Location of bores with water level data

Re-Analysis of Previous Deep Drainage Results

Deep drainage estimates under a range of land uses in the Queensland Murray-Darling Basin (QMDB) using water balance modelling, (Yee Yet and Silburn, 2003) is a study providing estimates of drainage for a range of land uses, soils and locations in the QMDB (which QMDB covers a large proportion of the recharge estimation study). Using soil moisture accounting models GRASP and PERFECT, the study produced tables of deep drainage estimates but did not map these results. Developing recharge maps using the tabulated data will act as a baseline to compare alternative estimates.

Two types of pastures were modelled using GRASP: native pastures and improved pastures (Yee Yet and Silburn, 2003). The PERFECT model was used to simulate the following cropping systems (Yee Yet and Silburn, 2003):

1. "winter cropping" (wheat-fallow-wheat rotation)
2. "summer cropping" (sorghum-fallow-sorghum rotation)
3. "opportunity cropping" (automatic planting dates for wheat and sorghum rotations)
4. "irrigated cropping" (irrigated cotton, where 'perfect irrigation' i.e. no drainage during irrigation is assumed).

Assumptions

During the development of the maps, the following assumptions were made:

1. Simplifications were used to translate available qualitative land use descriptions to the land use categories used in the look-up tables (see Table 4)
1. Due to the lack of detailed soils mapping, an average value of deep drainage per land use category, soil type and location was deemed adequate
2. As data were location specific, "drainage zones" were produced using modelled locations and climate data.

Methodology

The three data sets used to translate the tables to maps were:

1. The Atlas of Australian Soils by CSIRO's Australian Soil Resource Information System (ASRIS) (Figure 8)
2. Land use mapping – Queensland 1999 by the Department of Natural Resources and Mines (DNRM) (Figure 9) and

3. The results from "*Deep drainage estimates under a range of land uses in the QMDB using water balance modelling"* (Yee Yet and Silburn, 2003) (Appendix 2).

Several land use and soils descriptions available from the above sources were not consistent with the descriptions used in the deep drainage look-up tables. The DNRM land use data were reformatted into three of the land use categories used by Yee Yet and Silburn (2003). These were: Woodlands, Buffel Grass Pasture and Irrigated Summer Cropping. Table 4 shows the qualitative data conversion between DNRM land use mapping and land use categories used by Yee Yet and Silburn (2003).

Table 4 - Summary of Qualitative land use data reformatting

Original categories used by Yee Yet and Silburn (2003)	Corresponding categories on the DNRM maps
Channel/aqueduct	<void>*
Cropping	Irrigated Summer Cropping
Grazing natural vegetation	Buffel Grass Pasture
Intensive animal production	Buffel Grass Pasture
Intensive horticulture	Irrigated Summer Cropping
Irrigated cropping	Irrigated Summer Cropping
Irrigated perennial horticulture	Irrigated Summer Cropping
Irrigated plantation forestry	Woodlands
Irrigated seasonal horticulture	Irrigated Summer Cropping
Lake	<void>
Manufacturing and industrial	<void>
Marsh/wetland	<void>
Mining	<void>
Nature conservation	Woodlands
Other minimal Use	<void>

Perennial horticulture	Irrigated Summer Cropping
Plantation forestry	Woodlands
Production forestry	Woodlands
Reservoir/dam	<void>
Residential	<void>
River	<void>
Seasonal horticulture	Irrigated Summer Cropping

*<void> represents areas of the land use map which were excluded when assigning deep drainage results spatially.

For soils, the CSIRO data allow for identification of general soil types using the Australian Soil Classification (ASC) but the level of soil classification did not include soil colour. In contrast, Yee Yet and Silburn (2003) simulated deep drainage for a specific soil type including colour e.g. 'black Dermosol'. Because of the lack of detail in the CSIRO soils maps, the Yee Yet and Silburn (2003) data were averaged using general ASC soil types, e.g. the deep drainage rates for black, brown and red Dermosols were averaged to estimate the deep drainage rate for Dermosols. The tables provided in Appendix 2 are the deep drainage values reported by Yee Yet and Silburn (2003) for specific locations, land use types and soil types.

Lastly, to assign the deep drainage value to a specific area, the 35 locations modelled by Yee Yet and Silburn (2003) were used to produce "drainage zones". The PERFECT modelling generally relied on local climate data for each modelled location so the "drainage zones" were designed to represent an area around each modelled location while taking into account spatial trends in climate. The sizes of these "drainage zones" were therefore driven by the spacing between modelled locations and information on the spatial variability of rainfall throughout the QMDB. The zones can be seen in Figure 10. It is noted that the creation of these "drainage zones" was based on judgement regarding the translation shown in Table 3 so a degree of error is likely to be introduced using this approach. In particular, to improve the conversion between the look-up tables and the new maps, it is recommended that maps of more specific soil types are developed.

Finally, these drainage zones, combined with land use and soils mapping were used to assign the estimated deep drainage rates spatially.

Results

Figure 11 shows the long-term average deep drainage estimates in the QMDB part of the Surat Cumulative study area derived from the Yee Yet and Silburn (2003) look-up tables. The range of long-term average drainage values varies from 0 mm/yr to 455 mm/yr.

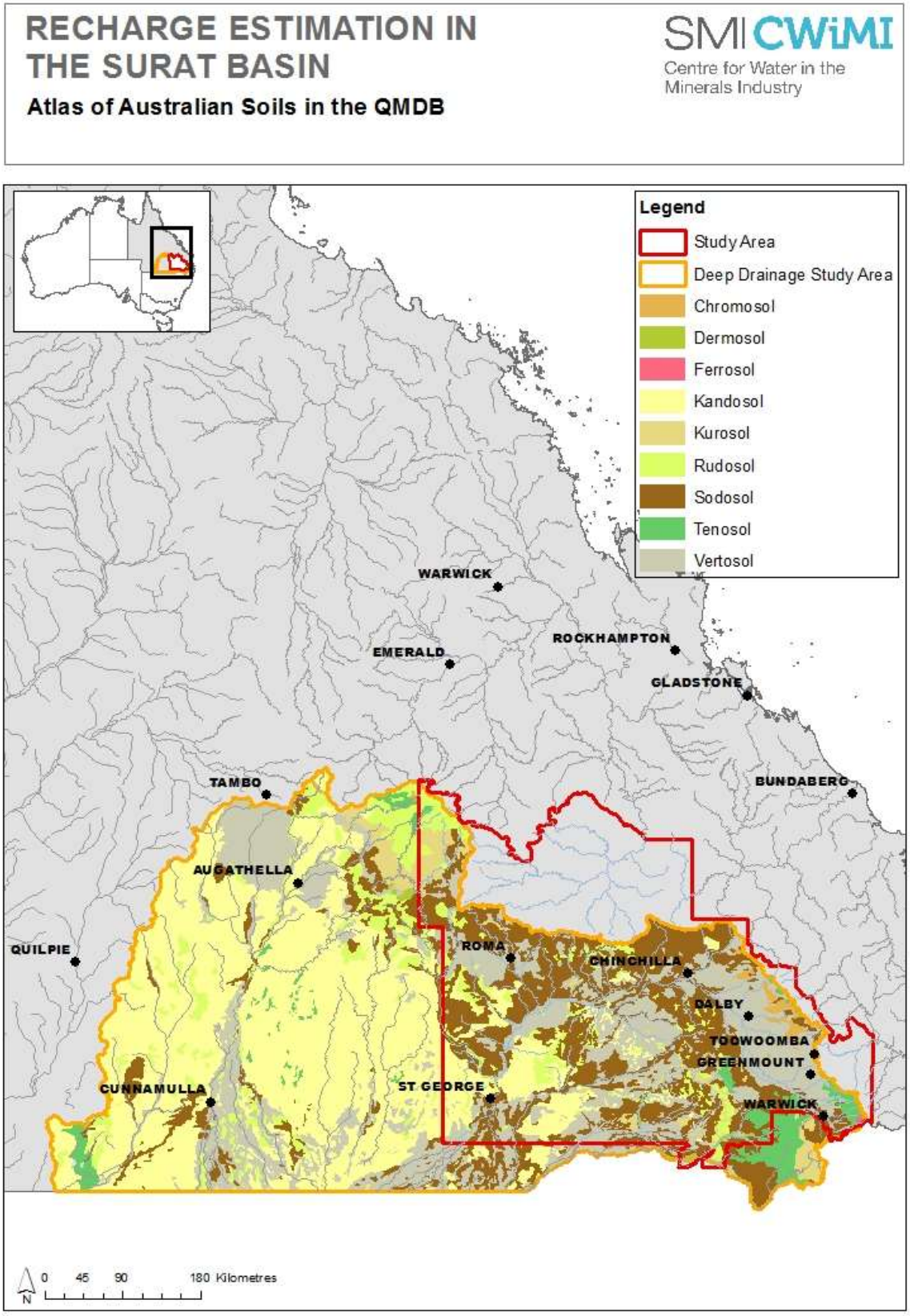

Figure 8 - Atlas of Australian Soils

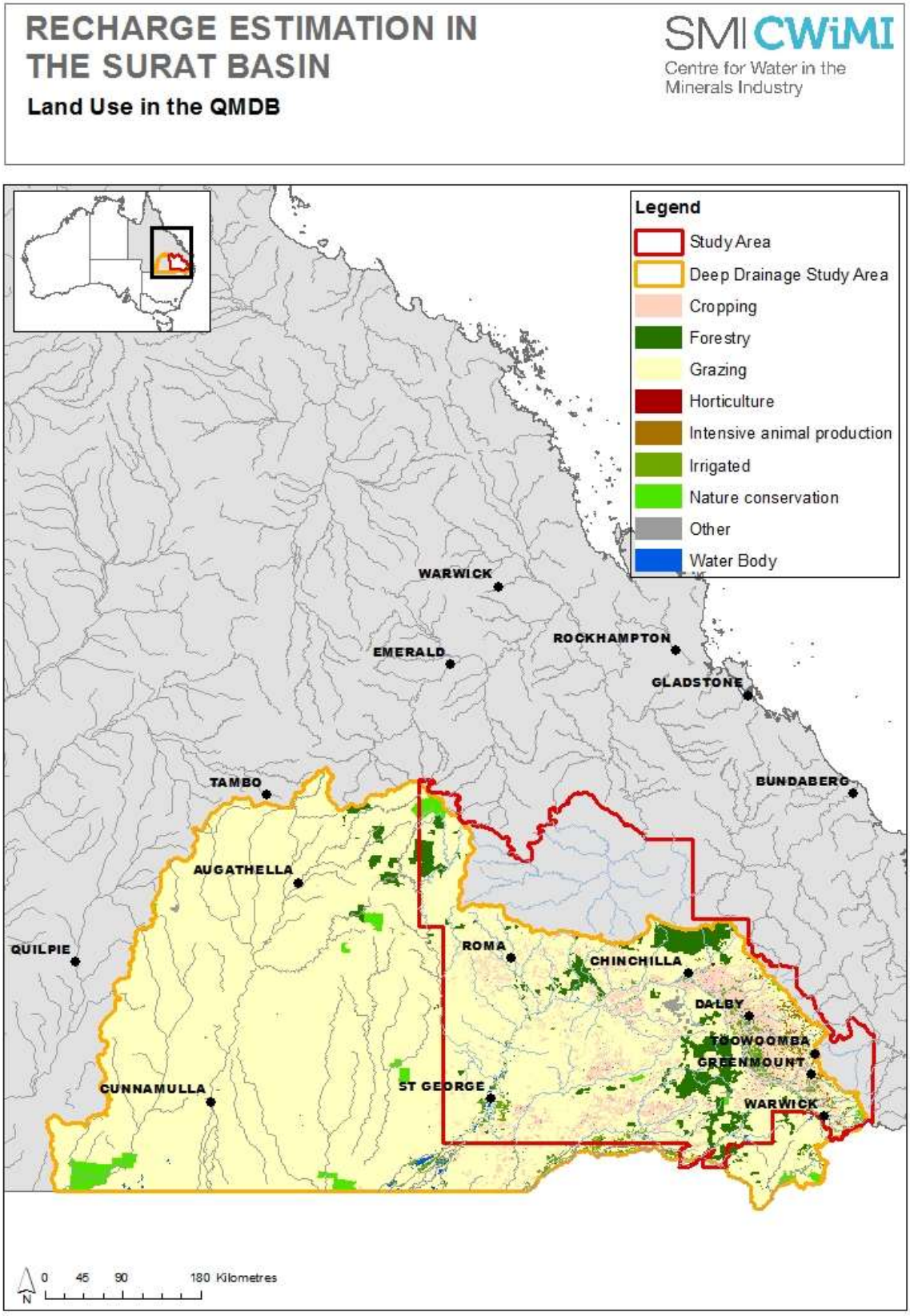

Figure 9 - Land Use Classifications in the QMDB

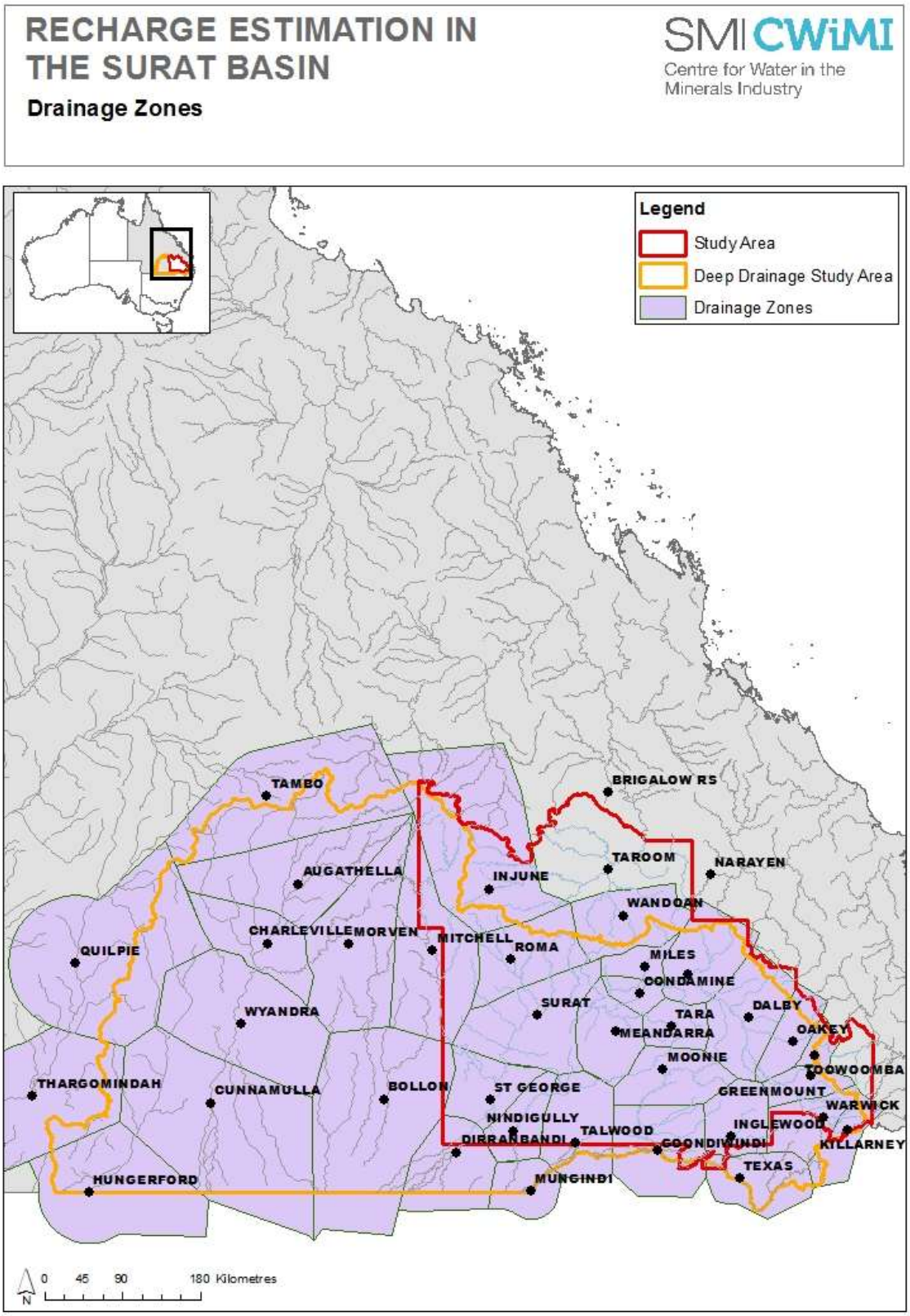

Figure 10 – Modelled Locations and Deep Drainage Zones

RECHARGE ESTIMATION IN THE SURAT BASIN

Deep Drainage Estimates in the Surat Basin

SMI CWiMI
Centre for Water in the Minerals Industry

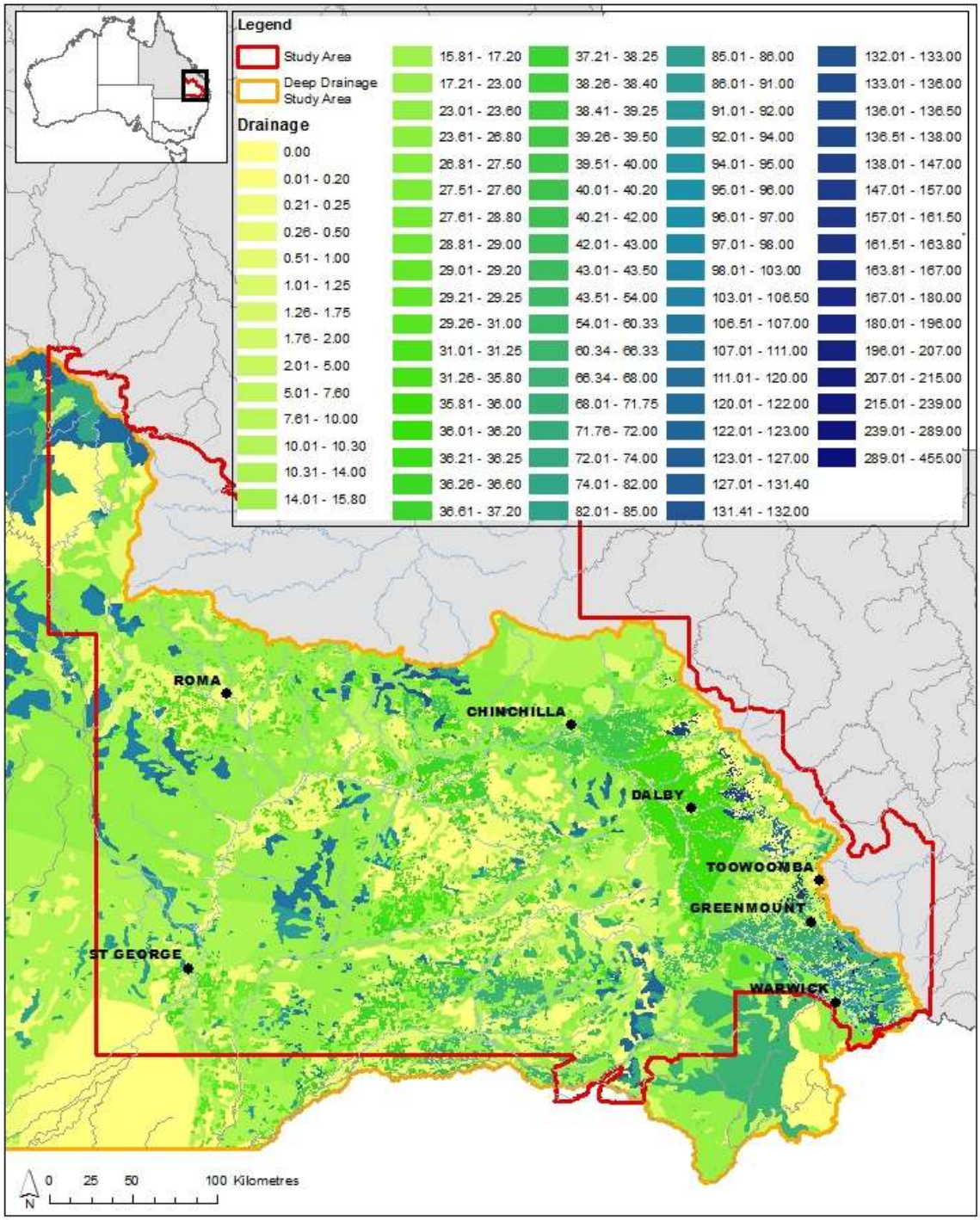

Figure 11 - Deep Drainage Results (mm/year)

Analysis of Groundwater Potentiometric Surfaces

Introduction

Groundwater potentiometric surfaces provide information on regional flow patterns within hydrogeologic systems, and can be used to identify potential recharge areas. Comparison of different groundwater surfaces can also provide information on the potential for groundwater flow between aquifers if they are vertically connected. This chapter investigates regional groundwater flow patterns of a number of younger geologic formations within the Surat CMA. Due to the major limitations of currently available datasets identified during this study, this chapter primarily demonstrates an approach for mapping regional groundwater flow patterns. It also provides a critical analysis of the quantity and quality of available water level data and its limitations. Preliminary results on groundwater flow patterns are presented, however these potentiometric surfaces have low reliability primarily due to data quality.

This chapter is made up of five further sections. A literature review on the current understanding of regional flow patterns within the Great Artesian Basin and Surat Basin is provided in Section 0. Section 0 and Section 0 discuss the various data sources that were used in producing groundwater potentiometric surfaces, the applied data processing techniques and data availability. Section 0 provides information on how groundwater surfaces were developed for the different geologic formations of the Surat Basin, the actual groundwater surfaces and also a discussion on the assumptions and limitations of the data and applied methods. Lastly, a conclusion and future recommendations are provided in Section 0.

Current Understanding of Groundwater Surfaces and Water Movement in the Great Artesian and Surat Basins

At the scale of the Great Artesian Basin, the dominant directions of groundwater flow are towards the southern, southwestern, western and northern margins (Habermehl (2002), Figure 12). Habermehl (1980) found potentiometric water levels in the confined portions of the Lower Cretaceous-Jurassic aquifers varied from approximately 40 m AHD in the southwest up to 400 m AHD in the east in the 1970s. Similar work has been carried out on the same aquifer

(e.g. Audibert, 1976; Habermehl, 1980; Radke et al., 2000; Welsh, 2000) with a thorough review available in Smerdon et al. (2012b). Most recently groundwater

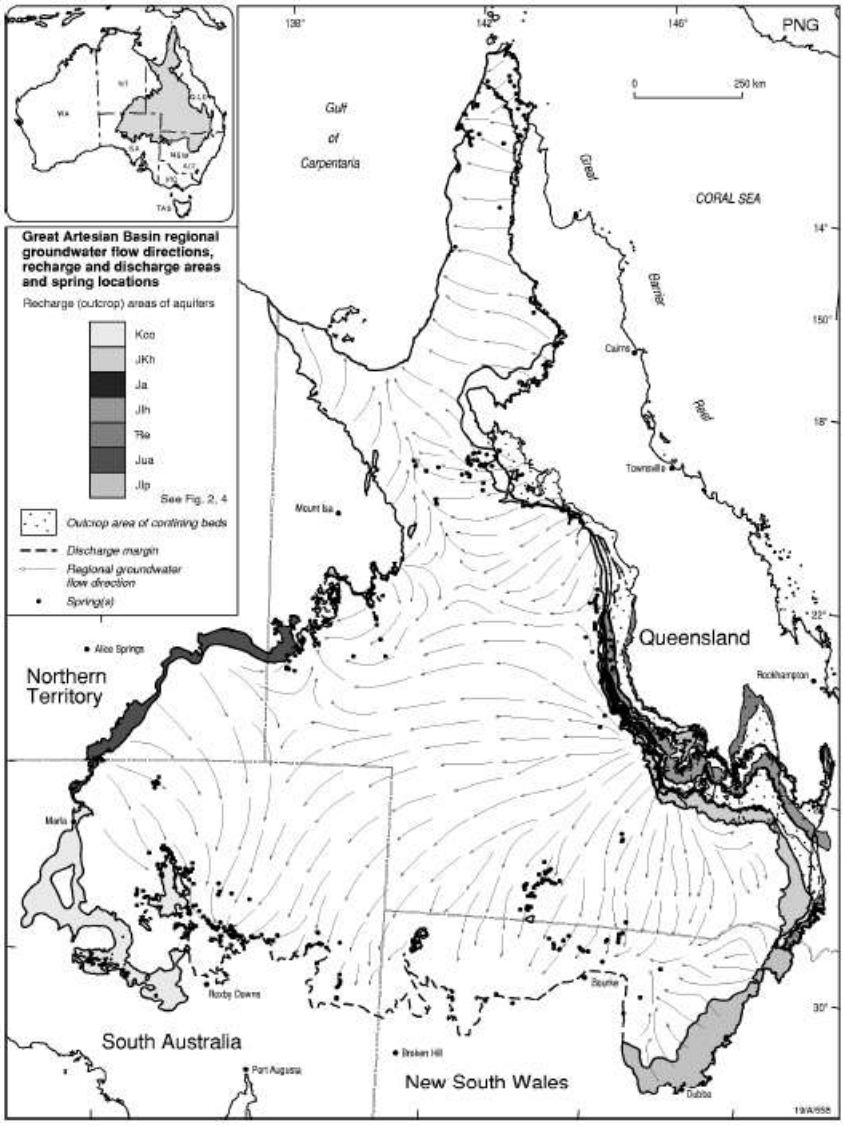

Figure 12 - Groundwater flow directions in the Cadna-owie Formation - Hooray Sandstone aquifers (from Habermehl (2002))

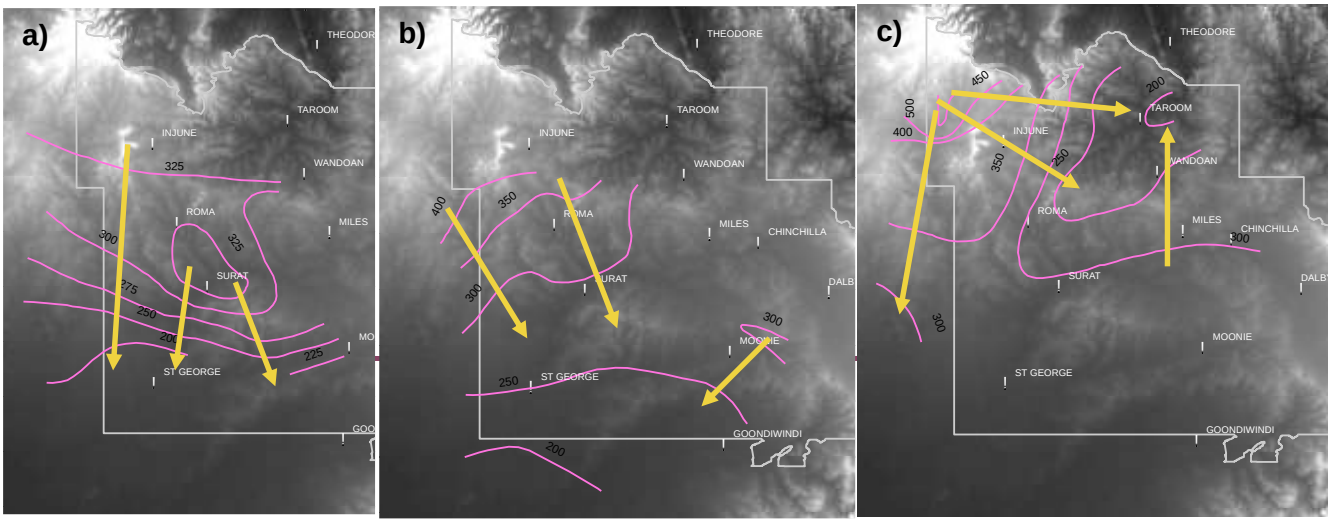

Figure 13 - Groundwater flow directions of the a) Mooga Sandstone, b) Gubberamunda Sandstone, and c) Hutton Sandstone (after Quarantotto, 1989)

surfaces of the Cadna-owie Formation – Hooray Sandstone have been produced at 20 year intervals, from 1900 to 2010, by Smerdon et al. (2012b).

Within the Surat Basin, located in the southeastern part of the Great Artesian Basin, the dominant flow directions in the Cadna-owie Hooray Sandstone are south and west (Smerdon et al., 2012b). Quarantotto (1989) investigated the groundwater surfaces of similar aquifers, however interpreted them as discrete units rather than investigating them as a single lumped system. Groundwater flow within the Gubberamunda Sandstone was found to be centripetal from the northwestern and eastern margins, while flow in the Mooga Sandstone was predominantly southerly (Figure 13). Flow directions within the Hutton Sandstone exhibited more similarity to the flow lines of the Cadna-owie Hooray Sandstone (Figure 12; Figure 13), with groundwater flow predominantly from northwest to south and east, with a secondary northerly component also evident. A similar trend was reported by Hodgkinson et al. (2010) and Australia Pacific LNG (2014) that further highlighted the significant components of flow in the north and eastern directions (Figure 14).

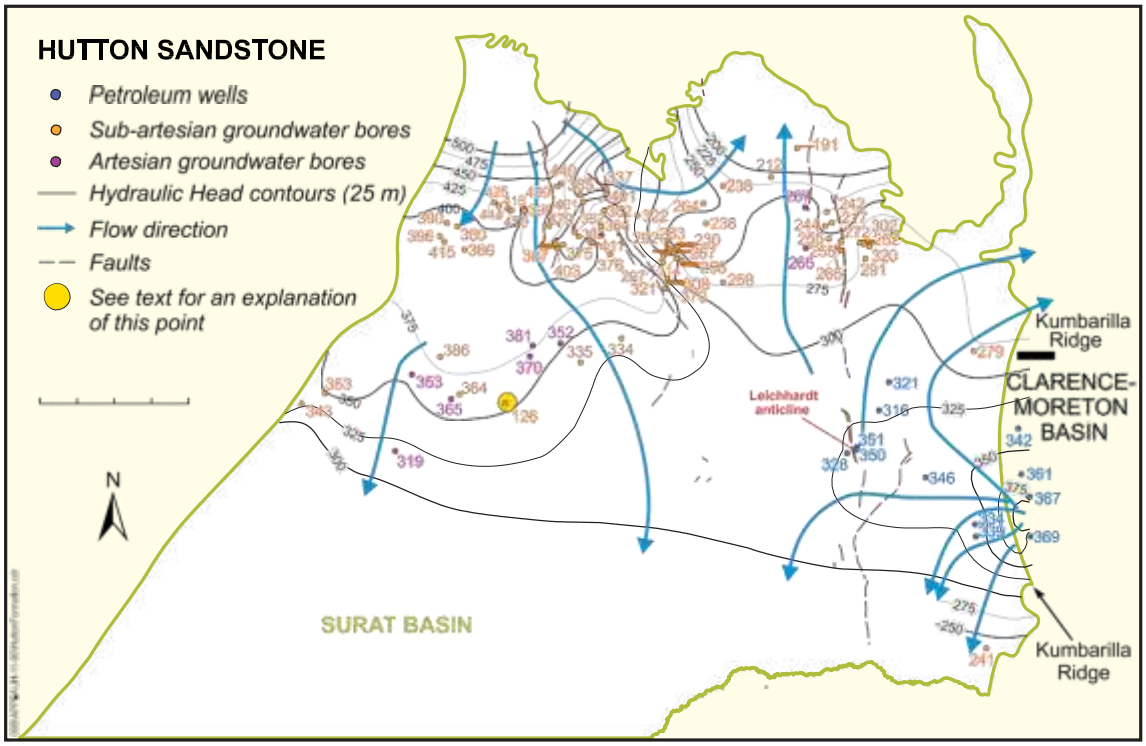

Figure 14 – Groundwater contours and flow directions for the Hutton Sandstone from 1960 to 1970 (from Hodgkinson et al. (2010))

Information on the groundwater surfaces of the other formations of interest from the Cretaceous and Jurassic age is limited to the reports by Golder Associates (2009), Schlumberger Water Services (2011), WorleyParsons (2012) and most recently Australia Pacific LNG (2014). Groundwater flow in the Kumbarilla Beds is predominantly westwards, radiating from a central highpoint of approximately 425 m (Schlumberger Water Services, 2011).

In the Walloon Coal Measures a general trend of water flowing westwards is present in both the Golder Associates (2009) and Schlumberger Water Services (2011) reports, however there is substantial dissimilarity between the two surfaces at a finer scale. Conversely, WorleyParsons (2012) and Australia Pacific LNG (2014) reported an easterly and northerly trend in groundwater flow in the northern parts of the basin around Taroom and Injune (Figure 15). Groundwater flows from the northwest to the south, southeast and east in the Springbok Sandstone, with groundwater levels varying from approximately 200 to 450 m AHD (Australia Pacific LNG, 2014; Golder Associates, 2009; Schlumberger Water Services, 2011).

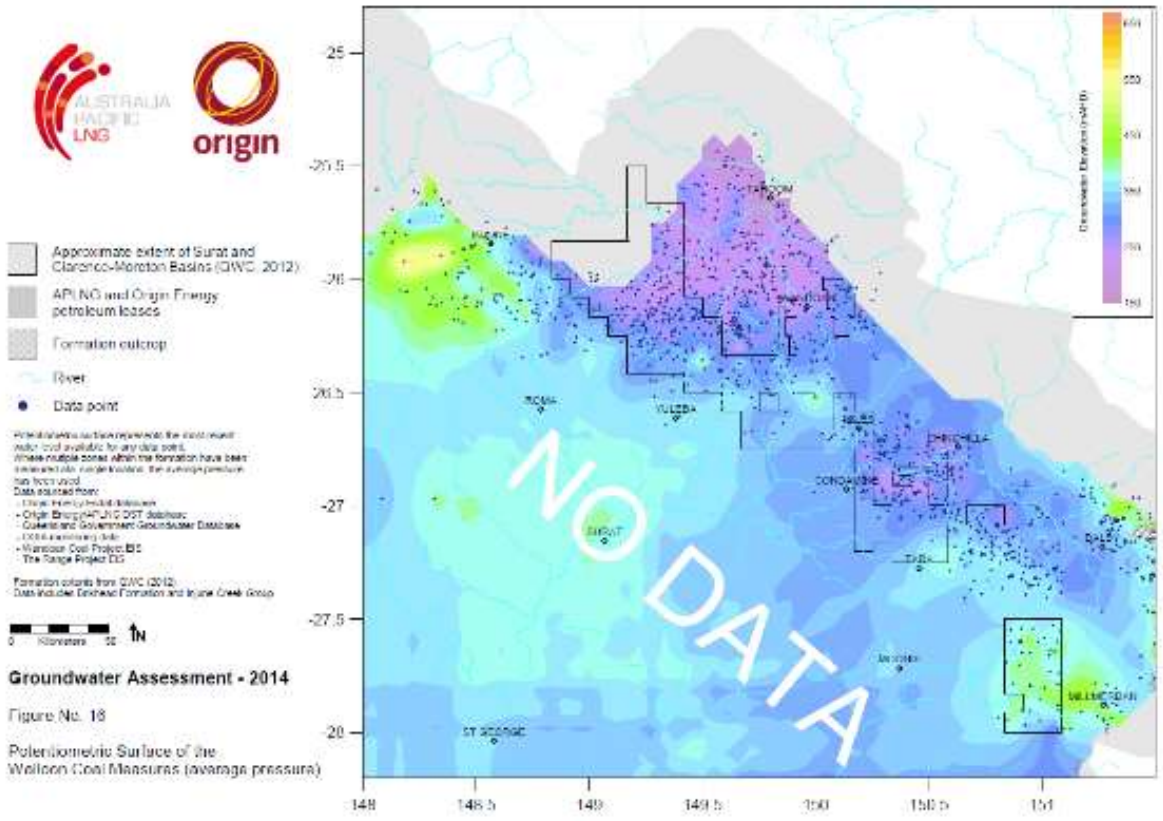

Figure 15 - Potentiometric surface of the Walloon Coal Measures (Source: Australia Pacific LNG 2014)

No information on the groundwater surface of the Main Range Volcanics was found. However, some further information on groundwater surfaces of other geologic formations in the Surat Basin was available. This predominantly focused on the Precipice Sandstone (Hitchon and Hays, 1971; Hodgkinson et al., 2010; Quarantotto, 1989) with less information available on the Evergreen Formation (Hodgkinson et al., 2010). However, this information was not included in this report as it did not address the target geologic formations.

Groundwater in the Condamine River Alluvium flows in a predominantly SE to NW direction, following the same general direction of the Condamine River (Dafny and Silburn, 2014). A secondary trend is present in a NE to SW direction, with water flowing from the neighbouring aquifers to the east. Hydraulic sinks are present in the central-southerly portions of the alluvium (east of the river), as a result of heavy development of the alluvium for agricultural purposes. A generally similar trend of groundwater flow in a SE to NW direction with hydraulic sinks was found by Schlumberger Water Services (2011). It should be noted that even though the alluvium is generally conceptualised as one continuous aquifer, in some localised areas there is evidence of perched aquifers where vertical hydraulic gradients are present (Dafny and Silburn, 2014). However, the alluvium does act as a single system on the whole (QWC, 2012b) .

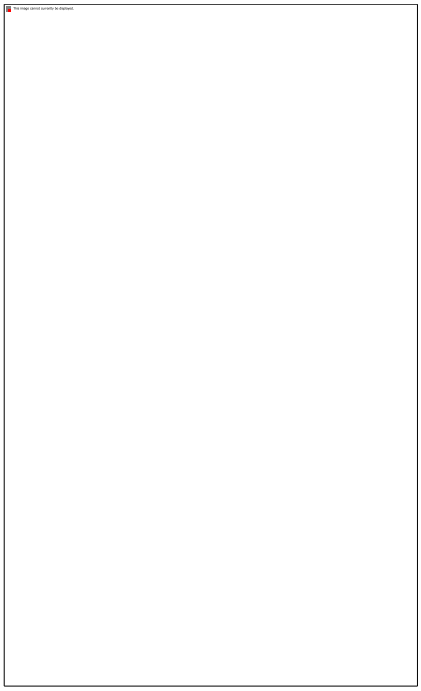

Figure 16 - Groundwater surface of the Condamine River Alluvium in 2011 (from Dafny and Silburn 2014)

Data Availability and Data Processing Methods

Introduction to Data Sources

This Section presents a detailed description of the data that were used to develop the groundwater level dataset into groundwater surfaces, and it also details the data processing and quality control methods that were implemented.

All groundwater level data were obtained from:

1. Queensland Groundwater Database (up to 16 June 2014) (QLD DNRM, 2014b)
2. Queensland Water Monitoring Data Portal (up to 16 June 2014) (QLD DNRM, 2014d)
3. Variety of references on the springs of the Great Artesian Basin and Surat Basin

Processing and Quality Control of Groundwater Database and Water Monitoring Data Portal

Preliminary Bore Selection Technique

The Queensland Groundwater Database (GWDB) was interrogated and a preliminary subset of data was identified based on the following:

1. Spatial extent – did the groundwater bore fall within the general vicinity of the study area?
2. Did the groundwater bore have any water level readings recorded within the 'WATER_LEVELS' attribute table?
3. Did the groundwater bore have any aquifer/stratigraphy record with the 'AQUIFER' and 'STRATIGRAPHY' attribute tables?
4. Did the groundwater bore have casing attributes which were indicative of where water would be entering the pipe? Only groundwater bores with a Material Description of 'OPEN', 'PERF', 'ENDD' and 'SCRN' in the 'CASING' attribute table were retained. This information would be used with aquifer and stratigraphy information to associate source aquifer(s) to the bores with larger confidence.

Aquifer and Stratigraphy Pipe Association

A source aquifer was associated to a groundwater pipe primarily based on the GWDB 'AQUIFER' attribute table. Data from the 'STRATIGRAPHY' table were used to supplement information on the rare occasions when a bore had no entry in the AQUIFER table. The

following procedure was applied in associating a source aquifer to each of the groundwater pipes:

1. A pipe was automatically associated to a source aquifer if only a single aquifer was listed in the AQUIFER table for that RN;
2. If multiple aquifers were listed in the AQUIFER table for a specific RN, depth information of the aquifer layers and pipe casing were cross-checked to identify the accurate source aquifer(s);
3. A pipe was included in the final dataset if it only had a single aquifer as a water source.

Once a final dataset of source aquifers to pipes was established, a quality control procedure was implemented to check and correct the source aquifer nomenclature. This was necessary to allow easy interrogation of the dataset, as there were general errors in data entry and also discrepancies in the naming of aquifers.

Water Level Calculation

The majority of the water level data was obtained from the GWDB and this was supplemented with additional and generally more recent data obtained from the Queensland Water Monitoring Portal. Water level depth data from these databases were converted to water level elevations with elevation data obtained from the ELEVATION table in the GWDB and also from a 9 Second Digitial Elevation Model (DEM) of Australia (AUSLIG, 2001). Elevation data were used from the ELEVATION table only in circumstances where there was confidence in the data quality, namely the 'Datum' attribute had to be AHD (Australian Height Datum) and the 'Precision' attribute was SVY (Surveyed). In all other circumstances elevations were extracted from a DEM. On occasion, the reference 'Measurement Point' between water level depths and elevations did not match. Accordingly, this reference was corrected by 0.5 m – the 'common' distance separating the top of a pipe from the natural elevation point. Lastly, a subset of the data was made that only included the target geologic formations in this study, namely the Condamine River Alluvium, Main Range Volcanics, Walloon Coal Measures, Kumbarilla Beds, Hutton, Springbok, Mooga and Gubberamunda Sandstones. Aquifers attributed as 'Basalts' that fell within the extent of the Main Range Volcanics were also taken as a part of the Main Range Volcanics.

Hydrograph Quality Control

All water level data taken for the geologic formations targeted in this study went through a quality control process. First, water level data classified as 'dry' in the GWDB were removed from the record. In addition, time series of the data records were visually inspected for each pipe, and portions that had clear errors in data logging were discarded (e.g. portions of time series where all readings were identical). The time series were also assessed for clear outliers which were discarded. Some of the data obtained from the Qld Water Monitoring Portal that were used to supplement the GWDB differed substantially from the rest of the time series for that pipe. In all cases this data had no quality assurance from the Queensland Water Monitoring Portal and as a result they were removed from the dataset.

In a limited number of circumstances, data were corrected where clear manual errors were made in data entry and these could be adjusted with confidence. For example, one pipe had some data entered without a 'negative'. In another example, five pipes were identified in the Main Range Volcanics with a similar time series pattern. Values of the hydraulic heads had increased by approximately 400 m in less than a year across all pipes. Here an error with the reference measurement point was identified and had to be manually corrected.

Gathering, Processing and Quality Control of Springs Data

A database of springs within the Surat Basin was compiled based off three principal sources: QWC (2012b), QWC (2012a) and Wolhuter et al. (In review). Even though data from four spring supergroups were considered, in the end only data on springs from the Springsure Supergroup were included. Springs from the other three supergroups were either not within the area of this study or had a source from a localised water system rather than being a discharge spring of a basin scale aquifer (Fensham and Fairfax, 2003).

Only five springs sourced by the Hutton Sandstone were incorporated into the final water level elevation dataset. Even though the size of the original database was substantially larger, the majority of the springs were sourced from deeper formations such as the Precipice Sandstone, had multiple aquifers attributed as potential sources, or were 'recharge' rather than 'discharge' springs. The water level elevations of the springs were also compared to the rest of the dataset to identify discrepancies and potential presence of regolith rather than regional aquifer springs. All data points that appeared to be outliers were removed. The final springs were assumed to have a water level depth of 0 m, or a water level elevation equal to the natural elevation at that point which was obtained from the 9 Second DEM of Australia (AUSLIG, 2001).

Petroleum and CSG Well Completion Reports Data

Data obtained from petroleum well completion reports (WCR) within the Surat Basin were also considered as a means of supplementing the GWDB and springs datasets. Hodgkinson et al. (2010) used petroleum well pressure data to investigate groundwater flow patterns within geologic formations after converting pressure data into equivalent hydraulic head values.

A repository in excess of 3000 Queensland petroleum well completion reports is available through the Queensland Digital Exploration Reports system (QDEX) managed by the Geological Survey of Queensland (Figure 17, QLD DNRM (2014c)), of which some has been integrated into the PressurePlot database (CSIRO, 2007). The CSIRO has also compiled information on WCRs not containing pressure data (Figure 17). Similar data are becoming available with QDEX for CSG WCRs (Figure 18, QLD DNRM (2014a)). Data already compiled into the PressurePlot database were interrogated and only 41 wells (predominantly in the Hutton Sandstone) contained any relevant pressure data. Petroleum well pressure data were not incorporated in this study due to limited data availability and the complexity of converting and correcting pressure data to equivalent hydraulic heads. However, there is future potential to expand the database, with the support of the CSIRO, and incorporate such data.

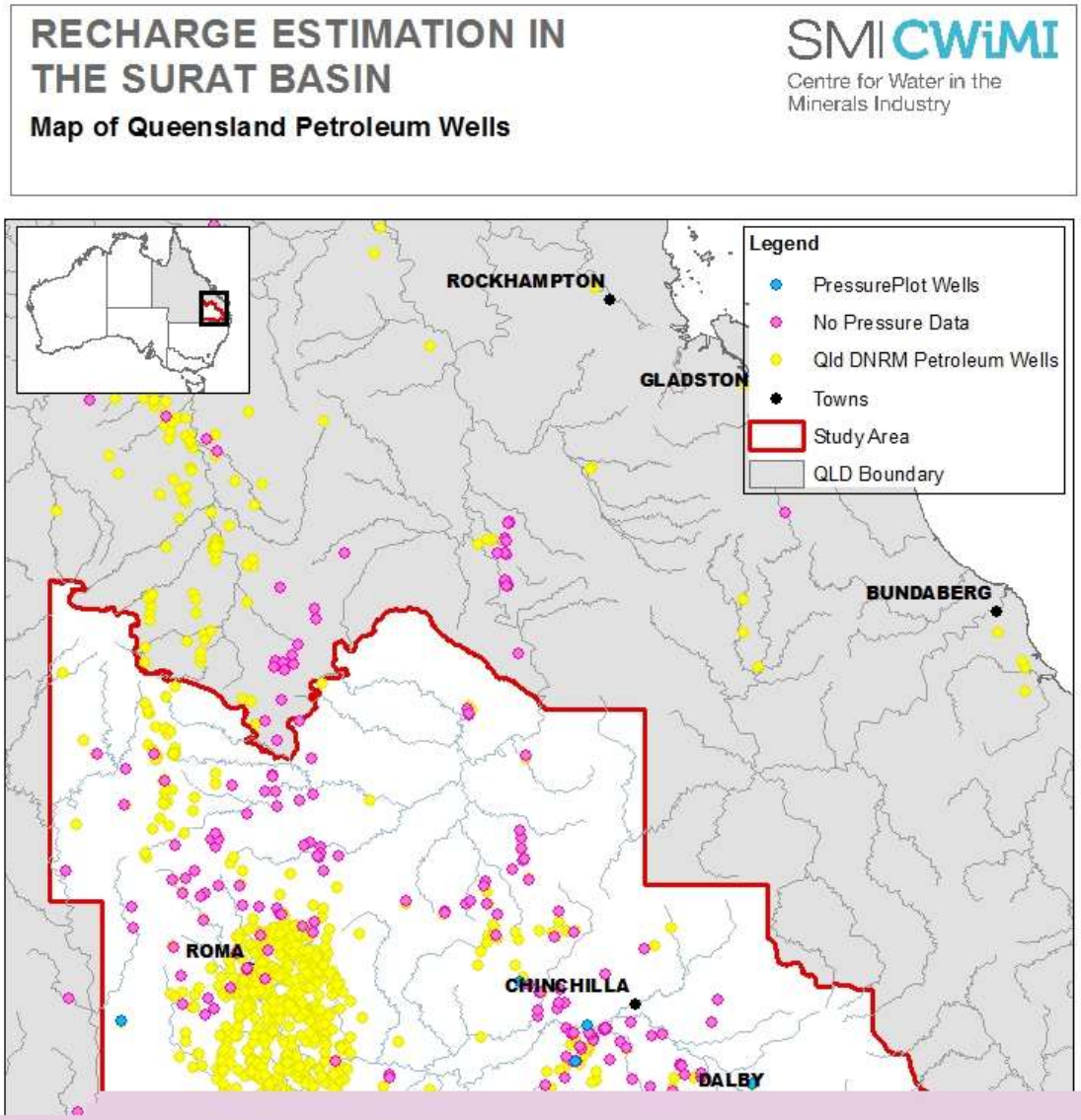
RECHARGE ESTIMATION IN THE SURAT BASIN
Map of Queensland Petroleum Wells
SMI CWiMI
Centre for Water in the Minerals Industry
Legend
PressurePlot Wells
No Pressure Data
Qld DNRM Petroleum Wells
Towns
Study Area
QLD Boundary
ROCKHAMPTON
GLADSTON
BUNDABERG
ROMA
CHINCHILLA
DALBY

Figure 17 - Map of all Queensland petroleum wells (QLD DNRM, 2014b), southern Qld petroleum wells with data contained in PressurePlot, and lastly petroleum wells with no pressure data reported in the WCRs. QLD DNRM material is licensed under a Creative Commons - Attribution 3.0 Australia licence

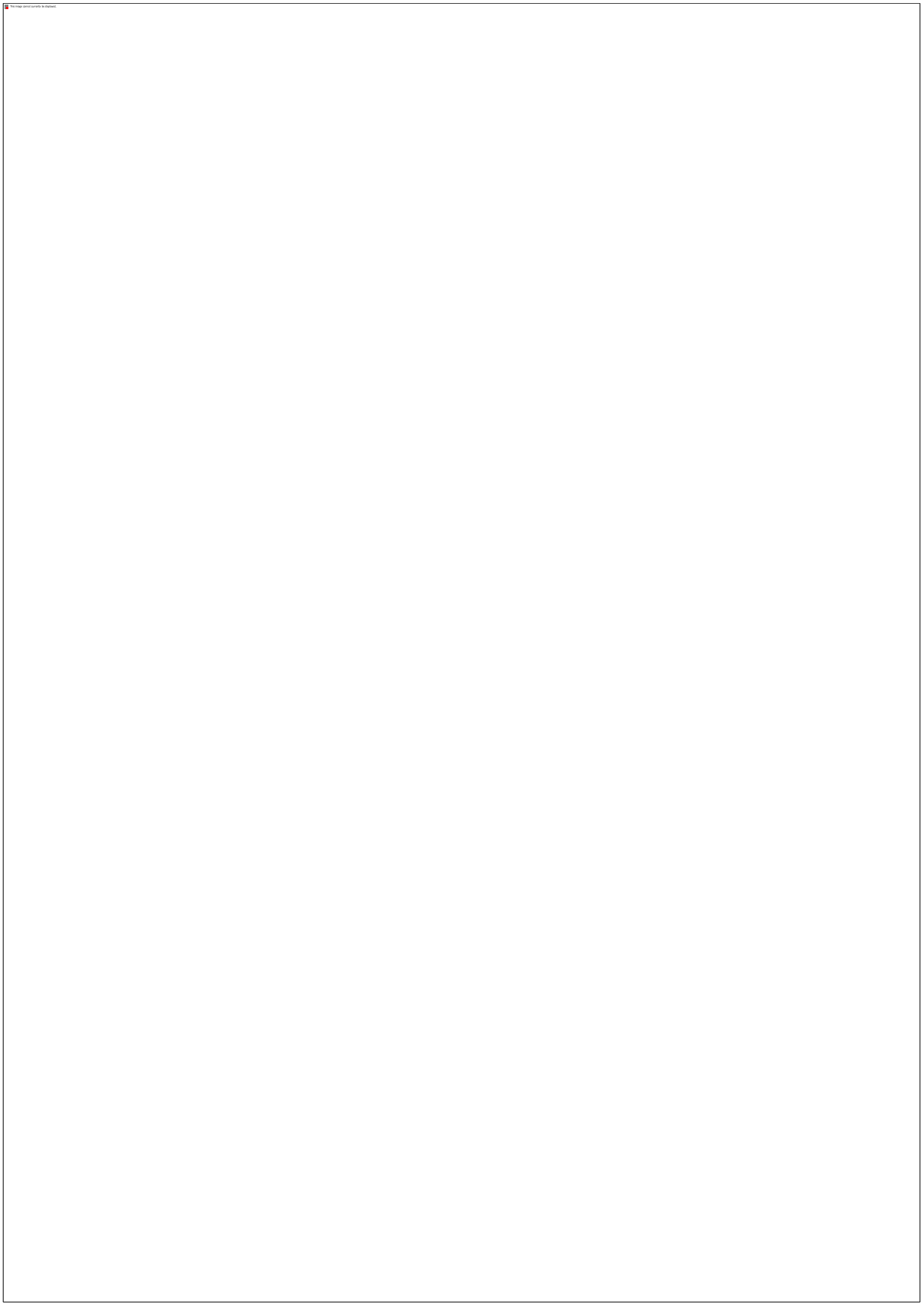

Figure 18 - Map of Queensland CSG exploration wells (QLD DNRM, 2014a). QLD DNRM material is licensed under a Creative Commons - Attribution 3.0 Australia licence.

Water Level Dataset and Single Reading Pipes

Initially, a general rudimentary analysis of the water level datasets for each geologic formation was carried out. A summary of the data is presented in Table 5, which contains information on the number of bores, pipes, springs and water level readings for each geologic formation, and the dates the first and last water level readings were taken. The Main Range Volcanics and Condamine River Alluvium have the largest datasets with over 1000 bores each (Table 5). Other than the Springbok Sandstone with a meagre 31 bores, the other geologic formations have a reasonable number of bores, varying between 183 for the Gubberamunda Sandstone and 469 for the Walloon Coal Measures. Springs data were only used to supplement the Hutton Sandstone dataset.

The locations of these datasets are depicted in Figure 19. The Condamine River Alluvium and Main Range Volcanics bores are all generally closely located on the eastern margins of the basin. The Walloon Coal Measures bores are located in the same general area, however appear to occur in two distinct spatial groups – west and east of the Great Dividing Range. These are most likely associated with the Walloons of the Surat and Clarence-Morton Basins. The bores of the Hutton, Mooga and Gubberamunda Sandstone are found further to the west and north. These bores are also more sparsely distributed over larger areas of the Surat Basin, with very few data points available in the southern and western sections of the basin.

Table 5 - Summary of available dataset for each geologic formation

Geologic Formation	No. Bore	No. Pipe	No. WL	No. Sprgs	Start Date	End Date
Condamine River Alluvium	1 123	1 244	70 926	0	1/01/1932	15/06/2014
Gubberamunda Sandstone	183	185	6 486	0	10/04/1919	15/06/2014
Hutton Sandstone	328	330	28 416	5	16/05/1897	15/06/2014
Kumbarilla Beds	269	278	464	0	1/01/1927	6/02/2014
Main Range Volcanics	1 698	1 822	44 905	0	01/07/1946	15/06/2014
Mooga Sandstone	293	296	7 020	0	27/05/1918	15/06/2014
Springbok Sandstone	31	31	31	0	1/10/1948	11/08/2011
Walloon Coal Measures	469	478	4 370	0	1/05/1936	26/02/2014
Total	**4 394**	**4 664**	**162 618**	**5**		

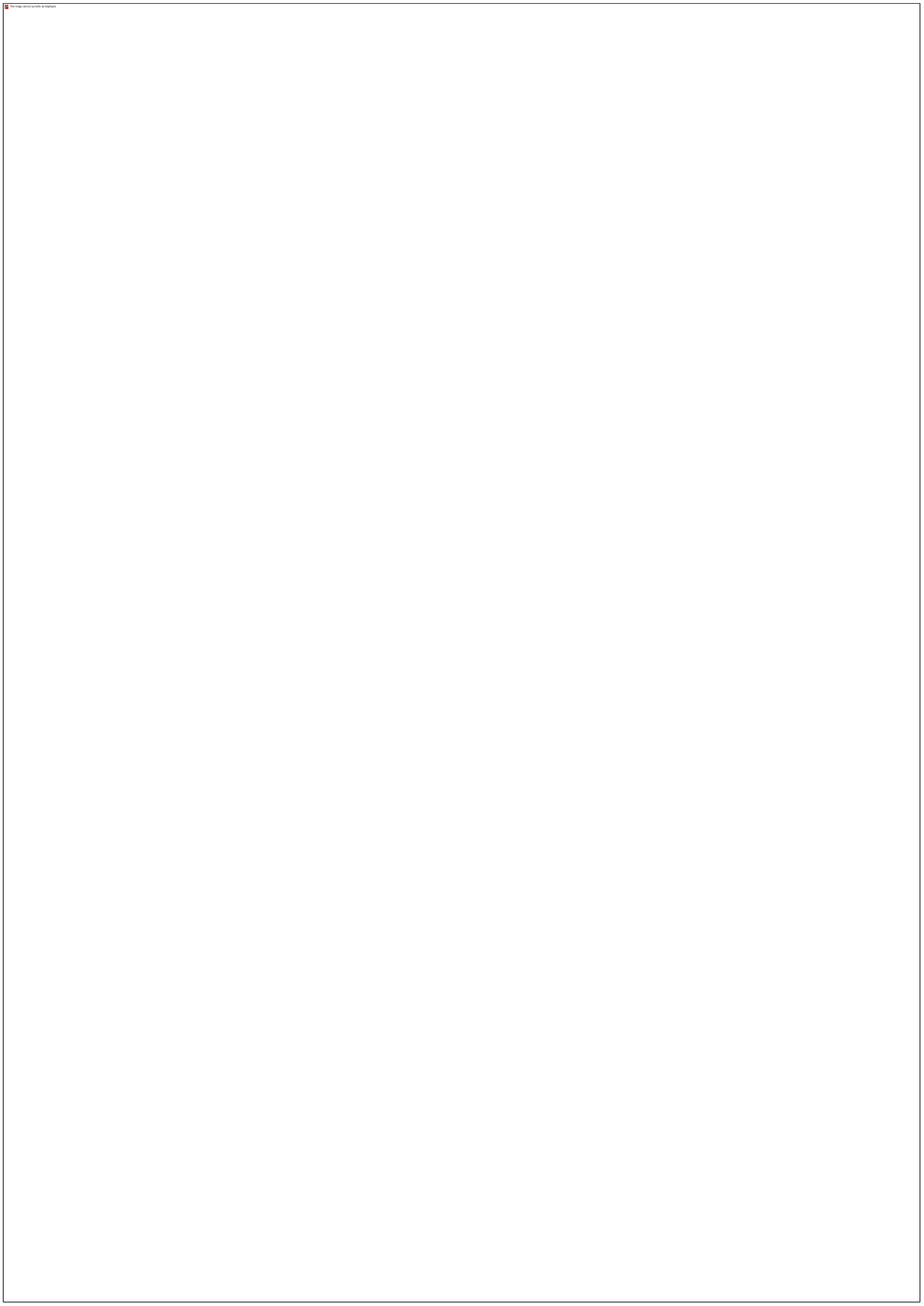

Figure 19 - Project study area and location of all data points

Single Reading Pipes

The first value taken at a pipe is not always an accurate representation of water levels/pressure of the geologic formation at that point. Depending on the physical attributes of the geologic formation, it can take a longer time to reach hydrodynamic equilibrium, which may not be captured by the first reading taken immediately after drilling. As a result, the possibility of removing the first value for each pipe was investigated.

From the quality control process undertaken on water level data, it was found that the first value was a clear outlier only on 11 occasions (equivalent to 1.9 percent out of a possible 569 pipes which had at least 3 water level readings each). Furthermore, the dataset is dominated by single reading pipes. Removing the first value would result in the loss of more than 85 percent of all pipes (Table 6), with only the Condamine River Alluvium (255 bores) and Main Range Volcanics (213 bores) geologic formation groups having adequately large datasets to attempt groundwater surface modelling. The Walloon Coal Measures have the next largest dataset of only 49 bores, while the Gubberamunda Sandstone has a meagre 14 bores. Consequently, only first water level readings identified in the quality control process were removed from the dataset. Pipes were categorised based on whether they are single (Category 2) or multiple (Category 1) water level reading pipes.

Table 6 - Summary of available dataset for each geologic formation if the first water level reading is removed. The final three columns indicate what proportion this dataset makes up of the entire data (refer to Table 4).

Geologic Formation	No. of Bores	No. of Pipes	No. of Water L	Start Date	End Date	% Bore	% Pipe	% WL
Condamine River Alluvium	255	286	69 682	29/08/1962	15/06/2014	22.71	22.99	98.25
Gubberamunda Sandstone	14	14	6 301	23/03/1928	15/06/2014	7.65	7.57	97.15
Hutton Sandstone	26	26	28 086	10/03/1960	15/06/2014	7.93	7.88	98.84
Kumbarilla Beds	31	31	186	21/01/1976	6/02/2014	11.52	11.15	40.09

Main Range Volcanics	213	242	43 083	29/09/1959	15/06/2014	12.54	13.28	95.94
Mooga Sandstone	32	32	6 724	10/02/1958	15/06/2014	10.92	10.81	95.78
Springbok Sandstone	0	0	0	NA	NA	0.00	0.00	0.00
Walloon Coal Measures	49	49	3 892	22/08/1963	26/02/2014	10.45	10.25	89.06
Total	**620**	**680**	**157 954**			**14.11**	**14.58**	**97.13**

Temporal Distribution of Data

Due to the importance of temporal variability in water levels, the temporal distribution of data was examined to gain a better general understanding of the data collection periods of individual geologic formations, and identify suitable time periods for which groundwater surfaces of the various geologic formations could be modelled. The numbers of bores with water level data were calculated for a number of different time periods and temporal 'windows'. Figure 20 and Figure 21 show the temporal distribution of the number of bores with water level readings for one year and ten year periods, starting from 1920.

The dominant data collection periods for the Kumbarilla Beds, Gubberamunda, Hutton and Mooga Sandstones were between 1950 and 1980, with the number of bores being monitored greatly reduced in the more recent decades. However, even through the more intensive monitoring periods, the number of bores being monitored is still rather limited. Generally less than ten bores were monitored in a year per formation, with the maximum number of 22 bores monitored in a year in the Hutton Sandstone (Figure 20). The Condamine River Alluvium, Main Range Volcanics and Walloon Coal Measures had the largest numbers of bores monitored in the 1970s (Figure 21). Currently, these are the formations with the largest number of monitored bores, of which majority are Category 1. The Condamine River Alluvium is the best monitored of all the aquifers, with between 100 and 150 bores monitored yearly over the last few decades (Figure 20). Approximately 75 Category 1 bores are monitored annually in the Main Range Volcanics, while in the last decade this number has varied between 20 to 40 bores in the Walloon Coal Measures.

In selecting a representative time period for the groundwater surface modelling of the various geologic formations, a number of factors were taken into account:

1. Using recent groundwater level data to have groundwater surfaces that are currently representative
2. Finding a balance between reducing temporal variability in data to prevent false trends (short temporal periods), and the need for larger datasets with greater spatial coverage (longer temporal periods)
3. Selecting the same temporal period for all the geologic formations to provide a consistent basis for comparison.

To account for the three points listed above, a moving window analysis was performed where the numbers of bores with water level data were calculated for different time periods (Figure 22). The time period calculations were carried out for 1, 2, 5 and then in five-year

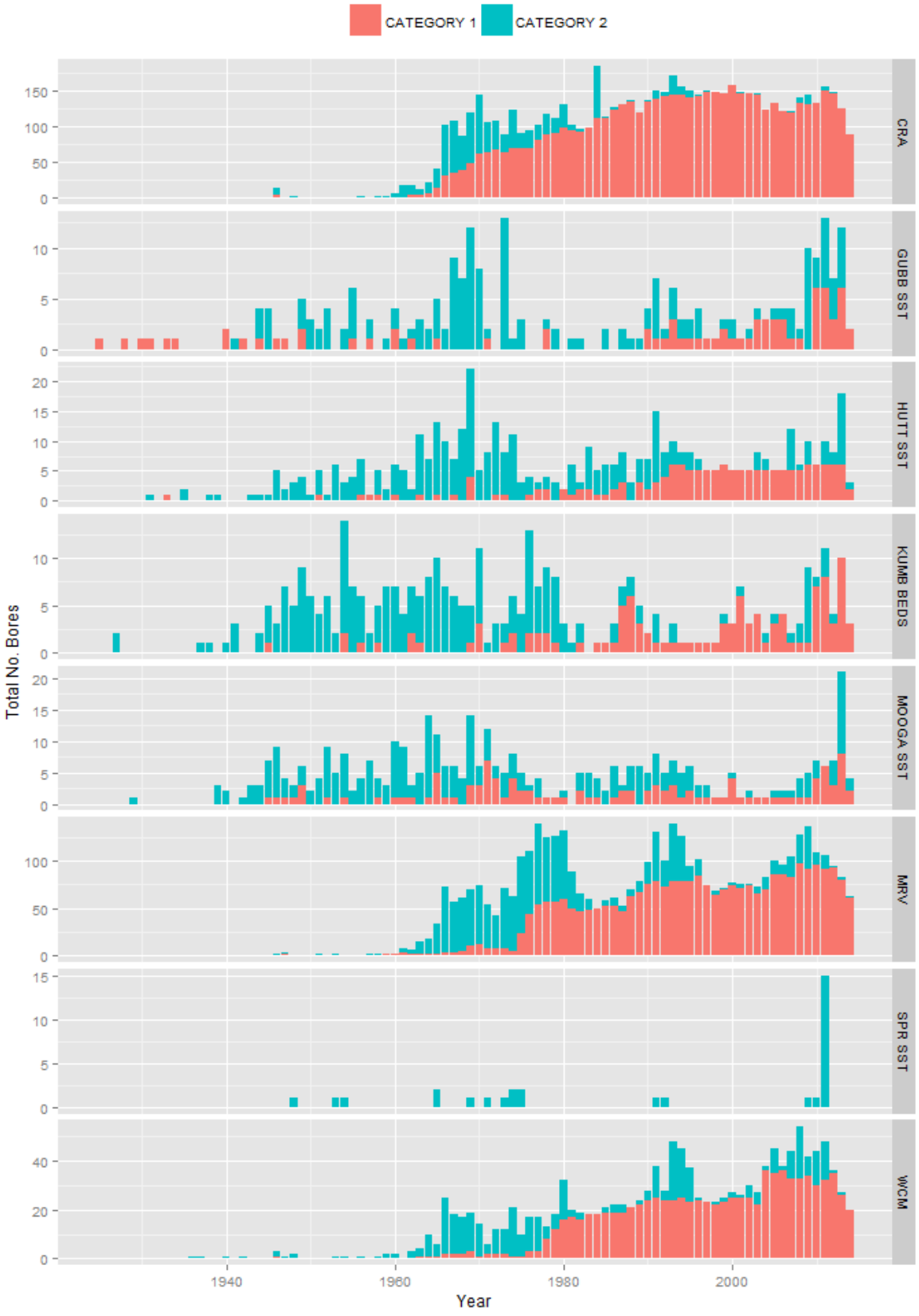
CATEGORY 1
CATEGORY 2
CRA
GUBB SST
HUTT SST
KUMB BEDS
MOOGA SST
MRV
SPR SST
WCM
Total No. Bores
Year
1940
1960
1980
2000

Figure 20 - Number of bores with water level readings for each geologic formation in annual increments, between 1920 and 2014


CATEGORY 1
CATEGORY 2
CRA
GUBB SST
HUTT SST
KUMB BEDS
MOOGA SST
MRV
SPR SST
WCM
Total No. Bores
Year
1920-1929
1930-1939
1940-1949
1950-1959
1960-1969
1970-1979
1980-1989
1990-1999
2000-2009
2010-2019

Figure 21 - Number of bores with water level readings in 10 year increments for each geologic formation


CATEGORY 1
CATEGORY 2
Total No. Bores
CRA
GUBB SST
HUTT SST
KUMB BEDS
MOOGA SST
MRV
SPR SST
WCM
1945-2014
1950-2014
1955-2014
1960-2014
1965-2014
1970-2014
1975-2014
1980-2014
1985-2014
1990-2014
1995-2014
2000-2014
2005-2014
2010-2014
2013-2014
2014-2014
YEAR_SPAN

Figure 22 - Number of bores of each category for each geological formation with water level data over different time periods relative to 2014

intervals up to 70 years. Based on this analysis and the work carried out by Smerdon et al. (2012b) (where twenty year intervals were used in modelling groundwater levels in the Cadna-owie Hooray Sandstone formations), a 20-year period from 1995 to 2014 was selected. Using a large time interval and data of different quality categories means that the groundwater surfaces modelled in this study are representative of long-term and regional groundwater levels and flow directions.

Groundwater Surfaces and Potential Movement of Groundwater

In this Section, first the different interpolation (contouring) methods that were attempted in groundwater surface contouring are discussed. This is followed by a presentation of the groundwater surface results for each of the geologic formations, and a comparison of these potentiometric surfaces with other published sources of the basin's groundwater surfaces. The Section concludes with a discussion about the uncertainties, limitations and difficulties in developing the groundwater surfaces.

Groundwater Surface Interpolation Methods

The water level values presented in Section 0, spanning from 1 January 1995 until present, were used to develop groundwater surfaces of the different geologic formations. If more than one water level measurement was measured at a bore during the 20 years, a weighted mean was used as a representative groundwater elevation. The weightings were proportional to the time span between consecutive readings. This weighting technique prevents the over-representation of short temporal periods with high monitoring frequency in the groundwater elevation calculations. If multiple pipes were accessing the same formation at the same bore, the data from the shallowest bore were used. Interpolation was carried out in a projected rather than geographic coordinate system to prevent large 'distortion'. No groundwater surface was interpolated for the Springbok Sandstone due to the limited dataset. A number of different deterministic and geostatistical techniques were attempted using Geostatistical Analyst (ESRI ArcGIS V.10.1) to produce interpolated groundwater surfaces.

First, the Inverse Distance Weighted (IDW) interpolation technique was attempted. IDW is a simple deterministic method where the predicted value at a certain point is equal to the weighted sum of neighbouring points. The weightings are a function of the inverse-distance to

a defined power between the target and known point, where the higher the power the larger the weighting to nearby points. The same power value is assumed within a sampling neighbourhood. The IDW interpolation technique is an exact interpolator, and all interpolated values are in the range of the dataset, i.e. no interpolated values can be smaller than the smallest data point or larger than the largest. A distinction of IDW interpolated surfaces is the presence of cone-like features (or bulls-eyes) at data locations due to the large weighting towards these points.

The Geostatistical Analyst tab (ESRI ArcGIS) was used. This tool allows the influence of the power value and neighbourhood assumptions to be evaluated both graphically and quantitatively. Neighbourhood characteristics (number, direction of points or search radius) can be adjusted so that unique subsets of the population meeting these parameters are used in interpolation. Using a subset of the data points instead of the entire population can result in improved interpolation because of increased similarity between spatially closer points. The 'Optimise' tool identifies the optimal power value for that sampling neighbourhood. Various neighbourhood sizes and neighbourhood directions were tested to identify the best-fitting groundwater surface model.

The second interpolation technique that was implemented was kriging - a commonly used geostatistical interpolation method essentially based on least-squares regression. Kriging interpolation methods are commonly described as 'best linear unbiased estimator' (BLUE) (Isaacs and Srivastava 1989), because they are linear interpolators that minimise the error variances of the predicted variable. Kriging interpolation methods not only produce a surface of predictions of the variable, but also a surface of standard errors of each prediction point. There are several variations of kriging (e.g. Goovaerts, 1997; Isaaks and Srivastava, 1989; Wackernagel, 2003).

Kriging estimates unknown values at specific locations in a similar manner to IDW. However, a major difference between the two methods is in the way that weightings to neighbouring points are determined. Unlike IDW methods, which determine weightings purely based on the inverse distance between points, kriging applies statistical methods that incorporate the spatial autocorrelation between sample points, which is usually estimated as a function of the distance between points and the direction of the line joining the points in the case of anisotropy. Weightings are determined in such a way to ensure minimum error variances of the predicted values are achieved. The modelling of the semivariogram (spatial

autocorrelation model) is the most difficult aspect of kriging, with Kitanidis (1997) describing it as more of an art than a science. Furthermore, kriging methods are better suited to normally distributed data. They can still be applied to other data distributions for predictions but with less meaning attached to predicted quantiles.

In this study, two main approaches were implemented depending on the geologic formation, namely ordinary and universal kriging. A requirement of ordinary kriging is second order stationarity, which is not met by data that exhibit strong spatial trends. In the instance of the Condamine River Alluvium and Walloon Coal Measures, strong spatial trends were evident both in a northerly and easterly direction (Figure 23) and as such universal kriging was applied, which incorporates a spatial trend model. Ordinary kriging was used on the other geologic formations where no evident spatial trend in groundwater elevation data was present (Figure 23). The Geostatistical Analyst tab (ESRI ArcGIS) was also utilised for kriging interpolations. Various semivariogram models, semivariogram parameters and prediction search neighbourhoods were tested to find a suitable semivariogram model that produced reasonable groundwater surfaces.

A commonly used model validation technique, known as cross-validation, was used to assess the accuracy/suitability of the different groundwater surfaces obtained. The cross-validation process involves removing a known data point and using all other data points to predict the value. This is repeated for all data points, and the cross-validation residuals provide information on the quality of the kriging model. A number of different measures of the accuracy of predictions, obtained from cross-validation were used. These were:

1. Mean of Prediction Errors – this should be approximately zero, and is an indicator of unbiasedness in predictions
2. Root Mean Square of Prediction Errors – this value should be as small as possible, and indicates how accurately points during cross-validation were estimated
3. Squared Standardised Error – this should be approximately equal to one; it is a measure of how similar the estimation errors are to the errors predicted by the model, and thus the ‘quality’ of the selected model (Wackernagel, 2003)

The groundwater surface rasters of each of the geologic formations were automatically contoured in ArcGIS and inspected. In some circumstances the groundwater surface contours were manually edited and smoothed. This was especially necessary with universal kriging surfaces where erroneous results were obtained away from the sample points due to the

global trend model. A change in sample neighbourhoods was another factor in producing 'step-like' features in the surfaces.

Due to the sparseness of sample points for most of the geologic formations, the possibility of incorporating secondary data in the form of digital elevation models was considered. This seemed a reasonable option due to the generally strong correlation between elevations and groundwater level elevations observed for most geologic formations (Figure 23). Initially, kriging with external drift was attempted in the R Statistical package, however this appeared to produce erroneous and unrealistic results and thus was scrapped. The cokriging tool in Geostatistical Analyst was also applied for this purpose, although the idea was aborted for a number of reasons. Firstly, numerical instability can occur when the secondary variable is much more densely sampled than the primary variable as is in this case (Goovaerts, 1997). Cokriging also requires three models instead of one to be fit to the data, increasing the complexity. Furthermore, the use of digital elevation models as secondary variables does not appear to be prevalent in the literature. Desbarats et al. (2002) used a DEM in modelling the groundwater table of the unconfined Oak Ridges Moraine aquifer, Canada. The dataset used was very large and densely sampled, however only improved RMSE by 0.1 m to ordinary kriging.

Groundwater Surface Models and Aquifer Flow Patterns

Condamine River Alluvium

A total of 234 data points were used in developing the groundwater surface of the Condamine River Alluvium (Table 7). The majority of the dataset was made up of higher quality points that had at least two water level readings in the entire GWDB (188 points classified as Category 1 data), while 46 points had only ever been sampled once (classified as Category 2 data). Category 1 data points were spread out over the entire Condamine River Alluvium, while Category 2 data points were spatially clustered within the area of Dalby, Chinchilla and Warwick with Category 1 data points in close vicinity (Figure 24).

Groundwater surfaces were generated using the IDW and universal kriging interpolation methods (Figure 24, Figure 25). Universal kriging was selected over ordinary kriging due to the groundwater elevation exhibiting a strong spatial trend both in an easterly ($\rho = 0.97$) and northerly ($\rho = -0.95$) direction (Figure 23). This trend is consistent with the general flow

direction of the Condamine River from the headwaters in the south-east flowing towards the north-west, represented in the kriging by a first-order trend model.

Groundwater surface elevations ranged from a maximum of approximately 480 m AHD in the Condamine River headwaters to approximately 290 m AHD in the North West of the alluvium (Table 7, Figure 24, and Figure 25). Groundwater surfaces produced by both IDW and universal kriging interpolation methods showed similar general trends in data. The primary trend that is evident in both figures is of groundwater flow in a north-westerly direction, consistent with the flow direction of the Condamine River. In addition, a major groundwater sink is present west of Oakey and extends north up to the region of Dalby, where water levels are up to 50 m below the surface. This is most likely due to the high level of water use and extraction from the alluvium for agricultural purposes (Dafny and Silburn, 2014). The universal kriging surface also infers a secondary flow trend from the east as observed by Dafny and Silburn (2014) to a greater degree, indicating lateral flow into the alluvium from neighbouring aquifers.

The groundwater surfaces presented here of the Condamine River Alluvium for the period 1995 to 2014 generally concur with the groundwater surface for 2011 reported by Dafny and Silburn (2014). The most noticeable difference present between surfaces is on the eastern boundary of the alluvium, where the Dafny and Silburn (2014) surface exhibits steeper and more prominent groundwater contours towards the west. This could be a result of the different number and distribution of groundwater bores used, but could also be indicative of larger lateral flow from the east during the wet periods of 2011.

Table 7 - Summary statistics of the water level elevation and water level depth of the Condamine River Alluvium

	Elevation (mAHD)	**Depth (m)**
Mean	357.03	-17.11
Median	339.9	-15
StdDev	48.10	9.93
Count	234	234

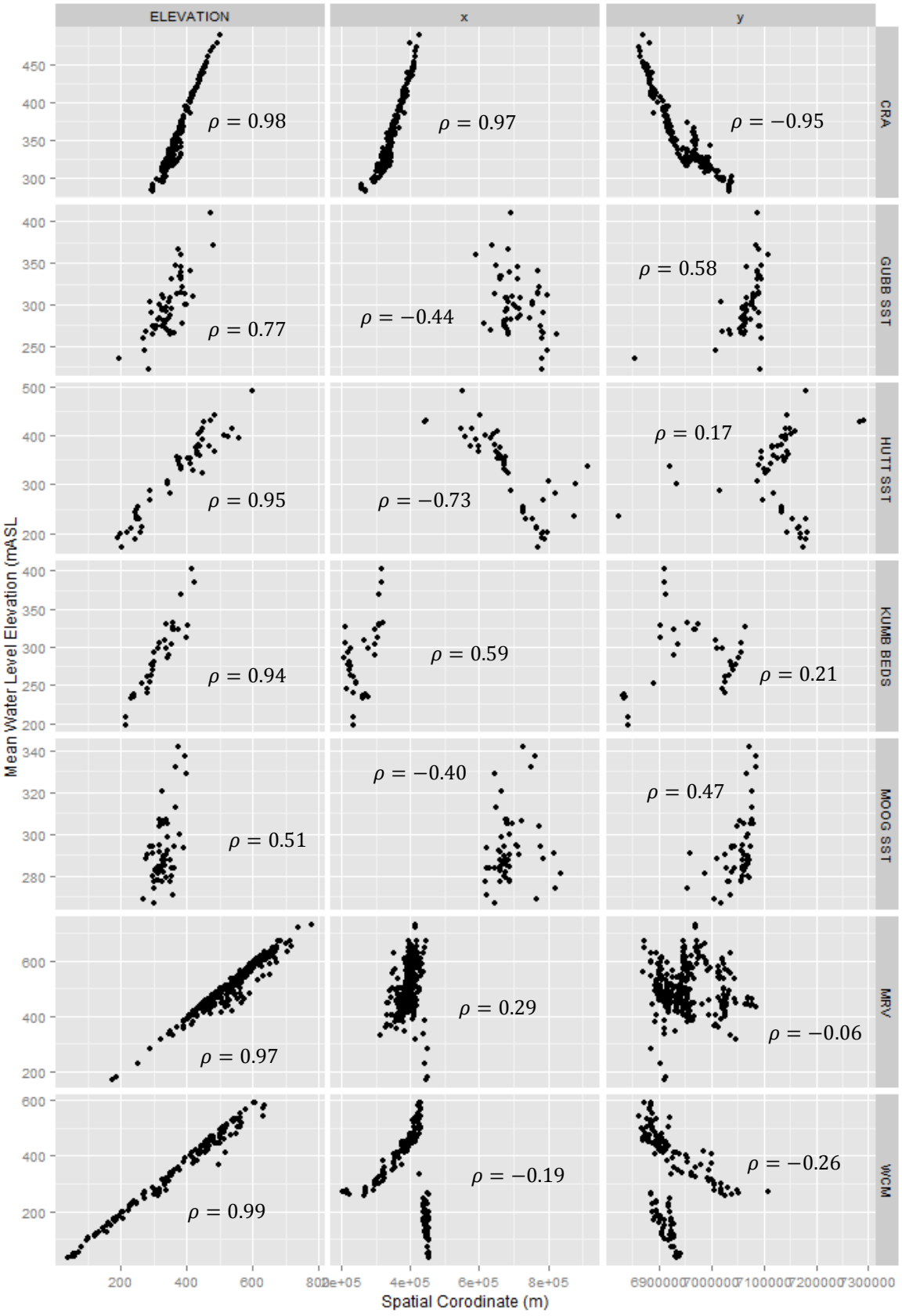
ELEVATION
x
y
CRA
GUBB SST
HUTT SST
KUMB BEDS
MOOG SST
MRV
WCM
ρ = 0.98
ρ = 0.97
ρ = −0.95
ρ = 0.77
ρ = −0.44
ρ = 0.58
ρ = 0.95
ρ = −0.73
ρ = 0.17
ρ = 0.94
ρ = 0.59
ρ = 0.21
ρ = 0.51
ρ = −0.40
ρ = 0.47
ρ = 0.97
ρ = 0.29
ρ = −0.06
ρ = 0.99
ρ = −0.19
ρ = −0.26
Mean Water Level Elevation (mASL
Spatial Corodinate (m)

Figure 23 - Scatterplot and correlation of mean water level elevation against elevation, easting and northing for each geologic formation

RECHARGE ESTIMATION IN THE SURAT BASIN

Map of Groundwater Surface Contours (IDW) of Condamine River Alluvium

SMI CWiMI
Centre for Water in the Minerals Industry

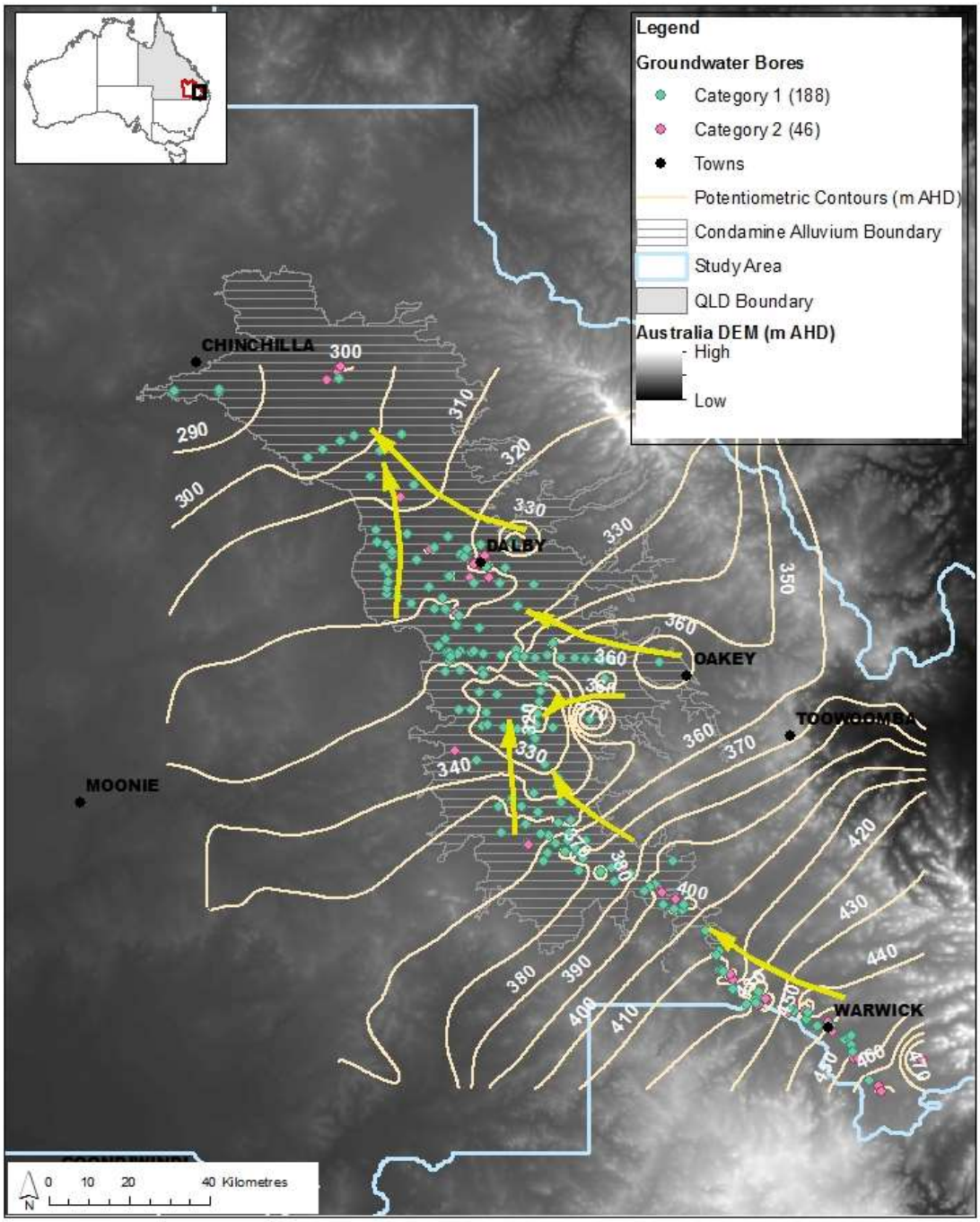

Figure 24 - Groundwater surface contours (10 m) of the Condamine River Alluvium (1995 - 2014) by IDW interpolation, with yellow arrows indicating general flow directions.

RECHARGE ESTIMATION IN THE SURAT BASIN

Map of Groundwater Surface Contours (Universal Kriging) of Condamine River Alluvium

SMI CWiMI
Centre for Water in the Minerals Industry

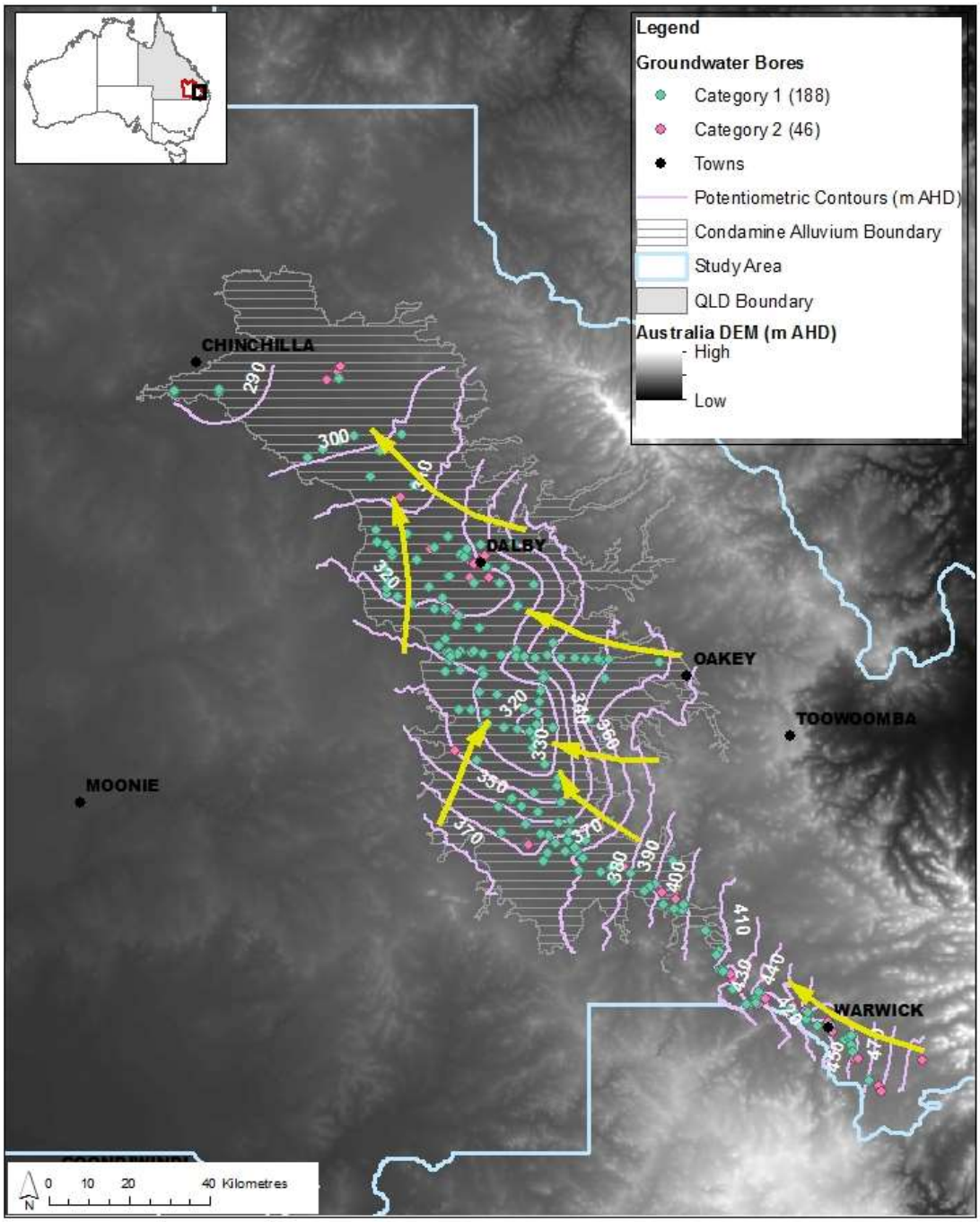

Figure 25 - Groundwater surface contours (10 m) of the Condamine River Alluvium (1995 - 2014) by universal kriging, with yellow arrows indicating general flow directions.

Gubberamunda Sandstone

A total of 56 data points were used to create the groundwater surface of the Gubberamunda Sandstone (Table 8, Figure 26, and Figure 27). Regional groundwater flow is predominantly in a southerly direction (Figure 26, Figure 27), with groundwater potentiometric elevations varying from approximately 360 m AHD north of Roma to approximately 230 m AHD north of Goondiwindi. A secondary flow direction is present south-west of Wandoan coinciding with the surface water divide, with groundwater flowing in a northerly and easterly direction. A similar trend was also observed by WorleyParsons (2012). A potentiometric low is present in the region of Roma, as also identified by Australia Pacific LNG (2014), due to water extraction for town water supply.

Sub-artesian flow is prevalent within the Gubberamunda Sandstones dataset, with artesian conditions present only in two bores located in the southern parts of the basin. Majority of the data points were clustered in the north around Roma and Wandoan, and as such due to limited data points it is only possible to infer general broad-scale flow patterns in the southern part of the basin. Figure 26 and Figure 27 also exhibit ‘bulls-eyes’ which can be indicative of the local potentiometric surface, errors in groundwater data or general data sparseness, and thus need to be interpreted with caution. The sparseness of Gubberamunda Sandstone data points coupled with topographical/hydrogeological variability makes it difficult to disentangle genuine errors in water level data. This problem also applies to upcoming potentiometric surfaces of other geologic formations as all suffer from data limitations, and are predominantly indicative of regional groundwater flows.

Table 8 - Summary statistics of the water level elevation and water level depth of the Gubberamunda Sandstone

	Elevation (mAHD)	**Depth (m)**
Mean	298.93	-47.49
Median	294.92	-44.62
StdDev	35.0	30.83

Count	56	56

RECHARGE ESTIMATION IN THE SURAT BASIN

Map of Groundwater Surface Contours (IDW) of Gubbermunda Sandstone

SMI CWiMI
Centre for Water in the Minerals Industry

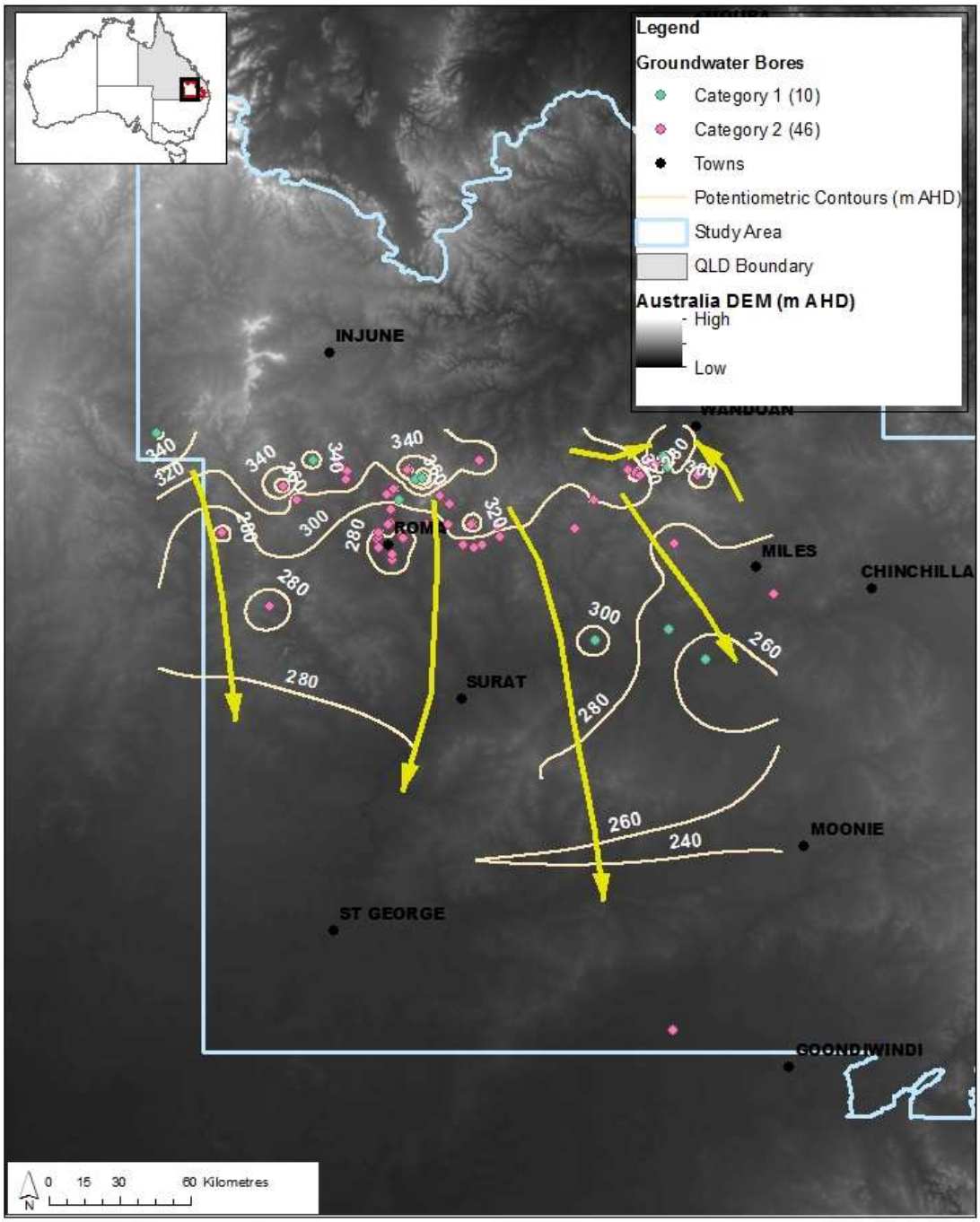

Figure 26 - Groundwater surface contours (20 m) of the Gubberamunda Sandstone (1995 - 2014) by IDW interpolation, with yellow arrows indicating general flow directions.

RECHARGE ESTIMATION IN THE SURAT BASIN

Map of Groundwater Surface Contours (Ordinary Kriging) of Gubbermunda Sandstone

SMI CWiMI
Centre for Water in the Minerals Industry

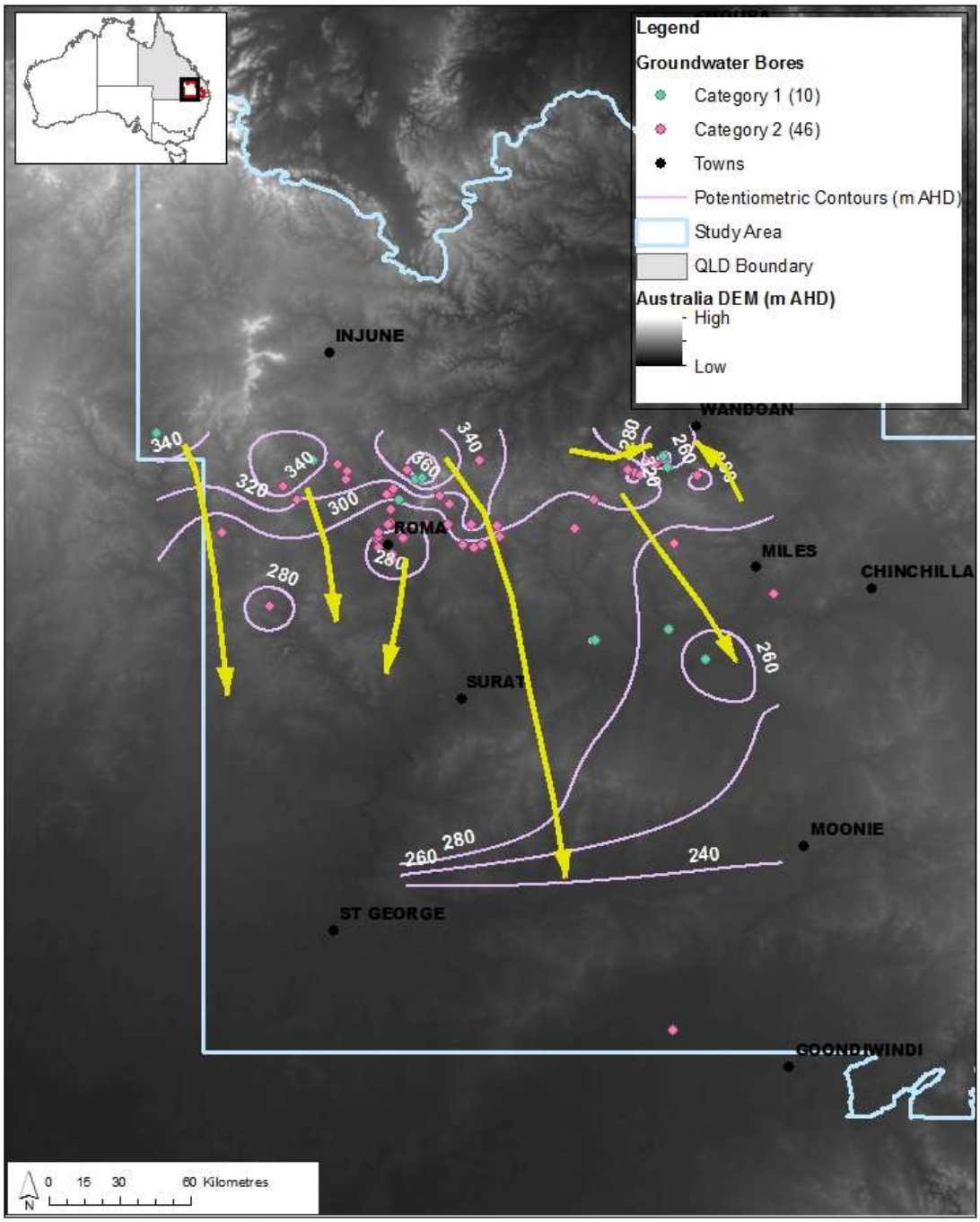

Figure 27 - Groundwater surface contours (20 m) of the Gubberamunda Sandstone (1995 - 2014) by ordinary kriging, with yellow arrows indicating general flow directions.

Hutton Sandstone

The groundwater potentiometric surface of the Hutton Sandstone was created using 53 data points, five of which were obtained from springs and 48 from groundwater wells. The majority of the points were Category 2 (Figure 28, and Figure 29). The data points are spread out over several hundred kilometres in a northerly and easterly direction. Most of the data are clustered west of Injune spreading south towards Roma, with a second cluster of data points located around Taroom and Wandoan. Similar to the Gubberamunda Sandstone, more southerly data points are scarce.

Groundwater potentiometric elevations varied from approximately 490 m AHD in the north-west to below 200 m in the north-east around Taroom. The regional groundwater flow within the Hutton Sandstone is complex and multi-directional. An easterly flow from west of Injune towards Taroom is prevalent. There is also evidence of flow from the elevated recharge zones southwards towards Surat, northerly groundwater flow from around Wandoan towards Taroom, and radiating groundwater flow from the eastern margins, which could be indicative of a recharge zone. There is also some evidence of westerly flow towards the Eromanga Basin from the high elevation zones (Orange lines, Figure 12), although sparse data points prevent better interpretation. The Nebine Ridge divides the Surat and Eromanga Basins, but stratigraphic data provides evidence of continuity in the younger and shallower stratigraphic formations, including the Hutton Sandstone (Hodgkinson et al., 2009).

Sub-artesian conditions were prevalent throughout the entire Hutton Sandstone. This is indicative of the clustering of data points in the northern outcropping areas. Artesian bores have been reported in the Hutton Sandstone primarily in the southern zone (Hodgkinson et al., 2010). The groundwater potentiometric surface of the Hutton Sandstone reinforces the findings of regional groundwater flow patterns in the northern region described by Quarantotto (1989) and Hodgkinson et al. (2010).

Table 9 - Summary statistics of the water level elevation and water level depth of the Hutton Sandstone

	Elevation (mAHD)	**Depth (m)**

Mean	328.90	-50.12
Median	353.14	-43
StdDev	80.90	37.38
Count	53	53

RECHARGE ESTIMATION IN THE SURAT BASIN

Map of Groundwater Surface Contours (IDW) of Hutton Sandstone

SMI CWiMI
Centre for Water in the Minerals Industry

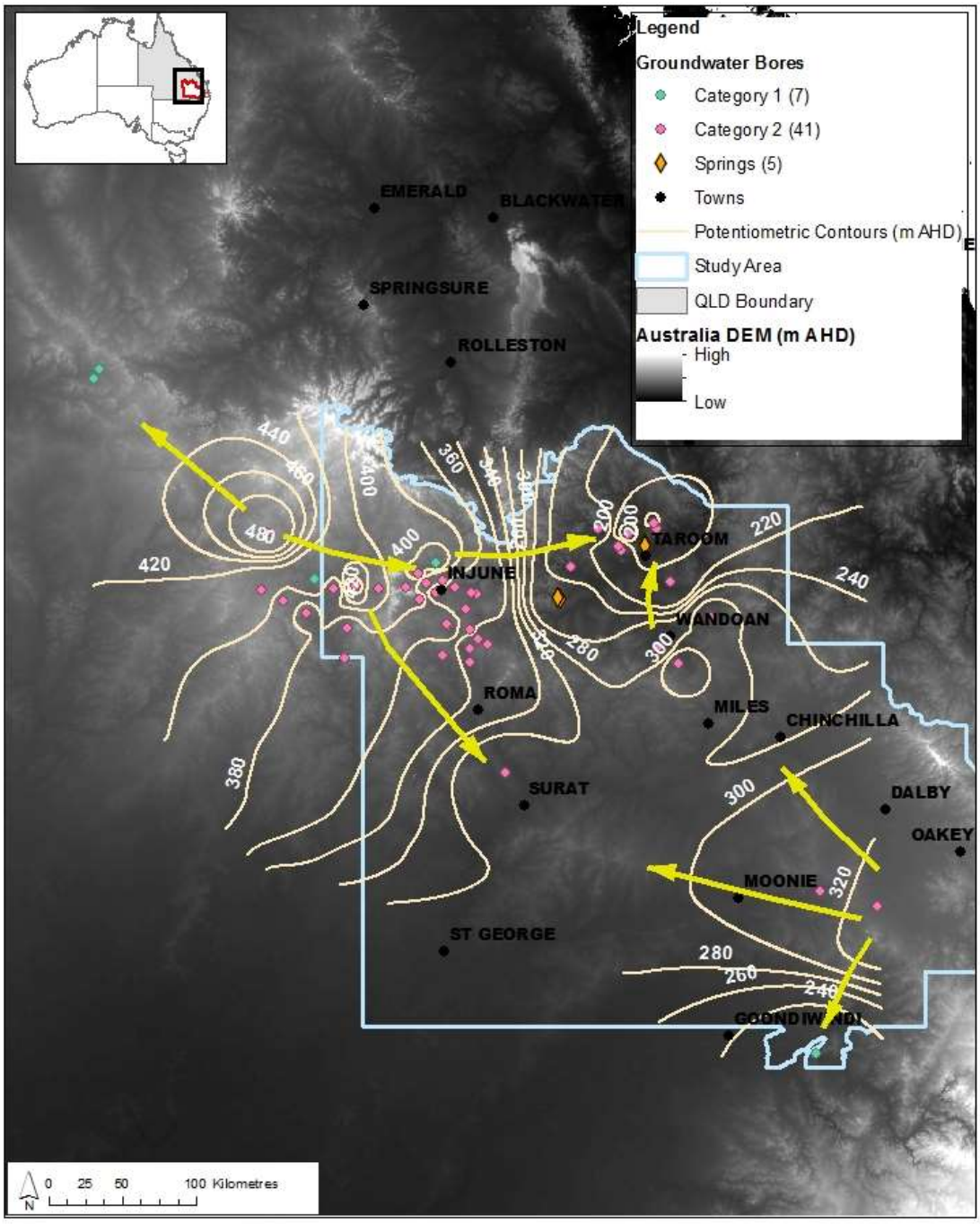

Figure 28 - Groundwater surface contours (20 m) of the Hutton Sandstone (1995 - 2014) by IDW interpolation, with yellow arrows indicating general flow directions.

RECHARGE ESTIMATION IN THE SURAT BASIN

Map of Groundwater Surface Contours (Ordinary Kriging) of Hutton Sandstone

SMI CWiMI
Centre for Water in the Minerals Industry

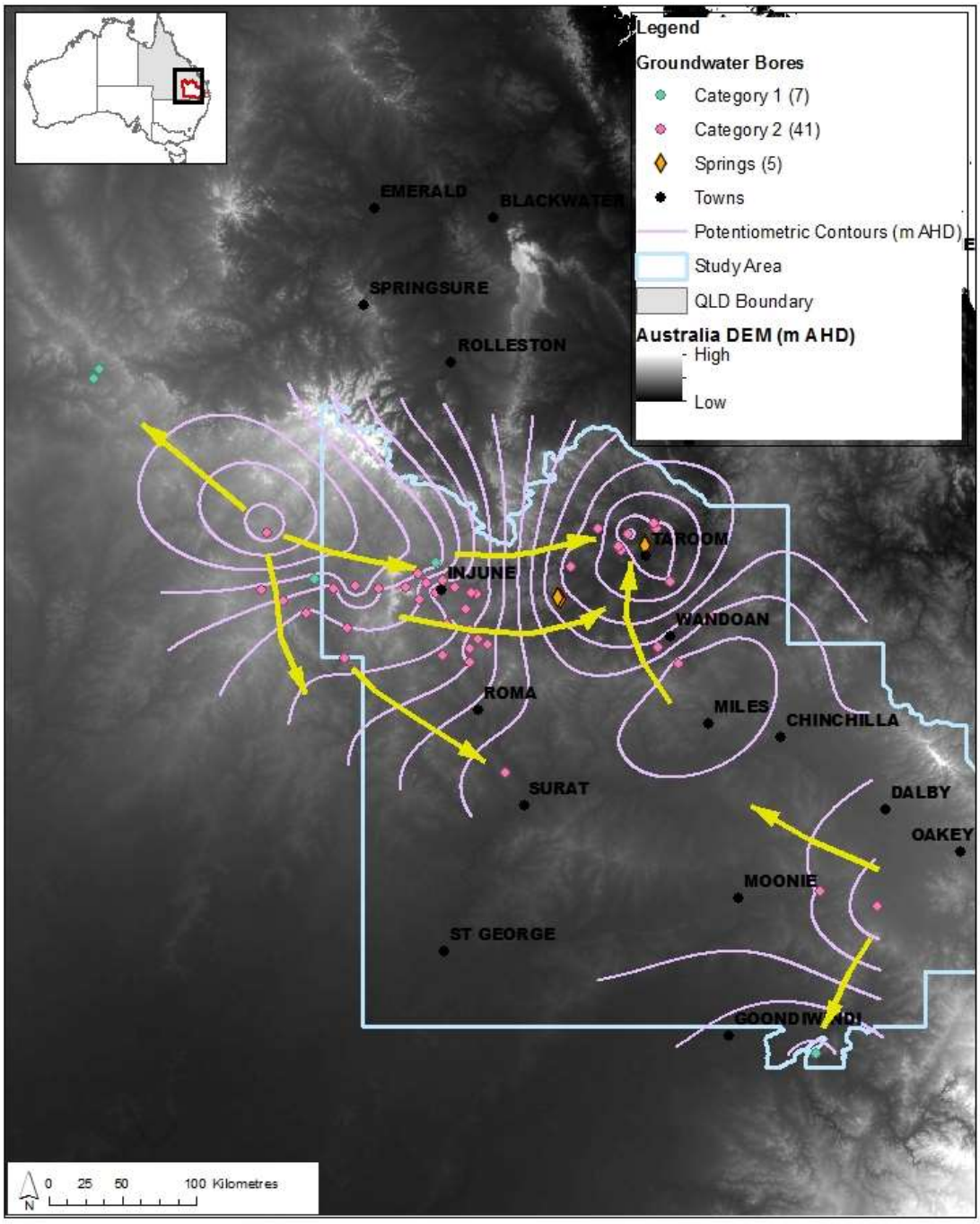

Figure 29 - Groundwater surface contours (20 m) of the Hutton Sandstone (1995 - 2014) by ordinary kriging, with yellow arrows indicating general flow directions

Kumbarilla Beds

The groundwater potentiometric surface of the Kumbarilla Beds was constructed from a mere 35 data points (Table 10), with data points clustered around Miles (Figure 30, Figure 31). Groundwater potentiometric elevations varied from approximately 400 m AHD on the eastern margins, to 200 m AHD by Goondiwindi. Groundwater flow is predominantly radial from the eastern higher elevation margins of the geologic formations. A secondary trend is present with groundwater flows also occurring southwards in the region of Miles. These groundwater flow patterns follow the general topographic trends in the region (Figure 31), however groundwater flow interpretations are severely restricted due to sparseness of data and clustering.

Table 10 - Summary statistics of the water level elevation and water level depth of the Kumbarilla Beds

	Elevation (mAHD)	**Depth (m)**
Mean	288.65	-28.15
Median	289.17	-24.48
StdDev	47.01	20.90
Count	35	35

RECHARGE ESTIMATION IN THE SURAT BASIN

Map of Groundwater Surface Contours (IDW) of Kumbarilla Beds

SMI CWiMI
Centre for Water in the Minerals Industry

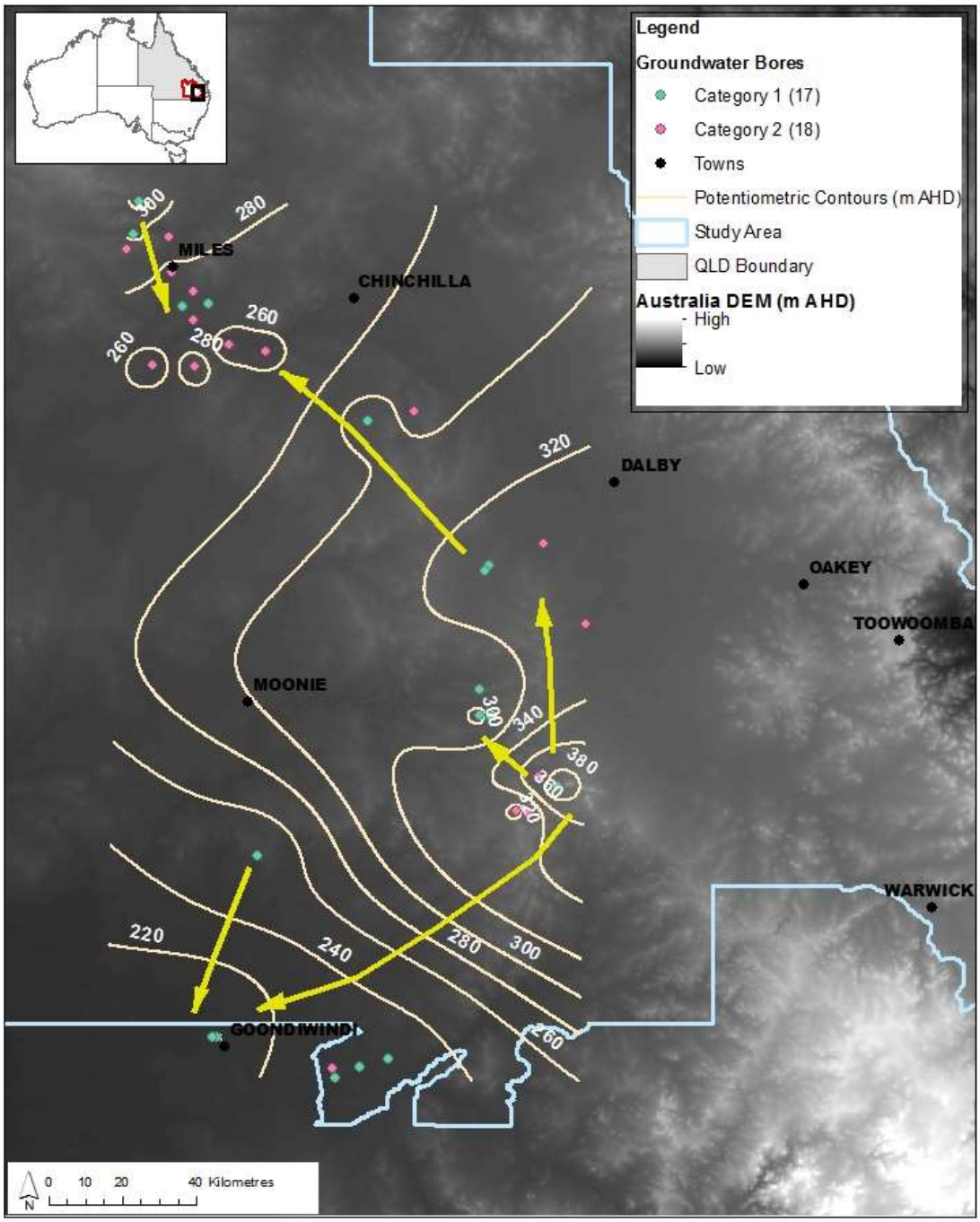

Figure 30 - Groundwater surface contours (20 m) of the Kumbarilla Beds (1995 - 2014) by IDW interpolation, with yellow arrows indicating general flow directions.

RECHARGE ESTIMATION IN THE SURAT BASIN

Map of Groundwater Surface Contours (Ordinary Kriging) of Kumbarilla Beds

SMI CWiMI
Centre for Water in the Minerals Industry

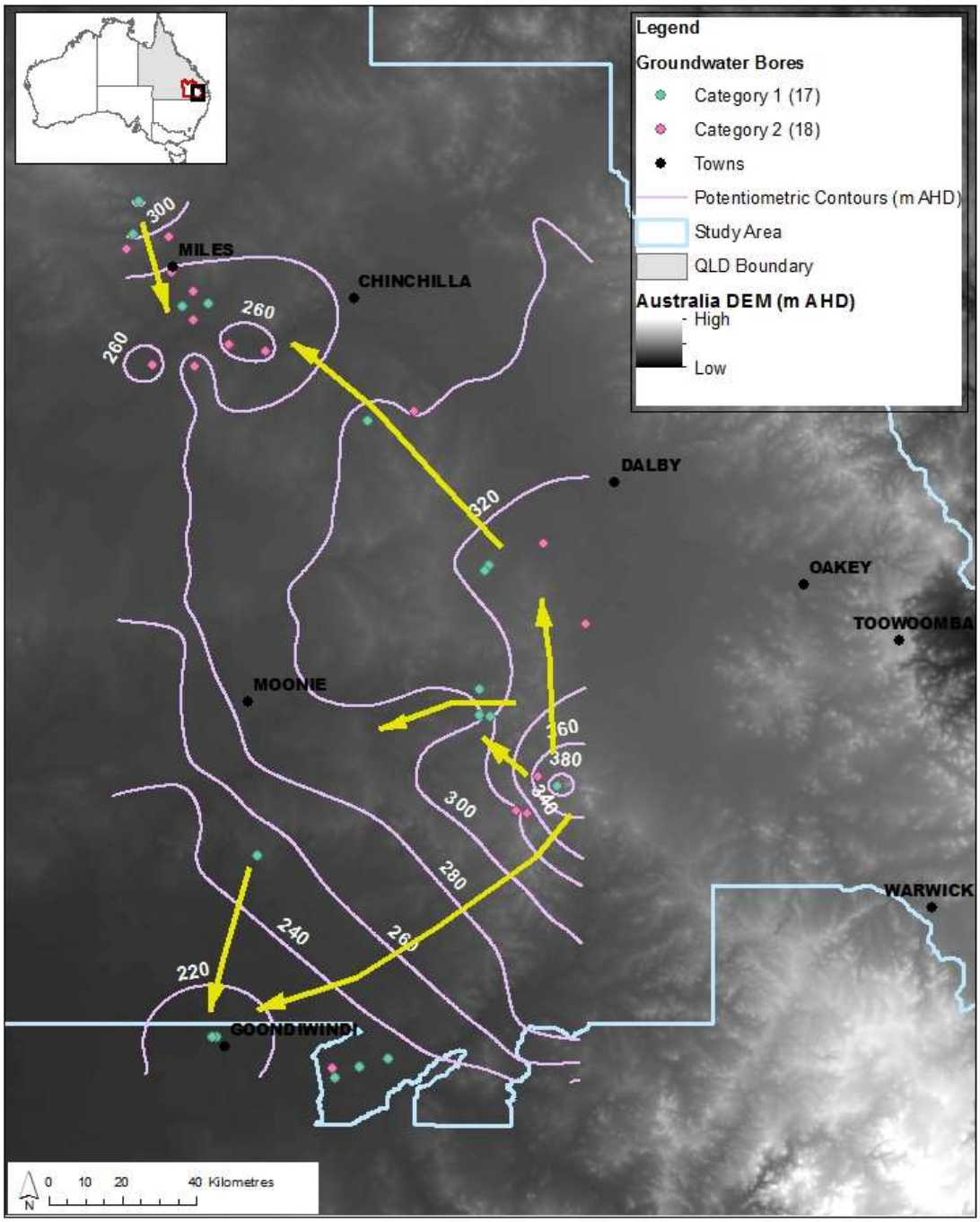

Figure 31 - Groundwater surface contours (20 m) of the Kumbarilla Beds (1995 - 2014) by ordinary kriging, with yellow arrows indicating general flow directions.

Main Range Volcanics

The groundwater surface of the Main Range Volcanics was interpolated from 373 points, the largest dataset available for any single geologic formation in the Surat Basin (Table 11). The majority of the data were located between Oakey and Warwick, and west of Toowoomba (Figure 32, Figure 33). Additional data points were found slightly north generally close to the Great Dividing Range.

Groundwater elevations varied substantially from more than 700 m AHD to less than 200 m AHD on the eastern edge of the Great Dividing Range. This variability is indicative of the topographical variability of the region, with topographical highs and steeply incised valleys in close proximity. Groundwater flow within the Main Range Volcanics exhibits a radial pattern outwards from the divide, indicating that the basalts are a potential recharge source to neighbouring aquifers. The groundwater surface contours exhibit a very similar pattern to the regional topography (Figure 33).

During the groundwater surface interpolation, anisotropic rather than isotropic behaviour of the semivariogram was identified and supported by improved cross-validation results. This anisotropic behaviour was incorporated into the kriging model, providing an explanation of the similarity between the groundwater contours and respective topography.

Table 11 - Summary statistics of the water level elevation and water level depth of the Main Range Volcanics

	Elevation (mAHD)	**Depth (m)**
Mean	492.73	-22.22
Median	476.34	-15
StdDev	80.20	20.46
Count	373	373

RECHARGE ESTIMATION IN THE SURAT BASIN

SMI CWiMI
Centre for Water in the Minerals Industry

Map of Groundwater Surface Contours (IDW) of Main Range Volcanics

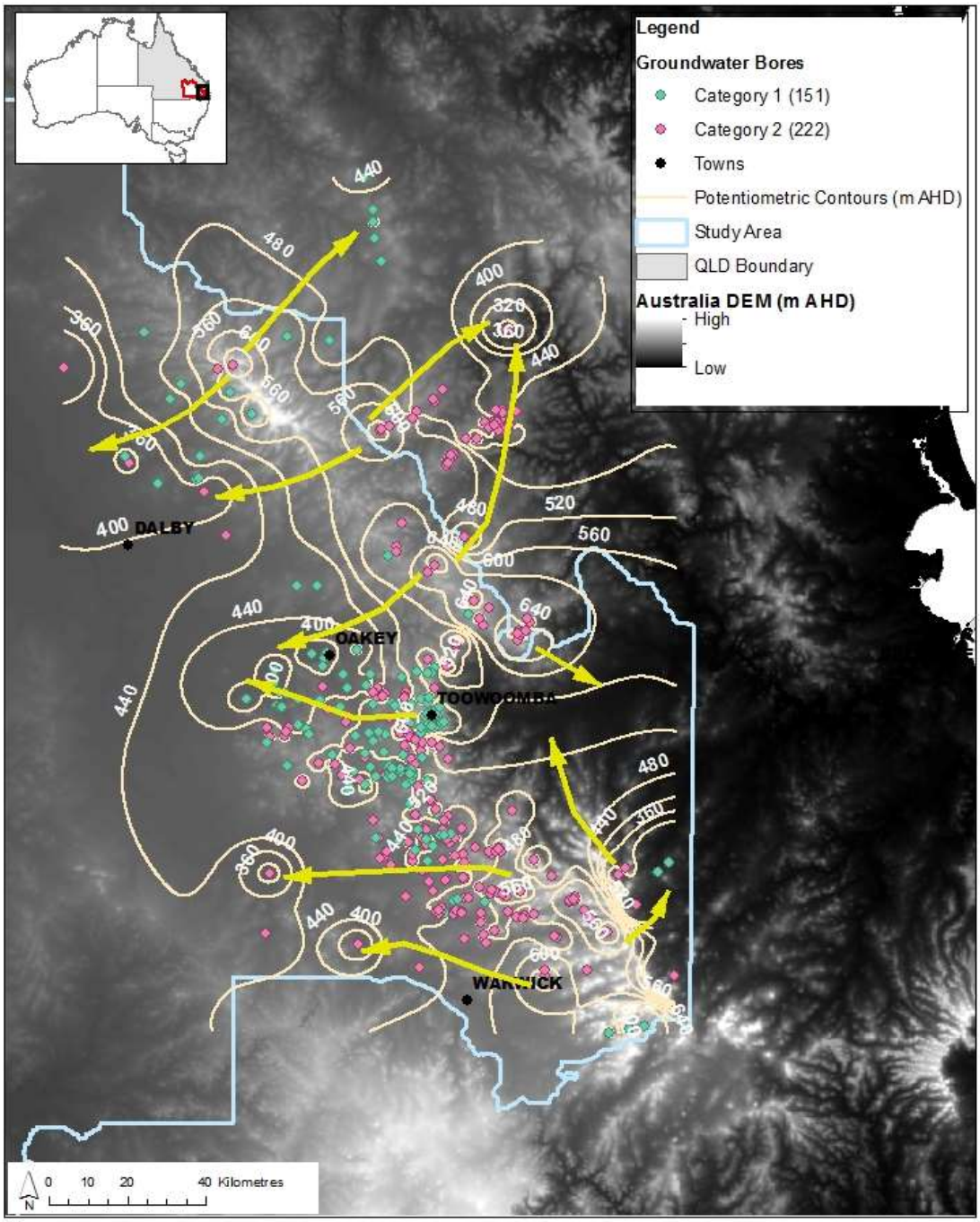

Figure 32 - Groundwater surface contours (40 m) of the Main Range Volcanics (1995 - 2014) by IDW Interpolation, with yellow arrows indicating general flow directions.

RECHARGE ESTIMATION IN THE SURAT BASIN

Map of Groundwater Surface Contours (Ordinary Kriging) of Main Range Volcanics

SMI CWiMI
Centre for Water in the Minerals Industry

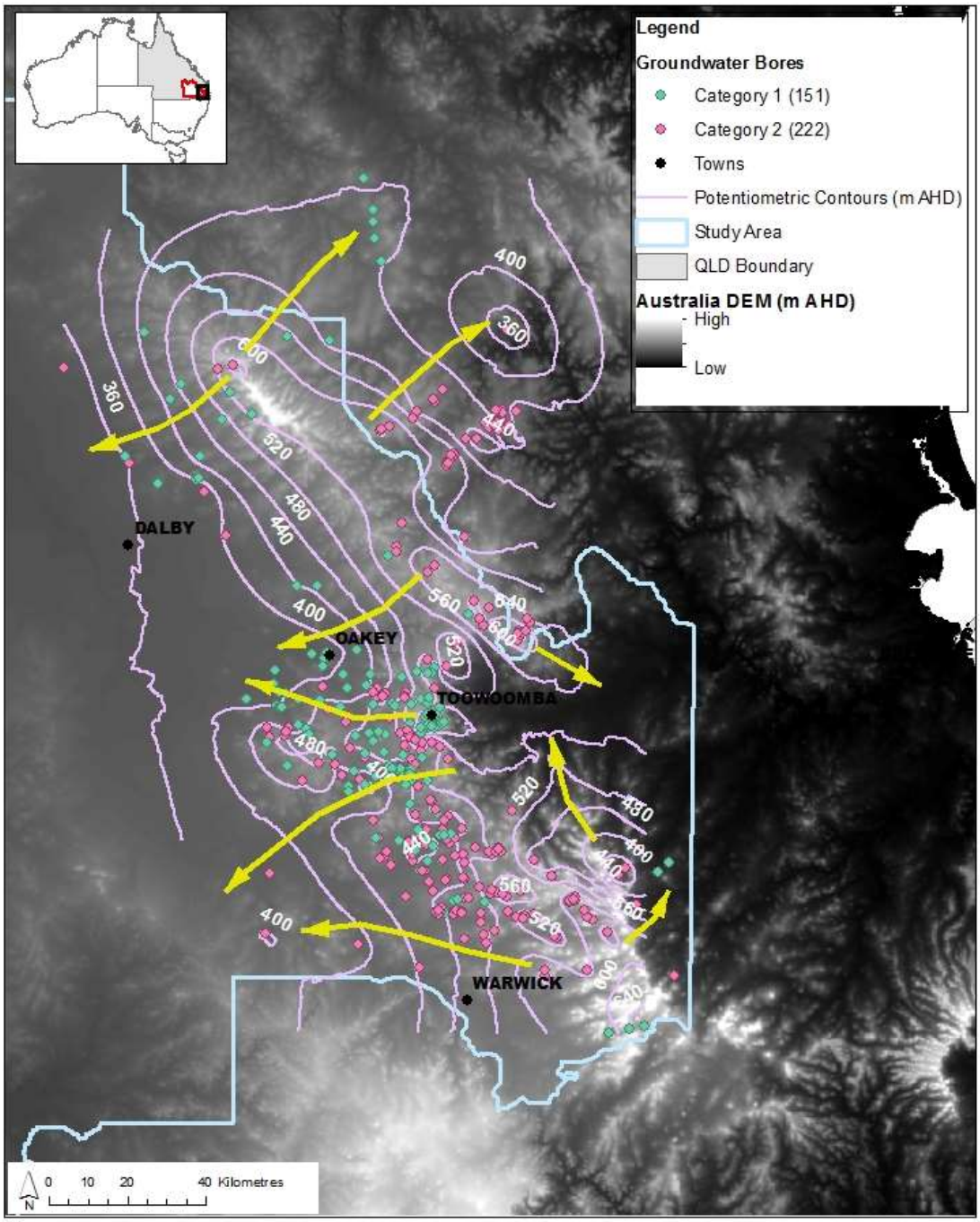

Figure 33 - Groundwater surface contours (40 m) of the Main Range Volcanics (1995 - 2014) by ordinary kriging, with yellow arrows indicating general flow directions.

Mooga Sandstone

The groundwater surface of the Mooga Sandstone was interpolated from 54 data points (Table 12), predominantly located around Roma and spread out eastwards towards Miles and Moonie (Figure 34, Figure 35). The Mooga Sandstone had the smallest variation in groundwater elevations of the all the geologic formations, with groundwater elevations varying from around 270 m AHD in the south-west to around 340 m AHD in the north. Groundwater flow is predominantly in a southerly direction for the entire Mooga Sandstone, as indicated by Quarantotto (1989). The groundwater surface interpolated by kriging does infer the possibility of westerly groundwater flow from the eastern margins (Figure 35). The limited number of data points does prevent further exploration of this trend.

Sub-artesian conditions are prevalent in the higher northern and western areas of the Mooga Sandstone. Four artesian bores are located in the lower lying central area of the geologic formation associated with the flatter valley-type landscape, as is observed in other confined aquifers such as the Gubberamunda Sandstone.

Table 12 - Summary statistics of the water level elevation and water level depth of the Mooga Sandstone

	Elevation (mAHD)	**Depth (m)**
Mean	292.28	-38.39
Median	288.05	-36.2
StdDev	16.62	25.37
Count	54	54

RECHARGE ESTIMATION IN THE SURAT BASIN

Map of Groundwater Surface Contours (IDW) of Mooga Sandstone

SMI CWiMI
Centre for Water in the Minerals Industry

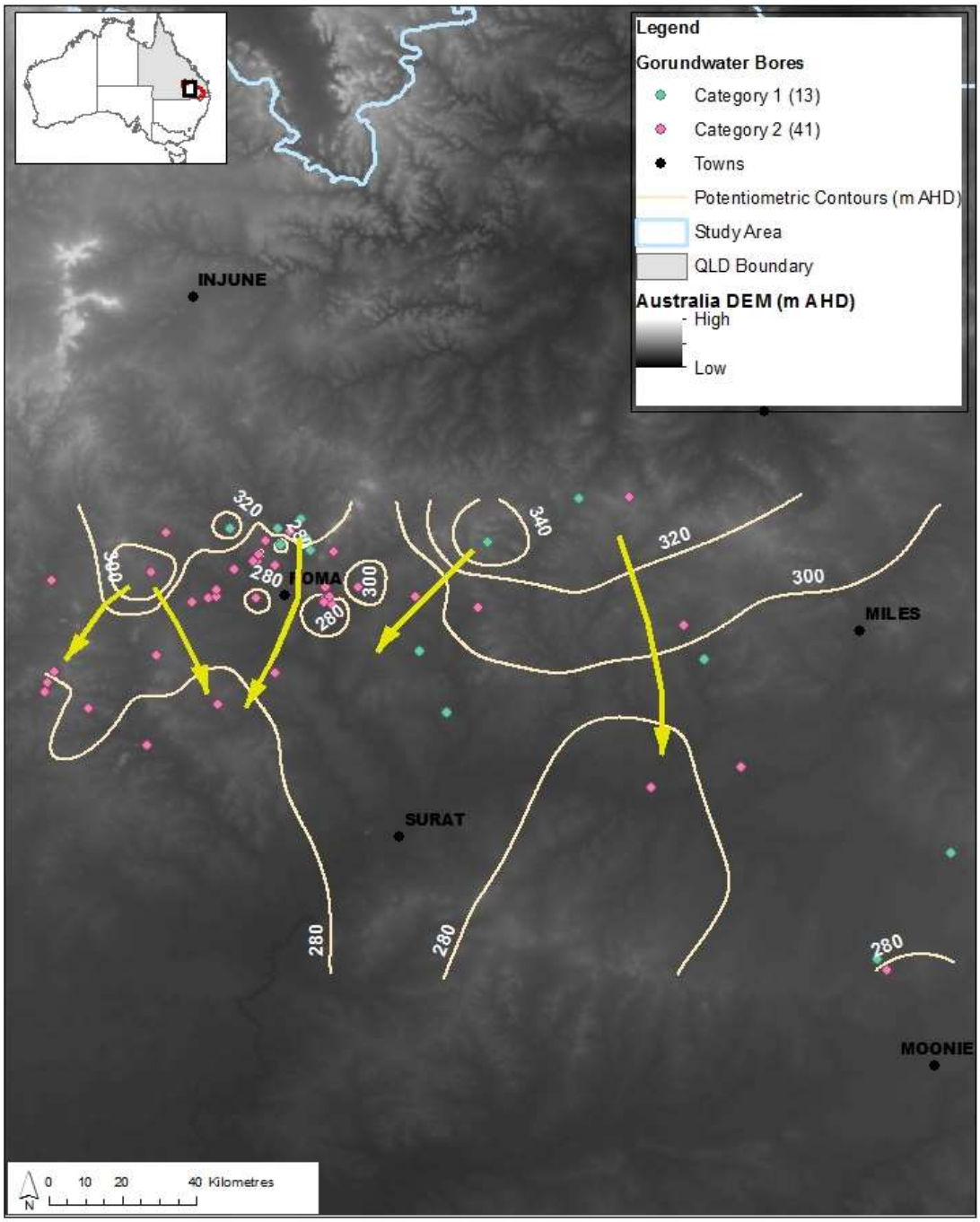

Figure 34 - Groundwater surface contours (20 m) of the Mooga Sandstone (1995 - 2014) by IDW Interpolation, with yellow arrows indicating general flow directions.

RECHARGE ESTIMATION IN THE SURAT BASIN

Map of Groundwater Surface Contours (Ordinary Kriging) of Mooga Sandstone

SMI CWiMI
Centre for Water in the Minerals Industry

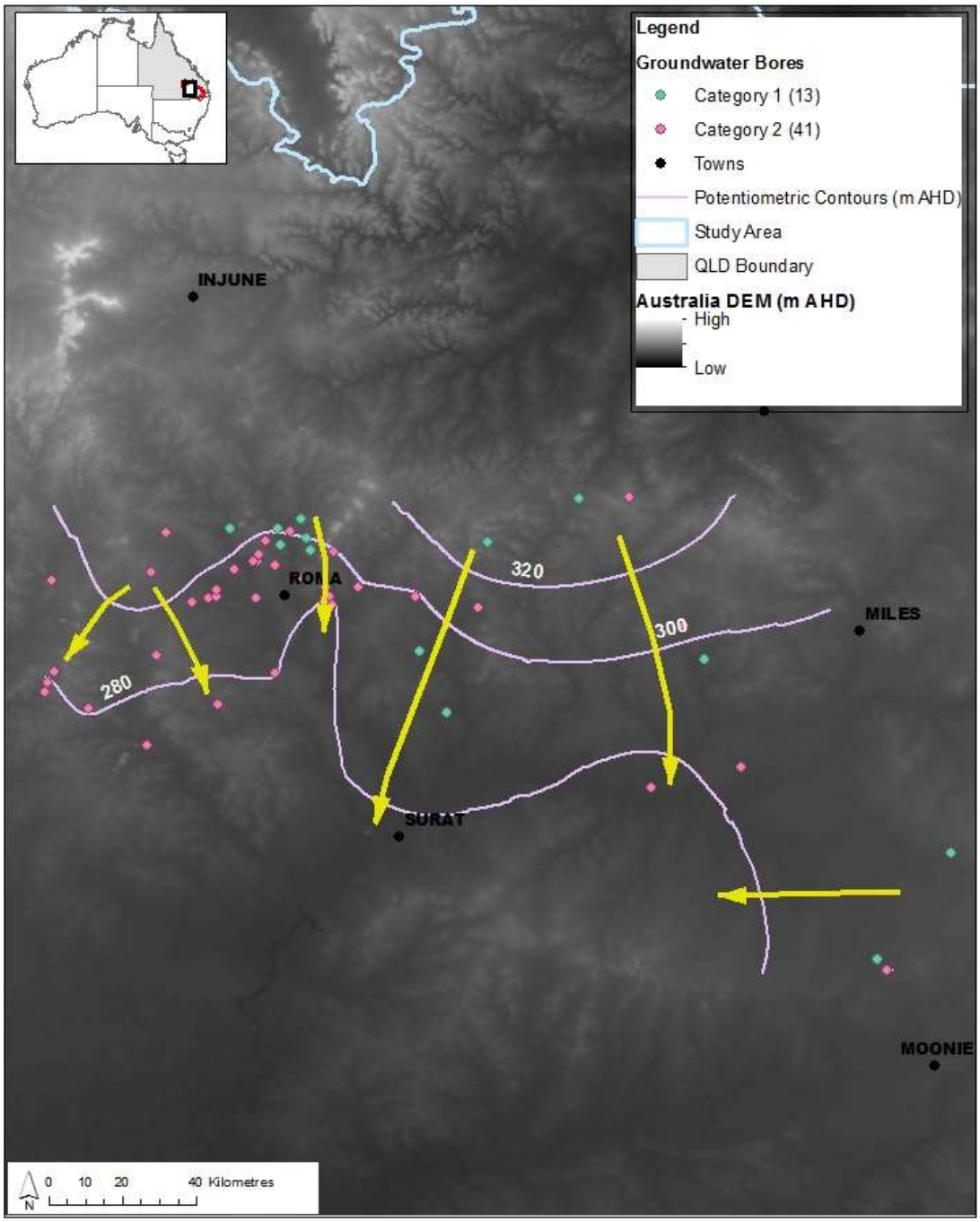

Figure 35 - Groundwater surface contours (20 m) of the Mooga Sandstone (1995 - 2014) by ordinary kriging, with yellow arrows indicating general flow directions.

Walloon Coal Measures

A total of 162 bores make up the Walloon Coal Measures 1995 to 2014 groundwater elevation dataset (Table 13). These bores are distributed between two geologic basins, both the Surat Basin to the west and Clarence-Moreton Basin to the east of the Great Dividing Range (Figure 36, Figure 37). The largest cluster of groundwater bores is located in the vicinity of Warwick, with groundwater bores extending all the way out to Wandoan in a somewhat sparse and linear arrangement. A second cluster of groundwater bores is located in the Clarence-Moreton Basin, east of the Great Dividing Range.

Table 13 - Summary statistics of the water level elevation and water level depth of the Walloon Coal Measures

	Elevation (mAHD)	**Depth (m)**
Mean	332.96	-22.69
Median	344.51	-16.15
StdDev	146.66	19.46
Count	162	162

The entire dataset was used to interpolate a groundwater surface of the Walloon Coal Measures using the IDW technique. However, groundwater bores located in the Clarence-Moreton Basin were excluded when interpolating groundwater elevations by kriging. The two subsets of groundwater bores have two distinct spatial structures associated with the two geologic basins, which is highlighted in the scatterplots of groundwater elevation vs. eastings and northings (refer to Figure 23). These distinct spatial structures made it difficult to model the spatial trend and a representative semivariogram. Considering the uncertainty on the continuity of hydrogeologic formations between the Surat and Clarence-Moreton Basins (Hodgkinson et al., 2009) and the focus of this study being the Surat Basin, the data set was split and interpolations were carried out only on the bores that were west of the divide. This reduced the dataset down from 162 to 112 data points (Category 1 with 33 points, Category 2 with 79 data points). The dataset had a strong spatial trend from south-east to north-west, best represented by a second order polynomial (ρ = 0.94 (Eastings), ρ = -0.90 (Northings)). As a result, universal kriging rather than ordinary kriging was applied, to account for the spatial trend in data.

RECHARGE ESTIMATION IN THE SURAT BASIN

Map of Groundwater Surface Contours (IDW) of Walloon Coal Measures

SMI CWiMI
Centre for Water in the Minerals Industry

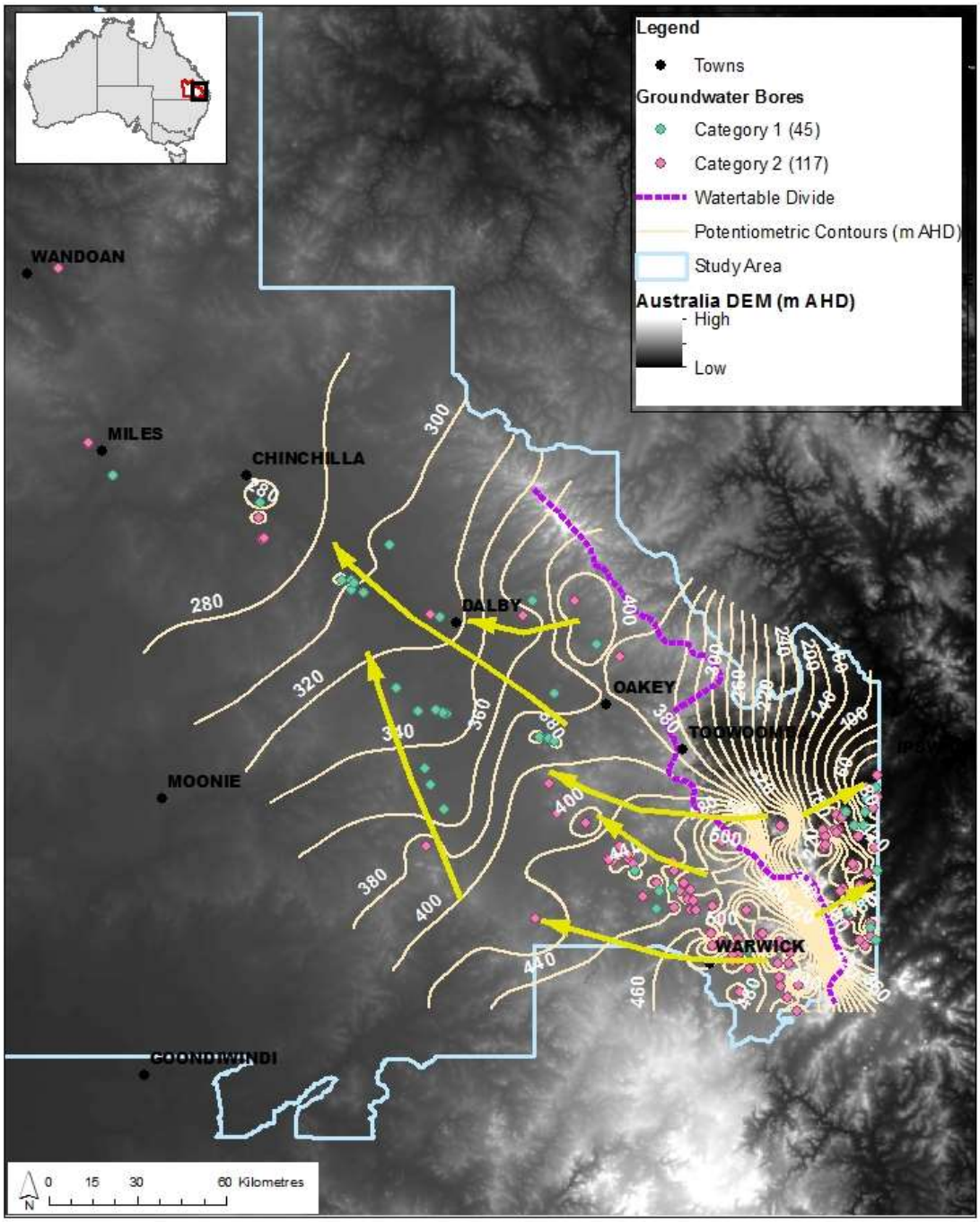

Figure 36 - Groundwater surface contours (20 m) of the Walloon Coal Measures (1995 - 2014) by IDW Interpolation, with yellow arrows indicating general flow directions.

RECHARGE ESTIMATION IN THE SURAT BASIN

Map of Groundwater Surface Contours (Universal Kriging) of Walloon Coal Measures

SMI CWiMI
Centre for Water in the Minerals Industry

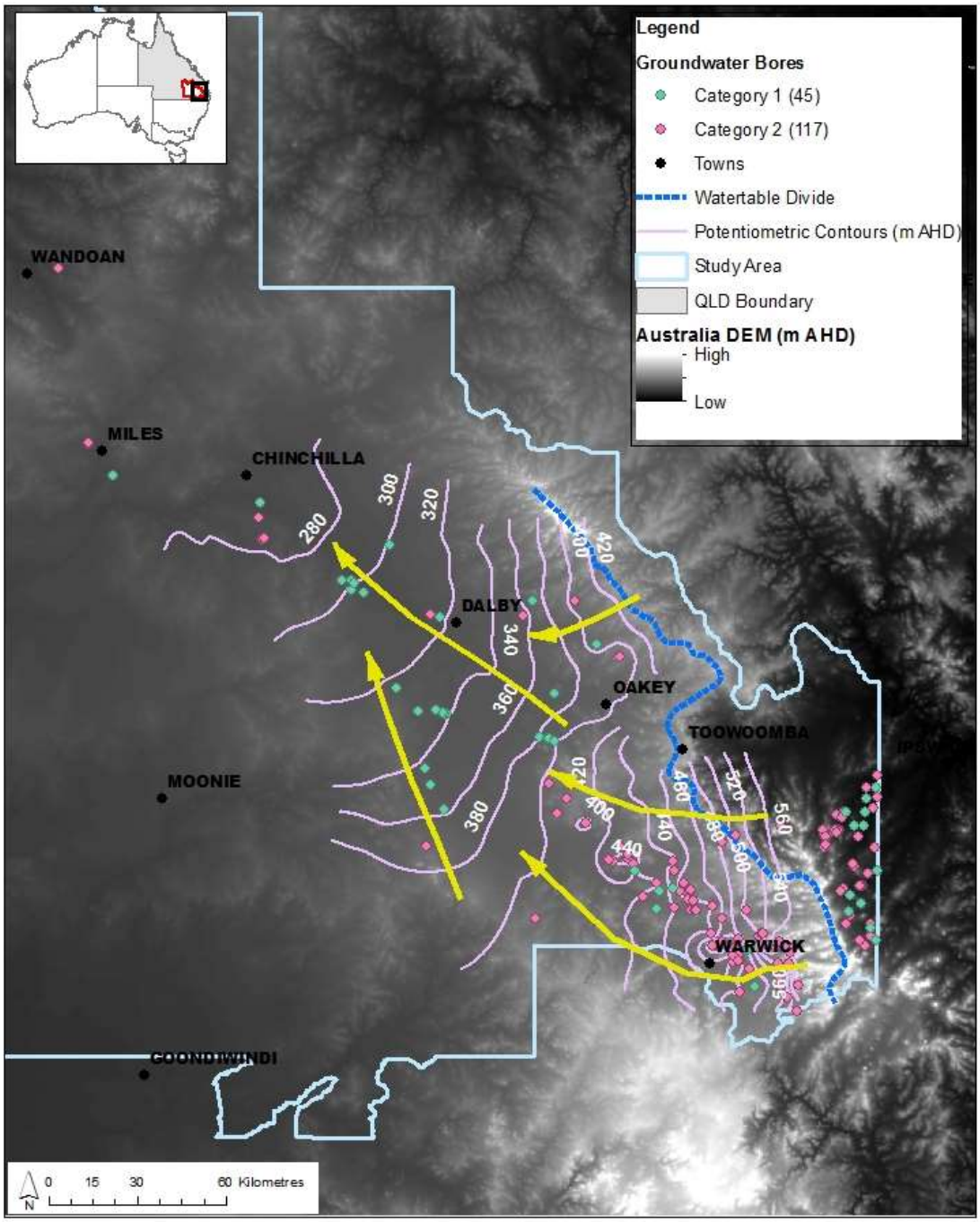

Figure 37 - Groundwater surface contours (20 m) of the Walloon Coal Measures (1995 - 2014) by universal kriging, with yellow arrows indicating general flow directions.

Groundwater potentiometric elevations varied between 260 m AHD in close proximity to Miles to approximately 590 m AHD east of Warwick in the high elevation zones. The dominant direction of groundwater flow in the Surat part of the Walloon Coal Measures was north-westerly (Figure 37). The groundwater flow directions showed similar trends to the regional topography, with westerly groundwater flows present around Dalby and Warwick. Sub-artesian conditions were prevalent throughout the entire Walloon Coal Measures.

Uncertainties, Limitations and Difficulties

Table 14 presents the cross-validation results of the kriged groundwater surfaces presented in the previous section. The quality of the geostatistical model predictions vary, with RMSEs for the Condamine River Alluvium being the best of the different geologic formations and reasonably low (RMSE = 6.1 m), followed by the Mooga Sandstone. The Main Range Volcanics have the largest prediction error (RMSE = 31.0 m) even with the largest dataset. A mean error of 1.27 m also indicates that values are being over-predicted on average. The RMSE of the other formations are around 20 m.

Table 14 - Cross validation errors for each geologic formation for all kriged surfaces

Geologic Formation	Kriging Technique	Mean Error (m)	RMSE (m)
Condamine River Alluvium	Universal	-0.014	6.1110
Gubberamunda Sandstone	Ordinary	-0.0836	22.626
Hutton Sandstone	Ordinary	0.3068	23.368
Kumbarilla Beds	Ordinary	0.0077	16.84
Main Range Volcanics	Ordinary	1.265	31.04
Mooga Sandstone	Ordinary	-0.0414	10.5442
Walloon Coal Measures	Universal	-0.2398	21.517

Currently, limited information is available on the success/difficulties of other attempts at interpolating groundwater surface elevations within the Surat and Great Artesian Basins, even though groundwater surface interpolation is not uncommon, especially with the recent CSG activity (e.g. Dafny and Silburn, 2014; Hodgkinson et al., 2010; Quarantotto, 1989; Smerdon

et al., 2012b; WorleyParsons, 2012). In addition, generally the implemented technique is either not identified or only identified in name with minimal description on the interpolation process. This limits our ability to compare the quality of the kriged groundwater surfaces in this report relative to others. Hodgkinson et al. (2010) did attempt both kriging and radial basis functions before settling for minimum curvature interpolation (i.e. spline functions), which produced better results with some manual tuning. However, minimum curvature interpolation has its own limitations, including inability for cross-validation to be performed and weak performance for closely spaced data.

Geostatistical techniques have been implemented successfully in interpolating groundwater and other environmental systems (e.g. climate) in the literature (e.g. Bohling and Wilson, 2006, 2012; Goovaerts, 2000; Hofstra et al., 2008; Kumar, 2007). For example, the Kansas Geological Survey (KGS) has been interpolating groundwater surface elevations and changes in water level of the High Plains aquifer on an annual basis for years (Bohling and Wilson, 2006, 2012). Desbarats et al. (2002) and Kumar (2007) also used kriging techniques to interpolate groundwater surface elevations, while Ahmadi and Sedghamiz (2007) used kriging to interpolate changes in groundwater levels and for time series interpolation. The studies reported RMSE values up to approximately 10 m. These values are generally smaller than those reported in this study (Table 14). However, there are substantial differences in the datasets (not all of these apply to all of the studies):

1. Higher quality data values, with groundwater levels surveyed during certain periods to allow for aquifer replenishment and over short time spans to capture the same 'event' (e.g. Bohling and Wilson (2006) surveyed 1266 wells over the winter months)
2. Larger number of data points that are more evenly distributed
3. Substantially smaller study areas
4. Higher density of data points
5. Interpolating water table levels in unconfined aquifers
6. Limited topographical variability.

There were a number of limitations, uncertainties and difficulties encountered in interpolating groundwater surfaces for the various geologic formations within the Surat Basin. These were associated with the quality of the available data, the complexity of the groundwater systems and the complexity of the interpolation techniques employed. These could explain some of the larger prediction errors. The main limitations and difficulties encountered were:

1. Temporal range of data

The data incorporated were sampled over a long period of time (20 years), with different points sampled during different events. Thus some data might reflect the average state of the aquifer over 20 years, other bores might be indicative of a flood or drought, and some might be indicative of a localised impact such as pumping. For example, some of the major outliers that were identified in the Main Range Volcanics during cross-validation were very closely spaced (less than a kilometre apart) but had groundwater elevations that differed by approximately 100m.

2. Inaccuracy in bores with only single readings taken at time of construction.

Sometimes there can be large discrepancies between these bores and neighbouring bores. Most of the datasets other than the Condamine River Alluvium were made up of single reading bores, where Category 2 data made up between 50 and 80 % of the datasets of each geologic formation.

3. Small datasets

Datasets for most of the geologic formations were generally either clustered or sparse (this was a major limitation also pointed out by WorleyParsons (2012)). Furthermore, the interpolated areas were large with variable topography, but generally a very low data point density. For example, most of the data points for the Gubberamunda Sandstone were located close to Roma, while there was only one data point in the southern parts of the Basin. This explains the peculiar groundwater surface contours in that region (Figure 27).

4. Uncertainty about the source aquifer

The aquifer assignments of all bores were wholly based on the GWDB logs and could not be checked with a Geological Model. There is doubt to the accuracy of the aquifer and stratigraphy logs of the GWDB. In some instances, the GWDB incorporates a number of different geologic formations that could not be individually identified in a single entry. The Kumbarilla Beds geologic formation is a good example of this.

5. Hydrogeologic complexity of geologic formations

The groundwater surfaces developed in this report are a simple representation of groundwater surfaces in the various geologic formations. Some of the challenges experienced in interpolation could be associated with the complexity of the geologic formation systems. For

example, in the Main Range Volcanics RN 42231660A and 42231662A are only 3 m apart but have water levels that differ by 80 m. These two bores have very different depths and are indicative of the strong vertical gradients within the volcanics. The groundwater surfaces did not explicitly account for screen depths and vertical behaviour in the geologic formations. Furthermore, no distinction was made in the interpolation between unconfined, semi-confined and confined regions which might behave differently and potentially have different spatial autocorrelation.

6. Uncertainties in locations of bores

Different bores in the Hutton Sandstone had the same spatial coordinates (RN330004A and 330005A, and RN330008A and 330009A). The quality control of the bore locations was also raised as a concern by project partners at the September 2014 project workshop.

7. Technical complexity of kriging interpolation technique

Kriging is a powerful but also complex technique that can require many inputs. Numerous parameters, especially associated with the semivariogram, need to be assumed and are at the discretion of the modeller. Hodgkinson et al. (2010) found minimum curvature functions to be better interpolators than kriging of the deeper geologic formations in the Surat Basin.

Conclusions and Recommendations

Regional flow patterns of hydrogeologic systems are important for system conceptualisation and can be used to identify potential recharge areas. This chapter demonstrated an approach for mapping regional groundwater flow patterns of geologic formations using the IDW and kriging interpolation techniques. Preliminary regional groundwater flow patterns were estimated for the Condamine River Alluvium, Main Range Volcanics, Walloon Coal Measures, Kumbarilla Beds, and the Gubberamunda, Hutton and Mooga Sandstones. However, the quality and reliability of groundwater flow patterns were limited due to the quality and quantity of available data for such an extensive area. Higher quality data are needed at both a finer temporal and spatial scale to be able to identify true groundwater flow within hydrogeologic units, and separate actual groundwater surfaces from inaccurate artefacts due to data quality such as false bulls-eyes in groundwater levels. Better identification of source aquifers and accurate groundwater well locations is also needed.

Groundwater hydrographs can be used to estimate groundwater recharge by applying the Water Table Fluctuation (WTF) method (Healy and Cook, 2002). The attraction of this method is that it is comparatively easy to use and makes no assumptions about the mechanisms by which water travels through the unsaturated zone (Healy and Cook, 2002). Therefore the presence of preferential flow paths within the unsaturated zone in no way restricts its application. The WTF method aims to be representative of recharge over several square meters around the borehole (Healy and Cook, 2002).

The rise in the water table due to rainfall (Figure 38) can be used to determine the recharge into the system. The standard equation is shown below.

$$R = S_y \frac{dh}{dt} = S_y \frac{\Delta h}{\Delta t}$$

Where *R* is equal to recharge, S_y is the specific yield and *dh/dt* is the rise in water level after a rainfall event.

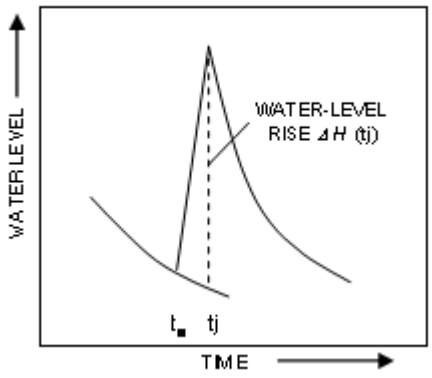

Figure 38. Water table fluctuation method (USGS, 2013)

It is important to ensure when using this method that any rise in the water table is due to a rainfall event as water tables can fluctuate due to other factors including evapotranspiration, atmospheric pressure, pumping and irrigation as well as the movement of entrapped air within the unsaturated zone (Healy and Cook, 2002) . It is recommended that any wells chosen for

analysis be located a sufficient distance away from pumping wells to ensure that water levels are not significantly lowered by pumping (Cuthbert, 2010). The circumstances under which the effect of pumping can be considered negligible are case dependent (Cuthbert, 2010).

Recharge rates are also substantially variable across the basin of interest due to differences in elevation, geology, land surface slope, vegetation and other factors (Cuthbert, 2010; Healy and Cook, 2002). Therefore the wells chosen with this method should ideally be representative of the basin as a whole (Healy and Cook, 2002) .

Limitations and Assumptions

The WTF method is best applied to shallow water tables that display sharp water level rises and declines. In some cases this method can be applied to deeper aquifers if they display seasonal water level fluctuation trends (Healy and Cook, 2002). The main assumptions in using the WTF method are:

1. Recharge rates can be calculated using water table fluctuations if it is assumed that water arriving at the water table goes immediately into storage and that all other fluxes e.g. evapotranspiration and pumping, are zero during the period of estimation (Healy and Cook, 2002).
2. Depth to water table should be low to reduce the amount of attenuation and lag that can occur after recharge events (Cuthbert, 2010).
3. Wells used for WTF should be representative of the catchment; if not, a number of wells should be used to get an average for the effects of spatial and temporal variability (Cuthbert, 2010; Healy and Cook, 2002).
4. The method is only applicable to unconfined aquifers (Healy and Cook, 2002).
5. No considerations are made for preferential flow or other flow mechanisms (Healy and Cook, 2002).
6. Specific yield values need to be determined in order for the method to be applied (Healy and Cook, 2002).

The main uncertainty with the WTF method is the specific yield value, which defines how high the water table will rise as a function of the net amount of water infiltrating the system. Its value can change between different sites within close proximity and at different depths.

There are many different methods to estimate specific yield ranging from pumping tests (Moon et al., 2004) to a simplified water balance. Due to the inherent uncertainty of this value it is recommended that several methods be utilised and that the chosen result should be representative of the in-situ conditions (Timlin et al., 2003). If there is insufficient data to complete multiple analyses a proxy method can be used to acquire a representative value. This proxy method is applied in conditions where it may be assumed that recharge is equal to rainfall. It uses the ratio of rainfall to water level rise to determine the specific yield (Gerla, 1992; Heliotis, 1989; Loheide et al., 2005; Rosenberry and Winter, 1997; Schilling and Kiniry, 2007).

$$Sy = \frac{rainfall}{water\ level\ rise}$$

The ratio method takes into account the following assumptions and recommendations:

1. Vertical infiltration (Gerla, 1992).
2. Negligible overland flow (Loheide et al., 2005; Timlin et al., 2003).
3. No change in unsaturated one storage (Loheide et al., 2005).
4. No evapotranspiration (Timlin et al., 2003).

Due to actual losses of water, this ratio generally provides an upper bound estimate of specific yield and is best calculated for a number of rainfall events to get an average specific yield value for each borehole (Timlin et al., 2003).

Methodology

As the method for calculating specific yield and groundwater recharge with WTF are highly interchangeable, many of bore selection criteria will apply to both methods and the following considerations need to be made:

1. There needs to be continuous daily readings of bore level over a significant period of time.
2. Aquifers must be unconfined. The depth to water table should be less than 20m or there should be significant evidence to prove that there is no confining layer. This will reduce the errors due totime lags, storage effects and lateral movement of water.
3. There needs to be a rainfall monitoring station in close proximity to collect rainfall rates as well as monitoring if the rise in water level is due to rainfall or other factors.

In order to get consistent results the following criteria were applied for borehole selection

4. Boreholes with obvious pumping or erratic levels over a daily period will be neglected. This includes pressure effects and earth tides.
5. Where possible, water years were used to get an accurate measure of recharge.
6. Appropriate boreholes from Kellett et al. (2003) were also used to determine if the method gave a reasonable estimate of specific yield.
7. Specific yield values calculated were compared to values in literature to determine if results are reasonable. These representative values are shown in Table 15 and Table 16.

The WTF method was applied to bores in the Main Range Volcanic area near Toowoomba where suitable groundwater hydrographs were readily available. The locations of the bores closest to Toowoomba are shown in Figure 39 along with the location of nearby “pumping” bores. The method could in future be extended to other aquifers that meet the bore selection criteria.

Table 15 - Specific Yield Values (Morris and Johnson, 1967)

Material	**Specific Yield (%)**
Gravel, coarse	21
Gravel, medium	24
Gravel, fine	28
Sand, coarse	30
Sand, medium	32
Sand, fine	33
Silt	20
Clay	6
Sandstone, medium	27
Sandstone, fine grained	21
Schist	26

Table 16 - Specific yield values (Heath, 1983)

Material	**Specific Yield (%)**
Soil	40
Clay	2
Sand	22
Gravel	19
Limestone	18
Sandstone (unconsolidated)	6
Granite	0.09
Basalt (young)	8

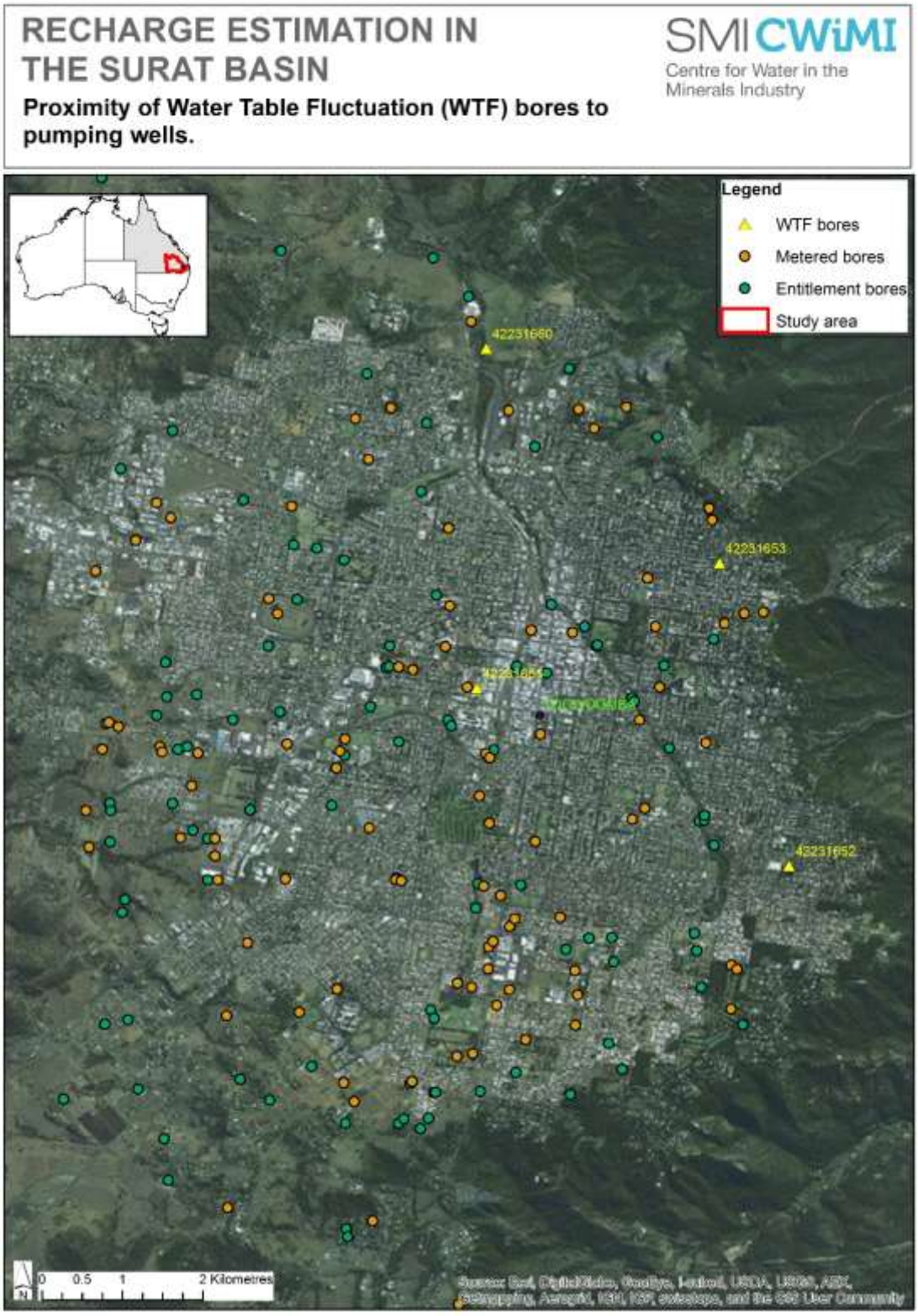

Figure 39 - Location of WTF bores close to Toowoomba

Results

The average recharge and specific yield values for the bore hydrographs analysed are displayed in Table 17. The annual recharge estimates are provided in Table 18.

Table 17 - Groundwater bore information

RN	Latitude	Longitude	Sy	Average Recharge (mm/year)	Years of Data	Aquifer
42231251	-27.694	151.907	0.127	13.4	1.5	Main Range Volcanics
42231655	-27.566	151.945	0.34	5.5	4	Main Range Volcanics
42230974	-27.705	151.860	0.085	9.44	5	Main Range Volcanics
42231652	-27.586	151.980	0.142	25.75	4.5	Main Range Volcanics
42231653	-27.552	151.972	0.043	21.3	4	Main Range Volcanics
42231478	-27.521	151.620	0.271	5.95	2	Main Range Volcanics
42231660	-27.528	151.946	0.433	37.4	.5	Main Range Volcanics
42220061	-26.409	148.655	0.233	4.2	4	Mooga Sandstone

Table 18 - Annual recharge values

RN	Year	Type of Data	Recharge (mm)
42231251	2011-2012	All daily readings	13.4
42231655	2009-2010	Water year	5.3
	2010-2011	Partial water year	7.3
	2011-2012	Water year	3.5
	2012-2013	Water year	5.8
42230974	2008-2009	Water year	4
	2009-2010	Water year	11.5
	2010-2011	Water year	11.4
	2011-2012	Water year	6.5
	2012-2013	Water year	13.8
42231652	2009	Partial year	10.7
	2010	Partial year	25.5
	2010-2011	Partial water year	19.1
	2011-2012	Water year	12.4
	2012-2013	Water year	46
42231653	2009-2010	Water year	28.2
	2010-2011	Partial water year	11.3
	2011-2012	Water year	Pumping?
	2012-2013	Water year	24.5
42231478	1993-1994	Initial data + water year	7.5
	1994-1995	Water year	4.4
42220061	2005-2006	Water year	2.1
	2008-2009	Water year	4
	2009-2010	Water year	4.1
	2010-2011	Water year	27.5
42231660	2009	Partial Year	37.4

Discussion

In determining if the ratio method was giving reasonable results a comparison was taken from borehole RN42220061 which is a shallow unconfined aquifer within the Mooga Sandstone. RN42220061 has an automated water level recorder as well as a rainfall data collector so measurements can be taken daily. This data can either be accessed from the Ground Water Database (GWDB) or the Department of Natural Resources and Mines (DNRM) Water Monitoring Portal. RN42220061 was used in the Kellett et al. (2003) report and was assumed to have a specific yield of 0.2. The value calculated from the ratio method of 0.23 corresponds closely to the Kellett et al. (2003) report. WTF recharge estimates were also compared and it was found that the Kellett et al. (2003) report gave recharge rates between 2.6 and 4.7 mm/yr which are comparable with the average found by applying the specific yield proxy method of 4.2 mm/yr.

Another bore from the Kellett et al. (2003) report was also considered (bore RN42220058) but there were too many fluctuations in the data for it to be properly assessed. Bore RN13030613 appears to be a confined or very deep aquifer so it was also dismissed even though it has continuous monitoring. Of the Kellett et al. (2003) report only these 3 boreholes are within the area of interest for this project.

The large specific yield value for RN42231655 of 0.34 was unexpected when compared with the specific yield for other bores nearby. This value is similar to values expected for soils or sand (Table 15 and Table 16). Analysis of the bore log enabled the identification of “honeycombed basalt” which explains the higher specific yield for this bore.

Most of the bores that were analysed are located in urban areas and this could lead to uncertainties in results. The recharge rates in urban areas can be much larger than expected even with the increased runoff and reduced surface area due to impermeable buildings (Lerner, 1990). Water can be introduced into the system through leaking service networks (mains or septic) as well as over-irrigation of gardens for aesthetic reasons (Lerner, 1990) . This could be problematic as the WTF method computes both infiltration from rainwater and domestic wastewater and it is recommended that geochemical analysis and interpretation can be used as a means to separate the two sources (Diouf et al., 2012). Upper and lower bound recharge estimation is also recommended due to the possibility of large uncertainties that can occur from leaking services in urban areas (Lerner, 1990) .

Evapotranspiration has not been considered in our hydrograph analysis approach and further testing is recommended. As most of the rainfall seems to occur within the summer months it would be hard to find events that occur within the minimal evapotranspiration periods, which has been suggested in some of the literature. As evapotranspiration and runoff have not been considered it may mean that the recharge estimates are upper bounds and it would be advisable to cross check these results with other methods.

Some water years included major flood events. Most of the partial water years are because of the halt in readings due to flooding. This is another potential source of bias when estimating time-averaged recharge using this approach.

Conclusions

The Water Table Fluctuation (WTF) method was applied based on the specific yield proxy method and an estimate of recharge was found for the Toowoomba and surrounding basalts. The method gave recharge estimates comparable to the independent estimates of Kellett et al. (2003). There are many assumptions in this method, which means that ideally results would be part of a multi-method approach to recharge estimation.

Even though the specific yield proxy method has many drawbacks and makes many assumptions it is still the most viable option to get representative in-situ values of specific yields. Other methods can then be applied to validate these values such as laboratory drainage testing of aquifer material or pump testing as mentioned previously.

Analysis of Remote Sensing Data

Introduction

Remote sensing has been a widely applied measurement tool within hydrology. Remote sensing cannot directly measure groundwater recharge; instead the data must be able to account for the other major elements in the water balance (evapotranspiration, surface runoff, soil water storage, surface storage and precipitation) and recharge inferred from this (Becker, 2006). Given that these elements are poorly constrained (especially runoff and soil water storage), remote sensing data are often combined with a simple water and energy balance modelling framework in order to derive recharge estimates (e.g. Bastiaanssen et al. (1998)).

This section investigates the spatial and temporal variability of recharge throughout the whole Surat, and for separate geological units (Walloon – Injune units, and Main Range Volcanics). Since the data available from remote sensing only allow a water balance in the top ~2 meters of soil, groundwater recharge here is more precisely called ”deep drainage”.

Methods

The combined remote sensing and model product from CSIRO, the Australian Water Availability Project (http://www.csiro.au/awap/) is utilised here. This dataset provides the past and present soil moisture and all water fluxes contributing to changes in soil moisture (precipitation, transpiration, soil evaporation, surface runoff and deep drainage), across the entire Australian continent at a spatial resolution of 5 km. The timescales of output availability are monthly and annually, 1900 – present. The data – model fusion methods, calibration, and uncertainties are described in detail within Raupach et al. (2009).

Briefly, the WaterDyn25M (version August 2008) is constructed as the mass balance interaction between two soil depths (M1 and M2):

$$\underbrace{dW_1/dt}_{\text{Change of soil water in layer 1}} = \underbrace{F_{WPrec}}_{\text{Precipitation}} - \underbrace{F_{WTra1}}_{\text{Transpiration from layer 1}} - \underbrace{F_{WSoil}}_{\text{Soil Evaporation}} - \underbrace{F_{WRun}}_{\text{Surface Runoff}} - \underbrace{F_{WLch1}}_{\text{Leaching from layer 1 to 2}} \qquad \text{(M1)}$$

$$\underbrace{dW_2/dt}_{\text{Change of soil water in layer 2}} = \underbrace{F_{WLch1}}_{\text{Leaching from layer 1 to 2}} - \underbrace{F_{WLch2}}_{\text{Deep Drainage}} - \underbrace{F_{WTra2}}_{\text{Transpiration from layer 2}} \qquad \text{(M2)}$$

M1 is the shallow soil layer, typically between 0 and 0.2m depth, and M2 is the deeper soil layer, typically 0.2 to 1.5m depth. The variable of interest here is deep drainage, which in this model is the residual drainage from the M2 mass balance.

Soil properties defining the soil moisture balance and deep drainage rates are derived from the digital Atlas of Australian Soils (McKenzie and Hook, 1992; McKenzie et al., 2000). This atlas classifies Australian soils into ~700 soil types, and is translated into soil physical properties using pedotransfer functions. Vegetation is also a critical component of the deep

drainage estimates, with the fractional vegetation cover typically derived from the Fraction of Absorbed Photosynthetically Active Radiation (FAPAR) from the SeaWiFS satellite.

Spatial deep drainage estimates are produced as whole record (~100 year) averages, as well as example 'wet' (2011) and 'dry' (2006) years to illustrate the influence of climatic variability on deep drainage for: 1. The entire Surat Basin, 2. the Walloon – Injune outcrop areas, and 3. the Main Range Volcanics Basalt outcrop areas.

Spatial Recharge Estimates

The deep drainage estimates presented in this section have been produced by CSIRO as part of the Australian Water Availability Project (http://www.csiro.au/awap/). This data set can be requested directly from CSIRO.

Whole Surat: Spatial average, wet and dry years

Taking the Surat as a whole, on average (1900 – 2014) high deep drainage estimates occur within the SE Main Range Volcanics as well as those NW of Toowoomba (near Oakey), the upper Condamine, within channel segments to the north of the Basin and across the surface catchment divides (Fitzroy catchment), and in the far NW of the Basin. Figure 40 shows the spatial variation of annual average deep drainage estimates across the Surat. The mean value over the whole Surat is 11 ± 7.9 mm/year (where the latter value is the standard deviation representing the spatial variation of the annual average value), although the distribution is highly skewed towards lower values. For the above average precipitation year (2011), mean deep drainage increased to 64.1 ± 39.7 mm/yr, and the distribution becomes more distinctly bimodal (Figure 41). In this example, high deep drainage values expanded across the whole length of the Main Range Volcanics, the upper Condamine, and much of the NW of the basin. Looking at 2006 as an example of a very dry year, the distribution of deep drainage values is even more positively skewed, and the mean deep drainage drops to 2.6 ± 3.1 mm/yr (Figure 42). Higher deep drainage values (~10 – 20 mm/yr) in this case are restricted to isolated pockets around the main river channels, Oakey and the northern Main Range Volcanics, and a small area west of Chinchilla. The maximum annual average over the Surat at this 5 km^2 scale was 105 mm/year (in the Main Range Volcanics), compared to the mean of 11 mm/year and minimum of 0.5 mm/year; confirming the importance of considering spatial variations.

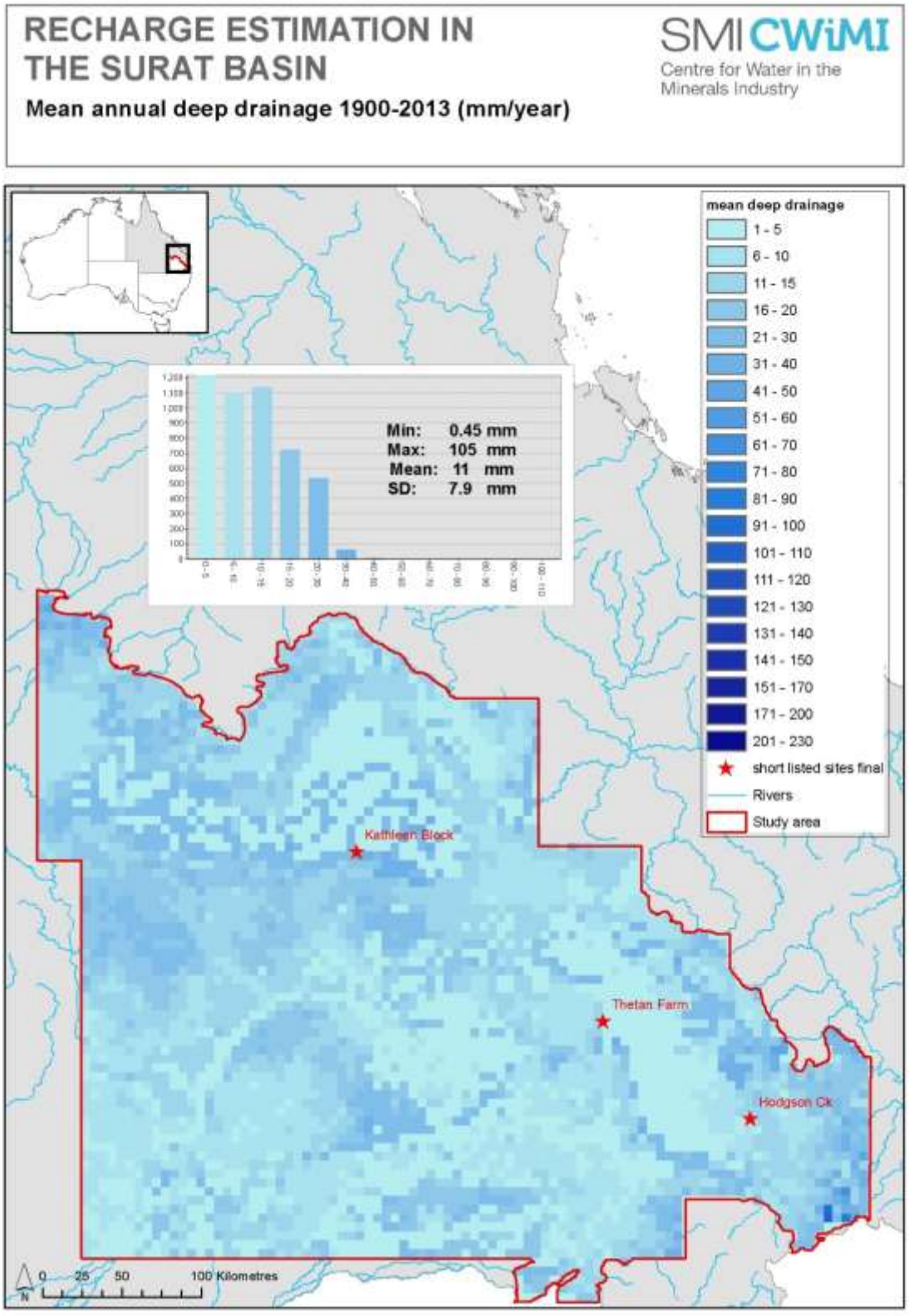
RECHARGE ESTIMATION IN THE SURAT BASIN
Mean annual deep drainage 1900-2013 (mm/year)
SMI CWiMI
Centre for Water in the Minerals Industry
mean deep drainage
1 - 5
6 - 10
11 - 15
16 - 20
21 - 30
31 - 40
41 - 50
51 - 60
61 - 70
71 - 80
81 - 90
91 - 100
101 - 110
111 - 120
121 - 130
131 - 140
141 - 150
151 - 170
171 - 200
201 - 230
short listed sites final
Rivers
Study area
Min: 0.45 mm
Max: 105 mm
Mean: 11 mm
SD: 7.9 mm
Kathleen Block
Thelan Farm
Hodgson Ck
0 25 50 100 Kilometres
N

Figure 40 - Average annual deep drainage estimates for the whole Surat CMA between 1900 – 2013 (data source: CSIRO AWAP 2014).

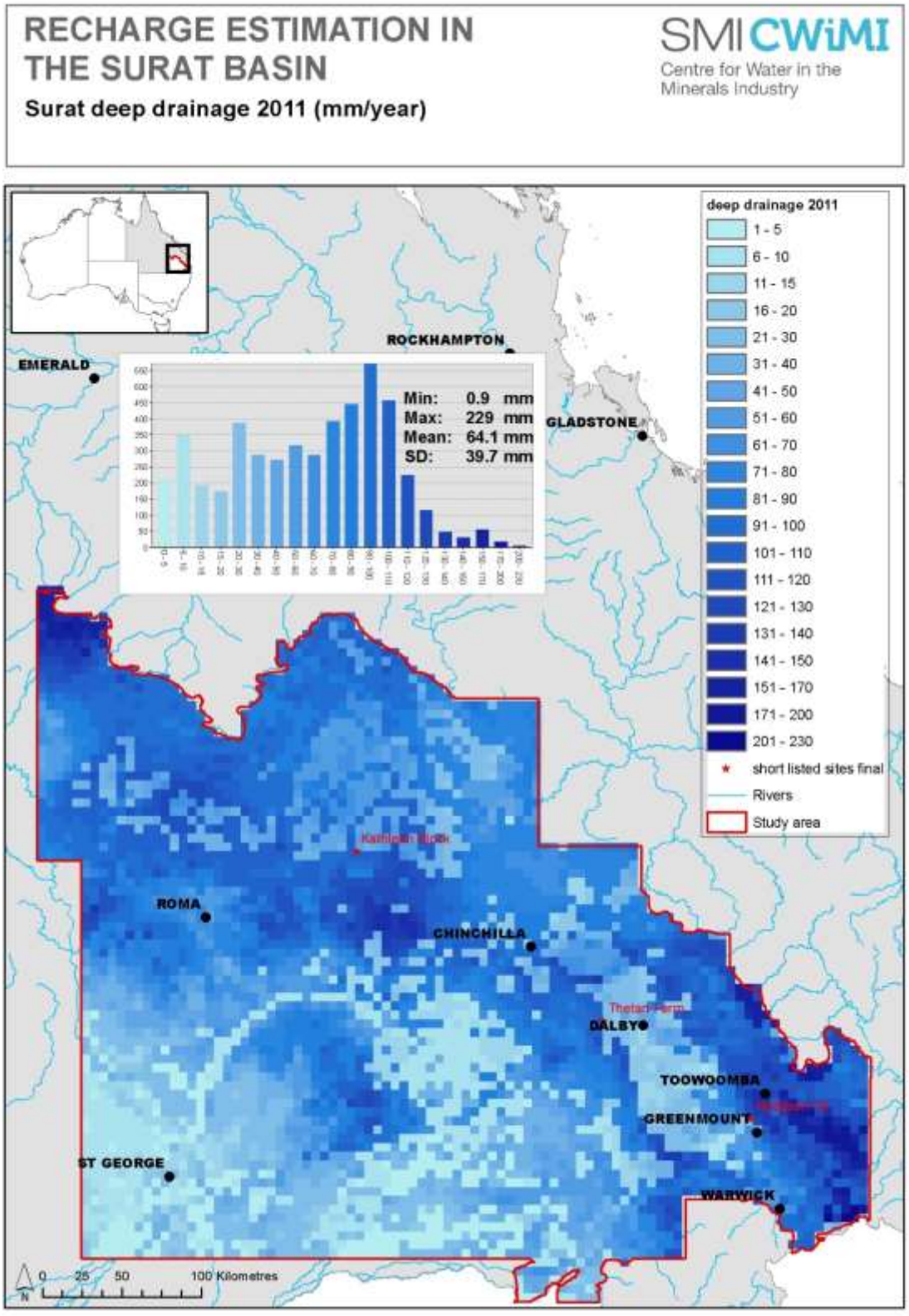
RECHARGE ESTIMATION IN THE SURAT BASIN
Surat deep drainage 2011 (mm/year)
SMI CWiMI
Centre for Water in the Minerals Industry
deep drainage 2011
1 - 5
6 - 10
11 - 15
16 - 20
21 - 30
31 - 40
41 - 50
51 - 60
61 - 70
71 - 80
81 - 90
91 - 100
101 - 110
111 - 120
121 - 130
131 - 140
141 - 150
151 - 170
171 - 200
201 - 230
short listed sites final
Rivers
Study area
Min: 0.9 mm
Max: 229 mm
Mean: 64.1 mm
SD: 39.7 mm
ROCKHAMPTON
EMERALD
GLADSTONE
ROMA
CHINCHILLA
DALBY
TOOWOOMBA
GREENMOUNT
ST GEORGE
WARWICK
0 25 50 100 Kilometres
N

Figure 41 - Average annual deep drainage estimates for the whole Surat CMA in an example wet year – 2011 (data source: CSIRO AWAP 2014).

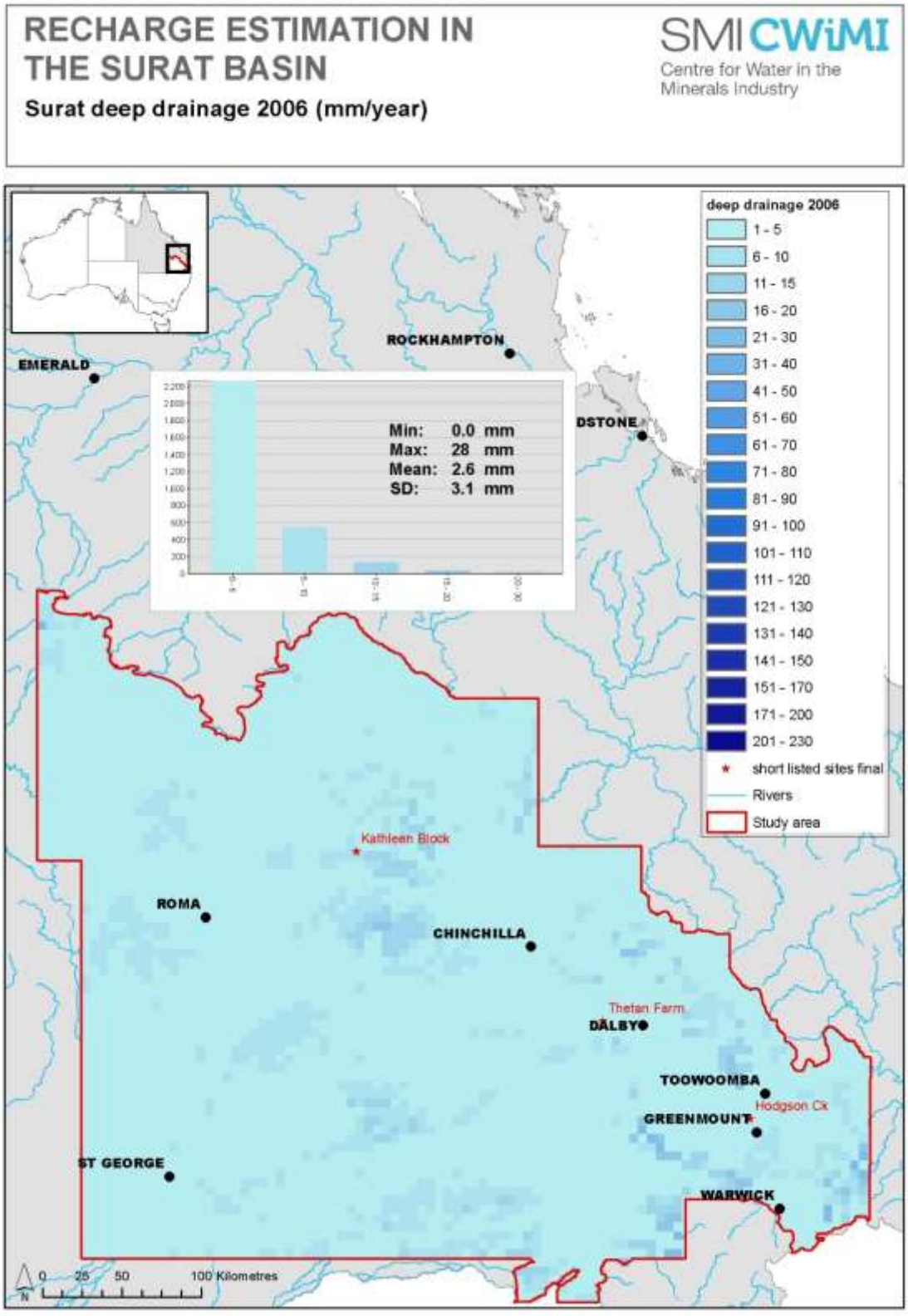
RECHARGE ESTIMATION IN THE SURAT BASIN
Surat deep drainage 2006 (mm/year)
SMI CWiMI
Centre for Water in the Minerals Industry
deep drainage 2006
1 - 5
6 - 10
11 - 15
16 - 20
21 - 30
31 - 40
41 - 50
51 - 60
61 - 70
71 - 80
81 - 90
91 - 100
101 - 110
111 - 120
121 - 130
131 - 140
141 - 150
151 - 170
171 - 200
201 - 230
short listed sites final
Rivers
Study area
Min: 0.0 mm
Max: 28 mm
Mean: 2.6 mm
SD: 3.1 mm
ROCKHAMPTON
EMERALD
DSTONE
Kathleen Block
ROMA
CHINCHILLA
Thetan Farm
DALBY
TOOWOOMBA
Hodgson Ck
GREENMOUNT
ST GEORGE
WARWICK
0 25 50 100 Kilometres
N

Figure 42 - Average annual deep drainage estimates for the whole Surat CMA in an example dry year – 2006 (data source: CSIRO AWAP 2014).

Walloon Coal Measures & Injune Creek Group: Average, wet and dry years

The combined Walloon and Injune beds deep drainage averages are difficult to evaluate spatially given the limited and patchy outcrop, especially in the SE of the basin, although here the deep drainage appears to be higher towards the east in association with the Main Range Volcanics (Figure 43). Within the north, higher deep drainage areas are quite discrete along channel networks, and become less discrete towards the west. The long term mean deep drainage exclusively for the Walloon – Injune units is 11.4 ± 10 mm/yr, with the distribution strongly positively skewed towards lower deep drainage estimates, although the higher deep drainage tail is slightly bimodal. During the wet example year there is a clear response towards increased deep drainage within the NW of the basin outcrop, and this is reflected in the shift towards a slightly negatively skewed (i.e. towards higher deep drainage), albeit bimodal distribution (Figure 44). This response is also clear from the very large shift in the mean outcrop deep drainage to 73.5 ± 32.1 mm/yr. In contrast, during the dry example year, the mean deep drainage is greatly reduced to 3.9 ± 3 mm/yr, and the resulting distribution of deep drainage is extremely positively skewed (Figure 45).

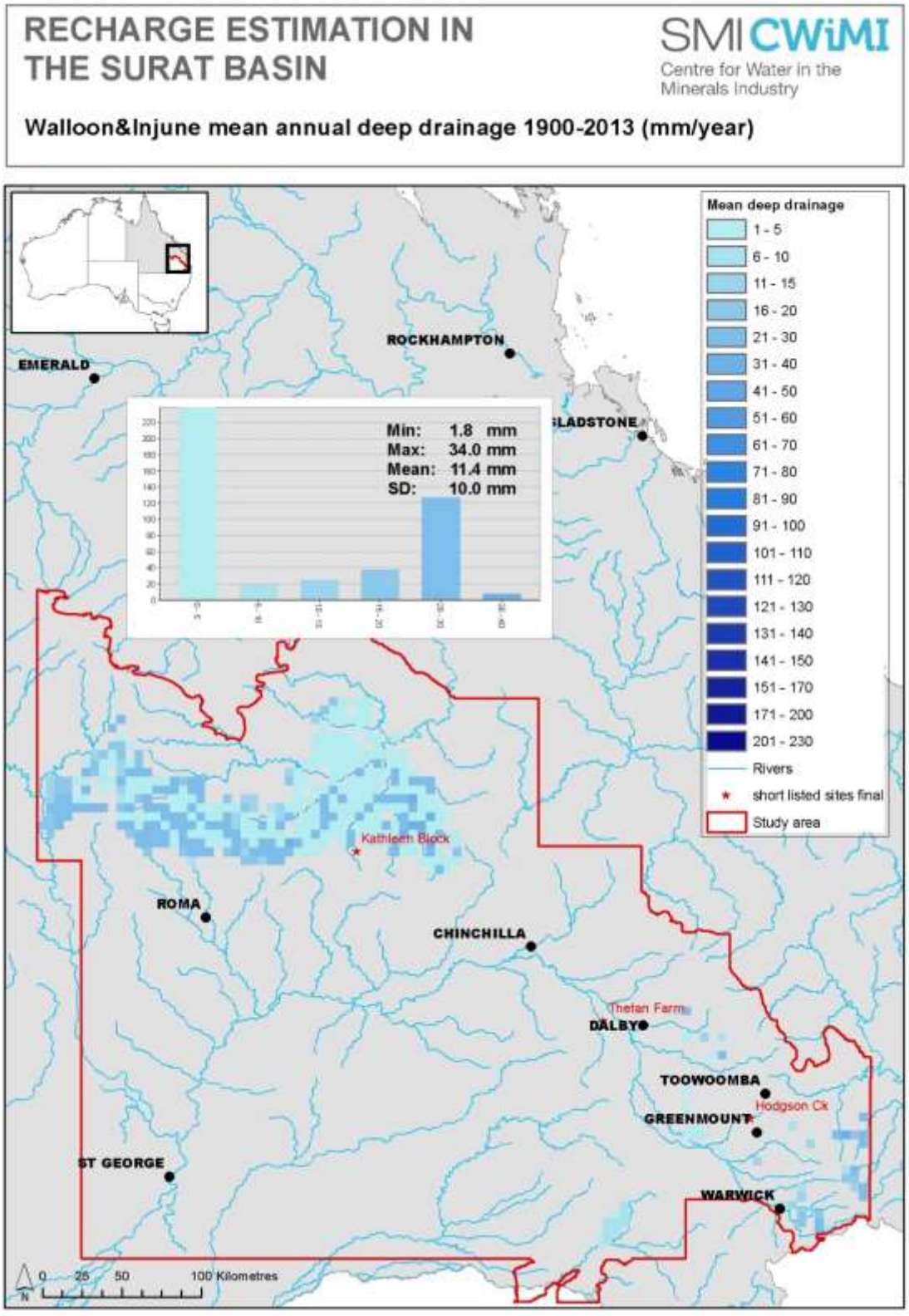
RECHARGE ESTIMATION IN THE SURAT BASIN
SMI CWiMI
Centre for Water in the Minerals Industry
Walloon&Injune mean annual deep drainage 1900-2013 (mm/year)
Mean deep drainage
1 - 5
6 - 10
11 - 15
16 - 20
21 - 30
31 - 40
41 - 50
51 - 60
61 - 70
71 - 80
81 - 90
91 - 100
101 - 110
111 - 120
121 - 130
131 - 140
141 - 150
151 - 170
171 - 200
201 - 230
Rivers
short listed sites final
Study area
Min: 1.8 mm
Max: 34.0 mm
Mean: 11.4 mm
SD: 10.0 mm
ROCKHAMPTON
EMERALD
GLADSTONE
Kathleen Block
ROMA
CHINCHILLA
Thetan Farms
DALBY
TOOWOOMBA
Hodgson Ck
GREENMOUNT
ST GEORGE
WARWICK
0 25 50 100 Kilometres
N

Figure 43 - Average annual deep drainage estimates for the Walloon Coal Measures and Injune Creek Group geologic units between 1900 – 2013 (data source: CSIRO AWAP 2014).

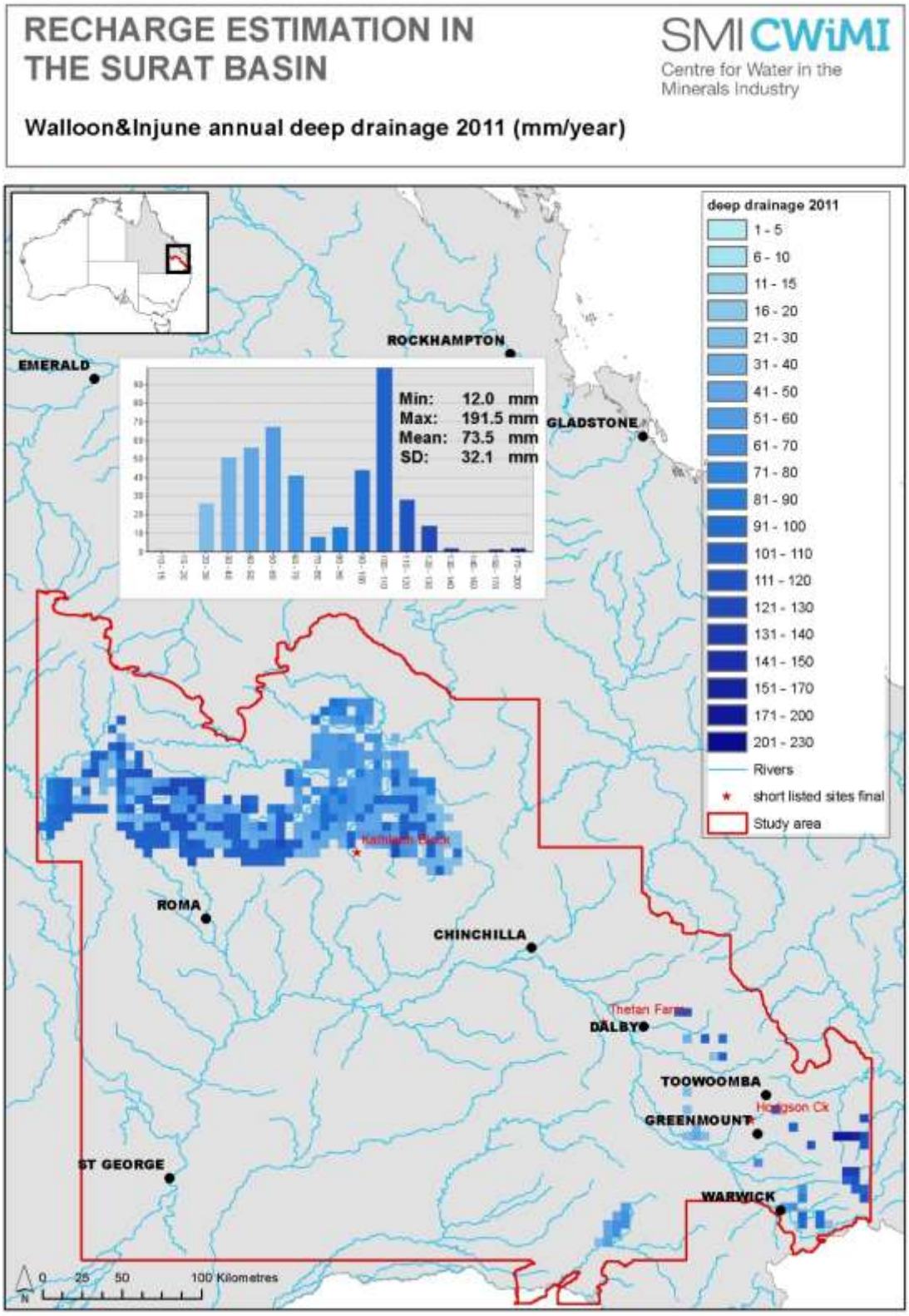
RECHARGE ESTIMATION IN THE SURAT BASIN
SMI CWiMI
Centre for Water in the Minerals Industry
Walloon&Injune annual deep drainage 2011 (mm/year)
deep drainage 2011
1 - 5
6 - 10
11 - 15
16 - 20
21 - 30
31 - 40
41 - 50
51 - 60
61 - 70
71 - 80
81 - 90
91 - 100
101 - 110
111 - 120
121 - 130
131 - 140
141 - 150
151 - 170
171 - 200
201 - 230
Rivers
short listed sites final
Study area
Min: 12.0 mm
Max: 191.5 mm
Mean: 73.5 mm
SD: 32.1 mm
ROCKHAMPTON
EMERALD
GLADSTONE
ROMA
CHINCHILLA
DALBY
TOOWOOMBA
GREENMOUNT
WARWICK
ST GEORGE
0 25 50 100 Kilometres
N

Figure 44 - Average annual deep drainage estimates for the Walloon Coal Measures and Injune Creek Group geologic units in an example wet year – 2011 (data source: CSIRO AWAP 2014).

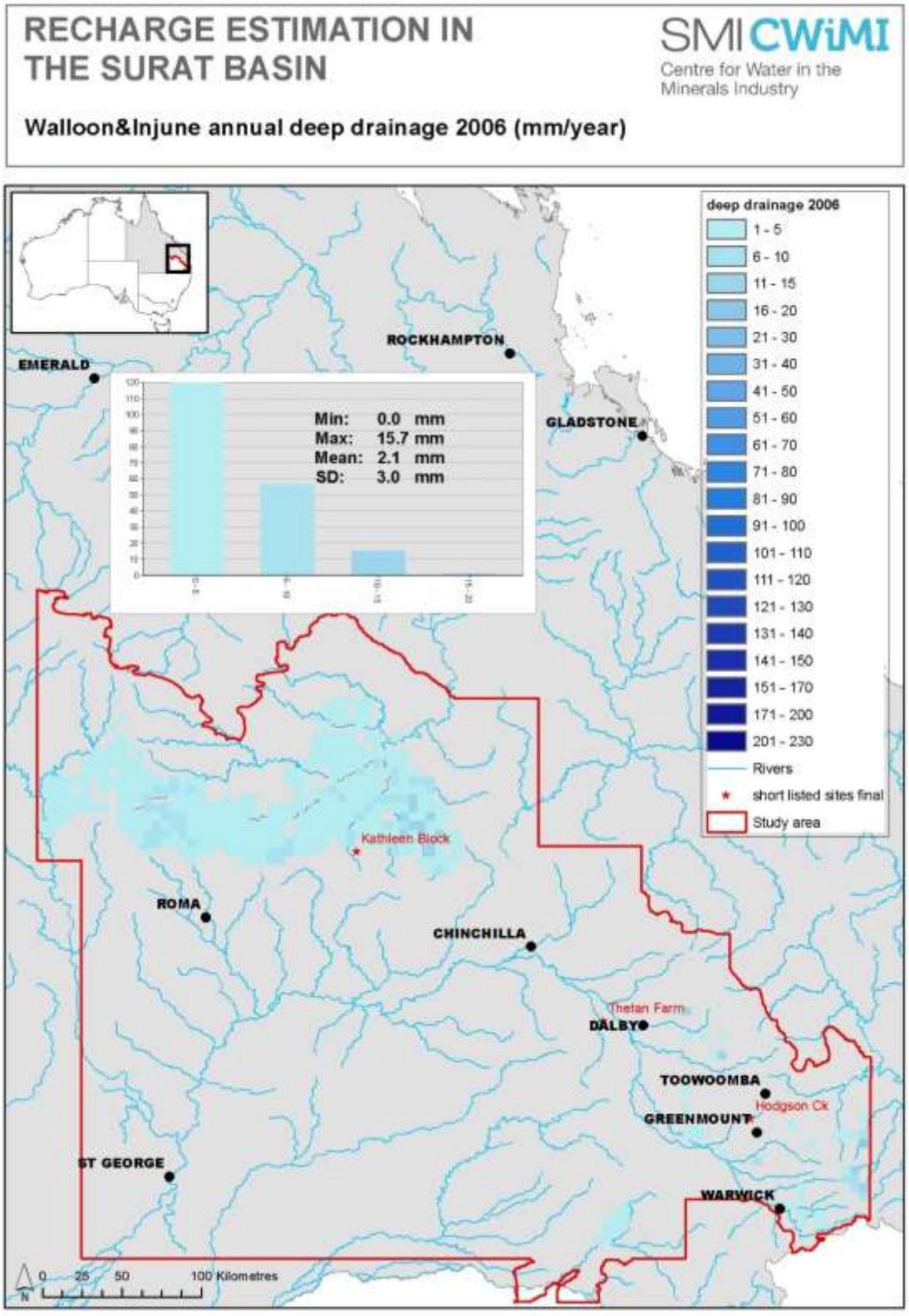
RECHARGE ESTIMATION IN THE SURAT BASIN
SMI CWiMI
Centre for Water in the Minerals Industry
Walloon&Injune annual deep drainage 2006 (mm/year)
deep drainage 2006
1 - 5
6 - 10
11 - 15
16 - 20
21 - 30
31 - 40
41 - 50
51 - 60
61 - 70
71 - 80
81 - 90
91 - 100
101 - 110
111 - 120
121 - 130
131 - 140
141 - 150
151 - 170
171 - 200
201 - 230
Rivers
short listed sites final
Study area
Min: 0.0 mm
Max: 15.7 mm
Mean: 2.1 mm
SD: 3.0 mm
ROCKHAMPTON
EMERALD
GLADSTONE
Kathleen Block
ROMA
CHINCHILLA
Thetan Farm
DALBY
TOOWOOMBA
Hodgson Ck
GREENMOUNT
ST GEORGE
WARWICK
0 25 50 100 Kilometres
N

Figure 45 - Average annual deep drainage estimates for the Walloon Coal Measures and Injune Creek Group geologic units in an example dry year – 2006 (data source: CSIRO AWAP 2014).

Main Range Volcanics: Average, wet and dry years

The spatial variation in the long term (1900 – 2014) mean deep drainage highlights higher values in the SE of the Main Range Volcanics, as well as NW of Toowoomba (near Oakey, Figure 46). The mean long term deep drainage for the Main Range Volcanics is 15.8 ± 13.8 mm/yr, higher than the Walloon – Injune and whole basin averages, and the distribution of deep drainage throughout the basalts is more Gaussian than the previous distributions. In the example wet year the spatial distribution is more uniform, although declining deep drainage to the west is still evident. The spatial mean deep drainage increases to 99 ± 42 mm/yr and the distribution becomes more bimodal (Figure 47). In the dry year example the spatial contrast becomes more apparent, with the areas in the very SE and just NW of Toowoomba dominating deep drainage, albeit at much lower rates (Figure 48). The spatial mean in this case drops to 3.9 ± 3.9 mm/yr, but the distribution returns to close to Gaussian.

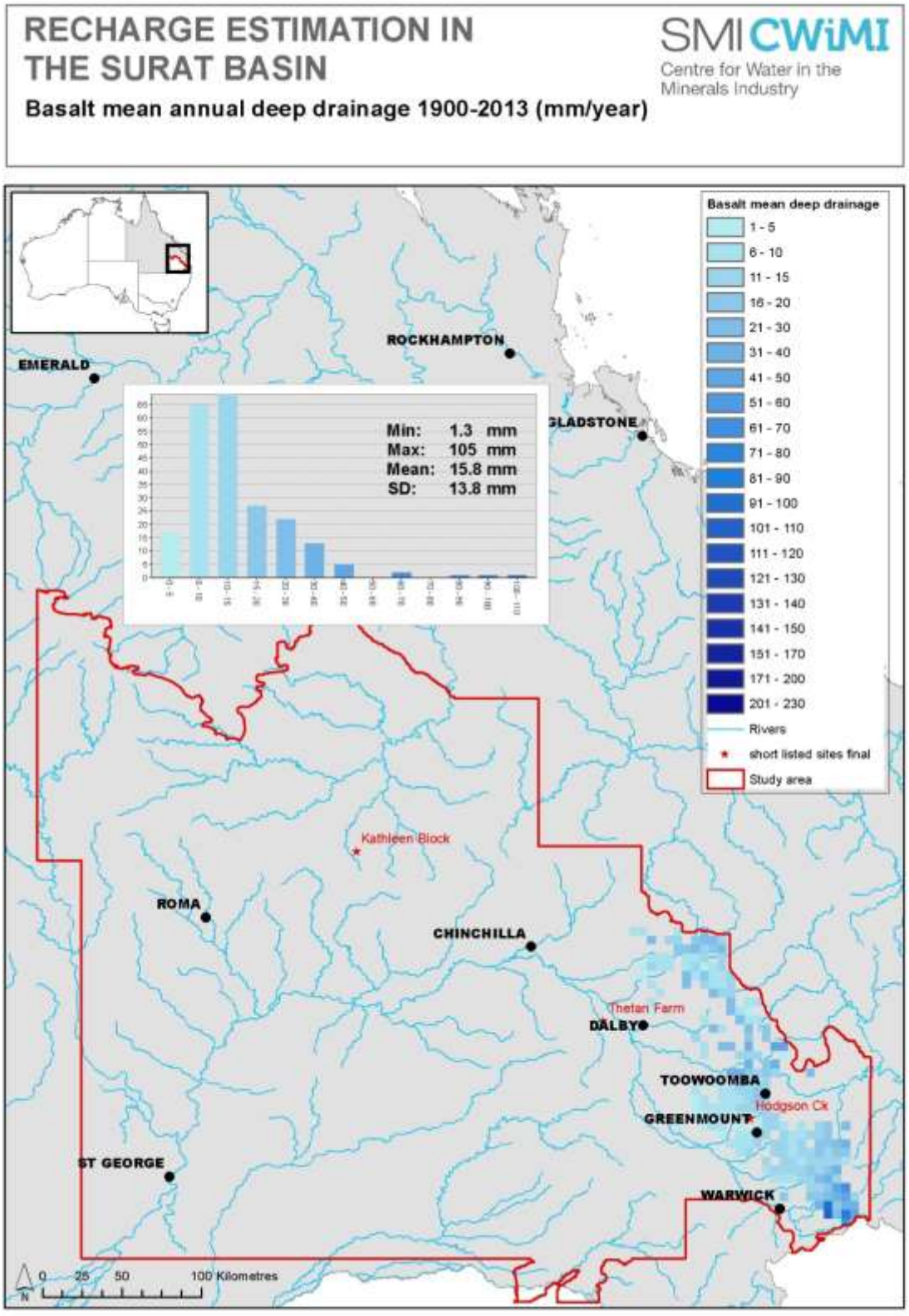
RECHARGE ESTIMATION IN THE SURAT BASIN
Basalt mean annual deep drainage 1900-2013 (mm/year)
SMI CWiMI
Centre for Water in the Minerals Industry
Basalt mean deep drainage
1 - 5
6 - 10
11 - 15
16 - 20
21 - 30
31 - 40
41 - 50
51 - 60
61 - 70
71 - 80
81 - 90
91 - 100
101 - 110
111 - 120
121 - 130
131 - 140
141 - 150
151 - 170
171 - 200
201 - 230
Rivers
short listed sites final
Study area
Min: 1.3 mm
Max: 105 mm
Mean: 15.8 mm
SD: 13.8 mm
ROCKHAMPTON
EMERALD
GLADSTONE
Kathleen Block
ROMA
CHINCHILLA
Thelan Farm
DALBY
TOOWOOMBA
Hodgson Ck
GREENMOUNT
ST GEORGE
WARWICK
0 25 50 100 Kilometres
N

Figure 46 - Average annual deep drainage estimates for the Main Range Volcanics (Basalts) between 1900 – 2013 (data source: CSIRO AWAP 2014).

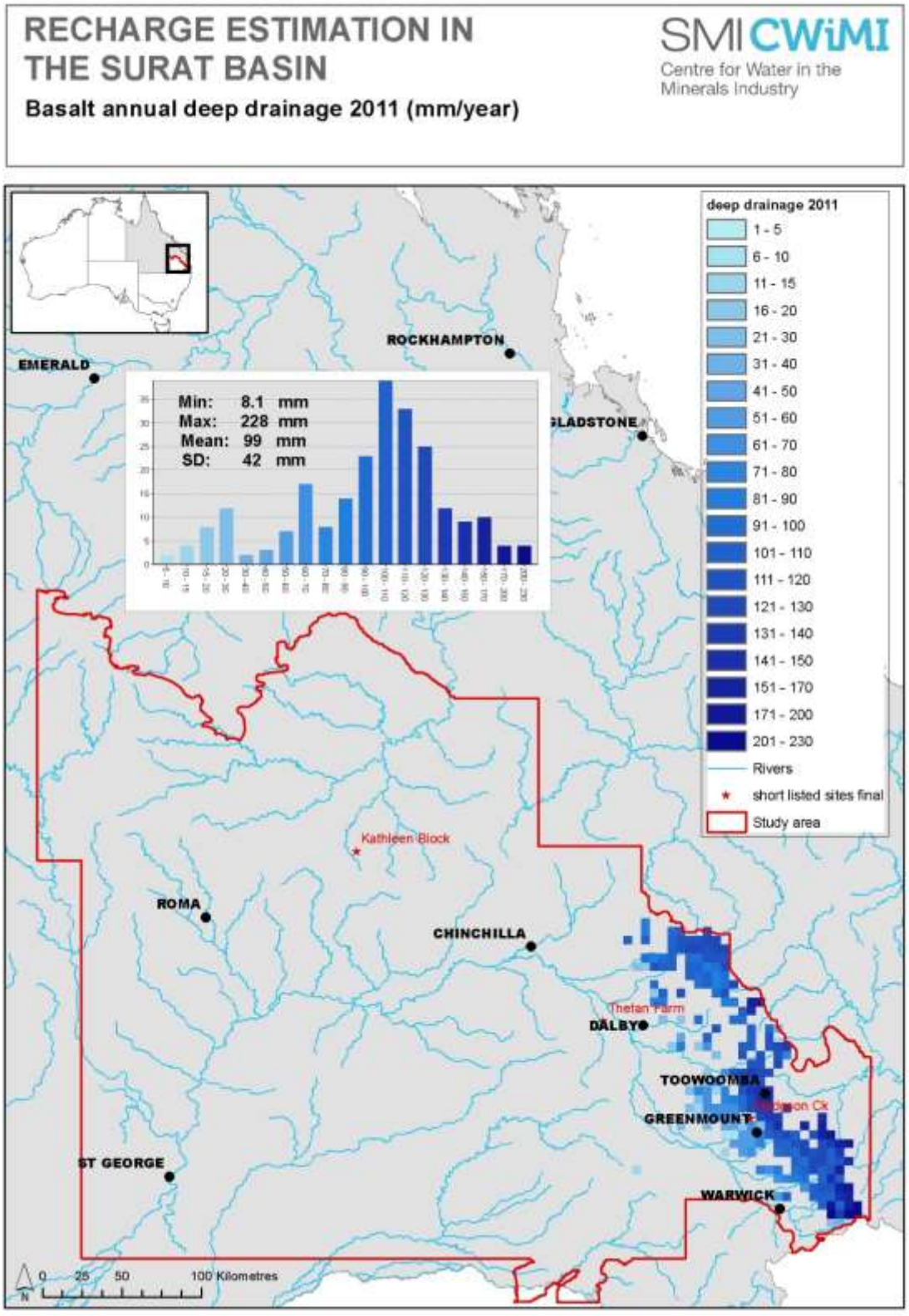
RECHARGE ESTIMATION IN THE SURAT BASIN
Basalt annual deep drainage 2011 (mm/year)
SMI CWiMI
Centre for Water in the Minerals Industry
deep drainage 2011
1 - 5
6 - 10
11 - 15
16 - 20
21 - 30
31 - 40
41 - 50
51 - 60
61 - 70
71 - 80
81 - 90
91 - 100
101 - 110
111 - 120
121 - 130
131 - 140
141 - 150
151 - 170
171 - 200
201 - 230
Rivers
short listed sites final
Study area
Min: 8.1 mm
Max: 228 mm
Mean: 99 mm
SD: 42 mm
ROCKHAMPTON
EMERALD
GLADSTONE
Kathleen Block
ROMA
CHINCHILLA
Thetan Farm
DALBY
TOOWOOMBA
GREENMOUNT
ST GEORGE
WARWICK
0 25 50 100 Kilometres
N

Figure 47 - Average annual deep drainage estimates for the Main Range Volcanics (Basalts) in an example wet year – 2011 (data source: CSIRO AWAP 2014).

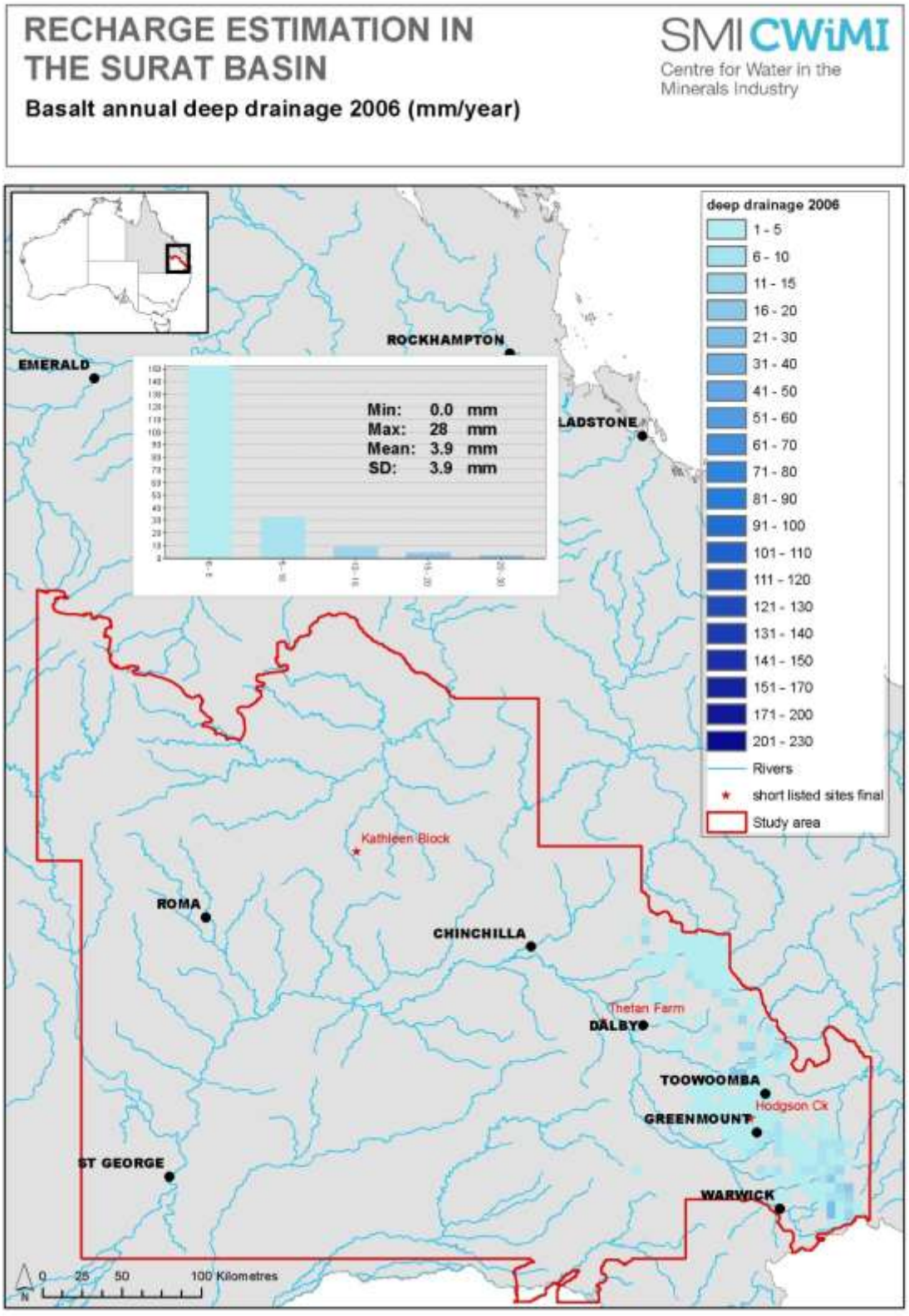
RECHARGE ESTIMATION IN THE SURAT BASIN
Basalt annual deep drainage 2006 (mm/year)
SMI CWiMI
Centre for Water in the Minerals Industry
deep drainage 2006
1 - 5
6 - 10
11 - 15
16 - 20
21 - 30
31 - 40
41 - 50
51 - 60
61 - 70
71 - 80
81 - 90
91 - 100
101 - 110
111 - 120
121 - 130
131 - 140
141 - 150
151 - 170
171 - 200
201 - 230
Rivers
short listed sites final
Study area
Min: 0.0 mm
Max: 28 mm
Mean: 3.9 mm
SD: 3.9 mm
ROCKHAMPTON
EMERALD
LADSTONE
Kathleen Block
ROMA
CHINCHILLA
Thetan Farm
DALBY
TOOWOOMBA
Hodgson Ck
GREENMOUNT
ST GEORGE
WARWICK
0 25 50 100 Kilometres
N

Figure 48 - Average annual deep drainage estimates for the Main Range Volcanics (Basalts) in an example dry year – 2006 (data source: CSIRO AWAP 2014).

Temporal Recharge Estimates

The annual time series of deep drainage shows a mean of 11 ± 11 mm/yr for the whole Surat (Figure 49) (where the latter value is the standard deviation representing the time variability of the spatial mean annual values). As a percentage of precipitation, the long term mean is just below 2% precipitation, although the role of sporadic high intensity wet periods is discernible (Figure 50).

Dividing the Surat into the Main Range Volcanic (Basalts) (Figure 13) and Walloon – Injune (Figure 51) geological units, the time variability of deep drainage in the Walloon – Injune is similar to that for the whole Surat, although the variability in the Main Range Volcanics is higher. This implies that during wet periods the Surat experiences more spatially widespread increases in deep drainage, and may explain the bimodal distribution (i.e. high deep drainage peak) in Figure 41.

Although these average values are useful, for further interpretation and any possible use as model inputs it is critical to better honour the large degree of climatic variability driving deep drainage within the Surat. Periods of above average precipitation clearly have an impact on the monthly deep drainage estimates for the Surat as a whole. As an example, above average precipitation occurred from 1995 – 1999, a prolonged drought period for 2000 – 2009, and a very above average precipitation period again 2010 – 2013. Despite the annual mean deep drainage of ~11 mm/yr, the period 1995 – 2000 experienced ~22.2 mm/yr, 2000 – 2009 only ~4.9 mm/yr, and 2010 – 2013 a much higher ~45.7 mm/yr (Figure 53). These large contrasts over ENSO timescales highlight that from dry to wet period's deep drainage rates can change tenfold.

Interestingly, comparing the Main Range Volcanic and Walloon – Injune geological units indicates that despite the similar average deep drainage values the rate is generally greater for the Main Range Volcanics, whereas the Walloon – Injune units have a proportionally greater response during very wet phases. This slight disparity explains the different trends in the cumulative distribution (Figure 54) which estimates that the Main Range Volcanics have transported ~500 mm additional deep drainage over the last ~100 years.

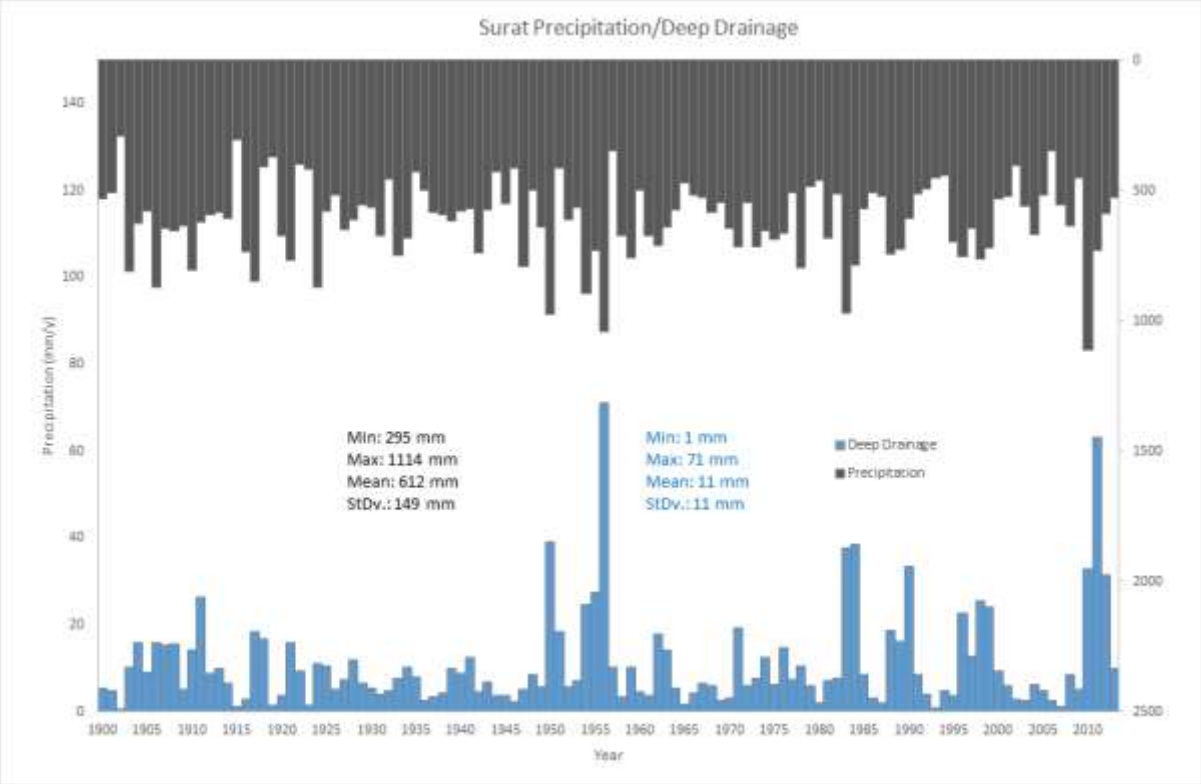

Figure 49 - Time series of annual precipitation and deep drainage for the whole Surat CMA as a spatial average for 1900 – 2014.

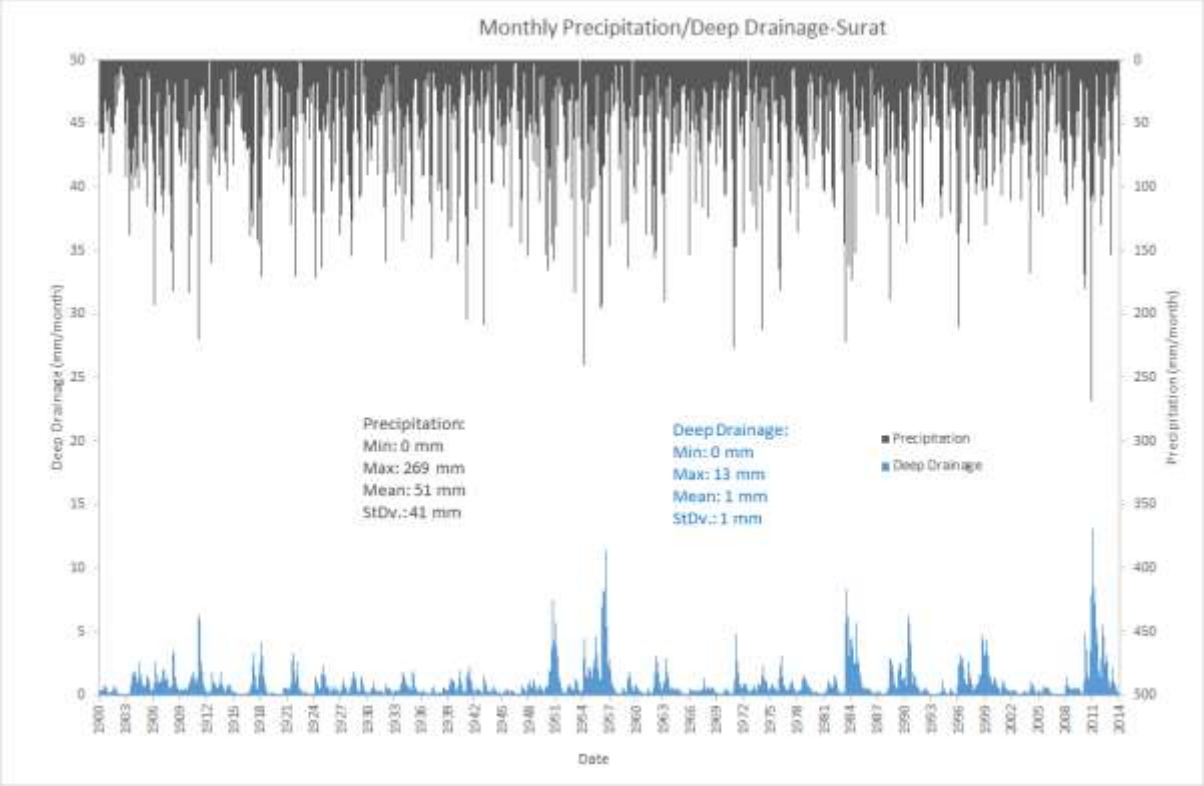

Figure 50 - Time series of monthly precipitation and deep drainage for the whole Surat CMA as a spatial average for 1900 – 2014.

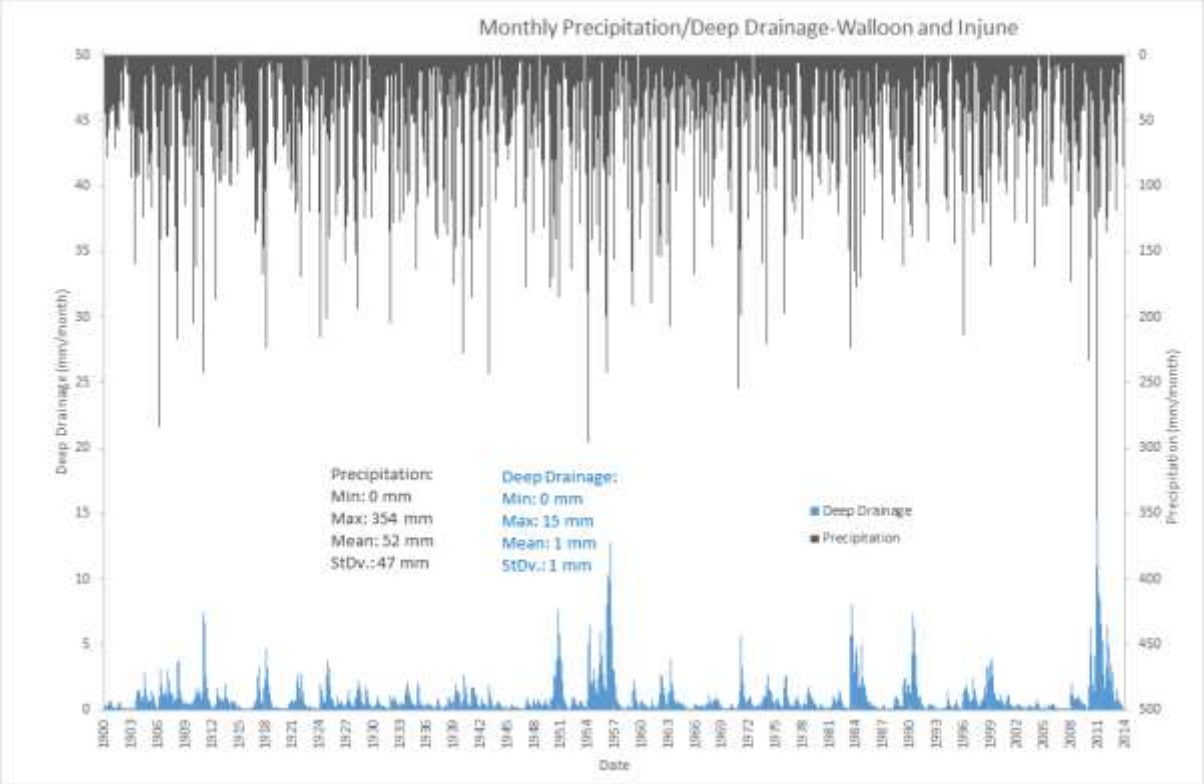

Figure 51 - Time series of monthly precipitation and deep drainage for the Walloon Coal Measures – Injune Creek Group geological units as a spatial average for 1900 – 2014.

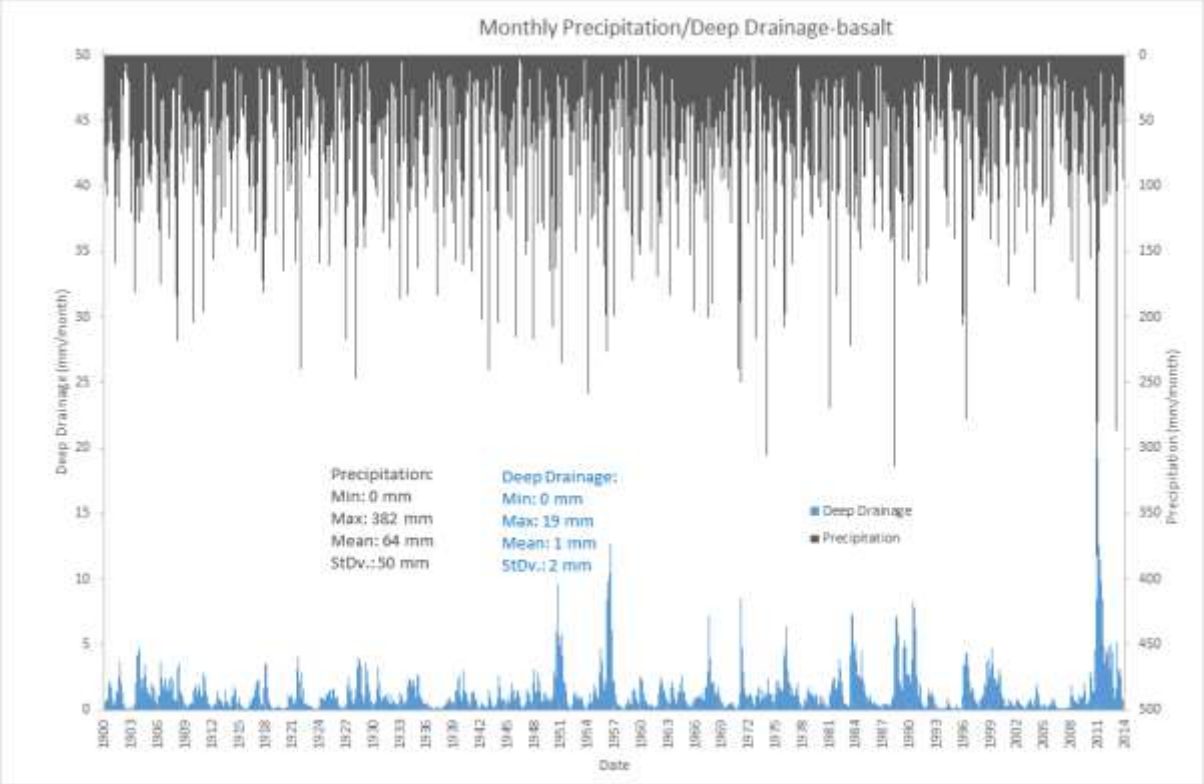

Figure 52 - Time series of monthly precipitation and deep drainage for the Main Range Volcanics (Basalts) geological unit as a spatial average for 1900 – 2014.

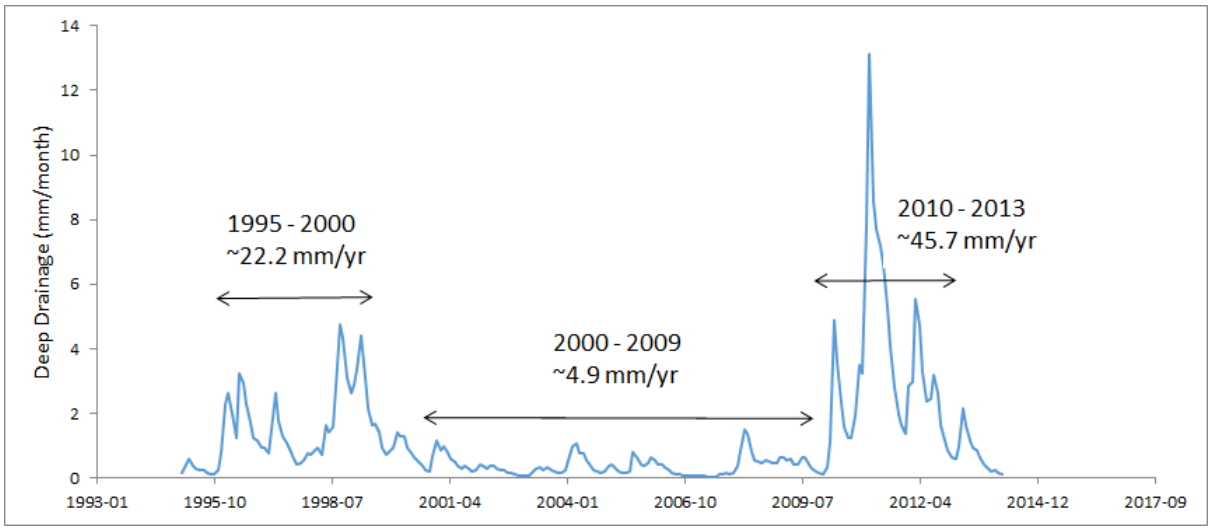

Figure 53 - Monthly rainfall time series for the whole Surat CMA between 1995 – 2013, highlighting the importance of ENSO induced wet and drought periods.

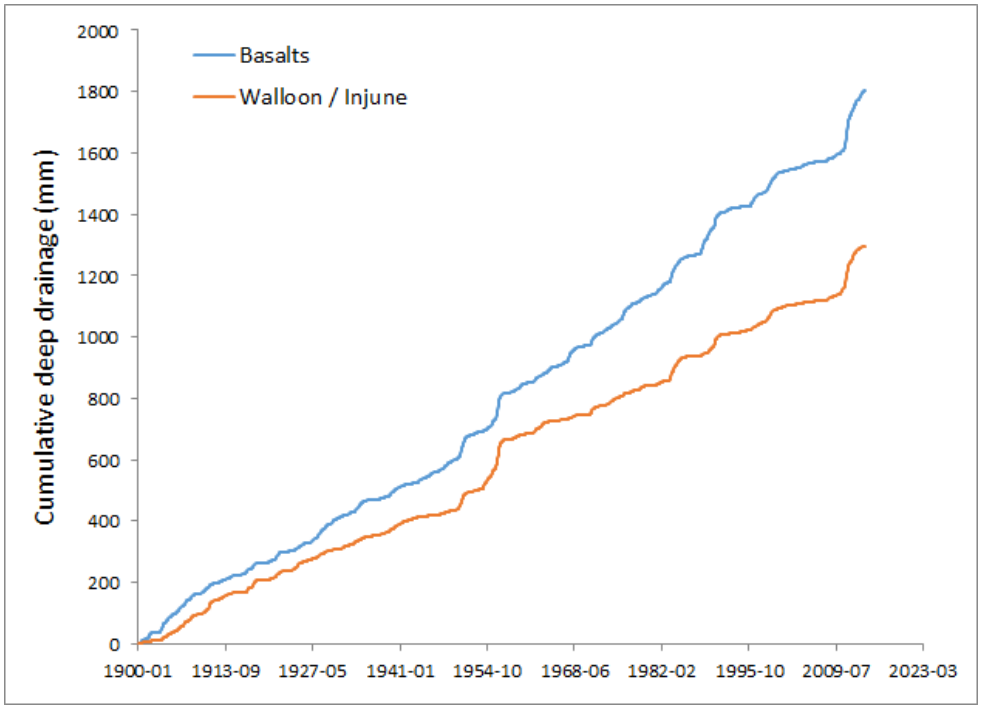

Figure 54 - Cumulative distribution of deep drainage in the Main Range Volcanics (Basalts) and Walloon Coal Measures – Injune Creek Group geological units.

Uncertainty

It is important to recognise the potentially high uncertainty in deep drainage estimates based on remote sensed and modelled data. Uncertainties in parameter estimation for WaterDyn25M followed a 3-step procedure (Raupach et al., 2009): 1. Reference parameter set was determined and then applied to a limited set of training data, 2. Sensitivities of key water fluxes to parameter values were determined. In terms of deep drainage fluxes, the greatest sensitivity was from the Priestly – Taylor co-efficient (within the evapotranspiration equation), the multiplier used for the deeper soil layer (M2) water saturation, and finally multipliers for emissivity and albedo. 3. The reference parameter set was subjected to several tests against a set of observations (e.g. actual soil moisture, measured runoff) over the national scale, with inevitable uncertainty arising about local accuracy. There would also be significant additional uncertainty in converting the deep drainage estimates to recharge.

Soil Moisture Comparisons

Another potentially signficant uncertainty is derived from the reliance on soil moisture data from the AWAP model. As a preliminary exploration of the accuracy of modelled soil moisture data, they were compared with the LANDSAT derived soil moisture (Figure 55 and Figure 56).

The Surface Soil Moisture data (SSM) were retrieved from the Metop ASCAT 25 km soil moisture images product of the Research Group Remote Sensing, Department for Geodesy and Geoinformation (GEO), Vienna University of Technology (TU-Wien). The product is provided as daily gridded images. These data were produced by using radar backscattering coefficients measured by the Advanced Scatterometer (ASCAT) onboard the Metop satellite. The relative soil moisture data ranging between 0% and 100% are derived by scaling the normalized backscattering coefficients between the lowest/highest values corresponding to the driest/wettest soil conditions. The derived soil moisture product represents the content in the first 5 cm of the soil in relative units between totally dry conditions (0%) and total water capacity (100%). The unit is degree of saturation, but can be converted into volumetric units with the help of soil porosity information. The Metop ASCAT data also is composed of some useful information such as error/noise of daily soil moisture and land surface conditions (i.e., unknown, unfrozen, frozen, temporary melting/water on the surface or permanent ice). The overlapping daily soil moisture data from (2006-2014) was extracted from Metop ASCAT data and compared with CSIRO AWAP daily soil moisture data.

The remote sensing soil moisture percentage is based on range between highest and lowest pixel values, whereas the AWAP soil moisture is based on a pedotransfer function (soil class) porosity and the shallow soil water balance equation. Also, the AWAP output is exactly monthly, where as remote sensing is much more haphazard, therefore the remote sensing is only crudely date adjusted so they can be compared (the AWAP data is a monthly average, whereas the remote sensing data is a monthly snapshot). Interpretation of the errors is challenging due to this timing issue, and due to the numerous potential sources of error in both the AWAP and LANDSAT-derived data. Nevertheless, we recommend further exploration of the spatial and temporal patterns of error over the Surat aiming to infer biases in these deep drainage estimates.

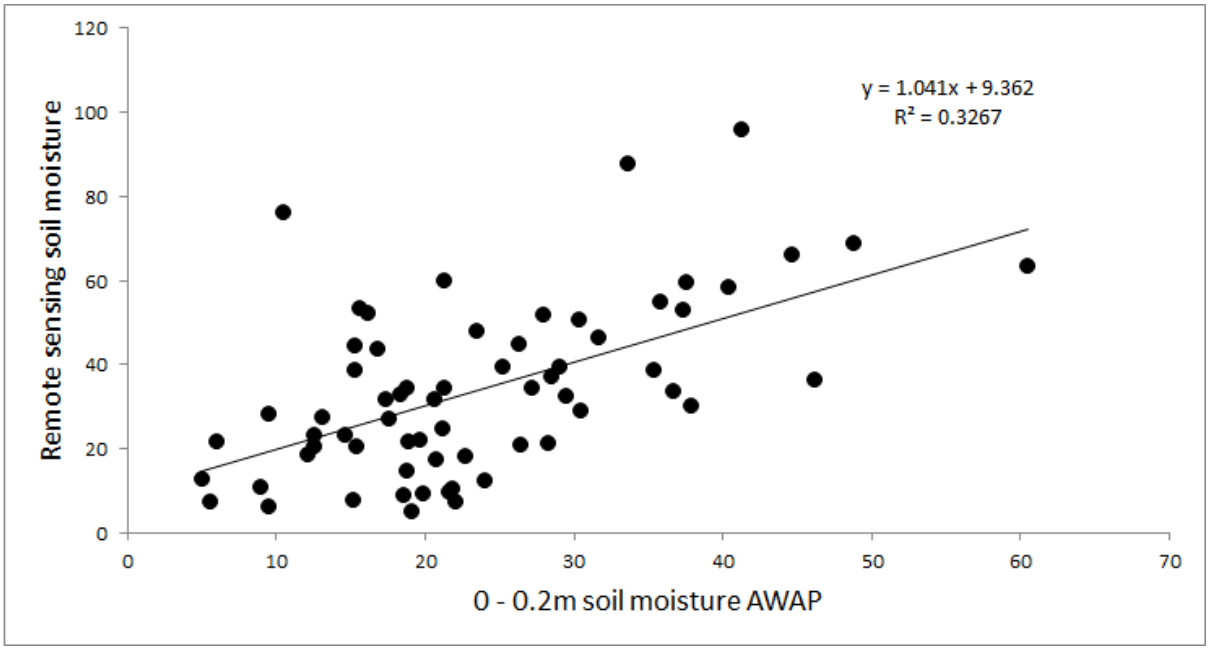

Figure 55 - Remote sensing soil moisture vs AWAP soil moisture, where soil moisture is expressed as a percentage.

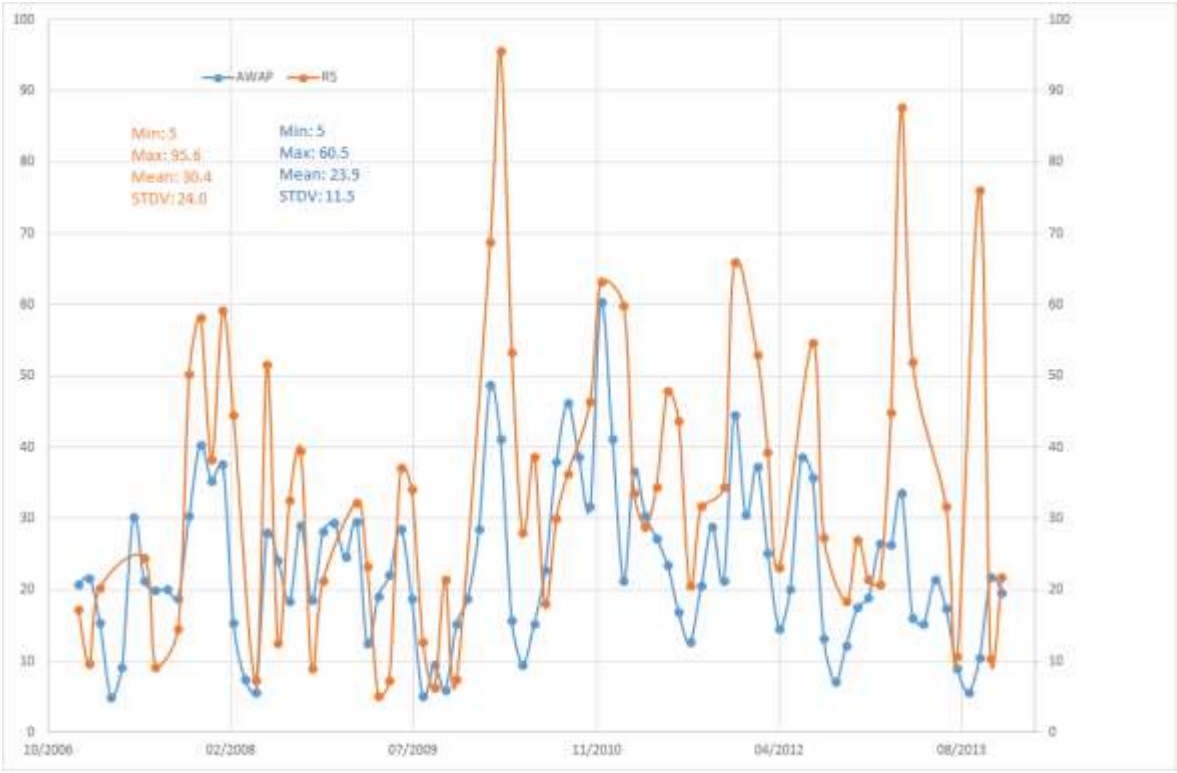

Figure 56 - Time series results for remote sensing soil moisture vs AWAP soil moisture, where soil moisture is expressed as a percentage.

Summary

Spatial variability

The analysis of the deep drainage estimates from the CSIRO Australian Water Availability Project (AWAP) illustrates that deep drainage within the Surat Basin as a whole has high spatial variability, and areas of higher deep drainage are driven by a combination of higher precipitation and /or soil and landscape properties. This spatial variability was also evident after separating the Surat into areas where the Walloon - Injune and Basalts are likely to be unconfined (i.e. outcrop areas of these units and the Main Range Volcanics which over-lie the Walloon Coal Measures). While caution is required due to the various modelling assumptions used to produce these estimates, the AWAP data can be used to illustrate the degree of variability. The long term (1900 – 2014) spatial range in deep drainage across the Surat is ~0 – 63 mm/yr, identical to the long term range for the Main Range Volcanics, although the long term range for the Walloon – Injune beds is much lower (~0 – 30 mm/yr). The data indicate that the Main Range Volcanics show the largest spatial sensitivity to variability from wet and dry phases, although the Walloon – Injune outcrop areas are also quite dynamic, and are certainly more sensitive to changes than the basin average.

Temporal variability

The temporal distribution of AWAP deep drainage data shows large variability around the long term means, strongly influenced by ENSO driven dry and wet phases. Although the Main Range Volcanics are again the most sensitive to this variability, the Surat as a whole can experience order of magnitude deep drainage changes between dry and wet periods. The results show the potential importance of including recharge as a time varying input (at least annually varying) to groundwater models.

Further investigation

Within the temporal distribution, the role of climatic variability as well as antecedent conditions and event intensity in driving deep drainage should be evaluated more explicitly.

Within the spatial distribution, the cause of variation in deep drainage distributions can be investigated further, specifically targeting potential hotspot recharge areas, as well as priority CSG impact areas.

For both the spatial and temporal distributions, more localised verification of the AWAP model using independent estimates of surface water and soil moisture from key recharge zones is required; and resolution of significant biases that may be uncovered.

Furthermore, relating the deep drainage estimates to actual recharge rates requires comparison with borehole hydrographs that have been interpreted as containing clear recharge signals. This would allow the soil moisture balance based deep drainage to be constrained by actual unconfined water table responses.

This would allow better estimation of a final recharge rate product for implementation within groundwater models for the Surat Basin. However, this also requires better propagation of uncertainty regarding deep drainage and recharge than is currently employed.

Analysis of Surface Water Hydrographs

Introduction

In this chapter, groundwater recharge on the eastern boundary of the Surat CMA is estimated with the use of streamflow data. Annual groundwater recharge is quantified in four stream catchments on the south-western extents of the Main Range Volcanics. The storage-discharge method developed by Kirchner (2009) was used to quantify groundwater recharge in the Surat CMA. This method has recently been applied to quantify seasonal mountain block recharge in semi-arid Arizona (Ajami et al., 2011). A very similar approach was implemented in this study to obtain a time series of annual recharge estimates from 1999 to 2014 for each catchment. The estimates are a lower bound as only changes in storage due to stream discharge are accounted for. Furthermore, a preliminary sensitivity analysis was carried out to investigate the impact of storage-discharge functions on recharge estimates.

This chapter is made up of three sections in addition to this introduction. The following section discusses the study area, the data and the methods applied in quantifying groundwater recharge and testing the sensitivity of these estimates to the main assumptions used. Section 3 presents the results of this study. The chapter concludes with a section discussing the limitations of the study, and putting forward recommendations for further work to improve and build upon these findings.

Estimating Groundwater Recharge – Study Area, Data and Methods

Storage – Discharge Theory and Method Formulation

The storage-discharge method developed by Kirchner (2009) is a catchment-based approach, where the change in catchment (aquifer) storage is described by the conservation of mass equation:

$$\frac{dS}{dt} = P - E - Q \qquad (1)$$

Where S is the volume of water in storage, P is the rate of precipitation, and E and Q are the rates of evapotranspiration and discharge. Furthermore, the storage-discharge method is based on the assumption that discharge (Q) is dependent on the amount of water in catchment storage (S). This relationship is quantifiable by the storage – discharge function:

$$Q = f(S) \qquad (2)$$

This relationship is also invertible, so that the magnitude of discharge provides a measure of the amount of water in catchment storage:

$$S = f^{-1}(Q) \qquad (3)$$

If it is assumed that the storage represents groundwater storage, which discharges only to surface streams, and the groundwater storage catchment area is known, increases in measured stream baseflow can be interpreted as changes in S and thus as changes in groundwater recharge. These are quantified as follows:

$$GWR_t = S_{t+1} - S_t = f^{-1}(Q_{t+1}) - f^{-1}(Q_t) \qquad (4)$$

Where GWR is groundwater recharge, S is catchment storage, Q is discharge, and t and t + 1 refer to the time periods before and after a precipitation event that results in groundwater recharge. The first step in the method is therefore to define the inverse function f^{-1}.

The inverse function f^{-1} is defined through analysis of the shape of recession curves. The derivative of the storage-discharge function, also known as the sensitivity function, can be determined directly from streamflow data when the catchment water balance (Equation 1) is dominated by discharge (Q >> P, Q >> E) (Kirchner, 2009):

$$g(Q) = \frac{dQ}{dS} \approx \left. \frac{-dQ/dt}{Q} \right|_{P \ll Q, ET \ll Q} \qquad (5)$$

The sensitivity function is derived by applying the recession plot method of Brutsaert and Nieber (1977). The recession plot data are binned and a least squares regression model is

fitted, defining the rate of change of discharge (-d*Q*/d*t*) as a function of discharge (*Q*). From this relationship, the inverse storage-discharge function can be derived as follows:

$$f^{-1}(Q) = \int dS = \int \frac{1}{g(Q)} dQ \qquad (6)$$

The remainder of this section will provide further details on how this method was applied in quantifying groundwater recharge in this study. This information is provided in four subsections. First, general information is provided on the streamflow and precipitation data used in the study. Second, the details of the methods applied in the recession plot analysis and deriving storage-discharge functions are provided for each catchment. Third, the manner in which recharge events were defined and respective discharge data extracted is explained. Last, the sensitivity analysis carried out on recharge estimates is described.

Streamflow and Precipitation Data and Quality Control

Daily streamflow data used to carry out storage-discharge analysis were obtained from Queensland's Department of Natural Resources and Mines (QLD DNRM, 2014e, 2014f). For a stream to be suitable for this method, the catchment had to have an identifiable storage – discharge relationship and closure of the mass balance was also necessary. As such, this restricts the method to small headwater catchments where the surface catchments can be assumed the same as the groundwater catchment, with no groundwater recharge bypassing the stream. This assumes that depletion of groundwater storage is only due to stream discharge, and that all groundwater recharge returns as stream baseflow. However, some components of groundwater recharge feed regional groundwater systems and not all recharge flow paths in the catchment are accounted for. Thus the answer may be considered as a lower bound estimate of groundwater recharge.

Five suitable gauging stations, with stream catchment areas varying between 35 and 148 km^2, were identified to provide initial estimates of recharge (Figure 57, Table 19). The streams are located on the western side of the Great Dividing Range from Toowoomba southwards towards the New South Wales border. The catchments of all the streams were predominantly located in the Main Range Volcanics geologic formation, which is likely to be the dominant source of groundwater to the streams. As such, the groundwater recharge estimates obtained from this study are believed to be indicative of recharge within the Main Range Volcanics.

Table 19 – General stream and gauging station information (QLD DNRM, 2014f)

Stream	Basin	Stream Gauging Station Number	Catchment Area (km^2)	Elevation (mAHD)
Swan Creek	Balonne - Condamine	422306A	83	536
Emu Creek	Balonne - Condamine	422313B	148	491
Spring Creek	Balonne - Condamine	422321B	35	552
Gowrie Creek	Balonne - Condamine	422326A	47	538
Condamine River	Balonne - Condamine	422341A	92	515

General quantity and quality analyses were carried out on the daily streamflow data. The possibility of using hourly streamflow data was explored. However, this was abandoned due to the increased levels of noise in the data at smaller discharges. In addition, hourly data were not available for the entire time series. For the majority of the streams the data record extended to the early 1970s, with the exception of Swan Creek which had a data record in

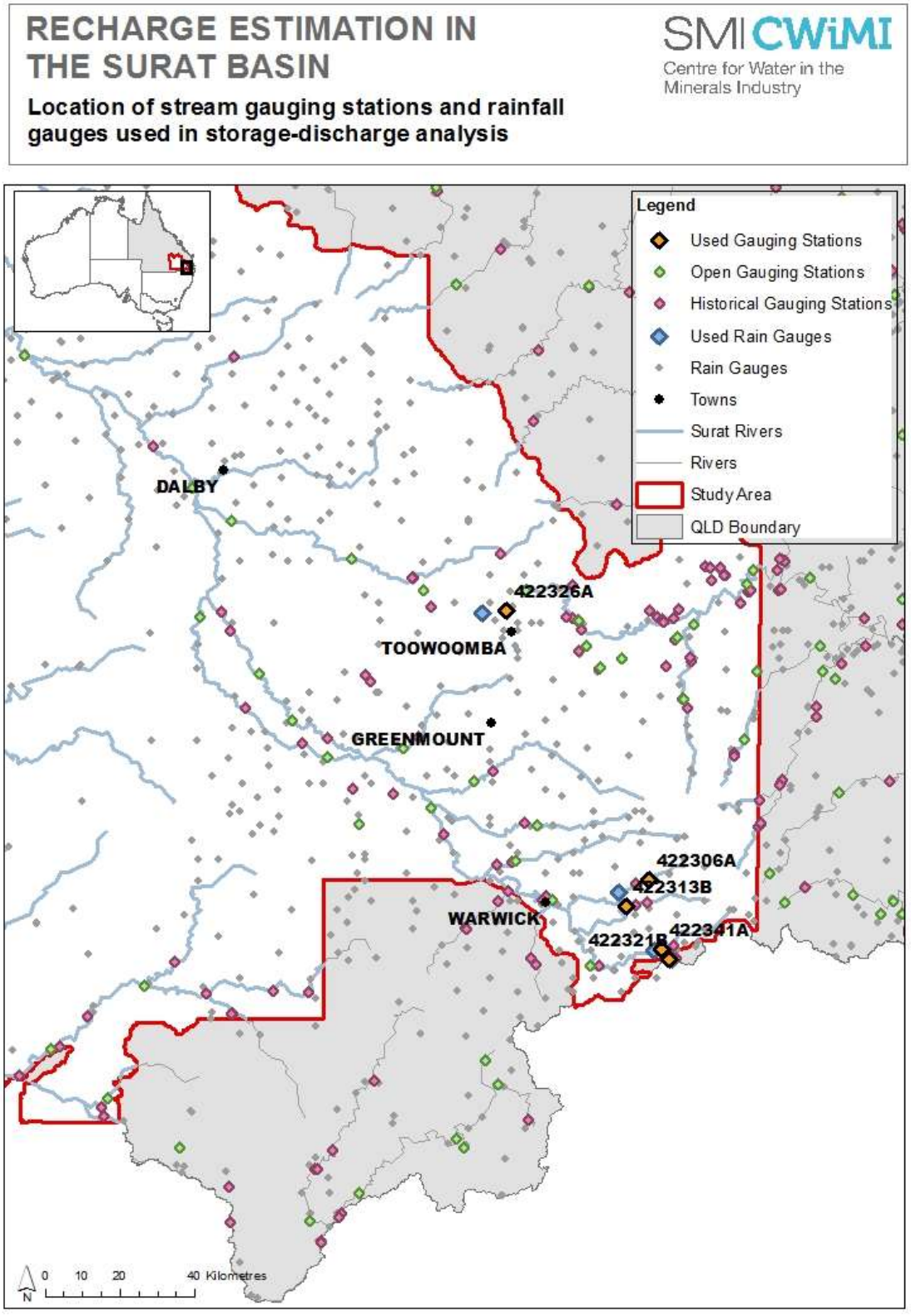
RECHARGE ESTIMATION IN THE SURAT BASIN
Location of stream gauging stations and rainfall gauges used in storage-discharge analysis
SMI CWiMI
Centre for Water in the Minerals Industry
Legend
Used Gauging Stations
Open Gauging Stations
Historical Gauging Stations
Used Rain Gauges
Rain Gauges
Towns
Surat Rivers
Rivers
Study Area
QLD Boundary
DALBY
422326A
TOOWOOMBA
GREENMOUNT
422306A
422313B
WARWICK
422321B
422341A
0 10 20 40 Kilometres
N

Figure 57 - Location of stream gauging stations used in storage-discharge analysis and respective rainfall gauges. The location of all open and historical stream gauging stations (QLD DNRM, 2014e, 2014f), and all rain gauges (BOM, 2014) is indicated.

excess of 90 years (Figure 59, Table 20). Swan Creek also had the largest number of missing data points, approximately 4.5 % of the total time series. Zero flow days made up less than 7 % of the remaining flow record for all the catchments (Table 20), with Swan and Emu Creek characterised by lower flows in comparison to Spring and Gowrie Creek (Figure 58). One assumption of the recession plot analysis is that the streams are perennial (Ajami et al., 2011). Even though the streams were not truly perennial, this limited number of zero flow days was assumed not to disqualify the approach.

Table 20 - Stream gauging station data distribution, quantity and quality (QLD DNRM, 2014f)

Stream	Stream Gauging Station	Period of Record - Start	Period of Record - End	Total Number of Data Points	% of Total Time Series	% of Net Time Series
Swan Creek	422306A	03/09/1920	21/08/2014	34 321	4.4	6.8
Emu Creek	422313B	24/01/1973	21/08/2014	15 185	0.3	6.1
Spring Creek	422321B	24/01/1973	20/08/2014	15 184	0.2	0.1
Gowrie Creek	422326A	20/11/1969	21/08/2014	16 346	2.7	0
Condamine River	422341A	27/05/1976	21/08/2014	13 966	2.3	4.2

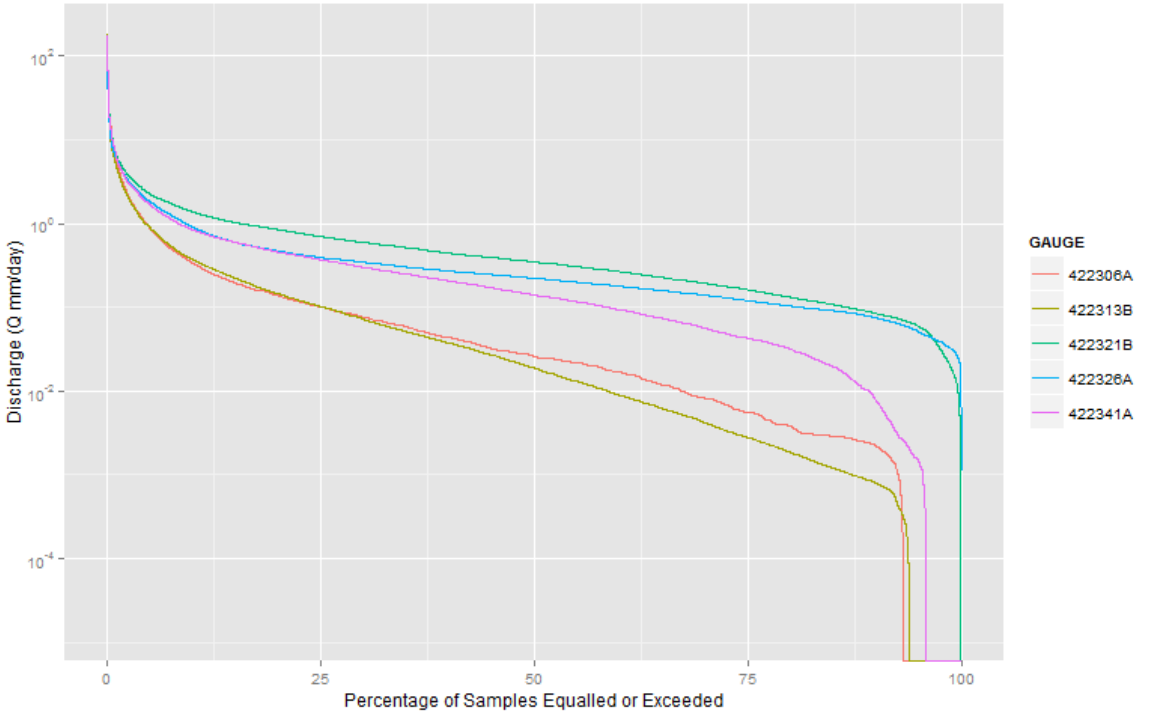

Figure 58 - Flow duration curves, normalised by catchment area, of the five stream gauging stations

Precipitation fluxes to the catchment had to be known for selecting baseflow recession periods. Rainfall data were obtained from the Bureau of Meteorology (BOM, 2014). Rainfall gauges were selected based on both the proximity of the gauge to the gauging station and the temporal overlaps in record with the stream gauging station (Figure 57, Figure 59, Table 21). In some circumstances one rain gauge was the optimal choice with respect to both criteria, while in other situations this was not the case. Generally, the length and quality of rainfall record was prioritised over the proximity as long as the rain gauge was within the vicinity (less than 10 km) of the stream gauging station and representative of rainfall in the catchment.

Table 21 - Information on rainfall gauge used for each stream gauging station (BOM, 2014)

Stream	Stream Gauging Station	Rainfall Gauge	Distance (km)	Period of Record - Start	Period of Record – End
Swan Creek	422306A	041120	8	01/01/1912	31/07/2014
Emu Creek	422313B	041120	4.1	01/01/1912	31/07/2014

Spring Creek	422321B	041208	0.7	01/02/1959	31/07/2014
Gowrie Creek	422326A	041369	5.9	01/05/1972	31/03/2014
Condamine River	422341A	041056	1.9	01/09/1903	31/08/2014

After further data interrogation and quality control, Gowrie Creek catchment (GS 422326A) was not included in the analysis. Gowrie Creek is on the northern outskirts of Toowoomba with the creek flowing through Toowoomba upstream. It appears that Toowoomba covers the majority of the stream catchment. Thus, streamflow would be heavily influenced by large areas of impermeable surfaces and stormwater diversions. This was evident from the Gowrie Creek hydrograph, which was highly responsive to rainfall but had a generally constant baseflow component indicating low groundwater recharge; however calculation of the sensitivity function is highly uncertain due to low values of dQ/dt and thus recharge was not quantified for this catchment.

Recession Plots and Storage – Discharge Relationships

Recession plots, as originally developed by Brutsaert and Nieber (1977), were used to estimate the catchment sensitivity function and thus the catchment storage-discharge relationship. To obtain recession plots of each of the four catchments, streamflow data were first normalised by surface water catchment area (assumed equal to the groundwater catchment) so that all water fluxes were in the same depth based units (mm/day).

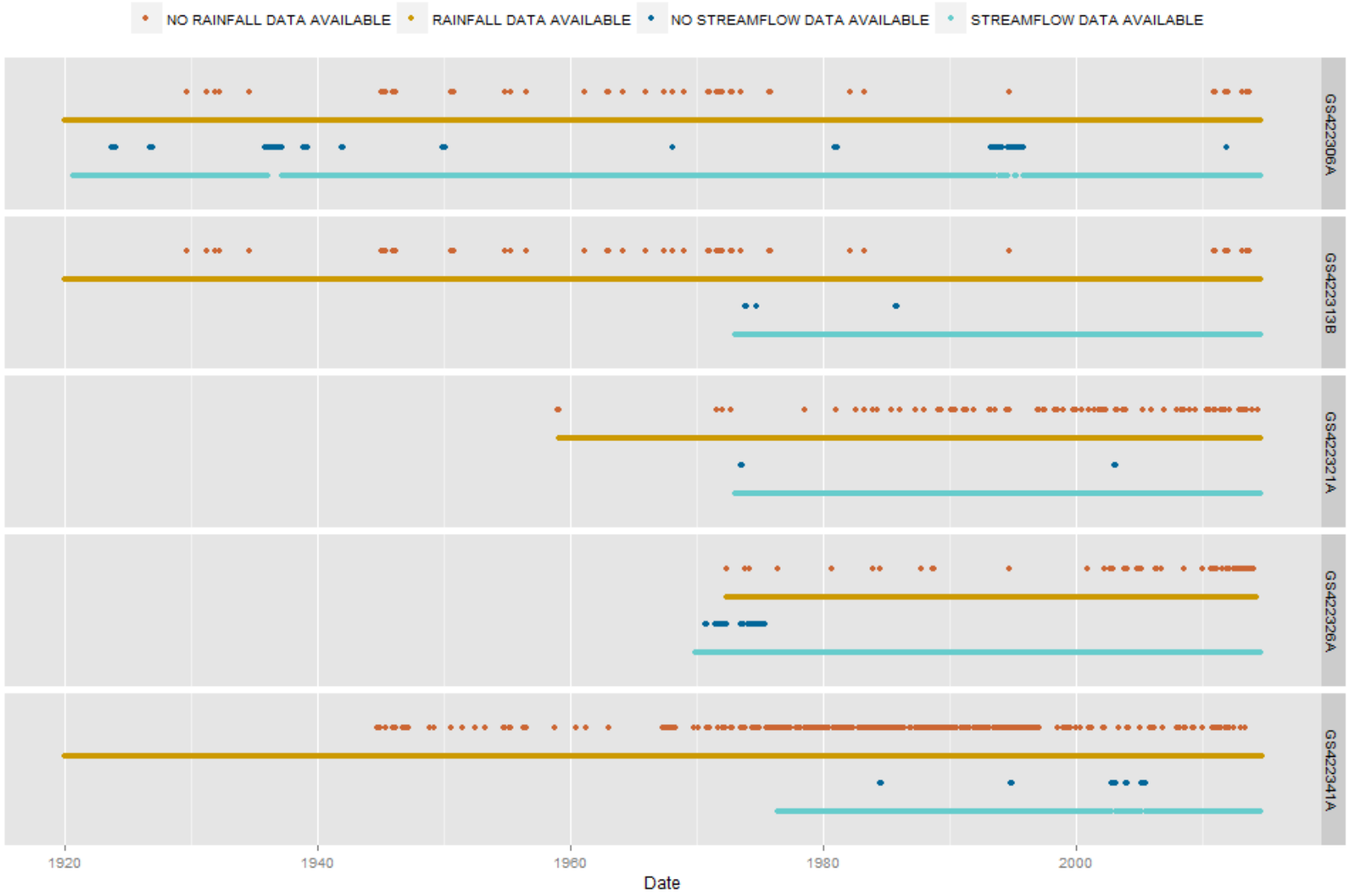
NO RAINFALL DATA AVAILABLE
RAINFALL DATA AVAILABLE
NO STREAMFLOW DATA AVAILABLE
STREAMFLOW DATA AVAILABLE
GS422306A
GS422313B
GS422321A
GS422326A
GS422341A
1920
1940
1960
1980
2000
Date

Figure 59 - Temporal distribution of stream flow and rainfall data for each stream gauging station, with distribution of missing data also indicated (BOM, 2014; QLD DNRM, 2014f)

A model was developed to automate recession curve extraction. A large variety of methods with different recession parameters have been applied in extracting baseflow recession data (e.g. Oyarzún et al., 2014; Stoelzle et al., 2013; Tallaksen, 1995; Wittenberg, 1999; WMO, 2008). In this study, recessions were defined as the component of the hydrograph where d*Q*/d*t* was negative, from two days after a peak until a day before a trough in discharge (or when missing data or constant discharge was encountered). This reduced the chance of including the effects of storm runoff and interflow on recessions. Only recessions that had a peak discharge higher than a specified cut-off value (Table 22) and lasted for a minimum of four consecutive days were used. This was done to increase the likelihood of extracting actual recessions rather than small fluxes in discharge that are especially evident at low flows, where data noise and gauging errors are more prevalent.

Table 22 - Peak discharge filter (cutoff) used in recession data extraction, and the number of bins used in determining storage-discharge relationships.

Stream	Stream Gauging Station	Cutoff Discharge (mm/day)	Number of Bins
Swan Creek	422306A	0.06	30
Emu Creek	422313B	0.06	50
Spring Creek	422321B	0.35	30
Condamine River	422341A	0.1	40

Rainy days and days with missing rainfall data were removed from the recession data, while the effects of evapotranspiration on recessions were assumed to be negligible as stream discharge was fed from groundwater storage (Ajami et al., 2011). The validity of this assumption varies between catchments, with groundwater storage losses to evapotranspiration (and thus recession behaviour) being more important in some catchments than others (Wittenberg, 1999). Kirchner (2009) indicated that precipitation and evapotranspiration fluxes did not need to be wholly absent, just relatively small compared to discharge. However, this could not be investigated due to a lack of adequate daily evapotranspiration data. A five year sample of the automatically extracted recession data for Spring Creek (GS 422321B) is depicted in Figure 60for the period January 2010 to August 2014.

Recession plots were generated from the filtered recession dataset. The rate of change of discharge (-dQ/dt) was plotted as a function of discharge (Q) in natural log space. These variables were calculated between all successive streamflow recession data points. The rate

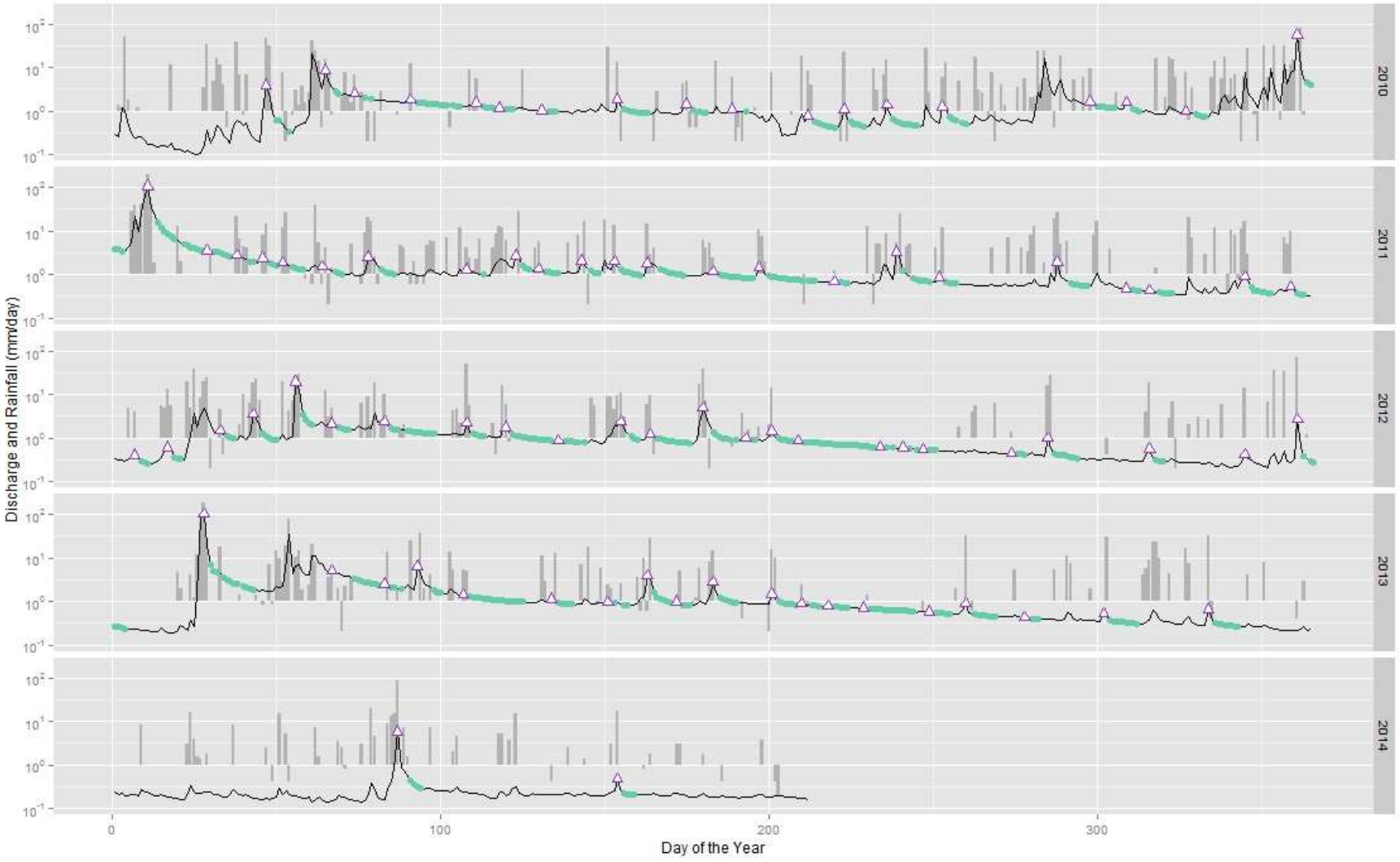
Discharge and Rainfall (mm/day)
2010
2011
2012
2013
2014
0
100
200
300
Day of the Year

Figure 60 - Daily streamflow (black line) and rainfall (grey bars) data from January 2010 to August 2014 for Spring Creek (GS 422321B), with rainless periods used in recession analysis highlighted in green and respective local flow peaks indicated by triangles. Downwards facing rainfall data represent rainfall less than 1mm in magnitude, as all the data are plotted on a lognormal scale.

of change of discharge and the corresponding discharge were estimated as follows (Brutsaert and Nieber, 1977):

$$-\frac{dQ}{dt} \approx \frac{Q_{t-\Delta t} - Q_t}{\Delta t} \qquad (7)$$

$$Q \approx \frac{Q_{t-\Delta t} + Q_t}{2} \qquad (8)$$

where Δt = 1 day. To determine the functional relationship between –d*Q*/d*t* and *Q*, recession plot data were binned based on the *Q* value (independent variable), and a least squares regression model was fitted to the binned values. The primary reason that recession plots were binned was to properly define recession behaviour at low discharges where scatter in data points is high (Kirchner, 2009). Two different binning techniques were employed as per Ajami et al. (2011), namely the quantile and equal interval binning techniques. The quantile binning technique bins data so that each bin contains approximately the same number of data points. On the other hand, the equal interval method bins data so that all bins span an equal width of log-transformed streamflows, resulting in bins with vastly different numbers of data points. The binned data undergo a quality control process, so that only bins where the standard error (-d*Q*/d*t*) is less than half mean (-d*Q*/d*t*) are kept (Kirchner, 2009). The number of bins was determined such that the relationship between Q and –d*Q*/d*t* was well defined (Table 22). Both linear and quadratic regression functions were fitted to the binned data. The most suitable of the four models that best represented the functional relationship between –d*Q*/d*t* and *Q* was selected for each catchment.

Storage-discharge relationships were derived from these regression functions by the methods outlined in Section 0 (Equation 5 and 6), where analytical solutions to the regression functions were already available (Ajami et al., 2011; Kirchner, 2009). The storage-discharge function of a linear regression equation of the form:

$$\ln\left(-\frac{dQ}{dt}\right) = \ln(a) + b.\ln(Q) \qquad (9)$$

was defined as:

$$S - S_0 = \frac{1}{a}\frac{1}{2-b}Q^{2-b} \qquad (10)$$

where ln(a) is the y-intercept , b is the slope and S_0 is a constant of integration. Similarly, the storage-discharge function of a quadratic polynomial regression equation of the form:

$$\ln\left(-\frac{dQ}{dt}\right) = c_1 + c_2\ln(Q) + c_3[\ln(Q)]^2 \qquad (11)$$

where the quadratic coefficient (c_3) is positive, was defined as:

$$S - S_0 = \frac{1}{2}\sqrt{\frac{\pi}{c_3}}\exp\left(\frac{(c_2-2)^2 - 4c_3c_1}{4c_3}\right)\mathrm{erf}\left(\sqrt{c_3}lnQ + \frac{\frac{c_2-2}{2}}{\sqrt{c_3}}\right) \qquad (12)$$

where erf is the error function.

Quantifying Annual Groundwater Recharge

Groundwater recharge was quantified on an event by event basis for the last 15 years (July 1999 to June 2014). This time period was selected for two primary reasons. First, high quality streamflow data with limited missing data were available across all catchments. Second, recharge estimates could be obtained for periods of both flood and drought, thus providing information over a range of climatic conditions. Groundwater recharge due to a precipitation event was estimated by calculating the change in catchment storage (i.e. recharge) before and after the event, using either Equation 10 or 12. The representative stream discharge values for each event were manually identified as depicted in Figure 61, which captures changes in catchment baseflow due to recharge. The values of groundwater recharge obtained are minimum estimates for three reasons: 1) only events that could be identified with confidence were incorporated; 2) any depletion of groundwater storage during the event was not considered, and 3) only groundwater recharge and respective changes in storage that returned as stream discharge was accounted for.

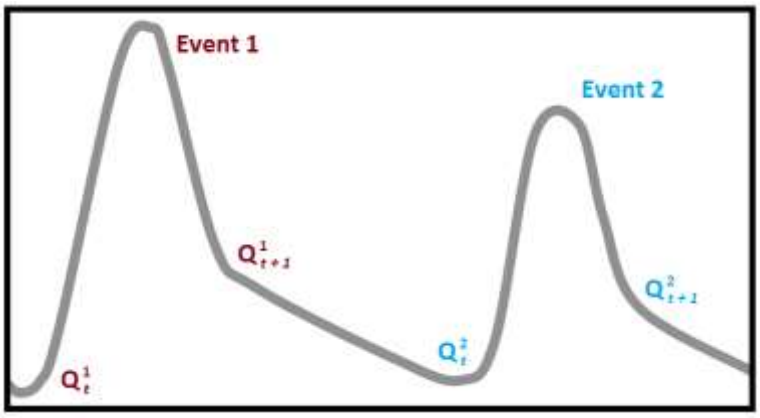

Figure 61 - Schematic of how representative discharge values are extracted from hydrograph to determine event-based recharge. A representative discharge is obtained before (Q_t) and after (Q_{t+1}) each recharge event (Figure after Ajami et al. (2011)).

Groundwater recharge estimates were aggregated into water years (July to June), where recharge events were assigned to the water year in which the event started. Aggregating the data allowed recharge estimates to be compared to the other estimates in this report. Total annual precipitation was quantified for the same time periods, and the percentage of rainfall resulting in recharge was evaluated.

Sensitivity Analysis

A sensitivity analysis was carried out to investigate the influence of the binning technique (quantile and equal interval) and the form of the regression equation (linear and quadratic) on predicted groundwater recharge values. Storage-discharge functions were derived for each of the four scenarios, and groundwater recharge values were estimated for each recharge event across all catchments. Annual groundwater recharge estimates for each scenario were quantified as discussed in Section 0. Groundwater recharge values were also compared to recharge data obtained for each catchment from the remote sensing analysis carried out in Chapter 0.

Results

Storage – Discharge Relationships

Simple quality control showed that only a limited number of recession points were lost due to missing rainfall record (Table 23). This was important as recession data were removed from the dataset if either rain was recorded on that day or if no rainfall data were available. Thus such a check ensured that large amounts of data were not being lost because of an incomplete rainfall dataset. The number of days lost due to incomplete rainfall record was calculated for the final dataset once recession data had been extracted from the stream flow time series, rather than for the entire rainfall record. A maximum of 1.4 % of recession points were lost across all four catchments (Table 23), which was considered satisfactory.

Table 23 - Assessment of the number of recession points lost due to missing rainfall data

Stream	Stream Gauging Station	Rainfall Gauge	No. of Recession Points	No. of NA Rainfalls	% of Total
Swan Creek	422306A	041120	6 112	6	0.10

Emu Creek	422313B	041120	3 758	3	0.08
Spring Creek	422321B	041208	2 736	20	0.73
Condamine River	422341A	041056	4 267	58	1.36

The recession behaviour of Spring Creek catchment (GS 422321B) was characterised by a cloud of recession points (Figure 62). The scatter in the recession plot, especially at lower discharge values, might be attributed to any of a number of factors, including: data measurement noise, gauging equipment limitations, impacts of evapotranspiration and precipitation on recession behaviour, and model simplification of real catchment (Kirchner, 2009).

After the recession data were binned, streamflow recession behaviour of Spring Creek catchment exhibited an upward curving, positive quadratic relationship for both the equal interval and quantile binning methods (Figure 62). In both instances, the relationship between rate of change of discharge ($-dQ/dt$) and discharge (Q) during streamflow recession was better defined by a quadratic rather than linear equation (Figure 63, Table 24). The quantile binning technique was selected because it defined catchment recession behaviour well with a suitable regression model (Figure 63, Table 25).

Figure 62 - Recession plots for Spring Creek (GS 422321B) based on daily rainless stream flow data. Black dots are binned data, error bars indicate standard error of each bin where the standard error was less than half the mean of –dQ/dt for each bin. Both the equal interval (left) and quantile (right) binning method were applied.

Quantile binning was also selected over the equal interval binning technique because all bin sizes were equal, thus preventing bins with very few data points having a large influence on the relationship. The storage-discharge function was derived from Equation 12, because the regression model had a positive quadratic coefficient and thus this analytical solution was suitable:

$$S - S_0 = 32.1 \, \mathrm{erf}(0.51 lnQ - 0.88)$$

Table 24 - Comparison of Spring Creek regression models for both equal interval and quantile binning methods

	Equal Interval Binning		**Quantile Binning**	
	Linear Model	**Quadratic Model**	**Linear Model**	**Quadratic Model**
ln*Q*	0.956	1.01	0.907	1.1
$(\ln Q)^2$	NA	0.19	NA	0.26

Intercept	-2.47	-2.85	-2.77	-2.91
Adjusted R^2	0.92	0.98	0.85	0.95
RMSE ($mm.day^{-2}$)	0.4	0.2	0.3	0.17
p Value	3.9e-15	2.2e-16	2.08e-13	2.2e-16

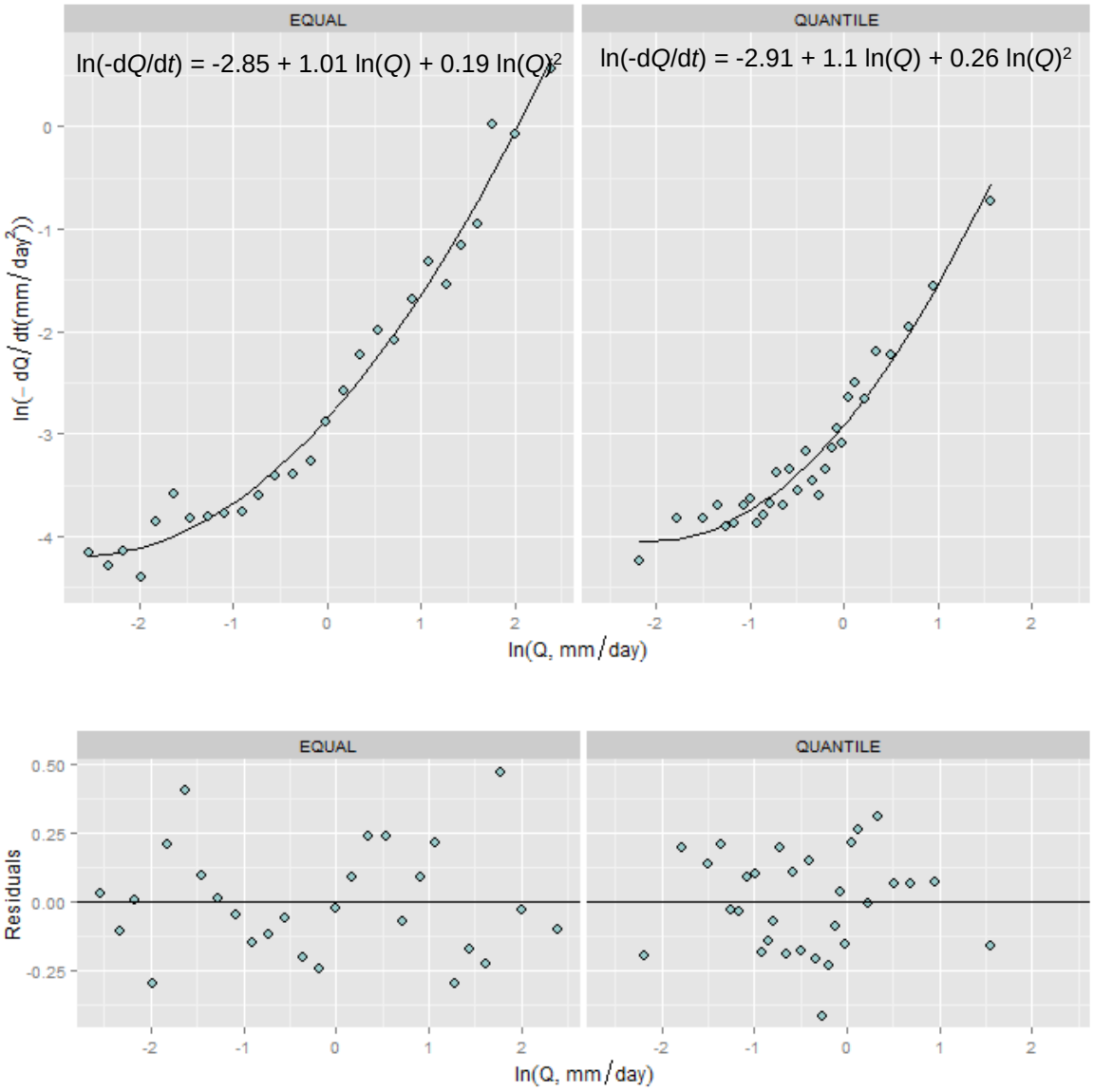

Figure 63 - Spring Creek quadratic regression models fitted to binned data (top) for both equal interval (left) and quantile (right) binning methods, with model residuals depicted below.

The other three catchments (Swan Creek, Emu Creek and Condamine River) all exhibited similar streamflow recession behaviour to Spring Creek (Figure 62, Figure 64). In each instance, the quantile binning technique and a quadratic regression function were found to be most suitable for defining the relationship between $-dQ/dt$ and Q. The least squares regression model was a good fit to the binned data with R^2 values varying between 0.97 and 0.99, while RMSE values were between 0.1 and 0.17 $mm.day^{-2}$ (Table 25). As with Spring Creek, the storage-discharge function of each catchment was derived from Equation 12.

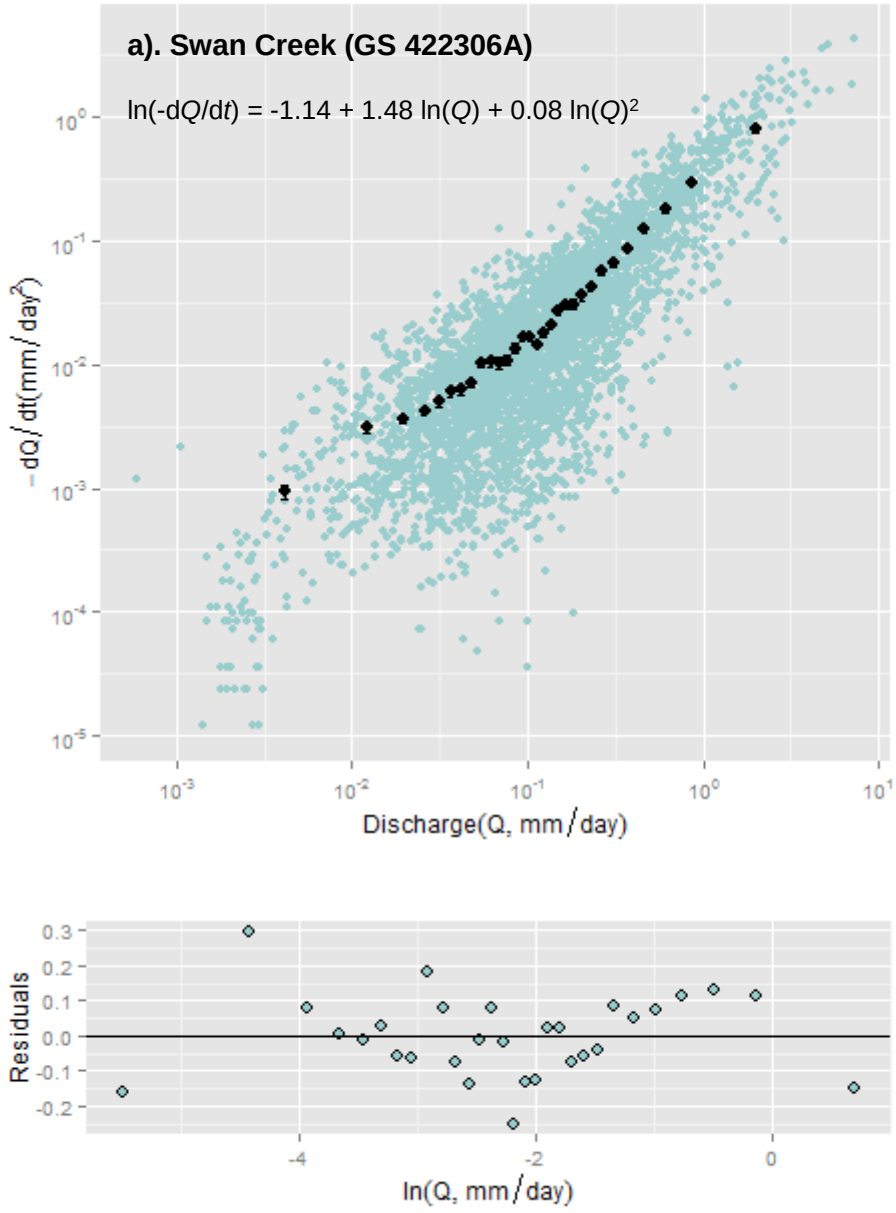

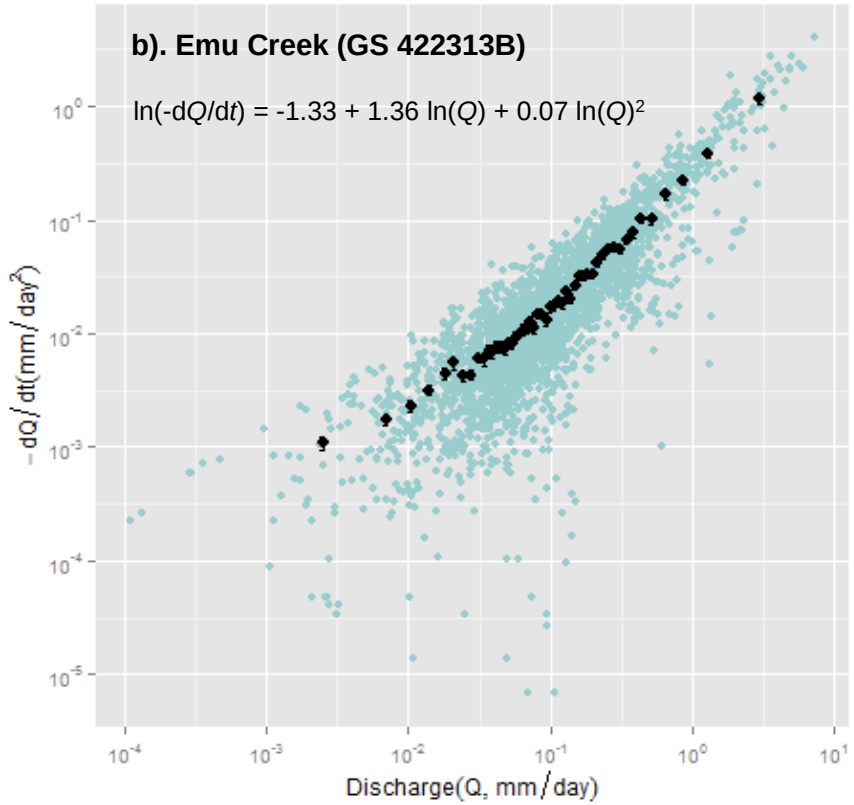
b). Emu Creek (GS 422313B)
ln(-dQ/dt) = -1.33 + 1.36 ln(Q) + 0.07 ln(Q)²
-dQ/dt(mm/day²)
Discharge(Q, mm/day)

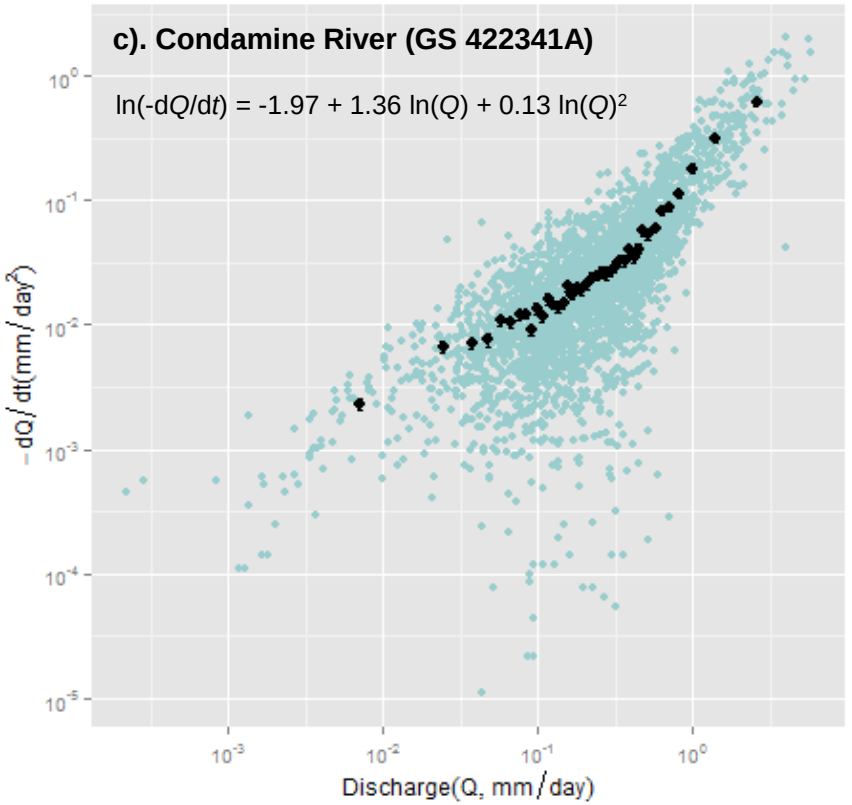
c). Condamine River (GS 422341A)
ln(-dQ/dt) = -1.97 + 1.36 ln(Q) + 0.13 ln(Q)²
-dQ/dt(mm/day²)
Discharge(Q, mm/day)

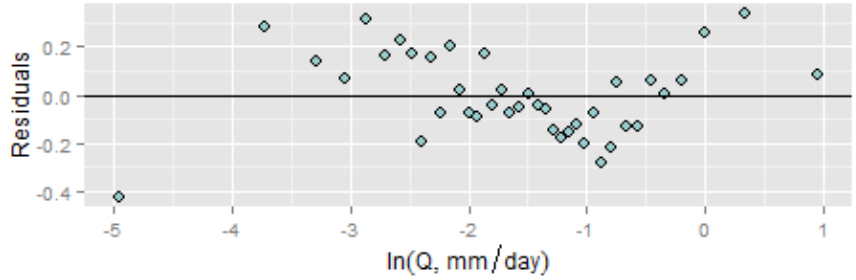
Residuals
ln(Q, mm/day)

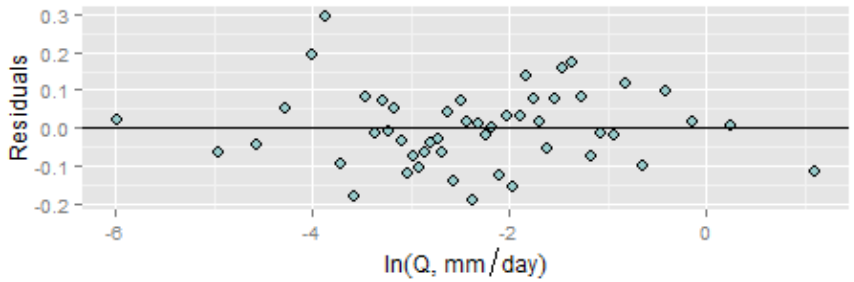

Figure 64 - Recession plots and model residuals of a) Swan Creek (GS 422306A), b) Emu Creek (GS 422313B), and c) Condamine River (GS 422341A)

Table 25 - Summary of the final storage – discharge functions used in estimating recharge for each catchment

Stream	Gauging Station	S – Q Function	Regression Type	Binning Technique	Adjusted R^2	RMSE ($mm.day^{-2}$)
Swan Creek	422306A	$S - S_0 = 19.7\ \mathrm{erf}(0.29lnQ - 0.91)$	Quadratic	Quantile	0.99	0.11
Emu Creek	422313B	$S - S_0 = 19.40\ erf(0.27lnQ - 1.17)$	Quadratic	Quantile	0.99	0.10
Spring Creek	422321B	$S - S_0 = 32.1\ erf(0.51lnQ - 0.88)$	Quadratic	Quantile	0.95	0.17
Condamine River	422341A	$S - S_0 = 23.21\ \mathrm{erf}(0.35lnQ - 0.90)$	Quadratic	Quantile	0.97	0.17

Recharge Estimates

Groundwater recharge estimates varied among the four catchments (Figure 65, Table 26) even though all gauging stations were within a 22 km range as the crow flies. Groundwater recharge for the period 1999 to 2014 was on average the largest at Spring Creek (13.0 mm/year), followed by the Condamine River (10.2 mm/year), Swan Creek (3.1 mm/year) and lastly Emu Creek (2.1 mm/year). The Condamine River (GS 422341A) streamflow dataset had some missing data during 2002, 2003 and 2005 and thus recharge during this time period is potentially underestimated. It appeared that only a small percentage of annual rainfall resulted in recharge in these catchments, with the Condamine River exhibiting the largest mean percentage turnover (1.3 %) while Emu Creek had the smallest with a meagre 0.3 % (Figure 66, Table 27).

This spatial variation in recharge estimates might be a result of a number of factors. The recharge rates are (unsurprisingly) correlated to the general streamflows in the catchments, with Emu and Swan Creek having the lowest area-normalised streamflows (Figure 58) and largest number of no-flow days (Table 20). There also appears to be a general north-south trend in groundwater recharge, with larger recharge rates occurring in the southerly (Spring Creek and Condamine River) as to the northerly (Swan and Emu Creek) catchments (Figure 57). Furthermore, Spring Creek has the smallest catchment area (35 km^2) and highest elevation (552 mAHD), while Emu Creek has the largest catchment area (148 km^2), lowest elevation (491 mAHD) and the gauging station might already be in alluvial deposits. These differences might be indicative of shallower recharge flow paths at higher elevations within the

Main Range Volcanics; while recharge might be deeper and more regional further from the outcrops, with less water returning to rivers as baseflow.

Table 26 - Summary statistics of annual recharge (mm/year) for each of the four streams. Respective water year indicated in brackets where relevant.

	Swan Creek (GS 422306A)	**Emu Creek (GS 422313B)**	**Spring Creek (GS 422321B)**	**Condamine River (GS 422341A)**
Mean	3.12	2.05	13.01	10.16
Median	1.87	1.89	8.56	7.79
Minimum	0 (*2006 - 2007*)	0.00 (*2006 - 2007*)	0.01 (*2006 - 2007*)	0.72 (*2006 - 2007*)
Maximum	10.18 (*2010 - 2011*)	7.84 (*2010 - 2011*)	49.82 (*2010 - 2011*)	27.30 (*2010 - 2011*)
Standard Dev.	3.15	2.13	14.48	8.04
Count	15	15	15	15

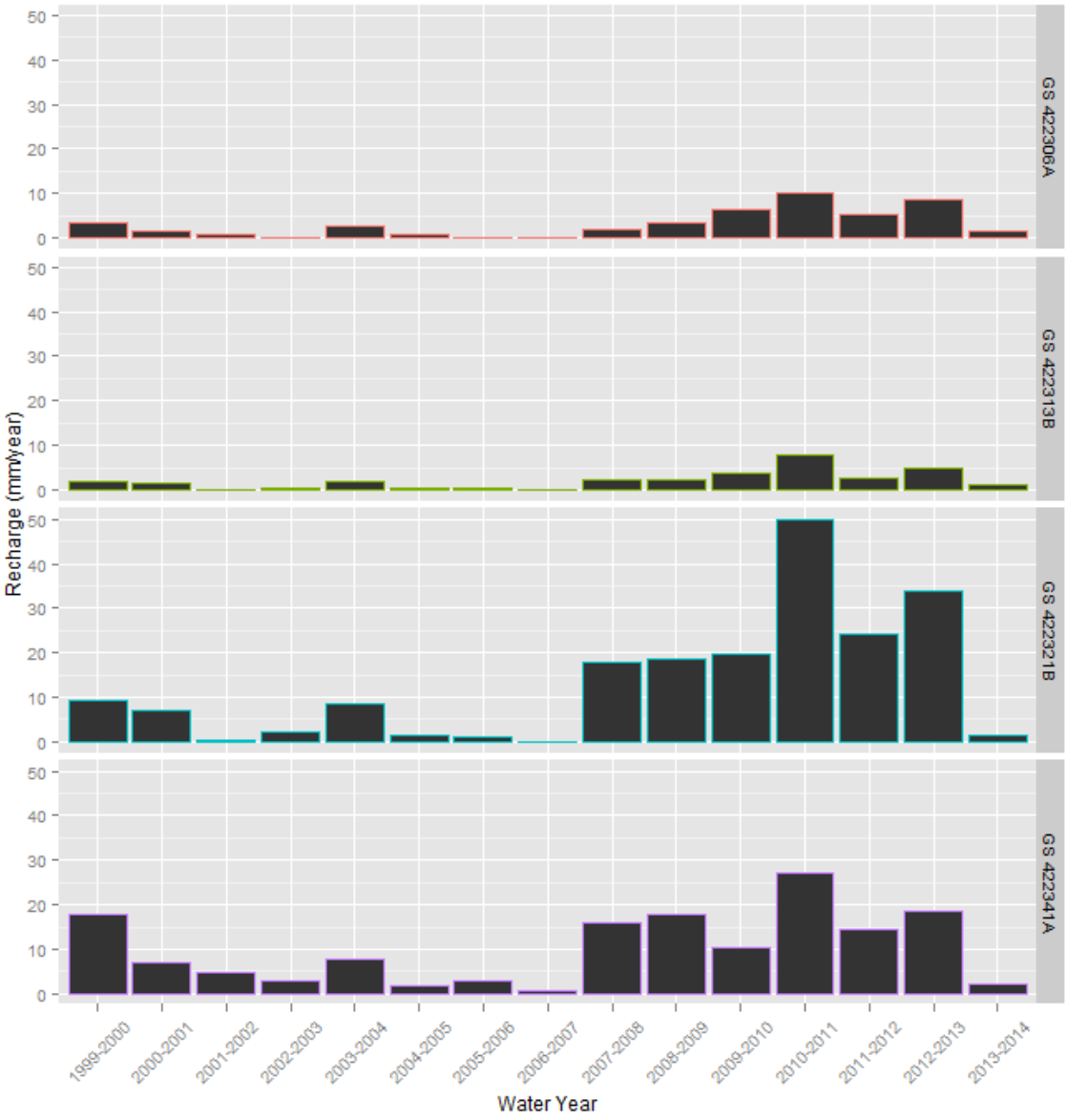

Figure 65 - Time series of groundwater recharge estimates for each of the four streams. Recharge is provided per water year (July - June), from July 1999 to June 2014.

Table 27 - Summary statistics of the percentage of annual rainfall that results in recharge, for each of the four streams. Respective water year indicated in brackets where relevant.

	Swan Creek (GS 422306A)	**Emu Creek (GS 422313B)**	**Spring Creek (GS 422321B)**	**Condamine River (GS 422341A)**
Mean	0.42	0.27	1.27	1.31
Median	0.30	0.25	1.02	1.33

Minimum	0 (*2006 - 2007*)	0.00 (*2006 - 2007*)	0.00 (*2006 - 2007*)	0.13 (*2006 - 2007*)
Maximum	1.37 (*2012 - 2013*)	0.80 (*2012 - 2013*)	3.17 (*2012 - 2013*)	2.32 (*2012 - 2013*)
Standard Dev.	0.40	0.24	1.14	0.82
Count	15	15	15	15

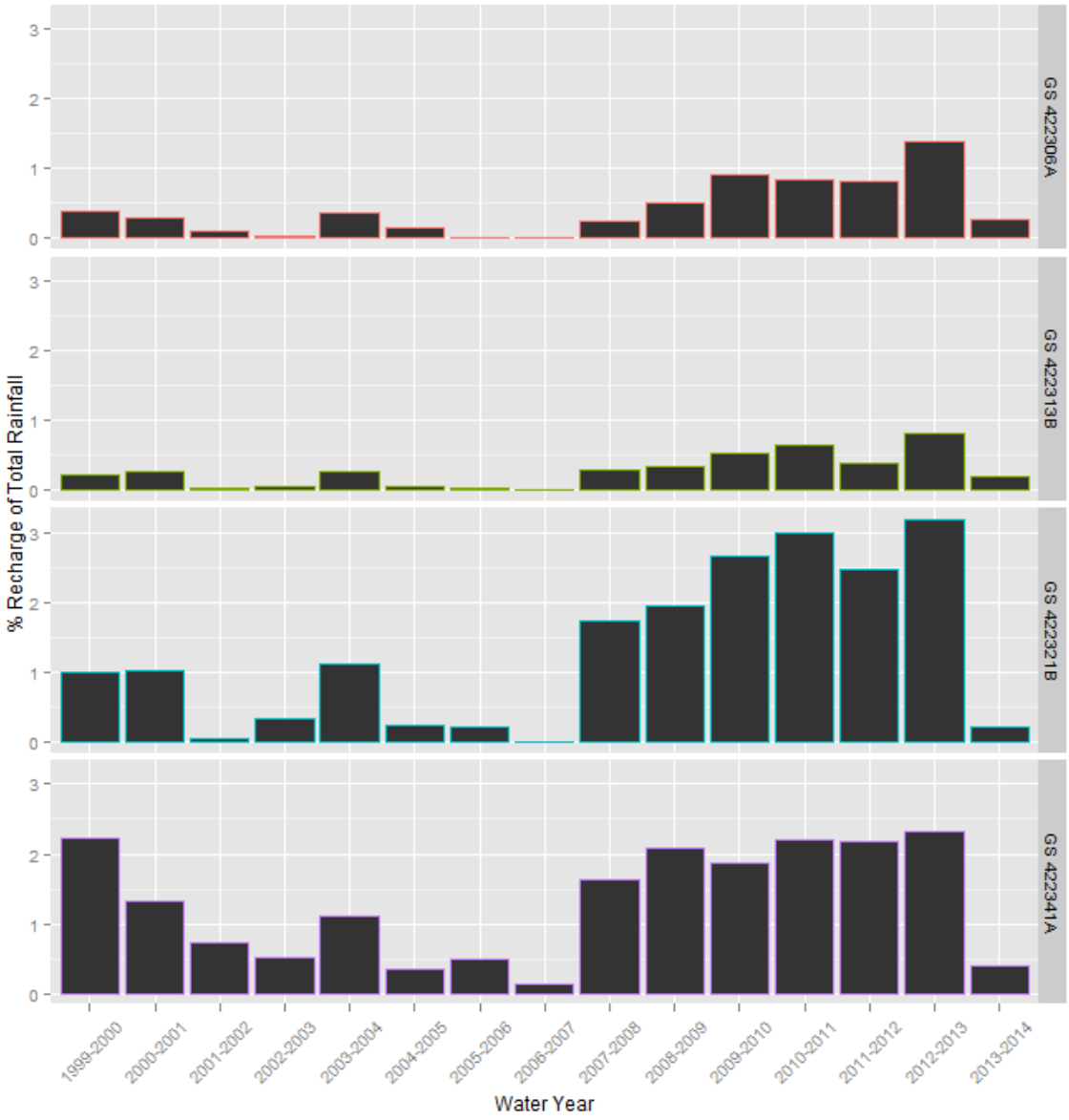

Figure 66 - Time series of percentage of rainfall resulting in groundwater recharge for each of the four streams. Percentages are provided per water year (July - June), from July 1999 to June 2014.

Groundwater recharge not only varied spatially but also substantial temporal variability was evident within each catchment (Figure 65, Table 26). During drought periods (e.g. 2006 - 2007), groundwater recharge was approximately zero for Swan, Emu and Spring Creek, while 0.7 mm of recharge occurred in the Condamine River catchment. On the other hand during flood periods (e.g. 2010 - 2011), recharge increased by many orders of magnitude with Spring Creek experiencing 50 mm. This variability in recharge rates is highlighted by the large standard deviations, with only the Condamine River catchment having a higher mean recharge rate than the respective standard deviation (Table 26). Similar trends were present in the amount of rainfall resulting in groundwater recharge (Figure 66, Table 27).

Sensitivity Analysis

Groundwater recharge estimates did vary depending on which storage-discharge function was used (Table 28). Generally, recharge estimates were the largest for storage-discharge functions derived from the linear recession behaviour regression models. Similarly, storage-discharge functions derived from data binned by the quantile technique resulted in larger estimates than from data binned into equal intervals. Recharge estimates derived from the quadratic regression model and equal interval binning technique were consistently the smallest. For three of the four catchments (Swan Creek, Emu Creek and Condamine River) predicted recharge estimates were substantially smaller than the recharge estimates that were derived from the other three storage-discharge functions (Table 28).

With the exception of the quadratic regression model fitted to equal interval binned data, recharge estimates were of the same order of magnitude giving confidence in the estimated values. Spring Creek had the largest range in mean recharge estimates (13.0 to 30.8 mm/year), while Swan Creek recharge estimates were very close between all models (3.0 to 3.7 mm/year). The groundwater recharge values used in this study (Model 4 - quadratic regression model fitted to quantile binned data) were consistently in the lower range of predicted values. Model 4 had the smallest RMSE across all catchments and also very high Adjusted R^2 (Table 28).

Table 28 - Summary of the different storage – discharge functions used in the sensitivity analysis, and respective estimates of mean annual recharge over the last 15 years. Four storage – discharge functions were derived for each stream for the sensitivity analysis. The influence of different regression functions (linear/quadratic) and binning techniques (equal interval/quantile) was investigated. Model 4 (quadratic regression function and quantile binning method) was used to estimate final recharge within each stream catchment.

Stream and Gauging Station Number	Model	S-Q Function (mm)	Regression Type	Binning Technique	Adjusted R^2	RMSE ($mm.day^{-2}$)	Mean Annual Recharge (mm/yr)
	1	$S - S_0 = 3.76\ Q^{0.84}$	Linear	Equal Interval	0.98	0.37	3.03
Swan Creek	2	$S - S_0 = 4.73\ Q^{0.90}$	Linear	Quantile	0.97	0.23	3.68
(GS 422306A)	3	$S - S_0 = 105\ \mathrm{erf}(0.09lnQ - 4.45)$	Quadratic	Equal Interval	0.98	0.36	2.5e-8
	4	$\boldsymbol{S - S_0 = 19.7\ erf(0.29lnQ - 0.91)}$	***Quadratic***	***Quantile***	***0.99***	***0.11***	***3.12***
	1	$S - S_0 = 3.95\ Q^{1.07}$	Linear	Equal Interval	0.96	0.54	3.81
Emu Creek	2	$S - S_0 = 5.12\ Q^{0.99}$	Linear	Quantile	0.97	0.23	5.17
(GS 422313B)	3	$S - S_0 = 20.31\ erf(0.25lnQ - 1.45)$	Quadratic	Equal Interval	0.995	0.18	0.873
	4	$\boldsymbol{S - S_0 = 19.40\ erf(0.27lnQ - 1.17)}$	***Quadratic***	***Quantile***	***0.99***	***0.10***	***2.05***
	1	$S - S_0 = 11.30\ Q^{1.04}$	Linear	Equal Interval	0.92	0.4	22.54
Spring Creek	2	$S - S_0 = 14.66\ Q^{1.09}$	Linear	Quantile	0.85	0.3	30.85
(GS 422321B)	3	$S - S_0 = 35.03\ erf(0.44lnQ - 1.13)$	Quadratic	Equal Interval	0.98	0.2	7.75
	4	$\boldsymbol{S - S_0 = 32.1\ erf(0.51lnQ - 0.88)}$	***Quadratic***	***Quantile***	***0.95***	***0.17***	***13.01***

	1	$S - S_0 = 5.74\ Q^{1.10}$	Linear	Equal Interval	0.95	0.55	13.72
Condamine River	2	$S - S_0 = 8.4\ Q^{1.10}$	Linear	Quantile	0.91	0.31	20.09
(GS 422341A)	3	$S - S_0 = 28.43\ \mathrm{erf}(0.22lnQ - 1.93)$	Quadratic	Equal Interval	0.96	0.45	0.40
	4	$\boldsymbol{S - S_0 = 23.21\ erf(0.35lnQ - 0.90)}$	***Quadratic***	***Quantile***	***0.97***	***0.17***	***10.16***

A limitation of this study is that it estimates recharge that subsequently discharges into the surface water system at the outlet of headwater catchments, rather than recharge that directly recharges to the Surat Basin groundwater system. Nevertheless, the estimates provide constraints on how much recharge may be directly entering the groundwater system from these headwaters and other areas of the Surat Basin with similar hydrological properties; and builds understanding of the surface flows.

The results presented in this report are only over a limited spatial and temporal scale, and can be expanded to get a fuller understanding of groundwater recharge in the Surat CMA. The catchments analysed in this study are located on the western side of the Main Range Volcanics from Toowoomba southwards towards the New South Wales border. There are other open gauging stations that can be analysed on the eastern extent of the Main Range Volcanics, and further historic stations both west and east of the divide. A handful of potential gauges have also been identified further west and north in the Surat Basin, however catchment areas at the gauging station locations might be too large to make these methods applicable. The time period of recharge estimates can also be expanded beyond the 15 years investigated in this report. There is potential for aggregating and expanding datasets from open and historical gauges in some circumstances.

The recharge estimates obtained here may be considered as a lower limit of groundwater recharge in the catchment. The methods account for groundwater flow paths from the aquifer to the stream, however this might not capture other recharge flow paths and inter-aquifer flows in the catchment (Ajami et al., 2011). The recession plot analysis of Brutsaert and Nieber (1977) is also based on the assumption that the investigated streams are perennial. Even though the streams investigated were only dry for less than seven percent of their flow record, this does result in underestimation of recharge events when pre-event discharge is zero as the actual level of catchment storage is unknown. There will also be some recharge that exits the catchment as streamflow during the events and therefore is not captured in the measured storage difference; and some recharge during the recession periods that the method assumes to be negligible

A preliminary sensitivity analysis was carried out on the impact of regression model and binning technique on recharge estimates. The methods applied in estimating groundwater

recharge have other assumptions whose impacts should also be further investigated. An automated technique was developed to extract recession data for this study that employed specific assumptions on recession length, start of recession, rate of recession and flow event magnitude. A recent study carried out on mesoscale catchments in Germany found that recession characteristics varied substantially depending on what method was applied, and recommended a multiple-methods approach to be implemented when possible (Stoelzle et al., 2013). Rupp and Selker (2006) developed a method to account for the scatter and noise in recession data at low discharges that might be valuable.

Further improvements in recession plot quality and quantifying recession behaviour can also be made by better identifying low precipitation and evapotranspiration days. The impacts of evapotranspiration on streamflow recession were not accounted for in the recession plots in this study. However, evapotranspiration can have substantial effects on baseflow recession in some systems and result in inaccurate interpretation of recession behaviour (Kirchner, 2009). Even though accurate daily evapotranspiration data are not available for these catchments, recession data can be selected for time periods of generally lower evapotranspiration rates. Improvements can be made in selecting rain free days by using spatially interpolated rainfall data or multiple rain gauges.

Recharge events and respective discharge values for quantifying groundwater recharge were manually identified in this study. Implementing such a manual hydrograph separation technique decreases objectivity, results are often not reproducible and separating the influence of multiple recharge events in close succession is difficult (Healy and Scanlon, 2010). The objectivity of results could be improved by looking at recharge on a larger time scale such as annual or seasonal, rather than on an event basis where errors can accumulate (Kirchner, 2009). Automated baseflow filters might also be valuable in reducing subjectivity in selecting recharge events and representative discharge values (Arnold et al., 1995; Chapman, 1999; Sloto and Crouse, 1996).

Furthermore, a number of different methods utilising streamflow data, such as the recession curve displacement method (Rorabaugh, 1964; Rutledge, 1998), have been applied in different studies to estimate groundwater recharge (Arnold and Allen, 1999; Arnold et al., 2000; Healy and Scanlon, 2010; Wittenberg, 1999). Applying different estimation techniques based on the same streamflow data might be fruitful in investigating the range in recharge estimates that are obtained by different streamflow recession methods and comparing to

values obtained from other recharge estimation approaches (e.g. water balance methods, water table fluctuation, etc.).

Conclusions

This section presents the main conclusions covering our literature review and analysis of existing data for the Surat Basin, including summary tables of previous and new recharge estimates. Recommendations follow in the next section.

A literature review was conducted to determine which recharge estimation methods used globally might be suitable for recharge estimation in the Surat Basin. Key findings from the literature review were: that multiple methods should be applied, and it is important to keep in mind the assumptions and limitations of each method. There is evidence that modelling methods can be readily combined with field measurements and that this combination of approaches may be suitable in the Surat Basin.

A number of recharge estimation methods have been applied in the Surat Basin prior to our study, e.g. groundwater hydrograph analyses, groundwater chloride mass balance, unsaturated zone chloride mass balance and soil water balance modelling. Of these methods, the soil water balance modelling resulted in the greatest range of recharge estimates (0 – 455 mm/year). Several methods resulted in estimated groundwater recharge rates that were higher than the groundwater recharge rates currently included in the OGIA model (see Table 29).

The previous recharge estimates included a range of spatial scales but the temporal scales were typically quite limited (see Table 29). Many of the previous studies reported long term average recharge rates but did not provide the finer detail of time-variable recharge estimates.

Our analysis and interpretation of available data has resulted in an improved understanding of the spatial and temporal distribution of groundwater recharge in the Surat Basin.

Re-analysis of the deep drainage results produced using the PERFECT model for the Queensland Murray Darling Basin resulted in a map of deep drainage for this region. However, the spatial distribution of these results is dependant on how the soil and land use classifications used by PERFECT are translated into available soil and land use maps.

Table 29 - Previous recharge estimates

Method Used	Spatial Scale	Time Period	Estimated Recharge Rate (mm/year)	Reference
Groundwater Hydrograph Analysis	Single bore in the Mooga Sandstone	1993-2001	4-7	(Kellett et al., 2003)
Groundwater Chloride Mass Balance	GAB intake beds	N/A	<0.5 - >10	(Kellett et al., 2003)
PERFECT Model	Queensland Murray Darling Basin	1900-2001	1-455	(Yee Yet and Silburn, 2003)
PERFECT Model	Fitzroy Basin	1900-2005	0-139*	(Owens et al., 2007)
PERFECT Model	Greenmount Site	1977-1996	12	(Owens et al., 2004)
Soil Chloride Mass Balance	Greenmount Site	1977-1996	14	(Tolmie et al., 2004)
Soil Chloride Mass Balance	13 cropped sites in the Queensland Murray Darling Basin	1985-2001	2-16	(Tolmie et al., 2004)
Soil Chloride Mass Balance	5 paired sites (pasture/annual cropping) in southern Queensland	N/A	0.1-25	(Silburn et al., 2011)
Lysimeters	7 irrigated sites in the Queensland Murray Darling Basin	2002-2009	0-235	(Gunawardena et al., 2011)
Groundwater Chloride Mass Balance	GAB intake beds	N/A	0-79	(Ransley and Smerdon, 2012)

OGIA groundwater model – calibrated "net recharge"	Surat CMA	N/A	0-5.2	(GHD, 2012)

*only recharge estimates for the portion of the Fitzroy Basin that coincides with the "Recharge Estimation Project Study Area" are reported here

The regional groundwater flow directions in different aquifers were plotted by fitting potentiometric surfaces to available borehole data. However due to various data limitations, the potentiometric surfaces are only broadly indicative of regional groundwater flow paths and require improvement. Higher quality and quantity of water level data is necessary with better characterisation of source aquifers and borehole location.

The water table fluctuation method was applied to available groundwater hydrographs to produce estimates of groundwater recharge. New recharge data were produced for the Main Range Volcanics, with rates varying between 6 and 37 mm/year (see Table 30). Yet the locations were restricted to bores with sufficient data where aquifers are unconfined, preferably where water tables are shallow, and pumping impacts are limited. If suitable locations are targeted for additional groundwater monitoring, this method could be extended to easily estimate recharge rates at further locations of interest.

Analysis of surface water data was also used to quantify groundwater recharge. This is a powerful method because it relies mainly on streamflow records; however it has important assumptions, including the assumption that a component of recharge (due to changes in storage) appears as stream baseflow at the outlet of the surface catchment. New recharge data were produced for the Main Range Volcanics area, with rates varying between 0 and 3.2 mm/year (see Table 30).

There are a number of potential ways forward for the surface water analyses including: extending it to other parts of the Surat Basin, looking at recharge on a larger time scale such as annual or seasonal basis, or applying alternative baseflow separation and recession analysis methods.

Data from the combined remote sensing and model product from CSIRO, the Australian Water Availability Project (http://www.csiro.au/awap/), were utilised to to investigate the spatial and temporal variability of deep drainage throughout the whole Surat Basin and for separate

geological units (Walloon – Injune units, and Main Range Volcanics) (summarised in Table 30).

Since the data available from remote sensing only allow a water balance in the top ~2 meters of soil, the term ”deep drainage” is used here in preference to “recharge”. Deep drainage within the Surat Basin as a whole was found to exhibit a high degree of spatial variability, and areas of higher deep drainage correlate to areas with a combination of higher precipitation and /or certain soil and landscape properties.

The temporal distribution of deep drainage shows large variability around the long term means. These results show the potential importance of including recharge as a time varying input (at least annually varying) to groundwater models.

Further work is required to improve the local and regional recharge estimates developed in Phase 1 of the Recharge Estimation project. This work includes: comparing the deep drainage estimates to recharge rates determined using borehole hydrographs; converting deep drainage into groundwater recharge; verification and adjustment of the CSIRO regional estimates and refinement by improved use of local data and remote sensed data; development of process knowledge to understand the causes for temporal and spatial variations in groundwater recharge; and merging local scale estimates and process knowledge with the regional scale data to produce spatial-temporal recharge data sets suitable for use in groundwater impacts assessment.

Table 30 - Recharge estimates from analysis of water table fluctuations, surface water hydrographs, and the CSIRO Australian Water Availability Project data.

Method Used	Locations	Spatial Resolution	Time Period	Estimated Recharge Rate (mm/year)
Groundwater Hydrograph Analyses[1]	Main Range Volcanics	A few metres	1993-2011	6-37
Surface Water Hydrograph Analyses (Storage/Discharge Relationships)[1]	Swan Creek	Small catchments	1999-2014	0-10.2
	Emu Creek		1999-2014	0-7.8
	Spring Creek		1999-2014	0-49.8

	Condamine River		1999-2014	0.7-27.3
	Regional (Recharge Estimation Project Study Area)		2006	0-28
			2011	1- 64
			1900-2013	1 - 105
Remote Sensing Based Water Balance (AWAP)[2]	Walloon-Injune Outcrop Areas	5 km x 5 km	2006	0 - 15.7
			2011	12 - 191.5
			1900-2013	1.8 - 34
	Main Range Volcanics		2006	0 - 28
			2011	8.1 - 228
			1900-2013	1.3 - 105

[1]Recharge, and [2]Deep drainage

Recommendations for further work on Recharge Estimation in the Surat Basin

The overall objectives of the groundwater recharge project, including the completed Phase 1 presented here and the future Phases 2 and 3, were:

1. To review existing recharge estimates and knowledge about recharge processes the Surat Basin (Phase 1)
2. To use existing data sets to develop new recharge estimates (Phase 1)
3. To identify priority experimental sites and experimental approaches (Phase 1)
4. To provide new evidence about recharge processes and rates at these selected priority recharge sites (Phase 2-3)
5. To regionalise this information to similar sites in the Surat (Phase 2-3)
6. To produce new broad-scale recharge estimates by merging estimation methods including remote sensing based methods (Phase 2-3)
7. To make recommendations for refinements to the recharge inputs used in the OGIA groundwater impacts assessment model (Phase 2-3)

Phase 1 of the project has met its objectives, with the overall conclusion that there is substantial scope to use local scale experiments and recharge estimation methods, merged

with improved remote-sensing based regional estimates, to produce more credible, time-variable inputs to the Surat CMA groundwater impacts assessment.

We recommend that Phase 2-3 addresses this conclusion and proceed according to the objectives outlined above and with the following approach:

1. Refinement of the CSIRO Australian Water Availability Project remote-sensing approach to include additional remote-sensed data (soil moisture, surface storage and additional climate variables), to use surface water data that is more relevant for the Surat, and to look at the value of including time-lags that convert deep drainage into groundwater recharge.
2. Extension of the groundwater hydrograph and surface water hydrograph methods to other key areas of the Surat Basin.
3. Implementation of the proposed field experiment program, details of which are included in the accompanying Field Experiment report.
4. Application of methods for merging the small scale data and process knowledge with the annual regional scale estimates to produce the best practicable accuracy and resolution for groundwater impacts assessment.

These recommendations are expanded upon in the Phase 2-3 proposal document.

References

Ahmadi, S. H., and Sedghamiz, A. (2007). Geostatistical Analysis of Spatial and Temporal Variations of Groundwater Level. *Environmental Monitoring and Assessment, 129*(1-3), 277-294. doi: 10.1007/s10661-006-9361-z

Ajami, H., Troch, P. A., Maddock, T., Meixner, T., and Eastoe, C. (2011). Quantifying mountain block recharge by means of catchment-scale storage-discharge relationships. *Water Resources Research, 47*.

Allison, G. B., Gee, G. W., and Tyler, S. W. (1994). Vadose-Zone Techniques for Estimating Groundwater Recharge in Arid and Semiarid Regions. *Soil Science Society of America Journal, 58*(1), 6-14.

Andreasen, M., Andreasen, L. A., Jensen, K., Sonnenborg, T. O., and Bircher, S. (2013). Estimation of Regional Groundwater Recharge Using Data from a Distributed Soil Moisture Network. *Vadose Zone Journal*, 18. doi: 10.2136/vzj2013.01.0035

Arditto, P. A. (1983). Mineral-Groundwater Interactions and the Formatin of Authigenic Kaolinite within the Southeastern Intake Beds of the Great Australian (Artesian) Basin, New South Wales, Australia. *Sedimentary Geology, 35*, 249-261.

Armstrong, D. (1974). Recharge and the Groundwater Regime of the Toowoomba City Catchment (pp. 25).

Arnold, J. G., and Allen, P. M. (1999). Automated methods for estimating baseflow and ground water recharge from streamflow records. *Journal of the American Water Resources Association, 35*(2), 411-424.

Arnold, J. G., Allen, P. M., Muttiah, R., and Bernhardt, G. (1995). Automated Base-Flow Separation and Recession Analysis Techniques. *Ground Water, 33*(6), 1010-1018.

Arnold, J. G., Muttiah, R. S., Srinivasan, R., and Allen, P. M. (2000). Regional estimation of base flow and groundwater recharge in the Upper Mississippi river basin. *Journal of Hydrology, 227*(1-4), 21-40.

Audibert, M. (1976). Progress report of the Great Artesian Basin hydrogeological study, 1972 - 1974. Record 1976/5. Canberra: Bureau of Mineral Resources, Geology and Geophysics.

AUSLIG. (2001). *AUSLIG 9 Second DEM (Version 2)*.

Australasian Groundwater & Environmental Consultants Pty Ltd. (2005). Great Artesian Basin Water Resource Plan - Potential River Baseflow From Aquifers of the GAB (pp. 19): Prepared for the Department of Natural Resources and Mines.

Australia Pacific LNG. (2014). 2013 - 2014 Groundwater Assessment Report (Q-LNG01-75-RP-0001).

Baram, S., Arnon, S., Ronen, Z., Kurtzman, D., and Dahan, O. (2012a). Infiltration Mechanism Controls Nitrification and Denitrification Processes under Dairy Waste Lagoon. *Journal of Environmental Quality, 41*, 1623-1632.

Baram, S., Kurtzman, D., and Dahan, O. (2012b). Water percolation through a clayey vadose zone. *Journal of Hydrology, 424-425*, 165-171.

Barron, O. V., Crosbie, R. S., Dawes, W. R., Charles, S. P., Pickett, T., and Donn, M. J. (2012). Climatic controls on diffuse groundwater recharge across Australia. *Hydrological and Earth System Sciences, 16*, 4557-4570.

Bastiaanssen, W. G. M., Merenti, M., Feddes, R. A., and Holtslag, A. A. M. (1998). A remote sensing surface energy balance algorithm for land (SEBAL). 1. Formulation. *Journal of Hydrology, 212-213*, 198-212.

Becker, M. W. (2006). Potential for Remote Sensing of Ground Water. *Ground Water, 44*(2), 1745-6584.

Bierwirth, P. N., and Welsh, W. D. (2000). Delination of recharge beds in the Great Artesian Basin using airborne gamma-radiometrics and satellite remote sensing (F. a. F. Department of Agriculture, Trans.) (pp. 34). Canberra: Bureau of Rural Sciences.

Bohling, G., and Wilson, B. (2006). Statistical and Geostatistical Analysis of the Kansas High Plains Water-Table Elevations, 2006 Measurement Campaign: Kansas Geological Survey.

Bohling, G., and Wilson, B. (2012). Statistical and geostatistical analysis of the Kansas High Plains Water-Table Elevations, 2012 Measurement Campaign: Kansas Geological Survey.

BOM. (2014). Climate Data Online - Rainfall. Retrieved 22 August 2014, from Commonwealth of Australia, Bureau of Metereology (BOM) http://www.bom.gov.au/climate/data/

Bond, W. (1998). Soil Physical Methods for Estimating Recharge. In L. Zhang (Ed.), *The Basics of Recharge and Discharge*. Collingwood, VIC: CSIRO.

Brunner, P. (2004). Using remote sensing to regionalize local precipitation recharge rates obtained from the Chloride Method. *Journal of Hydrology, 294*, 241-250.

Brutsaert, W., and Nieber, J. L. (1977). Regionalized drought flow hydrographs from a mature glaciated plateau. *Water Resources Research, 13*(3), 637-643. doi: 10.1029/WR013i003p00637

Chapman, T. (1999). A comparison of algorithms for stream flow recession and baseflow separation. *Hydrological Processes, 13*(5), 701-714. doi: 10.1002/(SICI)1099-1085(19990415)13:5<701::AID-HYP774>3.0.CO;2-2

Christiaens, K., and Feyen, J. (2001). Analysis of uncertainties associated with different methods to determine soil hydraulic properties and their propagation in the distributed hydrological MIKE SHE model. *Journal of Hydrology, 246*, 63-81.

Cook, P. G., and Herczeg, A. (1998). Groundwater chemical methods for recharge studies. Part 2 of 2. In L. Zhang (Ed.), *The Basics of Recharge and Discharge*: CSIRO.

Crosbie, R. S., Jolly, I. D., Leaney, F. W., and Petheram, C. (2010). Can the dataset of field based recharge estimates in Australia be used to predict recharge in data-poor areas? *Hydrology and Earth System Sciences, 14*, 2023-2038.

CSIRO. (2007). PressurePlot v2.0. Retrieved from http://www.pressureplot.com/

Cuthbert, M., and Tindimugaya, C. (2010). The importance of preferential flow in controlling groundwater recharge in tropical Africa and implications for modelling the impact of climate change on groundwater resources. *Journal of Water and Climate Change Vol, 1*(4), 234-245.

Cuthbert, M. O. (2010). An improved time series approach for estimating groundwater recharge from groundwater level fluctuations. *Water Resources Research, 46*(9).

Dafny, E., and Silburn, D. M. (2014). The hydrogeology of the Condamine River Alluvial Aquifer, Australia: a critical assessment. *Hydrogeology Journal, 22*, 705-727. doi: 10.1007/s10040-013-1075-z

Dahan, O., Talby, R., Yechieli, Y., Adar, E., Lazarovitch, N., and Enzel, Y. (2009). In Situ Monitoring of Water Percolation and Solute Tranport Using a Vadose Zone Monitoring System. *Vadose Zone Journal, 8*(4), 916-925. doi: 10.2136/vzj2008.0134

Davies, P. J., and Crosbie, R. S. (2011). *Australian 0.05 degree gridded chloride deposition*. Retrieved from: http://www.ga.gov.au/metadata-gateway/metadata/record/71620/

de Vries, J. J., and Simmers, I. (2002). Groundwater recharge: an overview of processes and challenges. *Hydrogeology Journal, 10*(1), 5-17.

Delin, G. N., Healy, R. W., Lorenz, D. L., and Nimmo, J. R. (2007). Comparison of local- to regional-scale estimates of ground-water recharge in Minnesota, USA. *Journal of Hydrology, 334*(1-2), 231-249.

Desbarats, A. J., Logan, C. E., Hinton, M. J., and Sharpe, D. R. (2002). On the kriging of water table elevations using collateral information from a digital elevation model. *Journal of Hydrology, 255*(1–4), 25-38. doi: http://dx.doi.org/10.1016/S0022-1694(01)00504-2

Diouf, O. C., Faye, S. C., Diedhiou, M., Kaba, M., Faye, S., Gaye, C. B., Faye, A., Englert, A., and Wohnlich, S. (2012). Combined uses of water-table fluctuation (WTF), chloride mass balance (CMB) and environmental isotopes methods to investigate groundwater recharge in the Thiaroye sandy aquifer (Dakar, Senegal). *African Journal of Environmental Science and Technology, 6*, 425-437.

Doll, P., and Fiedler, K. (2008). Global-scale modeling of groundwater recharge. *Hydrology and Earth System Sciences, 12*, 863-885.

Fensham, R. J., and Fairfax, R. J. (2003). Spring wetlands of the Great Artesian Basin, Queensland, Australia. *Wetlands Ecology and Management, 11*(5), 343-362. doi: 10.1023/B:WETL.0000005532.95598.e4

Free, D. (1989). Geology of the Main Range Volcanics and Hydrogeological Implications, Toowoomba District, South East Queensland (pp. 64).

Freeze, R. A., and Banner, J. (1970). The Mechanism of Natural Ground-Water Recharge and Discharge 2. Laboratory Column Experiments and Field Measurements. *Water Resources Research, 6*(1), 138-155.

Gee, G. W., and Hillel, D. (1988). Groundwater Recharge in Arid Regions - Review and Critique of Estimation Methods. *Hydrological Processes, 2*(3), 255-266.

Gee, G. W., Ward, A. L., Cadwell, L. L., and Ritter, J. C. (2002). A Vadose Zone Water Fluxmeter with Divergence Control. *Water Resources Research, 38*(8). doi: 10.1029/2001WR000816

Gerla, P. J. (1992). The relationship of water-table changes to the capillary fringe, evapotranspiration, and precipitation in intermittent wetlands. *Wetlands, 12*(2), 91-98.

GHD. (2012). Surat Cumulative Management Area Groundwater Model Report (pp. 290).

Golder Associates. (2009). QGC Groundwater Study Surat Basin, Queensland: Coal seam gas field component for environmental impact statement.

Goovaerts, P. (1997). *Geostatistics for natural resources evaluation*. New York: Oxford University Press.

Goovaerts, P. (2000). Geostatistical approaches for incorporating elevation into the spatial interpolation of rainfall. *Journal of Hydrology, 228*(1–2), 113-129. doi: http://dx.doi.org/10.1016/S0022-1694(00)00144-X

Greve, A., Andersen, M. S., and Acworth, R. I. (2010). Investigations of soil cracking and preferential flow in a weighing lysimeter filled with cracking clay soil. *Journal of Hydrology, 393*, 105-113.

Gunawardena, T. A., McGarry, D., Robinson, J. B., and Silburn, D. M. (2011). Deep drainage through Vertosols in irrigated fields measured with drainage lysimeters *Soil Research, 49*, 343-354.

Habermehl, M. (1980). The Great Artesian Basin, Australia. *BMR Journal of Australian Geology & Geophysics, 5*, 9-38.

Habermehl, M. (2002). *Hydrogeology, Hydrochemistry and isotope hydrology of the Great Artesian Basin*. GAB FEST 2002: A resource under pressure.

Habermehl, M., Devenshire, J., and Magee, J. (2009). Sustainable groundwater allocations in the intake beds of the Great Artesian Basin in New South Wales (recharge to the New South Wales part of the Great Artesian Basin). Final report for the National Water Commission. Canberra: Bureau of Rural Science.

Healy, R. W., and Cook, P. G. (2002). Using groundwater levels to estimate recharge. *Hydrogeology Journal, 10*(1), 91-109.

Healy, R. W., and Scanlon, B. R. (2010). *Estimating Groundwater Recharge*. Cambridge, New York: Cambridge University Press.

Heath, R. C. (1983). *Basic ground-water hydrology*. (2220). U.S. Govt. Print. Off.,.

Heliotis, F. D. (1989). Water storage capacity of wetland used for wastewater treatment. *Journal of Environmental Engineering, 115*(4), 822-834.

Herczeg, A., and Love, A. (2007). Review of Recharge Mechanisms for the Great Artesian Basin *Water for a Healthy Country* Glen Osmond, SA: CSIRO.

Hillier, J. R. (2010). Groundwater connections between the Walloon Coal Measures and the Alluvium of the Condamine River (pp. 24): A report for the Central Downs Irrigators Limited.

Hitchon, B., and Hays, J. (1971). Hydrodynamics and Hydrocarbon Occurrences, Surat Basin, Queensland, Australia. *Water Resources Research, 7*(3), 658-676. doi: 10.1029/WR007i003p00658

Hodgkinson, J., Hortle, A., and McKillop, M. (2010). The application of hydrodynamic analysis in the assessment of regional aquifers for carbon geostorage: preliminary results for the Surat Basin, Queensland. *APPEA Journal, 50th Anniversary Issue*, 445-462.

Hodgkinson, J., Preda, M., Hortle, A., McKillop, M., Dixon, O., and Foster, L. M. (2009). The Potential Impact of Carbon Dioxide Injection on Freshwater Aquifers: The Surat and Eromanga Basins in Queensland. In J. Draper (Ed.). Brisbane: QLD Department of Employment, Economic Development and Innovation.

Hofstra, N., Haylock, M., New, M., Jones, P., and Frei, C. (2008). Comparison of six methods for the interpolation of daily, European climate data. *Journal of Geophysical Research: Atmospheres, 113*(D21), D21110. doi: 10.1029/2008JD010100

Ireson, A. M., Wheater, H. S., Butler, A. P., Mathias, S. A., Finch, J., and Cooper, J. D. (2006). Hydrological processes in the Chalk unsaturated zone - Insights from an intensive field monitoring programme. *Journal of Hydrology, 330*, 29-43.

Isaaks, E. H., and Srivastava, R. M. (1989). *An introduction to applied geostatistics*. New York: Oxford University Press.

Kellett, J. R., Ransley, T. R., Coram, J., Laycock, J., Barclay, D. F., McMahon, G. A., Foster, L. M., and Hillier, J. R. (2003). Groundwater Recharge in the Great Artesian Basin Intake Beds, Queensland. Brisbane: Bureau of Rural Sciences and the Queensland Department of Natural Resources and Mines.

Kirchner, J. W. (2009). Catchments as simple dynamical systems: Catchment characterization, rainfall-runoff modeling, and doing hydrology backward. *Water Resources Research, 45*(2), W02429. doi: 10.1029/2008WR006912

Kitanidis, P. K. (1997). *Introduction to Geostatistics: applications to hydrogeology*. Cambridge: Cambridge University Press.

Kumar, V. (2007). Optimal contour mapping of groundwater levels using universal kriging—a case study. *Hydrological Sciences Journal, 52*(5), 1038-1050. doi: 10.1623/hysj.52.5.1038

Kurtzman, D., and Scanlon, B. R. (2011). Groundwater Recharge through Vertisols: Irrigated Cropland vs. Natural Land, Israel. *Vadose Zone Journal, 10*, 662-674.

Lerner, D. N. (1990). Groundwater recharge in urban areas. *Atmospheric Environment. Part B. Urban Atmosphere, 24*(1), 29-33. doi: http://dx.doi.org/10.1016/0957-1272(90)90006-G

Lerner, D. N., Issar, A. S., and Simmers, I. (1990). Groundwater Recharge: A Guide to Understanding and Estimating Natural Recharge (Vol. 8, pp. 372): International Association of Hydrogeologists.

Littleboy, M., Silburn, D. M., Freebairn, D. M., Woodruff, D. R., and Hammer, G. L. (1989). PERFECT, A computer simulation model of Productivity, Erosion, Runoff Functions to Evaluate Conservation Techniques (pp. 119): Queensland Department of Primary Industries.

Loheide, S. P. I., Butler Jr, J. J., and Gorelick, S. M. (2005). Estimation of groundwater consumption by phreatophytes using diurnal water table fluctuations: A saturated-unsaturated flow assessment. *Water Resources Research, 41*(7), 1-14.

Louie, M. J., Shelby, P. M., Smesrud, J. S., Gatchell, L. O., and Selker, J. S. (2000). Field evaluation of passive capillary samplers for estimating groundwater recharge. *Water Resources Research, 36*(9), 2407-2416.

Lu, X., Jin, M.-g., van Genuchten, M. T., and Wang, B.-g. (2011). Groundwater Recharge at Five Representative Sites in the Hebei Plain, China. *Ground Water, 49*(2), 286-294.

Marshall, M. R., Francis, O. J., Frogbrook, Z. L., Jackson, B. M., McIntyre, N., Reynolds, B., Solloway, I., Wheater, H. S., and Chell, J. (2009). The impact of upland land management on flooding: results from an improved pasture hillslope. *Hydrological Processes, 23*, 464-475. doi: 10.1002/hyp

McCown, R. L., Hammer, G. L., Hargreaves, J. N. G., Holzworth, D. P., and Freebairn, D. M. (1996). APSIM: A novel software system for model development, model testing and simulation in agricultural research. Agricultural Systems 50, 255-271 *Agricultural Systems, 50*(255-271).

McKenzie, N., and Hook, J. (1992). Interpretations of the Atlas of Australian Soils: Consulting report to the Environmental Resources Information Network (ERIN) (pp. 7). Canberra: CSIRO Division of Soils.

McKenzie, N., Jacquier, D. W., Ashton, L. J., and Cresswell, H. P. (2000). Estimation of soil properties using the Atlas of Australian Soils (pp. 24). Canberra: CSIRO Land and Water.

Mdaghri-Alaoui, A., and Eugster, W. (2001). Field determination of the water balance of the Areuse River delta, Switzerland. *Hydrological Sciences Journal, 46*(5), 747-760.

Moon, S.-K., Woo, N. C., and Lee, K. S. (2004). Statistical analysis of hydrographs and water-table fluctuation to estimate groundwater recharge. *Journal of Hydrology, 292*(1–4), 198-209. doi: http://dx.doi.org/10.1016/j.jhydrol.2003.12.030

Morris, D. A., and Johnson, A. I. (1967). *Summary of hydrologic and physical properties of rock and soil materials, as analyzed by the hydrologic laboratory of the U.S. Geological Survey, 1948-60*. U.S. Govt. Print. Off.,.

Ordens, C. M., Post, V. E. A., Werner, A. B., and Hutson, J. L. (2014). Influence of model conceptualisation on one-dimensional recharge quantification: Uley South, South Australia. *Hydrogeology Journal, 22*, 795-805.

Owens, J. S., Silburn, D. M., Forster, B. A., Chamberlain, T., and Wearing, C. (2007). Deep drainage estimates under a range of land uses and soils in the Fitzroy Basin. Brisbane: Department of Natural Resources and Water.

Owens, J. S., Tolmie, P. E., and Silburn, D. M. (2004). *Validating Modelled Deep Drainage Estimates for the Queensland Murray-Darling Basin*. ISCO 2004 - 13th International Soil Conservation Organisation Conference, Brisbane. July 2004, 6.

Oyarzún, R., Godoy, R., Núñez, J., Fairley, J. P., Oyarzún, J., Maturana, H., and Freixas, G. (2014). Recession flow analysis as a suitable tool for hydrogeological parameter determination in steep, arid basins. *Journal of Arid Environments, 105*(0), 1-11. doi: http://dx.doi.org/10.1016/j.jaridenv.2014.02.012

Parsons, S., Evans, R., and Hoban, M. (2008). Surface-groundwater connectivity assessment: A report to the Australian Government from the CSIRO Murray-Darling Basin Sustainable Yields Project (pp. 40): CSIRO.

Preston, R., Lawson, P., and Darbas, T. (2007). Landholder Practices, Attitudes, Constraints and Opportunities for Change in the Condamine Alliance Region. Brisbane: Condamine Alliance and the Department of Natural Resources and Water.

QLD DNRM. (2014a). Coal seam gas well locations - Queensland. Retrieved 15 August 2014, from QLD Department of Natural Resources and Mines (QLD DNRM) http://dds.information.qld.gov.au/dds/

QLD DNRM. (2014b). Groundwater Database - Queensland. Retrieved 16 June 2014, from QLD Department of Natural Resources and Mines (QLD DNRM) http://dds.information.qld.gov.au/dds/

QLD DNRM. (2014c). Petroleum well locations - Queensland. Retrieved 15 August 2014, from QLD Department of Natural Resources and Mines (QLD DNRM) http://dds.information.qld.gov.au/dds/

QLD DNRM. (2014d). Water Monitoring Data Portal. Retrieved 16 June 2014, from QLD Department of Natural Resources and Mines (DNRM) http://watermonitoring.derm.qld.gov.au/host.htm

QLD DNRM. (2014e). Water Monitoring Data Portal - Historical Streamflow Data. Retrieved 22 August 2014, from QLD Department of Natural Resources and Mines (DNRM) http://watermonitoring.derm.qld.gov.au/host.htm

QLD DNRM. (2014f). Water Monitoring Data Portal - Streamflow Data. Retrieved 22 August 2014, from QLD Department of Natural Resources and Mines (DNRM) http://watermonitoring.derm.qld.gov.au/host.htm

Quarantotto, P. (1989). Hydrogeology of the Surat Basin, Queensland. Record 1989/26. Brisbane: Queensland Department of Mines.

QWC. (2012a). Hydrogeological Attributes Associated with Springs in the Surat Cumulative Management Area (Vol. M09744A01). Brisbane: Queensland Water Commission (QWC).

QWC. (2012b). Underground Water Impact Report for the Surat Cumulative Management Area. Brisbane: Queensland Water Commission (QWC).

Radford, B. J., Silburn, D. M., and Forster, B. A. (2009). Soil chloride and deep drainage responses to land clearing for cropping at seven sites in central Queensland, northern Australia. *Journal of Hydrology, 379*, 20-29.

Radke, B. M., Ferguson, J., Cresswell, R. G., Ransley, T. R., and Habermehl, M. (2000). Hydrochemistry and implied hydrodynamics of the Cadna-owie - Hooray Aquifer, Great Artesian Basin, Australia (pp. 248). Canberra: Bureau of Rural Sciences.

Ransley, T. R., and Smerdon, B. D. (2012). Hydrostratigraphy, hydrogeology and system conceptualisation of the Great Artesian Basin (pp. 324): Australian Government, Department of Sustainability, Environment, Water, Population and Communties.

Ransley, T. R., Tottenham, R., Sundaram, B., and Brodie, R. (2007). Development of Method to Map Potential Stream-Aquifer Connectivity: a case study in the Border Rivers Catchment: Australian Government, Department of Agriculture, Fisheries and Forestry.

Raupach, M. R., Briggs, P. R., Haverd, V., King, E. A., Paget, M., and Trudinger, C. M. (2009). Australian Water Availability Project (AWAP): CSIRO Marine and Atmospheric Research Component: Final Report for Phase 3. Canberra: CSIRO and the Bureau of Meteolology.

Reading, L. P., Lockington, D. A., Bristow, K. L., and Baumgartl, T. (2010). *An analysis of the impacts of sodic soil hydraulic conductivity on deep drainage and groundwater recharge using the HYDRUS model*. American Geophysical Union (AGU) National Meetings, San Francisco, USA.

Rimon, Y., Nativ, R., and Dahan, O. (2011). Physical and Chemical Evidence for Pore-Scale Dual-Domain Flow in the Vadose Zone. *Vadose Zone Journal, 10*. doi: 10.2136/vzj2009.0113

Ringrose-Voase, A. J., and Nadelko, A. J. (2011). Quantifying deep drainage in an irrigated cotton landscape. Canberra: CSIRO.

Rockhold, M. L., Waichler, S. R., Saunders, D. L., Clayton, R. E., and Strickland, C. E. (2009). Soil Water Balance and Recharge Monitoring at the Hanford Site - FY09 Status Report (pp. 87): U.S. Department of Energy.

Rorabaugh, M. I. (1964). Estimating changes in bank storage and groundwater contribution to streamflow. *Inter. Assoc. Sci. Hydrol. Pub., 63*, 432-441.

Rosenberry, D. O., and Winter, T. C. (1997). Dynamics of water-table fluctuations in an upland between two prairie-pothole wetlands in North Dakota. *Journal of Hydrology, 191*(1-4), 266-289.

Rupp, D. E., and Selker, J. S. (2006). Information, artifacts, and noise in dQ/dt-Q recession analysis. *Advances in Water Resources, 29*(2), 154-160. doi: http://dx.doi.org/10.1016/j.advwatres.2005.03.019

Rutledge, A. T. (1998). Computer programs for describing the recession of ground-water discharge and for estimating mean ground-water recharge and discharge from streamflow records: update.: US Geological Survey Water-Resources Investigations Report 98-4148.

Rutter, H. K., Cooper, J. D., Pope, D., and Smith, M. (2014). New understanding of deep unsaturated zone controls on recharge in the Chalk: a case study near Patcham, SE England. *Quaterly Journal of Engineering Geology and Hydrogeology, 45*, 487-495. doi: 10.1144/qjegh2011-010

Sanford, W. (2002). Recharge and groundwater models: an overview. *Hydrogeology Journal, 10*(1), 110-120.

Scanlon, B. R., Healy, R. W., and Cook, P. G. (2002). Choosing appropriate techniques for quantifying groundwater recharge. *Hydrogeology Journal, 10*(1), 18-39.

Scanlon, B. R., Keese, K. E., Flint, A. L., Flint, L. E., Gaye, C. B., Edmunds, W. M., and Simmers, I. (2006). Global synthesis of groundwater recharge in semiarid and arid regions. *Hydrological Processes, 20*, 3335-3370. doi: 10.1002/hyp.6335

Schilling, K. E., and Kiniry, J. R. (2007). Estimation of evapotranspiration by reed canarygrass using field observations and model simulations. *Journal of Hydrology, 337*(3-4), 356-363.

Schlumberger Water Services. (2011). Groundwater Modelling of the Surat Basin: Prepared for Arrow Energy Limited.

Shanafield, M., and Cook, P. G. (2014). Transmission losses, infiltration and groundwater recharge through ephemeral and intermittent streambeds: A review of applied methods. *Journal of Hydrology, 511*, 518-529.

Silburn, D. M., and Montgomery, J. (2004). Deep drainage under irrigated cotton in Australia - A review *WATERpak: a guide for irrigation management in cotton* (pp. 29-40). Narrabri, NSW: Cotton Research and Development Corporation.

Silburn, D. M., Owens, J. S., Dutta, S., Cresswell, R. G., and McNeil, V. (2006). *Hodgson Creek, QMDB - salinity and recharge studies and 2CSalt modelling*. 10th Murray-Darling Basin Groundwater Workshop, Canberra, Australia. September, 2006.

Silburn, D. M., Tolmie, P. E., Biggs, A. J. W., Whish, J. P. M., and French, V. (2011). Deep drainage rates of Grey Vertosols depend on land use in semi-arid subtropical regions of Queensland, Australia. *Soil Research, 49*, 424-438.

Simunek, J., and van Genuchten, M. T. (2008). Modeling nonequilibrium flow and transport with HYDRUS. *Vadose Zone Journal, 7*(2), 782-797.

Sloto, R. A., and Crouse, M. Y. (1996). HYSEP: A computer program for streamflow hydrograph separation and analysis (pp. 46): U.S. Geological Survey Water-Resources Investigations Report 96-4040.

Smerdon, B. D., and Ransley, T. R. (2012). Water resource assessment for the Surat region: A report to the Australian Government from the CSIRO Great Artesian Basin Water Resource Assessment (pp. 142): Australian Government, Department of Sustainability, Environment, Water, Population and Communities.

Smerdon, B. D., Ransley, T. R., Radke, B. M., and Kellett, J. R. (2012a). Water Resource Assessment for the Great Artesian Basin (pp. 56): CSIRO.

Smerdon, B. D., Rousseay-Gueutin, P., Love, A., Taylor, A. R., Davies, P. J., and Habermehl, M. (2012b). Chapter 7: Regional hydrodynamics. In T. R. Ransley & B. D. Smerdon (Eds.), *Hydrostratigraphy, hydrogeology and system conceptualisation of the Great Artesian Basin. A technical report to the Australian Government from the CSIRO Great Artesian Basin Water Resource Assessment.* Australia.

Stoelzle, M., Stahl, K., and Weiler, M. (2013). Are streamflow recession characteristics really characteristic? *Hydrology and Earth System Sciences, 17*, 817-828.

Sukhija, B. S., Reddy, D. V., Nagabhushanam, P., and Hussain, S. (2003). Recharge processes: piston flow vs preferential flow in semi-arid aquifers of India. *Hydrogeology Journal, 11*, 387-395.

Tallaksen, L. M. (1995). A review of baseflow recession analysis. *Journal of Hydrology, 165*(1–4), 349-370. doi: http://dx.doi.org/10.1016/0022-1694(94)02540-R

Timlin, D., Starr, J., Cady, R., and Nicholson, T. (2003). Comparing Ground-Water Recharge Estimates Using Advanced Monitoring Techniques and Models. U.S. Department of Agriculture Agricultural Research Service Beltsville Agricultural Research Center.

Tolmie, P. E., Silburn, D. M., and Biggs, A. J. W. (2004). Estimating deep drainage in the Queensland Murray-Darling Basin using soil chloride. Toowoomba: Department of Natural Resources and Mines.

USGS. (2013). Water Table Fluctuation (WTF) Method. *Groundwater Resources Program.* Retrieved 14/08, 2014, from http://water.usgs.gov/ogw/gwrp/methods/wtf/

Wackernagel, H. (2003). *Multivariate Geostatistics: an introduction with applications* (3rd Edition ed.). Berlin: Springer-Verlag.

Welsh, W. D. (2000). GABFLOW: A steady state groundwater flow model of the Great Artesian Basin (pp. 75). Canberra: Bureau of Rural Sciences.

Winter, T. C., Harvey, J. W., Franke, O., and Alley, W. (1998). Ground water and surface water: a single resource. Denver, Colorado.: US Geological Survey.

Wittenberg, H. (1999). Baseflow recession and recharge as nonlinear storage processes. *Hydrological Processes, 13*, 715-726.

WMO. (2008). Manual on Low-flow Estimation and Prediction *Operational Hydrology Report No. 50* (pp. 136): World Meteorological Organization (WMO).

Wolhuter, A., Hines, K., Robbins, S., Vink, S., and Esterle, J. (In review). Final Report Volume 2 – Hydrogeological profiles of Great Artesian Basin springs; Springsure, Eulo, Bourke and Bogan River supergroups.

Wood, W. W. (1999). Use and Misuse of the Chloride-Mass Balance Method in Estimating Groundwater Recharge. *Ground Water, 37*(1).

Wood, W. W., and Sanford, W. E. (1995). Chemical and Isotopic Methods for Quantifying Groundwater Recharge in a Regional, Semiarid Environment. *Ground Water, 33*(3), 458-468.

WorleyParsons. (2012). Activity 1.2: Spatial Analysis of Coal Seam Gas Water Chemistry *Healthy HeadWaters: Coal Seam Gas Water Feasibility Study*: Prepared for the Department of Environment and Resource Management.

Yee Yet, J. S., and Silburn, D. M. (2003). Deep drainage estimates under a range of land uses in the Queensland Murray-Darling Basin using water balance modelling (pp. 76). Toowoomba: Queensland Department of Natural Resources and Mines.

Glossary

Aquifer: A saturated underground geological formation that can store water and transmit it to a bore or spring.

Aquitard: A geological formation that restricts the flow of water.

Baseflow Separation: Baseflow separation is often used to determine what portion of a streamflow hydrograph originates from baseflow and what portion originates from overland flow.

Confined Aquifer: A saturated aquifer bounded between low permeability materials like clay or dense rock.

Deep Drainage: Downwards movement of water across the bottom of the root zone.

Diffuse Recharge: Diffuse recharge is recharge that is distributed over large areas in response to precipitation infiltrating the soil surface and percolating through the unsaturated zone to the water table.

Focussed Recharge: Focussed recharge is the movement of water from surface-water bodies, such as streams to an underlying aquifer.

Piston Flow: The assumption that soil water moves vertically in a layered form.

Potentiometric Surface: A hypothetical surface representing the level to which groundwater would rise if not trapped in a confined aquifer. The potentiometric surface is equivalent to the water table in an unconfined aquifer.

Preferred Pathway Flow: Water flow through high permeability zones or cracks.

Process-Based Modelling: A modelling approach which focusses on simulating detailed physical processes that explicitly describe system behaviour.

Recharge: Groundwater recharge is the flux of water that reaches the groundwater table.

Unconfined Aquifer: A groundwater aquifer is said to be unconfined when its upper surface (water table) is open to the atmosphere through permeable material.

Appendices

Appendix 1 – Summary of available Research Outputs from Phase 1

Appendix 2– Deep Drainage Data

Appendix 3 – Water Table Fluctuation Analyses

Chapter 0: Deep Drainage Results, Surat CMA

Data ID Number	Data Description/ Location	Product	Spatial Data Resolution	Time Period	Temporal Data Resolution
1A	Surat Basin	Deep drainage estimates	Regional	NA	NA

Chapter 0: Groundwater Potentiometric Surfaces

Data ID Number	Data Description/ Location	Product	Spatial Data Resolution	Time Period	Temporal Data Resolution
2A	Condamine River Alluvium	Groundwater potentiometric surface – IDW Method	Regional scale aquifer	1995 - 2014	20 year interval
2B	Condamine River Alluvium	Groundwater potentiometric surface – Kriging Method	Regional scale aquifer	1995 - 2014	20 year interval
2C	Gubberamunda Sandstone	Groundwater potentiometric surface – IDW Method	Regional scale aquifer	1995 - 2014	20 year interval
2D	Gubberamunda Sandstone	Groundwater potentiometric surface – Kriging Method	Regional scale aquifer	1995 - 2014	20 year interval
2E	Hutton Sandstone	Groundwater potentiometric surface – IDW Method	Regional scale aquifer	1995 - 2014	20 year interval
2F	Hutton Sandstone	Groundwater potentiometric surface – Kriging Method	Regional scale aquifer	1995 - 2014	20 year interval
2G	Kumbarilla Beds	Groundwater potentiometric surface – IDW Method	Regional scale aquifer	1995 - 2014	20 year interval
2H	Kumbarilla Beds	Groundwater potentiometric surface – Kriging Method	Regional scale aquifer	1995 - 2014	20 year interval

2I	Main Range Volcanics	Groundwater potentiometric surface – IDW Method	Regional scale aquifer	1995 - 2014	20 year interval
2J	Main Range Volcanics	Groundwater potentiometric surface – Kriging Method	Regional scale aquifer	1995 - 2014	20 year interval
2K	Mooga Sandstone	Groundwater potentiometric surface – IDW Method	Regional scale aquifer	1995 - 2014	20 year interval
2L	Mooga Sandstone	Groundwater potentiometric surface – Kriging Method	Regional scale aquifer	1995 - 2014	20 year interval
2M	Walloon Coal Measures	Groundwater potentiometric surface – IDW Method	Regional scale aquifer	1995 - 2014	20 year interval
2N	Walloon Coal Measures	Groundwater potentiometric surface – Kriging Method	Regional scale aquifer	1995 - 2014	20 year interval

Chapter 0: Groundwater Hydrograph Recharge Estimates

Data ID Number	Data Description/ Location	Product	Spatial Data Resolution	Time Period	Temporal Data Resolution
3A	RN 42231251 (Main Range Volcanics)	Groundwater recharge estimates	Point estimate	2011 – 2012	Water Year
3B	RN 42231655 (Main Range Volcanics)	Groundwater recharge estimates	Point estimate	2009 – 2013	Water Year
3C	RN 42230974 (Main Range Volcanics)	Groundwater recharge estimates	Point estimate	2008 – 2013	Water Year
3D	RN 42231652 (Main Range Volcanics)	Groundwater recharge estimates	Point estimate	2009 – 2013	Water Year
3E	RN 42231653 (Main Range Volcanics)	Groundwater recharge estimates	Point estimate	2009 – 2013	Water Year
3F	RN 42231478 (Main Range Volcanics)	Groundwater recharge estimates	Point estimate	1993 – 1995	Water Year
3G	RN 42231660 (Main Range Volcanics)	Groundwater recharge estimates	Point estimate	2005 – 2011	Water Year

3H	RN 42220061 (Mooga Sandstone)	Groundwater recharge estimates	Point estimate	2009	Water Year

Chapter 0: Remote Sensing Recharge Estimates (available from the CSIRO http://www.csiro.au/awap/)

Data ID Number	Data Description/ Location	Product	Spatial Data Resolution	Time Period	Temporal Data Resolution
4A	Surat Basin	Deep drainage estimates	Regional	1900 - 2014	Yearly
4B	Surat Basin	Deep drainage estimates	Regional	1900 - 2014	Monthly

Chapter 0: Surface Water Hydrograph Recharge Estimates

Data ID Number	Data Description/ Location	Product	Spatial Data Resolution	Time Period	Temporal Data Resolution
5A	Swan Creek (GS 422306A)	Groundwater recharge estimates	Headwater catchment	July 1999 – June 2014	Water Year
5B	Emu Creek (GS 422313B)	Groundwater recharge estimates	Headwater catchment	July 1999 – June 2014	Water Year
5C	Spring Creek (GS 422321B)	Groundwater recharge estimates	Headwater catchment	July 1999 – June 2014	Water Year
5D	Condamine River (GS 422341A)	Groundwater recharge estimates	Headwater catchment	July 1999 – June 2014	Water Year

Table 31 - Drainage (mm/yr) matrix for Woodland

	SOIL TYPE																
	Vertosols				Dermosols			Kandosol	Tendosol	Sodosols					Rudosol	Chromosol	Ferrosol
	gre	bla	bro	red	bla	bro	red	red		yel	gre	bla	bro	red		red	red
Augathella	0	0	0	0	20	0	3	1	9	2	35	0	0	3	73	0	2
Bollon	0	0	0	0	12	0	1	1	4	1	22	0	0	1	53	0	1
Brigalow RS	0	0	0	0	32	0	5	3	14	3	59	0	0	7	100	0	5
Charleville	0	0	0	0	15	0	1	0	6	1	26	0	0	1	57	0	1
Chinchilla	0	0	0	0	23	0	3	1	8	2	48	0	0	3	94	0	3
Condamine	0	0	0	0	15	0	0	0	3	0	31	0	0	0	67	0	0
Cunnamulla	0	0	0	0	12	0	2	1	4	1	19	0	0	2	41	0	2
Dalby	0	0	0	0	19	0	1	0	4	0	37	0	0	1	82	0	1
Dirranbandi	0	0	0	0	12	0	1	1	5	1	21	0	0	2	53	0	1
Goondiwindi	0	0	0	0	19	0	2	1	7	1	36	0	0	2	74	0	2
Greenmount	0	0	0	0	20	0	1	1	6	0	43	0	0	2	89	0	1

Hungerford	0	0	0	0	10	0	1	1	3	1	16	0	0	1	33	0	1
Inglewood	0	0	0	0	17	0	2	1	7	1	34	0	0	3	77	0	2
Injune	0	0	0	0	22	0	2	1	9	1	43	0	0	3	80	0	2
Killarney	0	0	0	0	19	0	1	0	5	0	43	0	0	1	84	0	0
Meandarra	0	0	0	0	14	0	0	0	2	0	29	0	0	0	64	0	0
Miles	0	0	0	0	24	0	2	1	8	1	46	0	0	2	89	0	2
Mitchell	0	0	0	0	23	0	3	2	11	2	42	0	0	4	78	0	3
Moonie	0	0	0	0	10	0	0	0	2	0	22	0	0	0	54	0	0
Morven	0	0	0	0	22	0	3	1	10	2	38	0	0	3	76	0	2
Mungindi	0	0	0	0	15	0	1	0	4	1	27	0	0	1	60	0	1
Narayen	0	0	0	0	22	0	2	1	8	1	44	0	0	3	89	0	2
Nindigully	0	0	0	0	17	0	2	1	7	1	29	0	0	3	65	0	2
Oakey	0	0	0	0	12	0	1	0	3	0	25	0	0	1	58	0	1
Quilpie	0	0	0	0	10	0	1	0	3	1	16	0	0	1	36	0	1
Roma	0	0	0	0	23	0	1	0	6	1	40	0	0	2	81	0	1
St George	0	0	0	0	15	0	2	1	6	2	27	0	0	2	61	0	2
Surat	0	0	0	0	22	0	2	0	6	1	38	0	0	2	79	0	1

Talwood	0	0	0	1	21	0	2	1	7	2	36	0	0	3	78	0	2
Tambo	0	0	0	0	17	0	2	0	6	1	30	0	0	2	69	0	1
Tara	0	0	0	0	17	0	2	1	5	1	36	0	0	2	74	0	1
Taroom	0	0	0	0	33	0	3	2	13	2	60	0	0	4	105	0	3
Texas	0	0	0	0	15	0	2	1	6	1	32	0	0	2	72	0	2
Thargomindah	0	0	0	0	9	0	1	0	3	1	13	0	0	1	29	0	1
Toowoomba	0	0	0	1	56	0	11	8	36	6	108	1	0	15	168	0	11
Wandoan	0	0	0	0	22	0	1	0	6	1	44	0	0	2	88	0	1
Warwick	0	0	0	0	16	0	1	0	3	0	34	0	0	1	74	0	1
Wyandra	0	0	0	0	12	0	2	1	4	1	20	0	0	2	47	0	2
Average	0	0	0	0	19	0	2	1	7	1	36	0	0	2	72	0	2

Note: bla = black, gre = grey, bro = brown, yel =yellow

Table 32 - Drainage (mm/yr) for Buffel Grass Pasture

	SOIL TYPE																
	Vertosols				Dermosols			Kandosol	Tenosol	Sodosols					Rudosol	Chromosol	Ferrosol
	gre	bla	bro	red	bla	bro	red	red		yel	gre	bla	bro	red		red	red
Augathella	0	0	0	1	29	0	8	21	46	4	69	2	0	14	102	0	14
Bollon	0	0	0	1	19	0	4	12	31	2	50	1	0	8	77	0	8
Brigalow RS	4	1	5	8	52	5	21	41	79	12	108	8	2	32	139	5	31
Charleville	0	0	0	0	21	0	5	14	33	2	53	0	0	10	82	0	11
Chinchilla	2	0	2	4	45	2	14	37	77	7	101	5	1	24	137	3	23
Condamine	0	0	0	0	29	0	6	20	50	2	72	0	0	12	103	0	12
Cunnamulla	0	0	0	1	15	0	4	9	24	3	39	1	0	7	57	0	7
Dalby	0	0	0	1	37	0	10	28	64	4	90	2	0	19	127	0	19
Dirranbandi	0	0	0	0	20	0	4	10	28	2	49	1	0	7	77	0	8
Goondiwindi	1	0	0	1	33	0	9	25	58	4	76	2	0	16	110	1	15
Greenmount	1	0	2	2	48	0	13	40	83	6	112	2	0	26	147	0	26
Hungerford	0	0	0	0	12	0	2	6	18	1	30	0	0	4	44	0	5
Inglewood	2	0	2	3	38	2	12	30	65	6	87	4	1	20	123	2	20

Injune	1	0	0	2	36	0	10	26	59	4	85	2	0	18	117	1	17
Killarney	1	0	1	3	44	1	14	39	85	5	110	3	0	26	138	1	26
Meandarra	0	0	0	0	28	0	4	17	45	1	68	0	0	10	97	0	10
Miles	2	0	2	4	43	2	13	36	77	7	98	4	1	24	132	2	23
Mitchell	1	0	1	2	34	1	9	23	55	5	78	2	0	17	106	1	17
Moonie	0	0	0	1	23	0	5	14	36	2	59	1	0	10	86	0	10
Morven	0	0	0	1	31	0	9	21	49	5	74	1	0	16	105	0	16
Mungindi	0	0	0	0	24	0	4	11	33	1	58	0	0	7	86	0	8
Narayen	1	0	1	2	41	1	10	28	65	4	94	2	0	19	128	1	19
Nindigully	0	0	0	1	28	0	6	17	39	3	64	0	0	12	91	0	12
Oakey	0	0	0	1	25	0	5	16	41	2	68	1	0	9	99	0	10
Quilpie	0	0	0	1	13	0	4	9	22	3	34	1	0	6	50	0	7
Roma	0	0	0	1	37	0	10	27	59	4	83	1	0	19	115	0	19
St George	0	0	0	0	23	0	6	14	35	3	57	0	0	10	88	0	10
Surat	0	0	0	1	34	0	9	23	53	3	77	1	0	16	110	0	17
Talwood	1	0	1	1	33	1	7	21	49	3	74	1	0	14	108	1	15
Tambo	0	0	0	1	27	0	6	18	42	3	65	1	0	12	95	0	12

Tara	0	0	0	1	36	0	8	25	58	3	80	1	0	16	111	0	17
Taroom	1	0	1	3	51	1	15	36	78	7	107	3	0	26	143	1	25
Texas	1	0	1	3	36	1	12	33	67	6	85	3	0	21	122	2	21
Thargomindah	0	0	0	0	9	0	2	5	15	2	24	0	0	3	37	0	4
Toowoomba	10	1	11	19	103	11	52	99	180	25	209	22	4	79	235	11	74
Wandoan	1	0	1	1	39	1	10	29	66	4	92	2	0	19	128	1	19
Warwick	0	0	1	1	35	1	9	30	68	4	92	2	0	18	123	1	19
Wyandra	0	0	1	1	16	1	4	9	24	2	41	1	0	6	66	1	7
Average	1	0	1	2	33	1	9	24	54	4	77	2	0	17	106	1	17

Note: bla = black, gre = grey, bro = brown, yel =yellow

Table 33 - Drainage (mm/yr) for Summer Cropping

	SOIL TYPES																
	Vertosols				Dermosols			Kandosol	Tenosol	Sodosols					Rudosol	Chromosol	Ferrosol
	gre	bla	bro	red	bla	bro	red	red		yel	gre	bla	bro	red		red	red
Augathella	28	31	26	27	42	26	60	96	168	22	32	18	26	43	98	62	115
Bollon	26	28	19	22	43	19	47	79	136	19	28	15	24	35	81	50	96
Brigalow RS	44	47	39	39	55	39	90	149	233	32	46+	27	40	61	143	98	166
Charleville	23	23	20	21	37	20	46	80	143	16	29	15	19	37	81	48	97
Chinchilla	43	45	34	38	61	34	81	136	227	30	43	25	40	54	134	89	157
Condamine	42	44	33	34	58	33	68	113	178	30	39	25	39	48	111	77	127
Cunnamulla	16	44	13	14	30	13	34	55	101	12	18	10	15	24	57	35	69
Dalby	38	41	31	34	58	31	75	128	215	25	42	24	36	52	124	79	147
Dirranbandi	29	30	24	26	47	24	53	78	136	23	31	18	27	38	80	57	95
Goondiwindi	48	51	37	42	67	37	81	123	196	37	46	30	47	59	125	92	142
Greenmount	78	83	60	66	88	60	125	174	248	65	62	51	79	79	183	164	207
Hungerford	10	10	9	9	22	9	23	38	77	7	13	6	8	16	41	25	49
Inglewood	48	50	36	40	64	36	81	125	203	33	47	28	45	57	127	87	148

Injune	35	37	28	31	48	28	69	119	193	27	38	22	32	49	117	72	138
Killarney	144	148	123	131	124	123	193	222	289	141	118	111	133	154	251	233	270
Meandarra	40	42	30	33	55	30	66	107	169	30	39	24	38	48	110	77	124
Miles	46	47	35	40	60	35	82	138	222	31	44	27	42	57	133	90	154
Mitchell	34	36	28	30	52	28	64	110	183	24	35	19	31	45	110	73	131
Moonie	43	45	34	35	57	34	63	96	150	30	39	25	39	46	98	72	111
Morven	30	30	24	26	45	24	57	98	170	22	31	17	26	39	100	62	120
Mungindi	32	35	26	27	53	26	56	92	154	24	33	19	31	40	93	63	108
Narayen	42	45	34	38	58	34	82	139	221	28	43	25	39	55	134	89	157
Nindigully	31	33	26	27	49	26	59	92	155	24	33	19	29	40	94	64	109
Oakey	30	31	23	26	47	23	59	103	167	19	35	18	27	39	104	61	122
Quilpie	12	13	10	12	23	10	30	49	92	9	17	8	11	24	52	30	59
Roma	36	39	28	31	53	28	71	117	194	27	38	22	34	52	117	78	135
St George	34	36	26	29	53	26	61	95	159	25	36	20	31	46	97	67	114
Surat	37	40	29	32	56	29	69	113	188	27	39	22	36	50	112	77	132
Talwood	41	42	32	33	57	32	71	111	185	28	41	24	38	52	112	79	132
Tambo	25	28	22	21	39	22	50	90	157	18	28	14	24	36	89	54	108

Tara	43	46	33	36	59	33	73	118	191	29	41	24	40	52	120	82	138
Taroom	39	42	31	32	57	31	84	145	241	27	41	22	37	56	136	89	165
Texas	54	56	42	46	70	42	87	130	207	37	53	33	51	62	132	92	153
Thargomindah	8	9	7	8	18	7	20	35	70	6	11	6	7	15	37	19	43
Toowoomba	165	171	153	157	141	153	286	351	455	170	148	140	154	207	369	332	411
Wandoan	41	42	32	33	55	32	77	132	215	28	42	23	37	54	128	83	148
Warwick	117	122	89	98	108	89	147	175	239	104	87	77	111	111	196	189	213
Wyandra	19	19	15	17	34	15	39	65	114	12	23	11	16	30	67	42	79
Average	43	46	35	38	56	35	76	116	185	34	42	28	41	54	118	85	137

Note: bla = black, gre = grey, bro = brown, yel =yellow

Table 34 - Average Drainage (mm/yr) for Woodlands

	SOIL TYPES							
	Vert	**Derm**	**Kan**	**Ten**	**Sod**	**Rud**	**Chr**	**Fer**
Augathella	0	7.7	1	9	8	73	0	2
Bollon	0	4.3	1	4	4.8	53	0	1
Charleville	0	5.3	0	6	5.6	57	0	1
Chinchilla	0	8.7	1	8	10.6	94	0	3
Condamine	0	5	0	3	6.2	67	0	0
Cunnamulla	0	4.7	1	4	4.4	41	0	2
Dalby	0	6.7	0	4	7.6	82	0	1
Dirranbandi	0	4.3	1	5	4.8	53	0	1
Goondiwindi	0	7	1	7	7.8	74	0	2
Greenmount	0	7	1	6	9	89	0	1
Hungerford	0	3.7	1	3	3.6	33	0	1
Inglewood	0	6.3	1	7	7.6	77	0	2
Injune	0	8	1	9	9.4	80	0	2
Killarney	0	6.7	0	5	8.8	84	0	0
Meandarra	0	4.7	0	2	5.8	64	0	0
Miles	0	8.7	1	8	9.8	89	0	2
Mitchell	0	8.7	2	11	9.6	78	0	3
Moonie	0	3.3	0	2	4.4	54	0	0
Morven	0	8.3	1	10	8.6	76	0	2
Mungindi	0	5.3	0	4	5.8	60	0	1
Nindigully	0	6.3	1	7	6.6	65	0	2
Oakey	0	4.3	0	3	5.2	58	0	1
Quilpie	0	3.7	0	3	3.6	36	0	1

Roma	0	8	0	6	8.6	81	0	1
St George	0	5.7	1	6	6.2	61	0	2
Surat	0	8	0	6	8.2	79	0	1
Talwood	0.3	7.7	1	7	8.2	78	0	2
Tambo	0	6.3	0	6	6.6	69	0	1
Tara	0	6.3	1	5	7.8	74	0	1
Texas	0	5.7	1	6	7	72	0	2
Thargomindah	0	3.3	0	3	3	29	0	1
Toowoomba	0.3	22.3	8	36	26	168	0	11
Wandoan	0	7.7	0	6	9.4	88	0	1
Warwick	0	5.7	0	3	7	74	0	1
Wyandra	0	4.7	1	4	4.6	47	0	2

Note: Vert = Vertosol, Derm = Dermosol, Kan = Kandosol, Ten = Tenosol, Sod = Sodosol, Rud = Rudosol, Chr = Chromosol, Fer = Ferrosol

Table 35 - Average Drainage (mm/yr) for Buffel Grass Pasture

	SOIL TYPES							
	Vert	**Derm**	**Kan**	**Ten**	**Sod**	**Rud**	**Chr**	**Fer**
Augathella	0.3	12.3	21	46	17.8	102	0	14
Bollon	0.3	7.7	12	31	12.2	77	0	8
Charleville	0	8.7	14	33	13	82	0	11
Chinchilla	2.0	20.3	37	77	27.6	137	3	23
Condamine	0	11.7	20	50	17.2	103	0	12
Cunnamulla	0.3	6.3	9	24	10	57	0	7
Dalby	0.3	15.7	28	64	23	127	0	19
Dirranbandi	0	8	10	28	11.8	77	0	8
Goondiwindi	0.5	14.0	25	58	19.6	110	1	15
Greenmount	1.3	20.3	40	83	29.2	147	0	26
Hungerford	0	4.7	6	18	7	44	0	5
Inglewood	1.8	17.3	30	65	23.6	123	2	20
Injune	0.8	15.3	26	59	21.8	117	1	17
Killarney	1.3	19.7	39	85	28.8	138	1	26
Meandarra	0	10.7	17	45	15.8	97	0	10
Miles	2.0	19.3	36	77	26.8	132	2	23
Mitchell	1.0	14.7	23	55	20.4	106	1	17
Moonie	0.3	9.3	14	36	14.4	86	0	10
Morven	0.3	13.3	21	49	19.2	105	0	16
Mungindi	0	9.3	11	33	13.2	86	0	8
Nindigully	0.3	11.3	17	39	15.8	91	0	12
Oakey	0.3	10	16	41	16	99	0	10
Quilpie	0.3	5.7	9	22	8.8	50	0	7

Roma	0.3	15.7	27	59	21.4	115	0	19
St George	0	9.7	14	35	14	88	0	10
Surat	0.3	14.3	23	53	19.4	110	0	17
Talwood	0.8	13.7	21	49	18.4	108	1	15
Tambo	0.3	11	18	42	16.2	95	0	12
Tara	0.3	14.7	25	58	20	111	0	17
Texas	1.3	16.3	33	67	23	122	2	21
Thargomindah	0	3.7	5	15	5.8	37	0	4
Toowoomba	10.3	55.3	99	180	67.8	235	11	74
Wandoan	0.8	16.7	29	66	23.4	128	1	19
Warwick	0.5	15	30	68	23.2	123	1	19
Wyandra	0.5	7	9	24	10	66	1	7

Note: Vert = Vertosol, Derm = Dermosol, Kan = Kandosol, Ten = Tenosol, Sod = Sodosol, Rud = Rudosol, Chr = Chromosol, Fer = Ferrosol

Table 36 - Average Drainage (mm/yr) for Summer Cropping

	SOIL TYPES							
	Vert	**Derm**	**Kan**	**Ten**	**Sod**	**Rud**	**Chr**	**Fer**
Augathella	28	42.7	96	168	28.2	98	62	115
Bollon	23.8	36.3	79	136	24.2	81	50	96
Brigalow RS	42.3	61.3	149	233	40	143	98	166
Charleville	21.8	34.3	80	143	23.2	81	48	97
Chinchilla	40	58.7	136	227	38.4	134	89	157
Condamine	38.3	53	113	178	36.2	111	77	127
Cunnamulla	21.8	25.7	55	101	15.8	57	35	69
Dalby	36	54.7	128	215	35.8	124	79	147
Dirranbandi	27.3	41.3	78	136	27.4	80	57	95
Goondiwindi	44.5	61.7	123	196	43.8	125	92	142
Greenmount	71.8	91	174	248	67.2	183	164	207
Hungerford	9.5	18	38	77	10	41	25	49
Inglewood	43.5	60.3	125	203	42	127	87	148
Injune	32.8	48.3	119	193	33.6	117	72	138
Killarney	136.5	146.7	222	289	131.4	251	233	270
Meandarra	36.3	50.3	107	169	35.8	110	77	124
Miles	42	59	138	222	40.2	133	90	154
Mitchell	32	48	110	183	30.8	110	73	131
Moonie	39.3	51.3	96	150	35.8	98	72	111
Morven	27.5	42	98	170	27	100	62	120
Mungindi	30	45	92	154	29.4	93	63	108
Narayen	39.8	58	139	221	38	134	89	157
Nindigully	29.3	44.7	92	155	29	94	64	109

oakey	27.5	43	103	167	27.6	104	61	122
Quilpie	11.8	21	49	92	13.8	52	30	59
Roma	33.5	50.7	117	194	34.6	117	78	135
St George	31.3	46.7	95	159	31.6	97	67	114
Surat	34.5	51.3	113	188	34.8	112	77	132
Talwood	37	53.3	111	185	36.6	112	79	132
Tambo	24	37	90	157	24	89	54	108
Tara	39.5	55	118	191	37.2	120	82	138
Taroom	36	57.3	145	241	36.6	136	89	165
Texas	49.5	66.3	130	207	47.2	132	92	153
Thargomindah	8	15	35	70	9	37	19	43
Toowoomba	161.5	193.3	351	455	163.8	369	332	411
Wandoan	37	54.7	132	215	36.8	128	83	148
Warwick	106.5	114.7	175	239	98	196	189	213
Wyandra	17.5	29.3	65	114	18.4	67	42	79

Note: Vert = Vertosol, Derm = Dermosol, Kan = Kandosol, Ten = Tenosol, Sod = Sodosol, Rud = Rudosol, Chr = Chromosol, Fer = Ferrosol

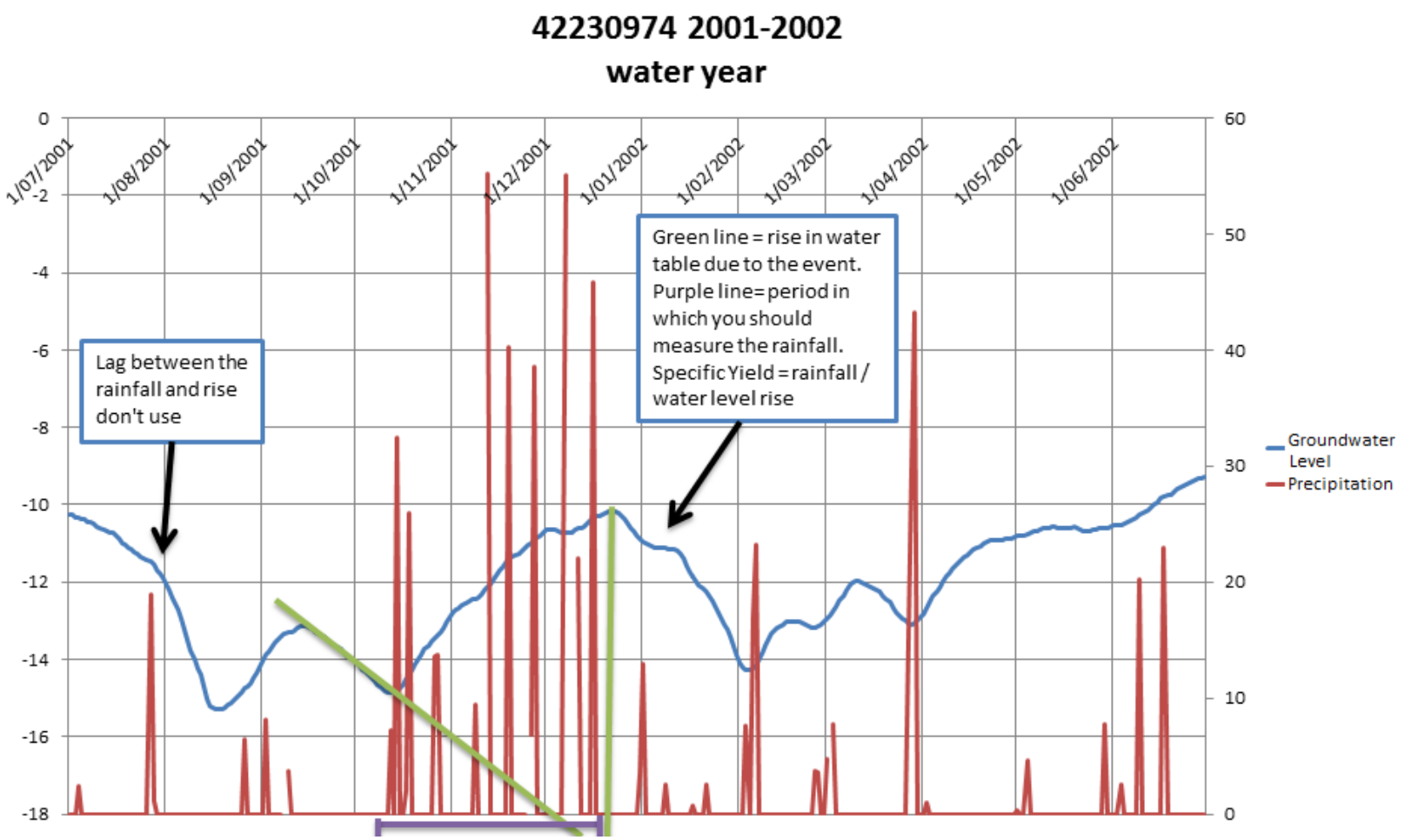

Figure 67 - Rainfall to water level rise method (Sy)

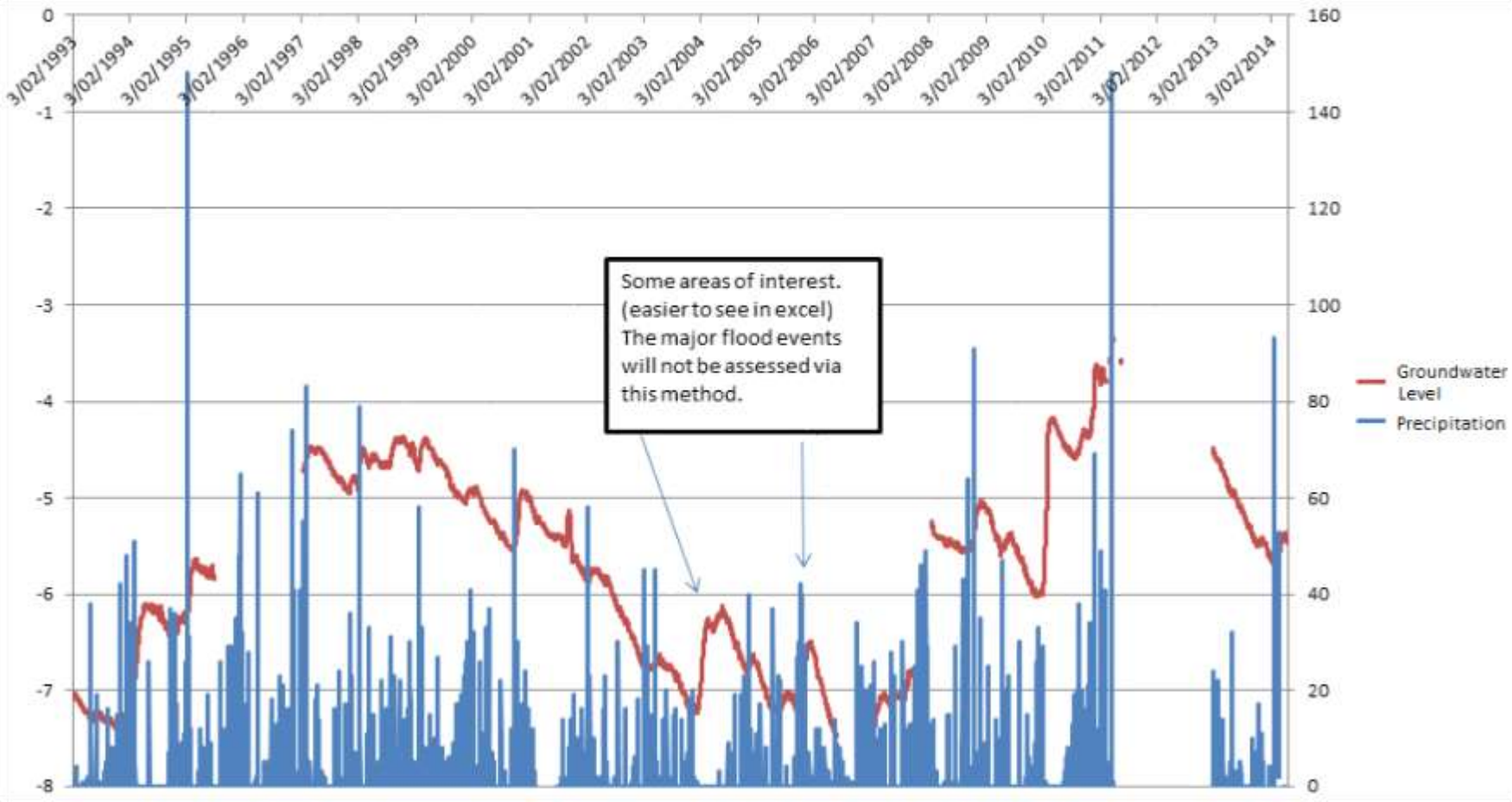

Figure 68 - All data bore RN 42220061

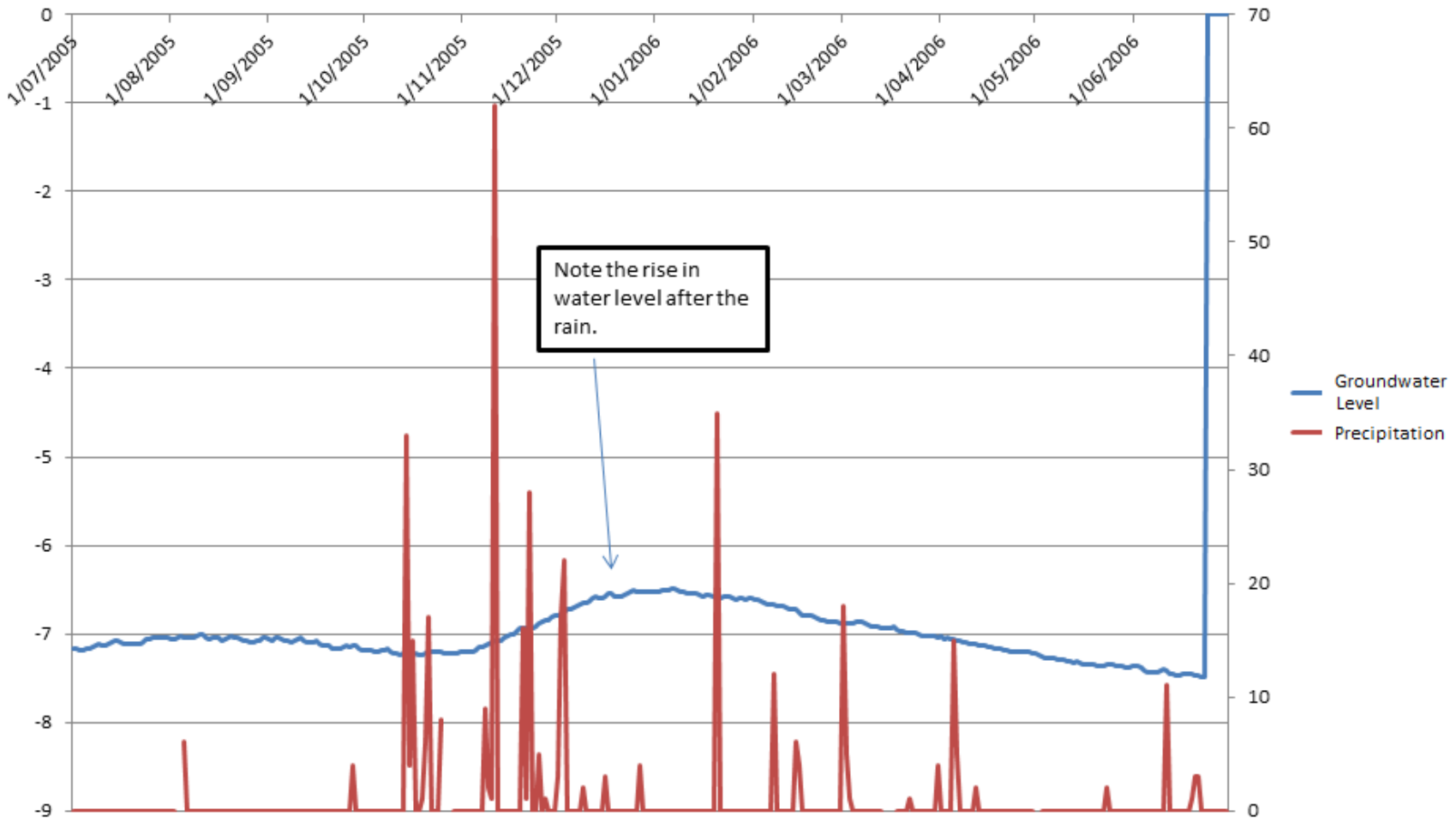

Figure 69 - 2005/2006 water year

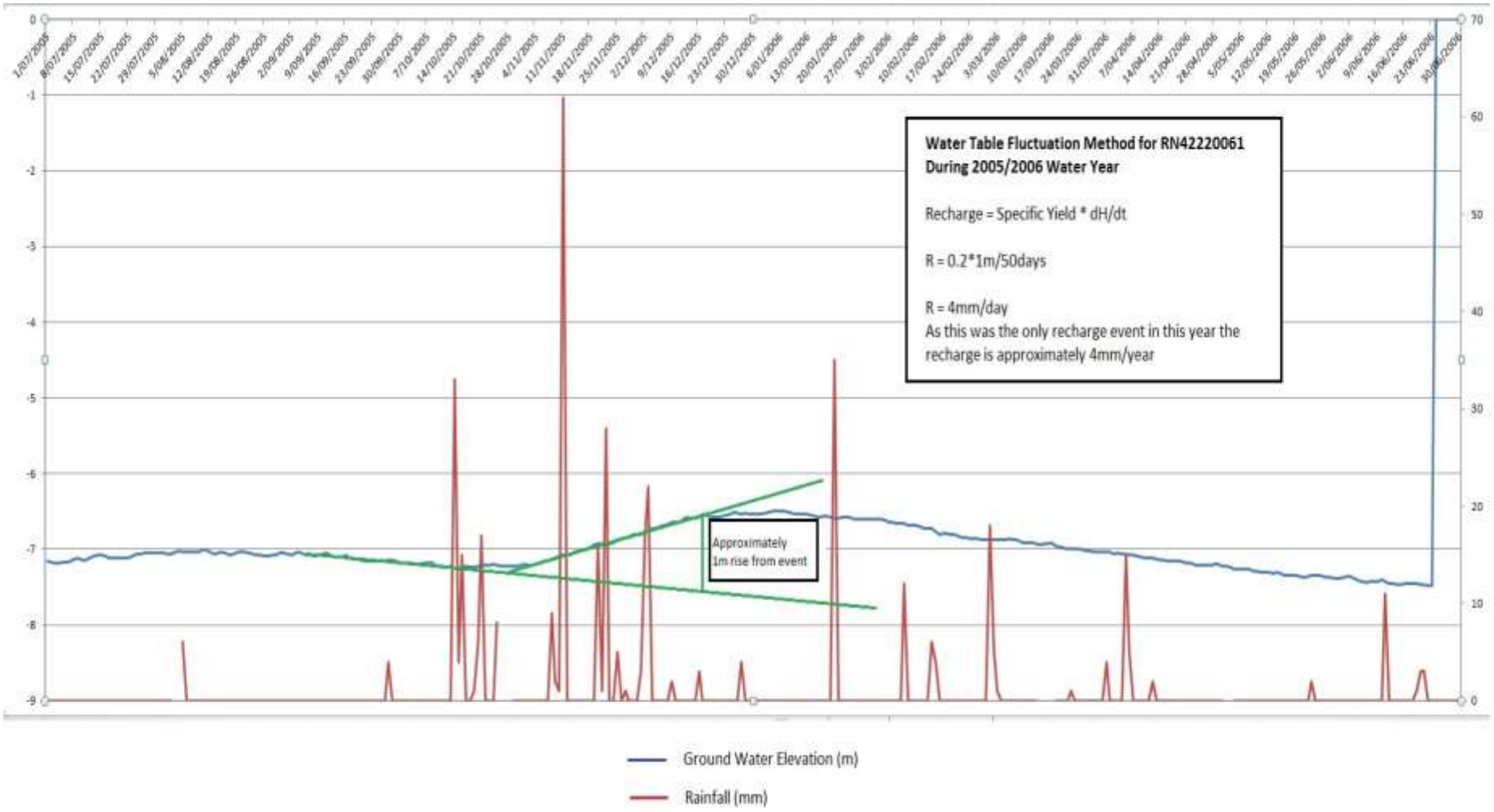

Figure 70 - WTF method applied to 2005/2006 water year

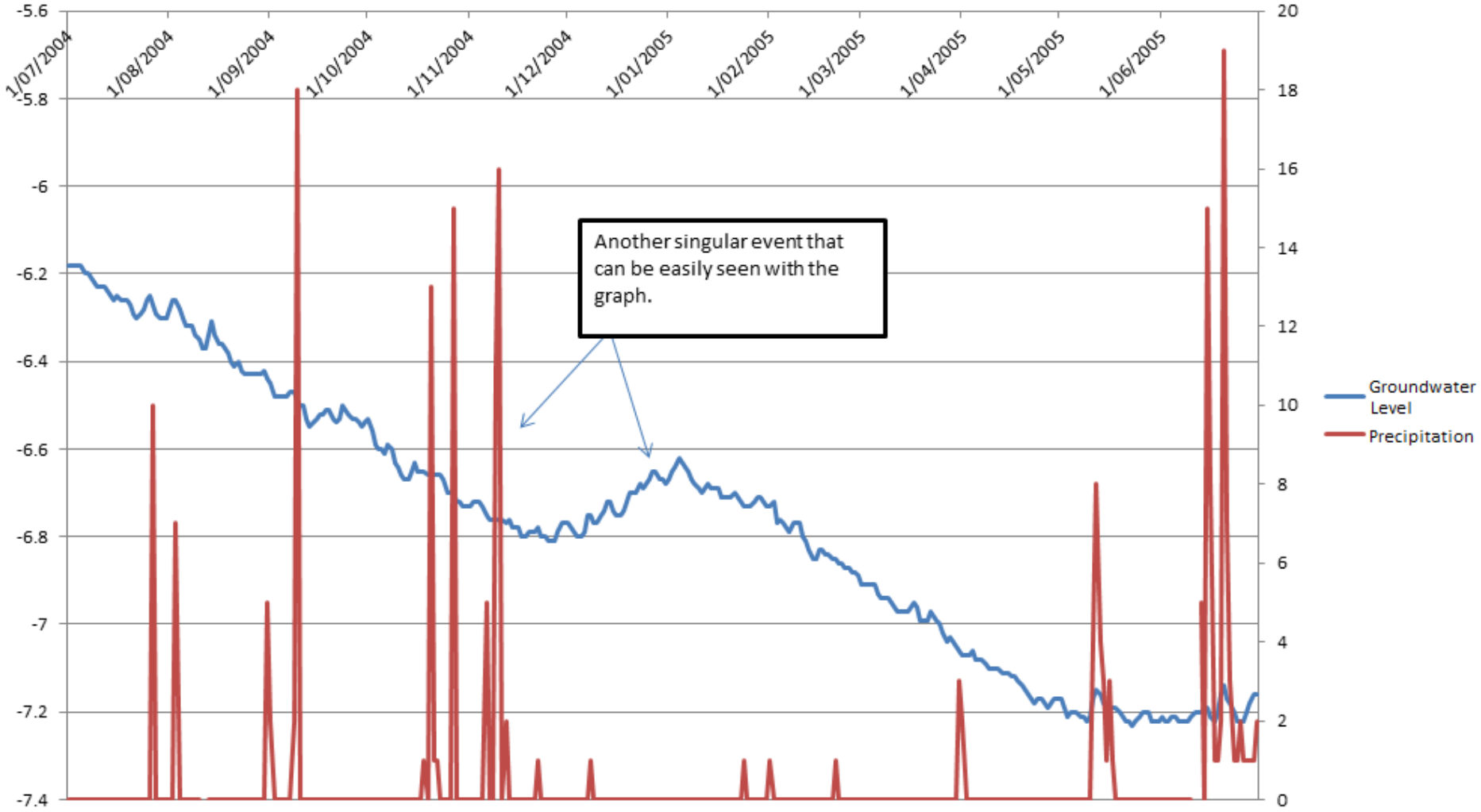

Figure 71 - 2004/2005 water year

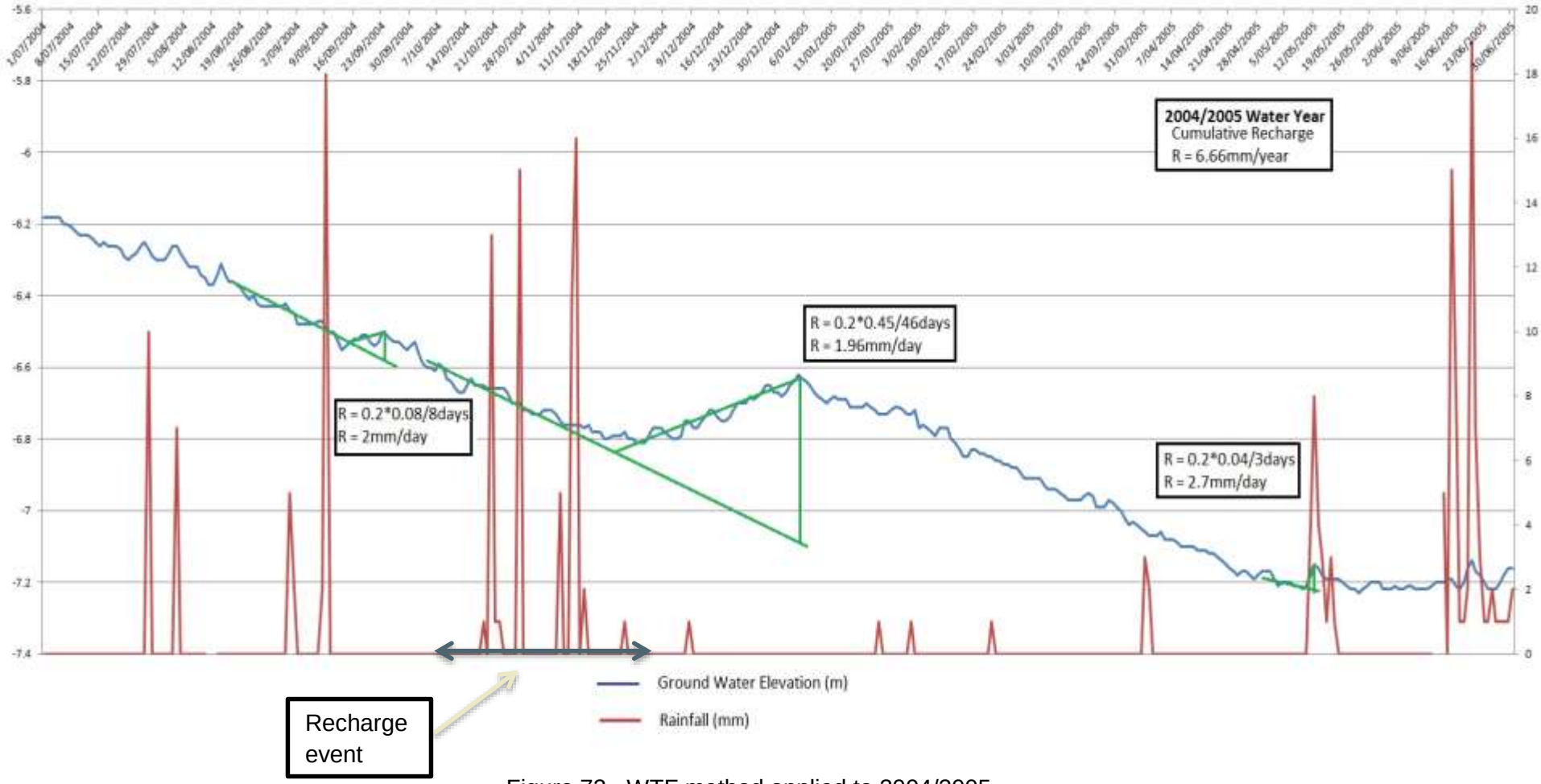

Figure 72 - WTF method applied to 2004/2005